Experimental studies on flat plate, single loop and multiloop, pulsating heat pipes

A Thesis

Submitted for the Degree of

Doctor of Philosophy

in the Faculty of Engineering

by

P.Srikrishna

Department of Mechanical Engineering

Indian Institute of Science

Bangalore 560012

July 2019

Abstract

Pulsating heat pipes (PHP) are a new addition to the family of heat pipes. These are meandering capillary tubes bent back and forth to form a loop with heat addition at one zone and heat removal at the other zone. These tubes are evacuated and partially filled with working fluid in saturated condition. The differential heating at various zones gives rise to differential pressures at various locations leading to pulsating motion of the two phase fluid. This fluid movement results in heat transfer from hot zone to cooler zones. PHPs are simple devices to fabricate but difficult in terms of understanding and design. Hence an experimental investigation has been carried out for various configurations of practical use of PHP.

PHPs in a form factor suitable for embedding in electronic assemblies are of great value in facilitating thermal management. In this aspect, a flat plate PHP configuration is more amenable for integration into a printed circuit board (PCB) due to its reduced thickness and higher density of channels within a given width of the PHP. Hence a flat plate closed loop PHP was experimentally investigated for its performance with respect various orientations, different heat loads and fill ratios with 3 different working fluids – methanol, water and FC 72. The first experiment (with water) was used to successfully benchmark the testing procedure and the test setup with the published data. Methanol was found to be fluid of choice in this configuration considering the inclinations and heat loads. A correlation has been evolved with deviation of less than ±20% for Kutateladze number (prediction of heat flux) with 146 data points across various fluids, fill ratios, inclinations and heat loads.

A single loop PHP is considered to be the building block of a PHP heat transfer device of multiple turns which may be in a single plane or sometimes arranged in multiple planes. The focus was given to start up characteristics of the PHP as this aspect is relatively less investigated especially for a single loop. A single closed loop PHP was tested with evaporator down mode. Methanol was chosen as the working fluid as it fulfilled most of the requirements of a PHP fluid. The tests were carried out for heat loads ranging from 10 W to 70 W in steps of 10 W and start-up characteristics (transient) were recorded. Most heat loads (on lower side) indicated a sudden start up where the evaporator temperature experienced an over shoot which was higher than the quasi steady state temperature for the heat load. Hence for practical cooling application care should be taken that the minimum heat flux is available for start-up as temperatures during start was higher than the steady state. At higher heat loads

the start was smooth with quasi steady state temperature being higher than the temperature at the start of PHP operation.

The single loop PHP was also investigated for the performance variations arising due to the bend radius. This aspect of PHP has been less studied and mostly the bend loss has been neglected in the simulation studies carried out for PHP geometries with lesser number of bends. As expected the smoother (larger radius) bend has performed better than the sharper bend. The flow regimes varied for the varying geometry and working fluids at lower heat loads. However, at higher heat loads unidirectional circulation has manifested for all inclinations tested. The tests have revealed that loss of pressure in the bends cannot be neglected even if the number of bends is small as almost 15% performance change was observed at lower inclinations due to the change in bend radius. The tests also indicated that the optimum angle of good heat transfer was not 90° but was found to be between the inclination angles of 60° and 70°. The effect of bend radius was less in methanol as its dynamic viscosity is much lesser than that of water. The insulating of the adiabatic section resulted in marginal improvement in heat transfer of the PHP of same geometry, working fluid, heat load at almost all inclinations. The insulation of the adiabatic section also widened the heat load range of both the working fluids tested. The frequency analysis carried out from the pressure transducer data has shown that with increase in heat load higher frequencies manifested. The frequencies have tended to be lower for near horizontal inclinations and less volatile working fluids.

A PHP with channels/tubing disposed in multiple planes with forced convective air cooling has been tested as this was reported in the literature to have greater orientation independence with respect to gravity. This device is akin to a fin array based on PHPs and can be a suitable replacement for heat sinks. Water has been employed as the working fluid for a fill ratio of 60% in three orientations with an aim to enhance the fin efficiency. The tests have shown that a PHP based heat sink with a substantial number of turns (in this case 18 numbers) can be deployed for gravity independent operation provided that the heat inputs are greater than the threshold of PHP operation initiation. The fin thermal conductivity was enhanced by a factor of about 5 over that of copper.

Acknowledgements

Every project big or small; tough or easy is successful largely due to the effort of a number of wonderful people who have always rendered their valuable support and advice. I sincerely appreciate the inspiration, support and guidance of all those people who have been instrumental in making this project a success.

I wish to express my gratitude and special thanks to my supervisor Dr G.S.V.L. Narasimham for accepting to guide me through this doctoral thesis. He was a tremendous support and gave me a valuable guidance, constant encouragement throughout the project and kept me on the right path not only in this project but throughout my career, academically and technologically.

I also wish to express my heartfelt gratitude to my Director as well as my internal supervisor Dr S. Umamaheswara Reddy who not only guided me throughout my investigation but also motivated me to pursue this venture in the first instance.

It is my glowing feeling to place on record my best regards, deepest sense of gratitude to all my colleagues within my group as well as across the my organisation MTRDC, DRDO for their valuable support and timely encouragement in the need of the hour.

I would like acknowledge with much appreciation my colleagues in the Precision Machining Division who helped me with the required hardware and necessary materials to complete the project.

I shall be failing in my duties if I fail to acknowledge the whole hearted support received from Mr. Varun, Scientist – C and Mr. Siddharth, Junior Research Fellow of the department, both of whom have left the organisation now. They spent long hours with me for testing without any hesitation and helped me complete several milestones in this dissertation.

I also thank my friends Yogendra, Sandeep, Hari Kumar, Narendra Babu and Bharath at my Refrigeration and Air-conditioning laboratory, IISc, Bangalore for stimulating discussions, support and fun which were always constructive and refreshing.

I would also like to thank Mr Vishweshwara Rao and his team from M/s Avac private limited, Bangalore for helping me realise the vacuum tight assemblies in time for completing my project.

I wish to thank Mr Mohan Kumar, glass blowing expert at Bharat Electronics, Bangalore for his skilful contribution in putting together the transparent pulsating heat pipes for visualisation studies.

I also profoundly wish to thank my undergraduate classmate, Mr Ramkumar for consistently persuading me to take up higher challenges in my career and motivating me to pursue the PhD.

I would take this opportunity to show my gratitude to my parents for their encouragement and instilling the good values and ethics in me which was instrumental in completing this project. A special thanks to my wife and daughter for cooperating patiently with me and helping me achieve my targets. They have been for days on end waiting for my arrival because I had to work late, and have shown tremendous support in that regard. Whether it was a failed test in the experiment or even minor hurdles during the course of my doctoral degree, they always encouraged me, lightened me up and boosted my confidence to pursue the work that I had planned for that day.

Even my entire lifetime would be insufficient to thank all of them who have contributed in completing this project, yet I thank them from the bottom of my heart for understanding and helping me through this tough yet enlightening journey.

Contents

List of Figures

List of Tables

Nomenclature

Symbols

A	area	m^2
b	breadth	m
Bo	Bond number = $d\left[g_{eff}(\rho_l - \rho_v)/\sigma\right]^{0.5}$	
Cp	specific heat capacity	J/kg-K
d	internal diameter	
D	external diameter	m
Fr	Froude number= $v/\sqrt{gd}$	
g	acceleration due to gravity	m/s^2
h	latent heat	J/kg
htc	heat transfer coefficient	W/m^2-°C
I	current	A
j	volumetric flux	m/s
Ja	Jakob number= $\frac{Cp_l(T_e - T_c)}{h_{fg}}$	
k	thermal conductivity	W/m-°C
Ka	Karman number= fRe^2	
Ku	Kutateladze number = $\frac{\dot{q}}{\dot{q_{max}}}$	
L	length	m
Mo	Morton number =$\frac{\mu_l^4 g_{eff}(\rho_l - \rho_v)}{\rho_v^2 \sigma^3}$	
n	number of turns	
Nu	Nusselt number = $htc*d/k$	
p	perimeter	m
P	pressure	N/m^2
Pr	Prandtl number = $\frac{Cp_l \mu_l}{k_l}$	

$\dot{Q}$	heat load	W
$\dot{q}$	heat flux	W/m^2
R	resistance or radius of bend	°C/W or m
R'	gas constant	J/kg/K
Ra	Rayleigh number = $\frac{g\beta(T_s - T_a)L^3}{\nu^2}$ Pr	
Re	Reynolds number = $\frac{\rho v d}{\mu}$	
t	depth of the channel	m
T	temperature	°C
v	velocity	m/s
V	voltage	V
Vol	Volume	m^3
w	width	m
We	Weber number = $\frac{\rho v^2 d}{\sigma}$	

Greek symbols

α	Property of fluid	
β	inclination angle or orientation of PHP / coefficient of expansion	degrees
δ	film thickness	m
Δ	difference	
ϕ	fill ratio	
μ	dynamic viscosity	Ns/m^2
θ	contact angle between solid and fluid	degrees
ρ	density	kg/m^3
σ	surface tension / Stefan Boltzmann constant	N/m
ν	kinematic viscosity	m^2/s

Subscripts

a	adiabatic
air	air
Al	aluminium
amb	ambient
avg	average
b	heat sink base
c	condenser
conv	convection
corr	correlated
crit	critical
cs	cross-section
e	evaporator
eff	effective
equiv	equivalent
exp	experimental
f	fin
fg	vaporisation
fill	fill ratio
fp	flat plate
h	horizontal
htc	heat transfer length in condenser
hte	heat transfer length in evaporator
i	inner
l	liquid
L	left
loss	loss of heat
m	mean
max	maximum
o	outer
PC	poly carbonate
PHP	pulsating heat pipe effect

R	right
rad	radiation
sat	saturation
t	total
th	thermal
trans	transducer
v	vapour
val	valve
vc	vertical in condenser
ve	vertical in evaporator
w	wetted

Abbreviations

BHM	bottom heat mode	
CFM	cubic feet per minute	ft^3/min
CGV	critical gas value	
CLPHP	closed loop pulsating heat pipe	
FFT	Fast Fourier Transform	
LPM	litres per minute	
OLPHP	open loop pulsating heat pipe	
PHP	pulsating heat pipe	
RMSE	root mean square error	
RPM	revolutions per minute	
SLPHP	single loop pulsating heat pipe	
THM	top heat mode	

1 Introduction

1.1 Need for efficient heat transfer

With the advancement of technology, heat removal problems associated with various thermal systems have accentuated. As the entire human kind is becoming well and truly aware of the energy crisis, efficient heat transfer mechanisms a have attained large significance. Another area that requires efficient heat transfer is the electronics industry where the combined effect of miniaturization and increased functionality has made thermal management (heat removal) a very serious aspect. In fact, this was predicted well in advance several decades ago by Gordon Moore, Intel co-founder through his Moore's law which states that the number of transistors on a chip will increase by two times for every two years. This law seems to be valid till date as seen in Figure 1-1 where actually the number of transistors have nearly doubled after every 18 months.

The shrinking size (miniaturization) and increased heat dissipation (increased functionalities) have resulted in manifestation of severe heat fluxes within small volumes as shown in Figure 1-2. This figure depicts the intensity of the thermal management in electronic assemblies and devices. The heat fluxes are comparable (of the order of 10^2 W/cm^2) to that of a nuclear blast. However, the maximum temperature which these devices can withstand are far less (around 100°C) and this maximum allowable temperature is very likely to remain in the same order for the foreseeable future. Hence very good thermal management tools are mandatory for the safe operation of these assemblies.

These thermal management tools can be classified as - heat transfer device where the heat at inaccessible spots are transported to a relatively manageable zones and heat spreaders where a severe heat flux at localised spot can be diffused to lower heat flux which can then be managed by more conventional strategies. Coupled with this heat transfer requirement these thermal management tools are needed to be energy and cost efficient for obvious reasons of energy shortage and market competitiveness. The passive two-phase heat transfer systems like heat pipes, thermosyphons, vapour chamber, pulsating heat pipes etc., are highly suitable devices for the above stated applications as they are inherently energy efficient.

Also these devices are more reliable due to absence of moving parts in their construction, thus can cater to the military and space applications where the reliability is of paramount importance.

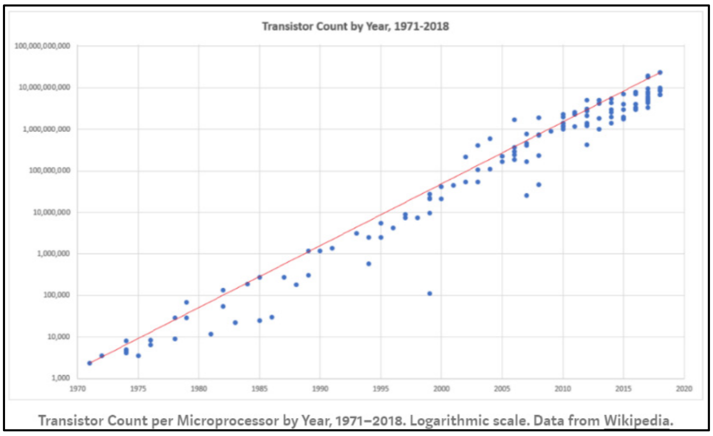

Figure 1-1: Number of transistors on a chip - Moore's law [1] and [2]

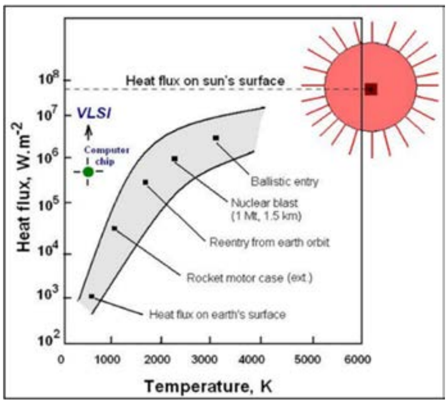

Figure 1-2: Heat flux vs maximum allowable temperature [3]

1.2 Heat pipes

Heat pipes are containers whose longitudinal dimension is larger than the lateral dimensions that are evacuated and filled with a working fluid (refer Figure 1-3). They are designed to have at least one heat absorbing zone (evaporator) and one heat dissipating zone (condenser) with an adiabatic section (which is not mandatory) [4]. The heat pipes are reported to have very large equivalent thermal conductivity compared to any known materials as heat is transferred from one zone to another by evaporation and condensation. As the heat transfer coefficients associated with these processes are very high the heat is transported from one end of the pipe to another with very small temperature gradient.

As shown in Figure 1-3, the heat added at the evaporator makes the working fluid to vaporize. The vapour due to increased pressure at the evaporator travel in the core (middle region) of the cross-section of the pipe. This vapour condenses when it encounters the cooler surfaces at condenser. The condensate travels back to the evaporator thus completing the cycle of operation. The condensate is taken back to the evaporator by capillary/wick structure attached to the walls of the container.

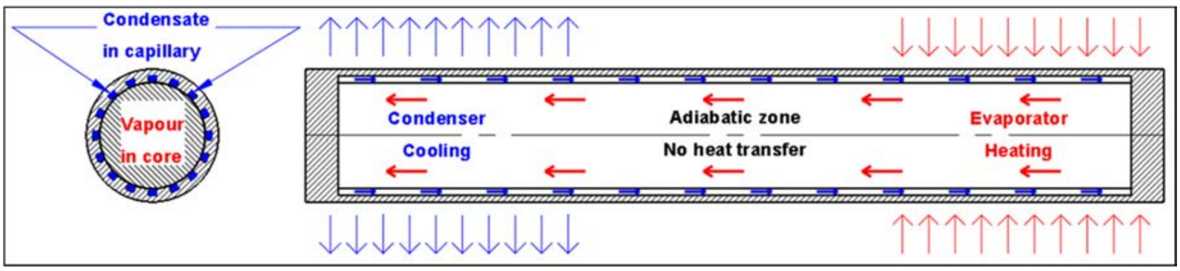

Figure 1-3: Working of a heat pipe

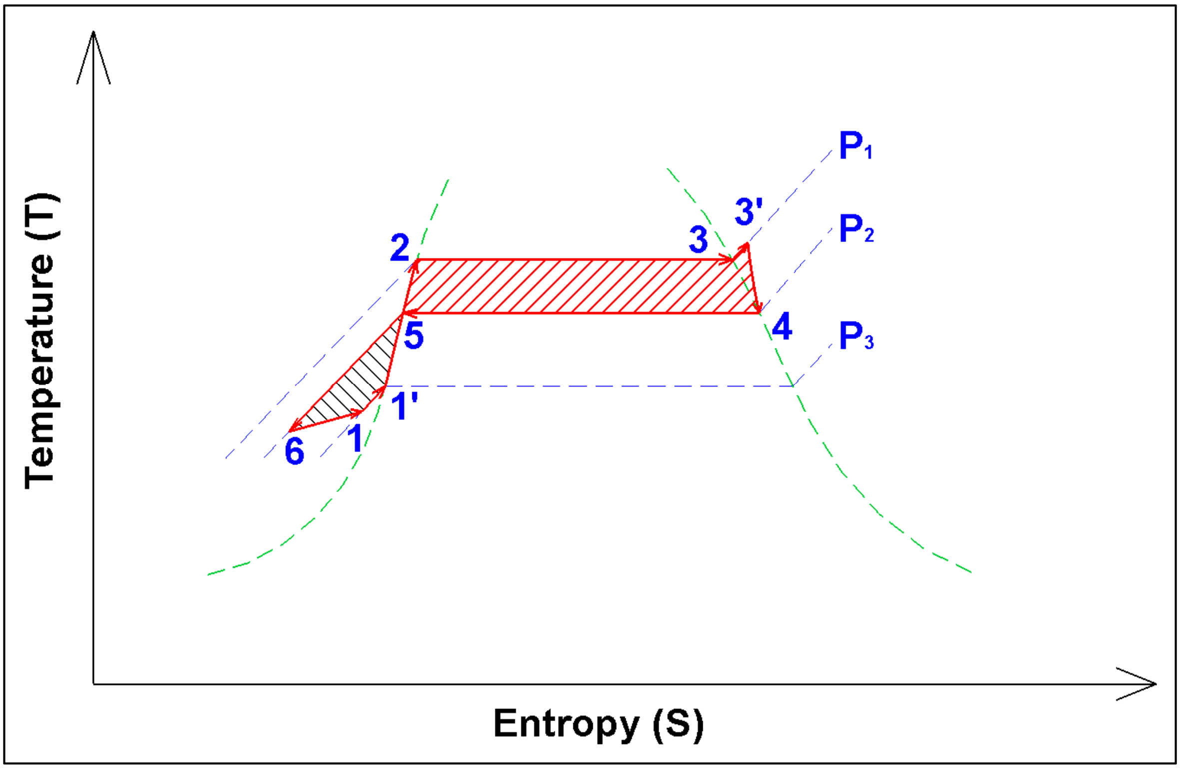

Figure 1-4: Thermodynamic cycle of a heat pipe

The thermodynamic cycle occurring within the heat pipe is akin to a power plant Rankine cycle (of course with substantially smaller pressure differences between the boiler and condenser). The thermodynamic cycle is shown in Figure 1-4. Beginning from state point 1, the liquid is heated by the evaporator heat addition (1-1'-2). This is followed by heat addition resulting in phase change and possibly slight superheating (2-3/3'). The vapour travel results in pressure loss as well as entropy increase and the same is represented by 3'-4. The vapour passing through the condenser undergoes change of phase from vapour to liquid and also sub cooling by rejection of heat (4-5-6). The liquid travelling back to evaporator through the capillary wick undergoes a pressure drop and entropy rise as represented by 6-1 which completes the cycle and this cycle is continuously repeated when the heat pipe is in operation. The area (2-3-3'-4-5), which resembles the Rankine cycle and the area (1-1'-5-6) are equal in magnitude to have the sole effect of heat transfer [5]. The work done in moving the fluid against friction in processes 6-1 and 3-4 is dissipated as heat. Therefore, the heat given out at the condenser includes this dissipated heat.

The heat pipes differ from thermosyphons as they have wick structure to return the condensate back to the evaporator. Thus heat pipes can work against gravity (condenser below evaporator) unlike two phase thermosyphons which are entirely dependent on the gravity to replenish the evaporator with the liquid.

1.3 Limitations of heat pipes

Though heat pipes are very efficient they have certain limitations [6] with respect to the temperature of operation for a given fluid for the given heat inputs at the evaporator. These limitations are as follows,

1. Continuum limit – which occurs for micro sized heat pipe at low temperatures where the low amount of vapour causes a rarefied condition thus preventing the heat transport.
2. Frozen start-up limit – while starting up from frozen state the vapour generated at evaporator can get frozen at the adiabatic section or condenser thus preventing the cycle from continuous operation by depleting the liquid at the evaporator.
3. Viscous limit – at lower temperature and lower heat inputs the vapour pressure at the evaporator is inadequate to overcome the viscous forces opposing the flow thus making the heat pipe non-functional.
4. Sonic limit – this occurs when the vapour velocity in the core region exceeds the sonic velocity. This leads to a choked working condition which can happen either during the start-up or during the regular operation.
5. Entrainment limit – occurs when the vapour velocity is substantially high that the shear force at the liquid-vapour interface tears the liquid confined to the wick and liquid particles get carried away with the vapour thus preventing replenishment of the liquid at the evaporator.
6. Capillary limit – occurs when the capillary pumping is unable to overcome the pressure head loss of the liquid travelling through the narrow wick structure and the gravity (if condenser is below evaporator). This also hinders the replenishment of the liquid at the evaporator.
7. Condenser limit –when the condenser is of limited capacity or if the non-condensable gases are present within the heat pipe then the heat transport is limited by the ability of the condenser to dissipate the heat.
8. Boiling limit – when the radial heat flux (thus the wall temperature) is high at the evaporator boiling of the liquid at the wick structure (as against required evaporation) starts. This results in drying out of the evaporator as the circulation (replenishment) of the liquid does not happen thus the heat pipe limit is reached.

The above limits are summarized pictorially in Figure 1-5.

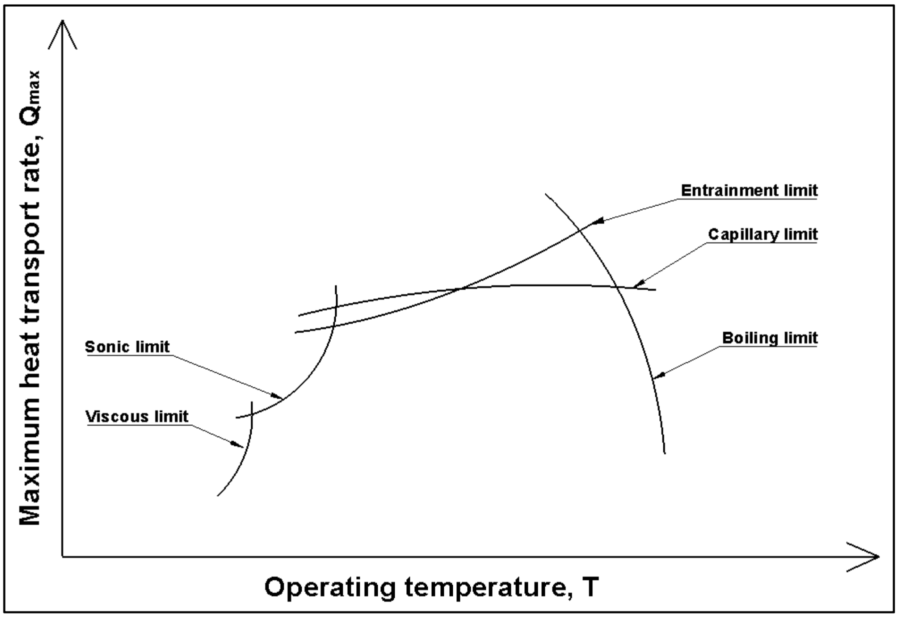

Figure 1-5: Heat transfer limitations for a heat pipe as a function of temperature [7]

1.4 Pulsating heat pipes

The pulsating heat pipes are the relatively recent addition to the family of heat pipes. They are heat pipes as they are closed, constant volume two-phase systems. They are also similar to thermosyphons in their construction as they have no capillary wick structure, but are not limited by the direction of gravity for the circulation of liquid back to the evaporator. These pulsating heat pipes (PHP) are defined as meandering tubes of capillary dimension bent back and forth to itself (refer Figure 1-6) forming a closed system charged partially with a working fluid after evacuation of the non-condensable gases [8], [9] and [10]. The liquid admitted inside tube self distributes into discrete liquid slugs and vapour plugs due to dominance of surface tension compared to gravity.

1.4.1 Working of pulsating heat pipes

The fluid inside the PHP is in the saturated condition to begin with (just after charging) and the liquid/vapour are distributed non-uniformly. Hence when heat is applied at the evaporator which is usually located at one end of the PHP the bubbles expand with rise in the vapour pressure at the evaporator. This pressure rise pushes the adjacent slugs to move towards the condenser where the exact opposite process occurs. In the condenser as the bubbles lose heat they shrink in size. This results in lower pressure thus making the net fluid movement towards the condenser. The nucleate boiling in the evaporator when the liquid traverses the evaporator causes new bubbles to appear. These bubbles either collapse at the condenser or agglomerate as larger plugs and travel with the fluid flow. Thus a quasi-steady oscillating but progressively axial movement of the fluid takes place from the evaporator to the condenser and back. This movement of the hotter fluid (two-phase mixture) between the evaporator and the condenser results in heat transfer which is predominantly sensible [11] and [12]. This is in contrast with the conventional heat pipes where the heat transfer is primarily latent. The latent heat contribution in PHPs are more confined to initiation and sustenance of the pulsations due to change of phase which leads to the pressure difference between evaporator and condenser.

1.4.2 Pulsating heat pipes in comparison to the conventional heat pipes

The pulsating heat pipes are reported to be between the latent heat conventional heat pipes and the single phase heat transfer of forced convection [13] in terms of efficacy of heat transfer. The primary difference between them is the fact that the PHPs are devoid of the capillary wick structure which is the main component of the conventional heat pipes in returning the condensate to the evaporator. However, it is shown that [14] the introduction of wick structure improves the performance of the PHPs. This aspect of non-requirement of wick structure renders the PHP to be simpler, less expensive and lighter than its conventional counterpart. As the channels are of capillary dimension and the surface tension effects are comparable to other forces in play (gravity and inertia) the countercurrent flow of liquid and vapour as occurring in conventional heat pipes do not happen in PHP. In PHP, the slug and plug move in unison in the same direction within a channel. Thus the entrainment limit of the conventional heat pipe is entirely removed. Since boiling is one of the active mechanism of bubble generation the boiling limit of the conventional heat pipe is also alleviated. This non-existence of the above two limits was documented in the first PHP patent by Akachi [8].

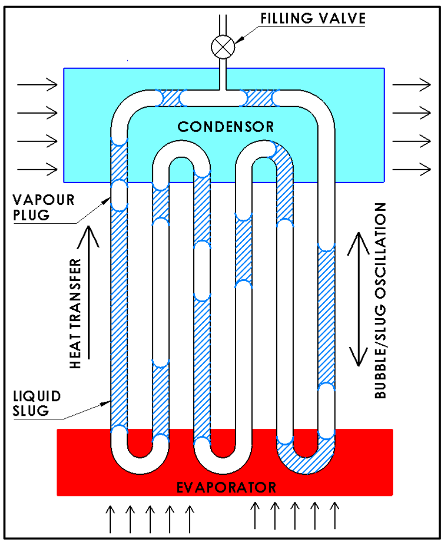

Figure 1-6: Schematic of pulsating heat pipe

1.4.3 Classification of pulsating heat pipes

Pulsating heat pipes can be classified with respect to various parameters – form factor, spatial orientation of the channels and type of end connection.

1.4.3.1 Flat plate and capillary tube configuration

The PHPs are classified as flat plate configuration and capillary tube configuration based on the form of construction as shown in Figure 1-7 (a) and (b). In flat plate configuration the PHP channels are usually machined into a flat plate substrate of desired material. The other side or the top side of the channel is closed with another plate which can be transparent for visualization or of the same material as that of the substrate. In this the number of channels that can be packed for a given width of the plate is maximum. On the other hand, a capillary tube can be bent back and forth to form several channels. Here the construction is made out of capillary tubes hence the name capillary tube PHP. Though capillary tube configuration might result in lesser tubes for a given width the performance of the capillary tubes are reported ([15] and [16]) to be superior to that of flat plate configuration. Some authors in literature have attributed the difference in performance due to reduced amplitude of oscillations in flat plate configuration as cross channel temperature homogenization and the pressure homogenization occurs more readily in the flat plate PHP. This is due to continuous substrate housing the channels as against the discrete channels of the capillary tube version.

1.4.3.2 Single plane and multiplane channels

PHPs are also classified according the orientation of the channels in the various planes. PHPs are called single plane PHP when the channels are deployed in the same plane as shown in Figure 1-7 (b). Whereas the PHP with its channels constructed in more than one plane as shown in Figure 1-7 (c) can be termed as multiplanar PHP. This kind of construction was termed as 'Kenzan fin' by Akachi [17]. This was also proposed by Akachi in his patent [18]. These multiplanar version of the PHP has the advantage of being gravity independent during their operation as the gravity aiding the return of condensate to the evaporator always has an active component when the channels are multiplanar [19] instead of single plane PHP for various inclinations.

1.4.3.3 Closed loop and open loop PHPs

Another classification of PHPs is based on the end connection of the capillary tubes or the channels. The PHPs are called open loop when the ends of the channels are not connected to each other (Figure 1-8 (a)) and sealed separately. When the two ends are joined to each other as in Figure 1-8 (b) then the PHP is called the closed loop. The closed loop PHPs are reported to be better in heat transfer performance owing to the provision for the fluid to circulate either clockwise or counter clockwise with superimposed oscillations thereby increasing the heat transfer from evaporator to condenser due to increased velocity of fluid flow. The open loop PHPs are advantageous from manufacturing and charging perspective but only permit oscillations and not circulation. The same concept of having circulation to enhance heat transfer has been extended by adding a check valve in a CLPHP-CV (refer Figure 1-8 (c)) to make the fluid motion in single direction and this was shown to have better performance than the CLPHPs with no check valves [20] and [21]. The check valves prevent the return of the fluid in the opposite direction thereby enhancing the flow velocity in one direction and thus the heat transfer.

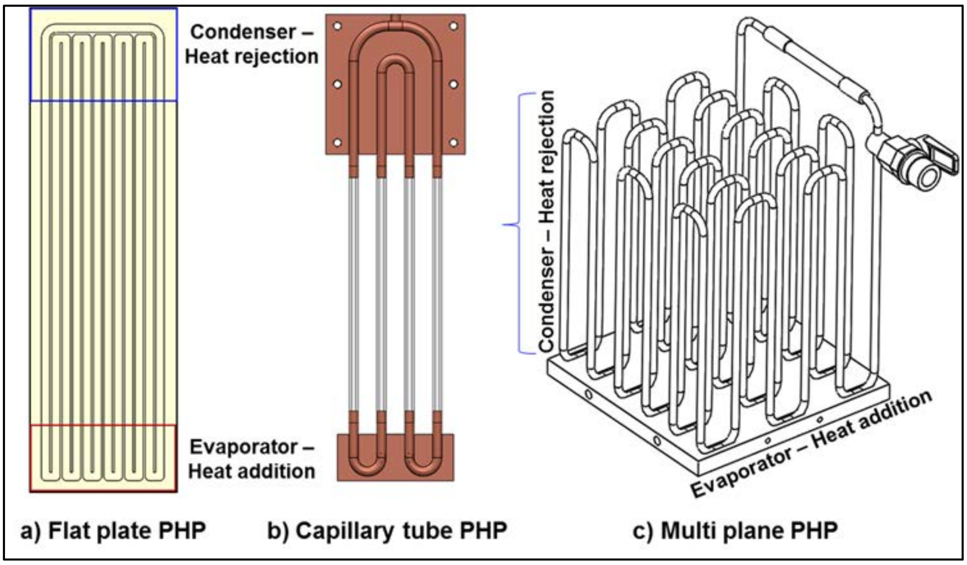

Figure 1-7: Configurations of PHP based on form of construction

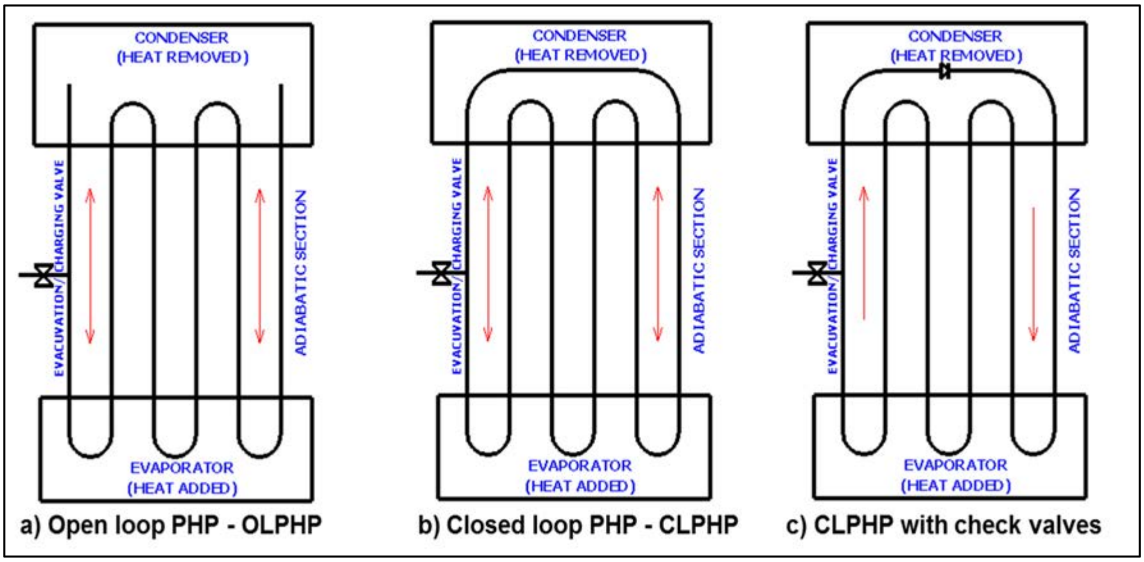

Figure 1-8: Configurations of PHP based on end connection

1.4.4 Parameters affecting pulsating heat pipe performance

The PHP performance can be altered by several parameters – geometry, working fluid, fill ratio, inclination angle and capacity of the condenser.

1.4.4.1 Geometry

The parameter of geometry can further be sub-divided into following

1. Inner diameter/channel size – The preferable channel size is reported to be the one which is small enough for the surface tension to be dominant (Bond number < 2) so as to get the formation of slug-plug alternately within the channel. However, there are incidences [22] where slight deviation of inner diameter on the higher side than the one prescribed by Bond number criteria worked well as PHP. Most of the work have been carried out with diameters 1 mm to 3 mm where the PHPs are found to yield the maximum heat throughput with larger diameters. In fact this was highlighted by Akachi in his first patent [8] and also by other researchers like [23]. The lower diameters yield nearly same thermal performance for varying orientations of operation [24].
2. Length of evaporator – Literature [25] states that shorter lengths of the evaporator yields lower thermal resistance hence better heat transfer.
3. Length of condenser – Larger condenser lengths are preferred as the heat removal capacity will be enhanced. It was also reported that enhancement of length of condenser or its capacity can be counterproductive as stated in [26].
4. Number of turns – larger number of turns not only increase the performance of the PHP but also makes their performance independent of gravity due to increased perturbations as stated in [19].

1.4.4.2 Working fluid

The desirable properties of a good PHP working fluid has been studied by various groups like [9] and [27]. The required properties are as follows

1. Surface tension – This parameter defines the size of the channel as per the Bond number static confinement criterion. Thus larger value would yield larger diameter thus greater inventory and better performance as performance tend to get better with larger diameters. However, it is stated in [26] that higher surface tension tends to increase the requirement of pressure difference for substantial oscillations to maintain pulsating flow. Thus surface tension of larger values can be used only with larger diameters and higher heat fluxes.

2. Latent heat – As mentioned earlier, in PHPs the role of latent heat is only to form the bubbles. For heat transfer (most heat transfer occurs through sensible mode) low latent heat leads to quicker evaporation and boiling thus faster and lower temperature start-up. Lower latent heat also leads to more vapour generation, leading to enhanced velocity of pulsations thus heat transfer is enhanced with lower latent heat fluids.
3. Specific heat – As majority of heat is transferred by sensible mode, a high specific heat will increase the amount of sensible heat transferred thus higher value is preferred.
4. Dynamic viscosity – As a lower dynamic viscosity will reduce shear stress along the wall and will result in reduced pressure drop in the channel a lower value is preferred as it results in greater velocities thus more heat transfer.
5. $(dP/dT)_{sat}$ – As the pulsations occur due to the variation of pressure arising due to the variation of temperature at evaporator and condenser a larger value is prescribed for the change in pressure for a given change in temperature by all research groups.

1.4.4.3 Fill ratio

The fill ratio is defined as the ratio of the volume of the fluid admitted inside the PHP to total volume of the PHP. This is one of most important parameters for the effective working of the PHP. It is widely accepted that the best range of working occurs between 30 % to 60 % fill ratio [9]. Too high a fill ratio results in lesser degrees of freedom for the oscillations to occur while too less a fill leads to dry out owing low amount of fluid inventory [26]. The good performing fill ratios vary with the shape of the cross-section of the channels, with the sharp angled cross-sections having their optimum fill ratio on lower side [28].

1.4.4.4 Orientation

Even after the conformance of the Bond number criterion for static confinement diameter it is seen in all the reported work that formation of slug-plug distribution at the time charging does not ensure deterioration of performance when the orientation of operation is changed. Bond number criteria shows that the gravity forces are relatively less compared to surface tension but still performance tests have indicated that the PHPs tend to perform inferior when operated in top heat mode than when compared to the bottom heat mode operation. However, PHPs with smaller diameters and larger turns are shown to be performing nearly orientation independent at higher heat fluxes. The orientation convention in this thesis is depicted in Figure 1-9. The angle of inclination is measured from the horizontal plane.

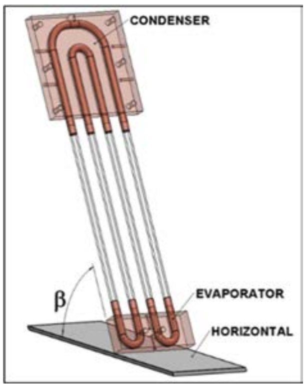

Figure 1-9: Definition of the inclination angle with respect to horizontal

1.4.4.5 Heat flux

Heat flux is another important parameter determining the thermal performance of a PHP. Invariably all the research works reported that the thermal performance of the PHP increases with the increase in the heat flux. This is due to the fact that higher energy leads to larger amplitude pulsations and higher velocities resulting in enhanced heat transfer. The PHPs are known to begin working only after a threshold heat flux is applied and this is called the start-up heat flux which is needed to overcome the viscous force of the tube wall to initiate and sustain the pulsations.

1.4.5 Types of modelling approaches

Various modelling approaches have been adopted in the last two decades to simulate the working of a PHP. The works of Khandekar [29] and [30] have given a comprehensive review of the various modelling approaches and their pros and cons. The initial way of modelling a PHP was considering it as a spring-mass-damper system as in [31]. Subsequently research groups have attempted at modelling from first principles using the conservation equations of mass, momentum and energy for the unit cell of one slug with two half plugs surrounding the slug. These initial attempts were made for a restricted scope like top heat mode, single turn and only slug flow regime [11], [12] and [32]. Due to the multitude of events happening within a short span of time inside a PHP, all these numerical simulations had certain limitations like simplified assumptions. A highly exhaustive numerical simulation was carried out by [14] and [33] in which authors have tried to capture most of the phenomena happening within the PHP. In [34] artificial neural networks were used to model the performance of the PHP and it was stated that a large number of experimental data points are required to train the network for the correct prediction. Subsequently many research groups have taken up correlation modelling as it is the method that can give the most reliable representation of the PHP working [29].

1.5 Objectives of the present work

In this doctoral work some configurations of PHPs of practical relevance are experimentally evaluated. The objective of the work includes:

- Investigation of PHPs in flat form factor with respect to heat load, working fluid, fill ratio and orientation so that the same can be embedded into an electronic device as thermal spreader to diffuse severe heat fluxes.
- Study of start-up characteristics of PHP and its practical relevance in case deployment of PHP for cooling of a device.
- Estimation of impact of geometric features like bends on the performance of PHPs with respect various orientations of operation and working fluid as sharper bends can be deployed for heat removal from relatively inaccessible/small hot spots.
- Study of PHP with orientation of the channels in multiple planes towards making the PHP performance gravity independent as well as realizing a heat sink with lighter but highly efficient fins composed of PHP.
- Study of PHPs with greater instrumentation (pressure as well as temperature) to get data for practical design of PHP based cooling solution.

1.5.1 Methodology

The work was carried out to meet the above mentioned objectives. The experimental setup was designed for various configurations listed above with the following provisions.

- Variation of orientation with resolution of 1° inclination angle from vertical bottom heat mode to vertical top heat mode.
- Heat loads (heat fluxes) with variation in steps of 5 W from as low as 5 W to 400 W.
- Valves and accessories to vary fill ratios in steps of 10% from as low as 10 % to 80%.

Thus temperature and pressure data was collected across fluids (water, methanol and FC 72), for different fill ratios, orientation and heat fluxes. The temperatures were measured at various locations (especially – evaporator and condenser) and was represented as thermal resistance values for comparison of performance for different cases for each configuration. A correlation was fitted using linear regression analysis with non-dimensional numbers. The pressure pulsations were monitored and the Fast Fourier Transform was used to predict the frequency of pulsations. For the multiloop configuration the temperatures were monitored at both root and the tip of the fin to predict the enhancement of the fin efficiency (thermal conductivity of the fin) due to the PHP operation in comparison to a unfilled PHP.

2 Literature survey

2.1 Evolution of PHP

The first applications which are close to operation of pulsating heat pipes can be found in mechanical toys which were popular in 1990s. These are the 'Drinking bird' and the 'Putt-putt boat'. In both these toys evaporation/boiling at one end makes the liquid adjacent to the expanding bubble to move. The condensation of the vapour generated restores the fluid in their respective positions for the cycle to repeat thereby making the toys to function continuously. These toys have utilized the physics [35] with very little understanding of the nuances of the two phase flow. The pulsating heat pipes are also based on the evaporation and subsequent condensation to make pulsations which results in heat transfer.

The first application or engineering utilisation of the pulsating heat pipes was proposed by Akachi [8] in his patent. This disclosed the pulsating heat pipe as a loop-type heat pipe carrying two phase fluid which circulates by repeated vaporisation and condensation at heat receiving zone and heat radiating (dissipating) zone respectively. The patent has documented 24 different configurations (Figure 2-1) of the PHP for use in various circumstances like cooling of electronics, power generation using turbine blades, electric motor winding cooling, cooling of underground cables, cooling of superconductor coils, etc. In this patent at least one check valve was advocated to promote the circulation in the preferred direction. The patent also outlined the limits like entrainment limit, wicking limit, length to diameter ratio limit, occurrence of water hammer as well as orientation dependent performance variation of the wicked heat pipe. The working principle of the PHP has been explained and the circulation enhancement due to check valve was elaborated. The construction of the check valve including the material of construction was documented. The inventor has advocated that for top heat mode (with adverse gravity situation) smaller diameter tubes have to be used. The inventor also states that the smaller diameter tubes result in lowering the heat transport capability of the PHP due greater flow resistance. The patent also enumerated different materials of construction of the tube. The patent shows the test results of PHP with water as well as Freon-11 as working fluid. The results show that the Freon-11 filled PHP performed better than the water filled ones. This has been primarily attributed to the higher saturation pressure and lower dynamic viscosity of Freon-11 in comparison with water. Based on the working fluid and applications like electrical isolation, alternate materials of construction of the PHP has been detailed.

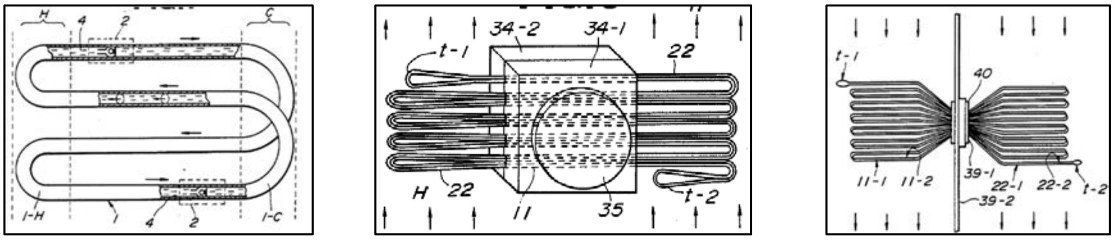

(a) (b) (c)

Figure 2-1: Various configurations of PHP proposed by Akachi, 1990 [8]

Akachi in his other patent [36] titled structure of micro-heat pipe proposed 8 more configurations in which PHP can be used. In this patent the inventor outlines the drawbacks associated with conventional heat pipes like deterioration of performance with respect to gravity, limitation arising due to counter flow of liquid and the vapour phases and lack flexibility in shape. The patent also states that the previous configuration introduced in the patent [8] suffers from the disadvantages of lack of reliability especially for long term usage due to use of check valves. These check valves lead to deployment of several joints and limits the inner diameter of the PHP. It is also stated that the open loop configuration is easy to charge and seal as compared to the closed loop PHP. In this patent a smaller inner diameter as compared to the previous patent [8] was proposed. As the inner diameter was reduced the inventor stated that the need for the check valves as well as precise fill ratio for better heat transfer are not mandatory. The patent shows that the performance of the PHP with ID 0.7 mm and OD 1.0 mm when filled with HCFC142b for fill ratios between 30% to 50% was orientation independent. The patent also advocates that the insulation of the adiabatic zone enhances the heat transfer as the entire PHP process works to homogenise the pressure (temperature) at the two different ends of the PHP. It is recommended to use liquid with higher thermal conductivity as working fluid. In one of the configurations the passage or the channel was crushed to 90% of the opening but the deterioration was shown to be negligible. The patent also showed that the thermal performance of same sized PHP in the sixth proposed configuration (Figure 2-2 (c)) was almost the same with or without the check valve irrespective of the orientation of the PHP. The seventh configuration indicates the method of deployment of smaller radii bends in the PHP. The last configuration indicates that the connections to the check valves if any are used or to the loop itself can be through threaded fittings rather than soldering or welding thus making the PHP to be flexible in its size and shape.

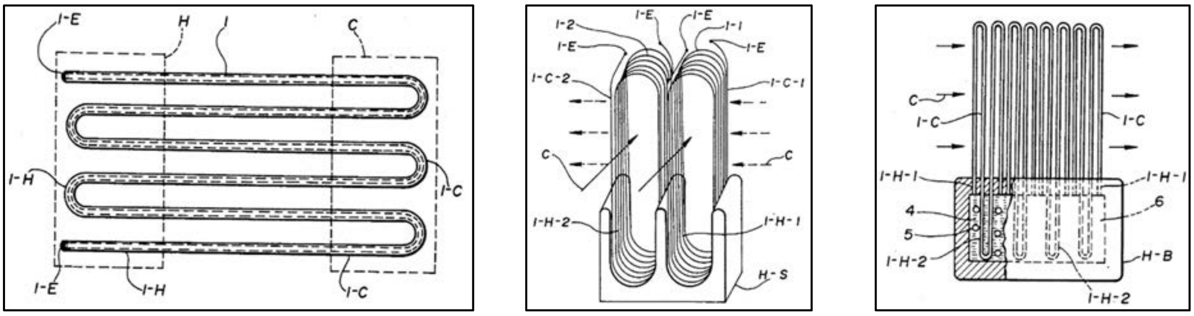

(a) (b) (c)

Figure 2-2: Configurations of Akachi patent 1993 [36]

Akachi in his patent [18] in 1996 proposed the use of PHP as pin-fins of a heat sink as shown in Figure 2-3. Although the pin-fins perform better than plate fins the patent states that the conventional pin-fins have drawbacks like greater difficulties in manufacturing, denser fins leading to lesser flow rates or use of larger fans, denser fins leading to higher weight, thinner fins being fragile, etc. Thus the proposed capillary tube wound in spiral form mitigates all the above mentioned disadvantages of the pin-fins as well as provide a large thermal conductivity to the pin-fin structure. The patent proposed that the tubing and the base of the heat sink to which the tubing is bonded to be made of aluminium to have reduced weight of the heat sink. The inventor has compared a conventional pin-fin structure of 30 mm height with 320 copper fins with 102 bends (204 pin-fins) of 30 mm height PHP heat sink and concluded that the deterioration of thermal performance for the PHP based pin-fins was lesser when compared with the conventional pin-fins when the air speed of cooling was reduced with the weight of the PHP heat sink being 36.2% lesser.

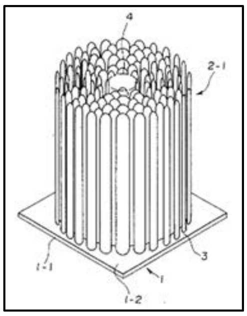

Figure 2-3: Pin-fin PHP by Akachi, 1996 [18]

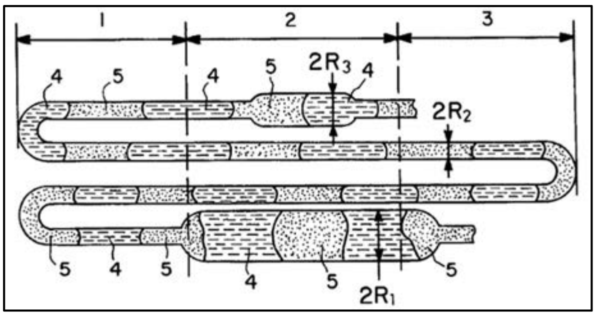

Figure 2-4: Asymmetry in geometry proposed by Smyrnov [37]

Smyrnov in his patent [37] in 2004 has explained the method of action of the PHP and its construction with additions for storage of kinetic energy, heating elements (other than evaporator zone), porous zones to enhance and regulate the flow thereby improve the heat transfer. This patent states that the drawback of using check valves is that the diodicity of the valves are low in low flow rates and the valves offer hydraulic resistance thereby reducing the thermal performance. The patent emphasises that the driving force in PHP is the imbalance caused by the varying local vapour pressures at different locations. This pressure variation is due to the fact that the liquid film near the wall around a vapour bubble appears at different locations in the adjoining branches at different points in time. The imbalance may not exist if the geometric, physical, constructional and thermal factors are identical in adjacent branches. Hence the L_e, L_c, R (like in Figure 2-4) and pitches between branches if made different can act as facilitating factors for the pulsations. The patent defined the radius of the tubing for effective PHP working and the maximum length of the liquid slug that can be sustained for the given radius. The patent has highlighted various configurations/additions/modifications in the PHP to make them perform better. The modifications can be inclusion of bellows which can stretch when the pressure inside the PHP is high and release the mechanical energy to sustain the two-phase flow when there is a pressure fall. The same effect can be replicated by fitting an elastic material over the outer diameter of the tubing at few locations. Few chambers of piston/membrane can be added to enhance the performance of the PHP. The inclusion of alternate rough (porous) and smooth internal surface can add to the imbalance that sustains the two-phase flow. The use of porous inserts at few locations can introduce additional meniscus at several locations thus introducing difference in pressures in the order of thousands of Pascal thus sustaining the PHP action. The patent advocates the use of auxiliary heaters at predetermined locations other than the evaporator that can be operated periodically to enhance pulsations. The thermal contact between adjacent branches can also enhance pulsations. Thus this patent has advocated thermal and hydraulic discontinuities as enhancement factors though these discontinuities are usually viewed as impediments. Finally, the patent states that the fluid of choice governs the material of construction of PHP where both fluid and material can be selected based on the application/requirement from a variety of combinations.

Based on Akachi's proposed configurations different research groups have carried forward the research in various directions and for various form factors of PHPs. The various reasearch efforts can be broadly classified into study of the operating parameters alongwith flow visualisation, form factor variations, numerical modelling, correlation modelling, heat transfer enhancement studies.

2.2 Study of operating parameters and flow visualisation

Khandekar and Groll in [26] discuss the critical design parameters of a successful PHP operation. The authors also describe the difference between a conventional heat pipe and a PHP. It is reinforced that the PHP has more share of sensible heat transfer whereas the conventional heat pipe transfers majority of energy by latent heat. The various flow regimes that are possible in the PHP operation have been discussed. The authors state that the net circulation takes place with superimposed oscillatory motion leading to the alternate channels of down-comers being relatively colder than the adjacent hot up-headers. The authors have made an attempt to plot the thermodynamic cycle of a PHP with the uncertainties also being stated. It is shown that the mass quality of vapour inside the PHP for the fill ratios at which PHP operates is very low. It is stated that the internal diameter chosen should satisfy the Bond number criteria ($Bo < 2$) for the slug-plug formation of the fluid which is essential for the PHP performance. If the internal diameter is larger than the one prescribed by Bond number criteria, the liquid in the PHP will stratify thus making it work as a thermosyphon (operating only in the vertical bottom heat mode). Within the range of the prescribed diameter the heat throughput continuously increases with increasing diameter. The importance of fill ratio was also emphasised. The authors state that at low fill ratios the PHPs dry out at low heat loads whereas at very high fill ratios exceeding 80% of the internal volume the number of bubbles (plugs) are low leading to lesser oscillations thus lower performance. Thus, an optimum fill charge exists. The exact range will differ for different working fluids, operating parameters and construction. It is also stated that increasing the condenser capacity need not necessarily improve the heat transfer like that in conventional heat pipes. If the condenser capacity is raised there can be chance of dry-out in case of PHP. The paper summarizes that the desirable properties of working fluid are high $(dP/dT)_{sat}$, lower dynamic viscosity, lower latent heat combined with higher specific heat capacity, lower surface tension and lower contact angle hysteresis. It is concluded that instead of individual thermophysical properties, groups of properties affect complex real systems like PHPs. As the PHP has great dependency on the flow pattern for its thermal performance, different operating regimes of the device are likely to be affected by different groups of thermophysical properties.

The paper by Khandekar and Groll [13] attempts to define the PHP in terms of controllable thermo-mechanical boundary conditions. This is deemed necessary to benchmark the operational performance limits and to help in system analysis. The advantages of PHP over an air cooled solid fin in terms of heat transfer and over a forced liquid cooling system in terms of cost and simplicity of construction was highlighted. The authors also state that the most defining parameter for PHP to work as a heat pipe and not just as an interconnected thermosyphon is the internal diameter. The Bond number criteria of $Bo < 2$ was prescribed as a prerequisite for the PHP to function with slug flow. It was as well stated that the performance of the PHP goes down with decrease in internal diameter after the criteria of Bo number is met. This is attributed to the fact that the smaller diameter leads to greater friction for the pumping action of the bubbles leading to diminished performance as well as lower fluid inventory thus lesser sensible heat transfer. It is also stated that after a certain diameter range, the pulsating device will gradually loose its fundamental character of PHP. Instead, it will behave as an interconnected array of two phase thermosyphons which may be thermally a better option, at least for a certain range of inclination angles. It is affirmed that CLPHPs may never be as good as an equivalent heat pipe or thermosyphon system which are based on pure latent heat transfer but can be optimized towards classical heat pipes or thermosyphons, as a limiting case. The authors state that the operating heat flux will directly affect the level of perturbations inside a CLPHP thereby affecting the thermal performance of the device. The lower heat flux results in lower oscillation amplitudes thus poorer heat transfer followed by slug flow and annular flow with increasing heat flux leading to better heat transfer. When heat flux is further increased it results in the net circulation of the semi annular and annular flow leading to the best heat transfer where one limb will act as down-comer while the adjacent limb acts as up-header. Finally, it is confirmed that the unfilled PHP and the 100% filled PHP cease to behave as PHP. The more bubbles (lower fill charges), the higher is the degree of freedom but simultaneously there is less liquid mass for sensible heat transfer. Less bubbles (higher fill charges) cause less perturbations and the bubble pumping action is reduced thereby lowering the performance. Thus an optimum fill charge exists in between 20% to 80% where adequate number of bubbles are available for pumping and sufficient fluid is available for sensible heat transfer.

Khandekar et al. [9] presents the results of the 2 mm internal diameter copper – glass PHP of 5 turns in the evaporator for 3 fluids – R123, ethanol and water. A wide fill ratio was deployed for the study starting from 0% (dry tubes) to 100%. The results for the vertical bottom heat mode indicate that the optimum fill ratio for all three fluids do not exceed 55%. In this study the heat load was applied as heat flux in evaporator and the condenser was air cooled with air velocity of 5 m/s. The adiabatic section was not present in the study. The requirements of a good PHP fluid like – high $(dP/dT)_{sat}$, low viscosity, low latent heat, low surface tension and high specific heat were detailed. The authors stated that the 100% fill was having better performance than the 85% to 95% fill due to additional pressure drop within the loop caused by the one or two bubbles in the higher fill ratios. The study also states that though the Bond number criteria of 2 or lesser was adhered the gravity had profound influence in the working of the PHP making it non-operational at horizontal orientation. The authors concluded that the horizontal operation did not occur due to the limitation of the T_e (100°C for water and ethanol; 60°C for R123) and also due to the limited number of turns leading to decreased perturbations.

The authors in [19] have carried out an exhaustive study to characterise the effects of orientation, number of turns, internal diameter, section lengths and type of fluid. On the whole 11 copper capillary tube PHPs were studied with 2 mm and 1 mm internal diameter, 5 different number of turns (5, 7, 11, 16 and 23) and section lengths of 100 mm and 150 mm. Three fluids – R123, ethanol and water with constant filling ratio was used with the orientation being monitored in 5 angles of 0° being horizontal to 90° being vertical bottom heat mode with angles varied almost in steps of 10°. The authors have considered the closed loop PHPs (CLPHP) rather than the open loop ones (OLPHP) and the closed loop ones with check valves for the study for the reasons of better thermal performance of CLPHPs over OLPHPs and their simplicity of construction than CLPHPs with check valves. The study concluded that though the Bond number criteria of less than 2 was adhered the gravity had major effect on the working of the PHPs. It was concluded that up to 60° the effect was same as that of vertical orientation. The study stated that the internal diameter being larger and the number of turns being higher leads to PHPs having higher heat throughput. The study as well stated that for 2 mm diameter the critical number of turns was 16 and that for internal diameter of 1 mm the critical number of turns was higher to make the PHPs work in horizontal mode (Figure 2-5). The authors have also proposed alternate structures of PHPs were the gravity vector will be actively aiding the working of the device in all orientations apart number the increased number turns which leads to more stochastic distribution of void fraction leading to the working of the PHPs in varying orientations with respect to gravity. The study concluded that water was a good fluid in vertical bottom heat mode but ethanol and R123 with higher $(dP/dT)_{sat}$, lower latent heat and lower viscosity were found to be more suitable fluids for orientations away from vertical mode and even for lower diameter tubes.

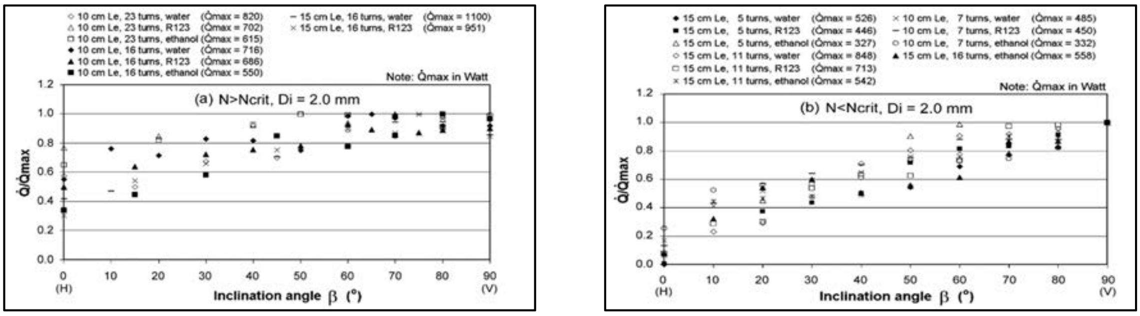

(a) Turns greater than critical number (b) Turns less than critical number

Figure 2-5: Critical number of turns for horizontal operation for a given diameter [19]

Charoensawan and Terdtoon in [25] have investigated the performance of horizontal closed loop pulsating heat pipes with distilled water and ethanol. The fill ratio was varied as 30, 50 and 80%. The PHPs were constructed out of copper tubes of internal diameter 1, 1.5 and 2 mm. The evaporator lengths were 50 and 150 mm. The lengths of the evaporator, adiabatic and condenser sections were maintained to be equal. The number of turns was varied as 5, 11, 16 and 26. The heat load was provided at the evaporator as a constant temperature boundary between 40°C to 90°C in increments of 10°C. The heat was removed at condenser by forced air convection with air velocity of 0.4 m/s at 25°C of room temperature. The authors state that the evaporator temperature of operation to start-up depends on the inner diameter and number of turns. The greater the inner diameter and the number of turns, lower is the temperature of start-up. The authors also inferred that at each T_e the R_{th} was lower for the higher inner diameter for water whereas the trend is reverse for ethanol. This is being attributed to the fact that smaller tube leads to larger friction thus hindrance to pulsations in case of water and ethanol with lower surface tension and viscosity manifested a different trend. At larger inner diameter water had distinct higher performance. At 1 mm inner diameter the two fluids showed comparable R_{th}. The authors also concluded that shorter evaporator lengths (also shorter PHP length as the sections are of equal lengths) performed better than the ones with longer evaporator lengths. For a short evaporator length R_{th} was found to reduce with increase in number of turns. For a long evaporator length, the number of turns strongly affected the R_{th} which reduced sharply as the number of turns was increased. However, the best performance of all the HCLOHPs remains at the maximum number of 26 turns. None of PHPs with minimum number of turns of 5 could operate. This was attributed to the fact that with an increase in the number of turns, the unbalanced pressure in the tubes between the evaporator and condenser sections increases thus enhancing the fluid motion (hence heat transfer). The study showed that for 150 mm evaporator length best heat transfer performance was found occur at 30% fill ratio whereas for the 50 mm evaporator length the fill ratios of both 30% and 50% was found to yield the similar thermal performance.

The paper by Mameli et al. [38] describes the thermo-fluid-dynamic investigation on a CLPHP with four parallel tubes with 2 turns in the evaporator. In this study, the fluid pressure as well as the fluid temperature are recorded. Thus the investigation was able to estimate the local heat transfer coefficient (Figure 2-6) in a chaotic flow boiling process. This was possible as the fluid temperature and the solid wall temperature at nearly the same axial location was monitored. The internal diameter of the PHP was 2 mm. The adiabatic section consisted of glass tubing thus paving way for flow regime identification. The fluid pressure was monitored at a sampling frequency of 6 Hz as the characteristic frequency was estimated as not more than 3 Hz in the literature [39]. The experiments were conducted with ethanol and ethanol-water azeotropic mixture at 65% fill ratio. The experiments were carried out for 2 different behaviour of PHP. First set of experiments were targeted to heat loads where the PHPs start-up behaviour was monitored. These experiments indicated that the PHP did not start or reached high evaporator temperatures for heat loads less than 40 W. Even if the heat loads were increased incrementally from 40 to 50 W, the PHP was not found to operate as a heat pipe. During these lower heat fluxes the PHP operated in heat switch mode - fluid temperature and pressure raised when fluid oscillations are poor and again decreased, when more vigorous flow motion is activated. Once the starting heat load was above 50 W the PHP operated successfully from thereon up to 110 W when actual dry-out occurred. During the successful start-up net circulation was observed with super imposed oscillations. The heat transfer coefficient was estimated to be 4600 W/m^2-K and an equivalent thermal conductivity was estimated to be 6000 W/m-K. The flow regime for the majority of the study was reported to be slug flow in the down-comer and annular flow in the up-header. The authors have also reported that the enhancement of heat transfer with increase of heat load is due to the thin film evaporation due to flow transition from slug to annular apart from increased oscillations. A Fast Fourier Transform (FFT) of the pressure oscillations indicated no characteristic frequency of oscillation. On the whole six orientations 90°, 75°, 60°, 45°, 30°, 15° and 0° with the angle measured from vertical position were investigated. Thus 0° correspondents to vertical bottom heat mode and 90° corresponds to horizontal position. The PHP did not start in horizontal mode of operation. This has been attributed to the limited number of turns in the PHP construction which makes this device performance more susceptible for the orientations. The result indicated an interesting occurrence that the 30° inclination gave a wider range of heat flux (even more than 0°- BHM) between start-up and before dry-out. The authors also reported that the azeotropic mixture of ethanol and water did not show any appreciable performance improvement over pure ethanol for the same fill ratio and heat fluxes.

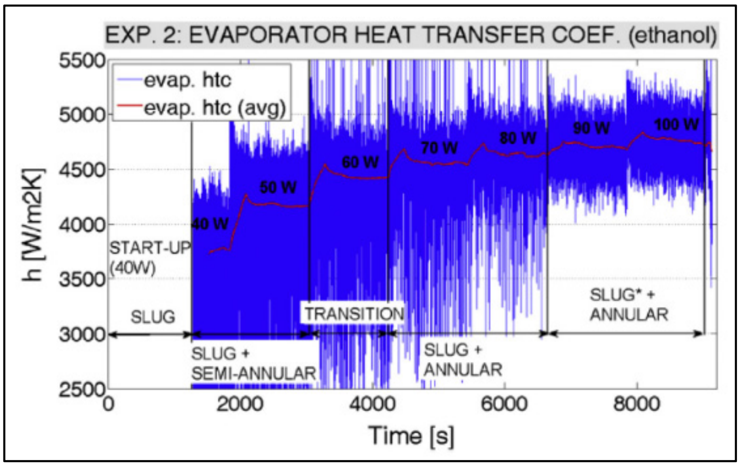

Figure 2-6: Experimental estimation of heat transfer coefficient in PHP [38]

Mameli etal. [40] conducted experimental investigation with copper tube of ID 1.1 mm and OD 2.0 mm filled with FC-72 to assess the impact of inclination (effect of gravity) on the performance of CLPHP. The PHP consisted of 31 bends with a relatively very short evaporator length (6 mm) nearly the entire length acting as condenser (180 mm) with condenser cooled by fans. The heat load was applied from 10 W to 100 W in steps of 10 W. The characterisation was made with respect to inclination starting from horizontal position to the vertical bottom heat position in steps of 15°. The fill ratio was maintained at 50% for all tests. The test was conducted with both temperature measurements at evaporator and the condenser as well as pressure measurement at the condenser. The sampling frequency of the measurement was made at 0.2 Hz. The authors have reported unstable performances at higher heat loads for vertical operation in comparison with horizontal operation. The authors also state that despite the small diameter and the high number of bends gravity plays a major role in the performance of the CLPHP. The PHP started-up at nearly 10-20 W and operated normally between 30 W and 60 W. The dry-out or the instability started at heat loads of 90 W – 100 W. The bottom heat mode showed more instability (higher R_{th} and larger temperature oscillations) at higher heat loads than the more horizontal orientation though at the normal operating heat loads the trend was reverse. The normal operation mode for most heat loads showed that only the near horizontal orientations were affected by the gravity and the rest of the R_{th} were similar to the gravity assisted bottom heat mode. During the start-up heat loads the vertical orientation shows that the gravity is a source of instability as the repeatability was not achieved like it was achieved with the horizontal orientation. The authors have reported that the PHP reaches performance crisis at higher heat loads which can be attributed to the combined effect of gravity and heat flux. It was reported that the gravity aids in maintenance of oscillations at higher heat loads. The study also reveals that the instability (leading to large temperature oscillations) is not affected by hysteresis as shown by the comparison of R_{th} for sudden heating at maximum load versus the incremental heat loads as the two R_{th} values settle at the same average value.

The authors in [41] have investigated the effect of gravity on a CLPHP of internal diameter 1.1 mm and outer diameter 2 mm with FC-72 as working fluid for a fill ratio of 50%. The PHP consisted of 32 parallel channels (16 turns) with bend radii of 3 mm. The PHP had a heating (evaporator) length of 6 mm. The condenser was of 180 mm length cooled by aluminium heat sink and 4 fans. The PHP was tested both on ground also in flight for a parabolic flight trajectory where the gravity varies from aiding the PHP to neutral to impeding the PHP. The PHP was fitted with pressure transducer and 14 thermocouples. The signal sampling rate was 16 Hz. The PHP was tested for 10 to 100 W in steps of 10 W. In the ground tests the PHP was tested for heating up (10 to 100 W) as well as heating down (100 to 10 W) modes. The PHP tested required a minimum of 3.5 W/cm² heat flux for an instant start-up. The authors observed that only partial dry-out (few channels) occurred and total dry-out never occurred. The horizontal operation did not show partial dry-out though its performance in terms of R_{th} in standard PHP operation was higher than the vertical one. The pressure signals indicated that the horizontal operation resulted in large amplitude pulses followed by small amplitude ones of higher frequency whereas the vertical operation had pulsations of smaller amplitude consistently. However, the Fast Fourier transform of the signal for 60 W did not reveal any dominant frequency. The PHP was tested on ground for sudden vertical – horizontal – vertical orientations for the investigation of the hysteresis effects. The PHP when suddenly moved to the adverse horizontal orientation took more time (about 180 s) to attain the pseudo-steady state than when the PHP was moved to a more favourable vertical position. This experiment was done to assess the PHP performance in the parabolic flight where the gravity varied from 1g to 1.8g to 0g to -1.8g to -1g. However, in the flight tests the time provided between the micro gravity and the hyper gravity condition was only 20 s. The tests in flight revealed that the thermal regime of a planar PHP subjected to 20 s of microgravity environment reached the same regime of a PHP operating on ground in horizontal position. However, for the horizontal orientation of the PHP in the flight the variation of the performance with respect to the varying gravitational field was not pronounced. The authors concluded that the vertical position was more dependent on the heating history (heating up or heating down) than the horizontal position. The authors also observed that for a 2-D PHP in horizontal position - the horizontal operation on ground is the most similar to the microgravity operation in flight. In Appendix – A, the criteria of critical internal diameter for PHP based on We < 4 and Ga other than the usual Bo < 2 criteria were provided. The authors state that the PHP inner diamater can be larger in case of microgravity than in case of the normal terrestrial applications.

The authors in [27] have studied the performance variation of the 5 turn, 2 mm internal diameter CLPHP with 4 fluids – deionized water, methanol, ethanol and acetone. The fill ratio was varied from 20% to 95% and heat load was varied from 5 W to 100 W. The condenser was air cooled with air velocity of 1.5 m/s. The evaporator and the adiabatic section was enclosed in a double wall container for thermal insulation. The authors have made a systematic comparison of the thermal and physical properties of the various fluids included in the study. The authors have concluded that most of the properties do not vary appreciably with temperature and even when there is a variation the relative values from fluid to another fluid remain the same (i.e., the larger ones tended to be larger). The authors have indicated that of all properties that are perceived to be relevant for an efficient PHP working water possesses the best values except for the $(dP/dT)_{sat}$ and surface tension. The authors have brought out the difficulty in repeatability of the tests for lower fill ratios (< 35%) and lower heat loads < 35 W) and they attribute this to the variation of the distribution of the void fraction in lower fills and loads. For higher fill ratios between 60 to 90% the repeatability could be achieved. At each filling ratio, the PHP was first tested from low to high heat input step by step; the second test run started after it was cooled to the room temperature. The PHP with acetone started up at the lowest power of 10 W and ethanol was the fluid which required the largest power of 35 W for start-up. The authors state that the dynamic viscosity was the most influencing parameter for the start-up of PHP as the dynamic viscosity of liquid acetone was the lowest whereas that of ethanol was the highest. The authors have stated that the higher liquid dynamic viscosity is the largest influencing parameter for the large amplitude and low frequency temperature oscillations associated with water and ethanol as compared to acetone and methanol. The difference of the temperature oscillations between fluids reduced as the heat load was increased due to reduction in dynamic viscosity as well as increase in inertial force. They also stated that the lower latent heat fluid tended to have dry out at lower heat loads. It was also stated that water out performed most of the fluids due to its high C_p

and h_{fg} at higher heat loads with moderate fill ratios. Thus at higher heat loads larger h_{fg} was also favourable for the PHP working. At higher fill ratios methanol performed the best even for higher loads due to larger $(dP/dT)_{sat}$ and lower dynamic viscosity. According to the study the best fill ratios occurred between 62-70% with R_{th} being the lowest for all the fluids under consideration. The authors conclude that at higher heat loads the fluid choice becomes less relevant as the R_{th} becomes nearly the same if the dry-out does not occur. The authors also state that after certain threshold heat load the PHP R_{th} is governed by the limiting of the cooling at the condenser apart from the material and structure of the PHP. The authors have made a thorough study of the various properties and their effects on the PHP working at various fill ratios. The authors have also stated that the sampling of the temperature data was done at 1.5 s interval which might be missing out on the pulsation frequency investigation as the literature [38] predicts the frequency of pulsations in the order of 0.1 Hz to 3 Hz.

Kearney and Griffin in [42] investigated the effects of various fluids (ethanol, Novec 649 and Novec 7200), different fill ratios (30%, 50% and 70%), orientations (vertical bottom heat to horizontal through intermediate 45°) on the performance of a flat plate open loop PHP. The PHP was made of FR4 with 4 layers of 400 μm of copper. The PHP was made with channels of 1.55 mm wide and 1.9 mm deep (with hydraulic diameter of 1.7 mm) with 13 turns at the evaporator. The visualisation provision was made by having a polycarbonate cover on top with silicone sheet to prevent transport of fluid between adjacent channels. The investigation was targeted to provide an in-situ heat spreader in less conducting printed circuit board material. The tests were limited to sub-ambient pressures and the same was monitored by a pressure transducer at one end of the open loop whereas the other end of the loop was used for vacuuming and charging of the PHP. The authors have acknowledged the findings of [23] that the optimum fill ratio is lower for the channels with sharp angled corners than the equivalent hydraulic diameter circular channels. This they attributed to the fact that the corners facilitated the flow of the liquid towards evaporator even when the vapour flows towards the condenser. The tests in this study could not be pursued with Novec 7200, as the fluid was found incompatible with silicone seal. At a given fill ratio, the study indicated that T_e was lower with Novec 649 but the range of heat fluxes was limited for Novec 649 as the P_{sat} exceeded the P_{amb} for the fluid. The authors have pointed out that at higher heat fluxes the Bond number criteria based D_{crit} for Novec 649 was lower leading to rise in the T_e. The Novec 649 had the best performance at 30% fill ratio. There was very little difference in performance for ethanol between 30% and 50%. At lower heat fluxes ethanol at higher fill ratio was better performing due to the higher C_p of ethanol. Though PHPs are perceived to be gravity independent the orientation had significant effects on the performance of the PHPs – 90° (bottom heat mode) was the best performing followed by 45° and subsequently 0°. The PHPs did not operate at -90° orientation. The performance degradation for Novec 649 from 90° to 45° was not substantial indicating that the performance had a non-linear dependence on the orientation. The authors concluded that Novec 649 was the most suitable fluid for use with FR4 material due to its higher $(dP/dT)_{sat}$, with respect to compatibility, electrical isolation and heat transfer performance of all the conditions tested in the study.

The various parametric studies conducted by several research groups have been summarised in Table 2-1.

Table 2-1: Summary of investigations on various operating parameters of PHP

Ref.	Inner diameter and material	Geometric variations	Inclinations	Fluid and fill ratio	Boundary conditions	Salient Conclusions
[9]	2 mm; copper	5 turns; closed loop	BHM to horizontal	Water, ethanol and R123; 0 to 100%	5 to 65 W; Forced air cooled condenser	25 to 65% fill ratio was optimum for heat transfer; No horizontal operation possible; Bo criteria not mandatory for vertical operation and does not guarantee horizontal operation;
[19]	2 and 1 mm; copper	5 to 23 turns; Section lengths 0.1 m and 0.15 m; closed loop	BHM to horizontal	Water, ethanol and R123; 50%	Constant T_e; Liquid cooled Condenser	Gravity affects performance; Critical number of turns needed for horizontal operation; Larger internal diameter larger heat throughput;
[25]	2, 1.5 and 1 mm; copper	5, 11, 16 and 26 turns; Evaporator length 0.1 and 0.15 m	Horizontal	Distilled water, ethanol; 30, 50 and 80%	T_e 40 to 90ºC; Forced air cooled condenser	Horizontal operation better for higher T_e and higher number of turns; Lower number of turns failed to start up; Critical number of turns to start-up dependent on inner diameter; Shorter evaporator leads to better performance;
[27]	2 mm; copper	10 turns; closed loop	BHM	DI water, methanol, ethanol and acetone; 20 to 95%	5 to 100 W; Liquid cooled condenser	Lower boiling fluid leads to earlier dry out; At lower heat loads μ and $(dP/dT)_{sat}$ important and at higher heat loads larger latent heat of vaporisation was more important; At higher heat loads performance independent of fluids and constrained only by condenser capacity;
[38]	2 mm; copper and glass	2 turns; closed loop	BHM to horizontal	Ethanol and ethanol water mixture; 65%	20 to 100 W; Liquid cooled condenser	Minimum flux needed for operation; Net circulation with superimposed oscillation pattern; Heat transfer coefficient at evaporator by experiment; No difference in performance between 2 fluids; Pressure signals yield no characteristic frequency;

Ref.	Inner diameter and material	Geometric variations	Inclinations	Fluid and fill ratio	Boundary conditions	Salient Conclusions
[40]	1.1 mm; copper	31 turns; closed loop	BHM to horizontal	FC 72; 50%	10 to 100 W; Forced air cooled condenser	At normal heat loads the BHM performed better. However, at higher heat loads the horizontal operation was better performing; Effect of gravity pronounce only for near horizontal inclinations; Gravity is a source of instability during start-up for vertical orientation, horizontal operation showed repeatable start-ups;
[41]	1.1 mm; copper	16 turns; closed loop	BHM-Horizontal-BHM	FC 72; 50%	10 to 100 W; Forced air cooled condenser	Ground tests – vertical to horizontal shit takes more time to attain steady state whereas horizontal to vertical takes less time for steady state; Horizontal orientation of the PHP in the flight the variation of the performance with respect to the varying gravitational field was not pronounced; Vertical position was more dependent on the heating history (heating up or heating down) than the horizontal position; 2-D PHP in horizontal position - the horizontal operation on ground is the most similar to the microgravity operation in flight.
[42]	1.7 mm; FR 4	13 turns; open loop	BHM to horizontal to THM	Novec 649, Novec 7200, Ethanol; 30, 50 and 70%	0.4 to 2.5 W/cm²; Liquid cooled Condenser	Fluid with higher $(dP/dT)_{sat}$ more suitable at lower heat fluxes; Dielectric fluids useful for integration into electronics; Performance highly dependent on fill ratio, orientation and fluid;

2.3 Start-up characteristics

Tong et al. in [43] carried out a thorough visualisation study of the flow patterns in the various sections of the PHP. They carried out their study with pyrex glass tube (inner diameter 1.8 mm) 7-turn PHP of 160 mm x 160 mm dimension. The PHP was filled with methanol at a fill ratio of 60% and evaluated the flow at vertical and horizontal inclinations at 50 W. The authors concluded that the start-up period is characterised by large amplitude oscillations of the liquid slugs and vapour plugs followed by the unidirectional circulation of the slugs superimposed with oscillations after the start-up. The circulation direction can be arbitrary for the same set of test conditions. That is the circulation can be clockwise or counter clockwise for the same inclination, fill ratio and heat input. The authors attributed the random direction of circulation to the void fraction (slug-plug locations) distribution at the start of the experimental run. The authors stated that the PHP required a minimum heat input of 30 W for start-up. The study indicated that the circulation resulted in higher heat transfer and the amplitudes of the oscillations became reduced. The authors stated that the boiling at each bend of the evaporator was different due to the varying temperatures as the slugs and plugs keep changing their locations. The authors have described the flow pattern in the evaporator as nucleation boiling when the bulk fluid is saturated or sub-cooled, vapour expansion and forced convection boiling when liquid enters the evaporator. The nucleation results in large number of small bubbles and they coalesce to form larger bubbles. The smaller bubbles form Taylor bubbles and these when they expand breaks a long slug into shorter slugs. The study showed that the slugs are formed due to the propagation of inertia waves. As the amplitude of the wave becomes larger than the diameter of the tube, it results in formation of a slug. The authors reasoned these occurrences for the changing number of slugs and plugs. In the condenser the flow becomes slug flow as the short slugs are penetrated by fast moving plugs to result in larger plugs and slugs. At the evaporator bends which form the lowest portion of the PHP the liquid started to collect as the slugs left behind them the liquid film which over time formed a slug and was carried away by the flow. The authors concluded that the velocity of the flow increased with heat input and the entire process of PHP was summarised as combination of nucleate boiling, coalescence of bubbles, propagation of waves and forced convection boiling and condensation.

Xu and Zhang [44] have investigated a three turn 2 mm internal diameter CLPHP of copper with FC 72 as working fluid. The evaporator length was 50 mm and the overall length was 180 mm. The distance between adjacent channels was 25 mm. The portion other than the evaporator was allowed to act as condenser with natural convection cooling. The fill ratio used in the study was 70%. The authors reported two types of start-ups. One type being the temperature overshoot start-up which is characteristic of low heating power, where the evaporator temperatures raise higher than the quasi-steady operating temperature before falling suddenly to stabilise at a quasi-steady value. The other type of start-up is the smooth type where the evaporator temperatures steadily raise and reach a maximum value of the quasi-steady state operation, which is characteristic of higher heat loads. The authors have provided an explanation for the different type of start-ups as well as for the fluctuations of the wall temperatures monitored on the PHP. The FFT of the temperature fluctuations for a low heating power and the higher heating power was plotted and the authors have concluded that at least in the higher heating power the fluid in the capillary tube is oscillating with a characteristic frequency. The oscillating flow can be considered as quasi periodic, inferring that the vapour plug and liquid slug are quasi uniformly distributed in the capillary tube at the high heating power. In other words, higher heating power makes the distribution of the vapour plug and the liquid slug more uniform.

In [45] the condition for start-up of a PHP was studied both qualitatively and quantitatively. The quantitative investigation was made from 27 copper PHPs with internal diameters 0.66, 1.06 and 2.03 mm, 3 different section lengths of 50, 100 and 150 mm and 3 different number of turns (5, 10 and 15). For the visualisation study pyrex glass PHPs with length scale installed adjacent to the PHP, of inner diameters of 1.5 and 2 mm were used with section length of 50 mm. In all cases each section length was same for a given PHP and the fluid used was R123. The authors have explained the concept of operating pressure in PHP. The operating pressure is the pressure of the liquid slugs and it has a value which lies between the saturation pressure corresponding to temperatures of evaporator and condenser. The vapour has a higher pressure at evaporator and lower pressure at the condenser but the liquid phase will have a single pressure which is the operating pressure throughout the PHP. The authors also detail the mechanism by which the evaporator section is continuously replenished by the liquid from the condenser. The authors have explained the phenomenon of circulation in a preferred direction and also have explained the alternate direction switching of the circulation due to varying condensation rate in the adjacent limbs near the condenser. The study concludes that the circulation starts to happen when the net collapse in the vapour plug volume across the PHP is larger than the net expansion. When the reverse occurs the vapour cannot move from evaporator to the condenser thus a dry out can occur. A method was developed to predict the minimum temperature required at the condenser for successful start-up with the initial temperature, fluid, fill ratio and T_e as the input variables. The authors have also stated that the temperature difference needed for successful start-up was slightly under predicted and the ones for the failed start-up was over predicted by the model when compared with the experimental values. However, the number of data points which were not adhering to the prediction of the model was very less (only six) within 16%. The model also indicated that once the inner diameter satisfies the slug-plug formation criteria and with L_e being equal to L_c the PHP geometry does not have any effect on the temperature difference required between evaporator and condenser. It was concluded that a suitable start-up condition is not only governed by the superheat level at the evaporator section but also by the control of temperature difference between the evaporator and condenser section. In addition, the model indicated that the filling ratio also has an effect on the temperature difference for a suitable start-up condition. In the case of a fixed evaporator temperature and a small fill ratio, a large temperature difference is needed in order to have a successful start-up and the opposite is true for a large fill ratio.

Hua et al. [46] have investigated the CLPHPs with larger inner diameter. In this study the PHPs of 4 mm inner hydraulic diameter with rectangular cross section were tested for various fill ratios (30% to 70% in steps of 10%) of deionized water. The lengths of the evaporator and condenser sections were maintained the same (80 mm) and the adiabatic section length was 90 mm. The study included only one orientation – vertical position with evaporator down. The heat load was varied from 80 W to 360 W in steps of 40 W. It was concluded that the start-up of the PHP was sudden with evaporator temperature overshoot in case of lower heat loads whereas the start-up was smooth for larger heat loads (as shown in Figure 2-7). The start-up heat load needed for various fill ratios for the rectangular channel PHP was larger than the ones needed for the circular channels of comparable size in the existing literature. This was attributed to the larger cross-section of the rectangular channels thus larger fluid inventory when compared with circular ones. The best fill ratio was recorded as 30% which was lesser than the best filling ratio of 40% for circular channels. This was attributed to the corners providing greater capillary force in rectangular channels to form liquid films thus the transfer of heat between the channel walls and the liquid film was more efficient. Also the R_{th} was found to reduce with heat loads in case of both circular and rectangular channels.

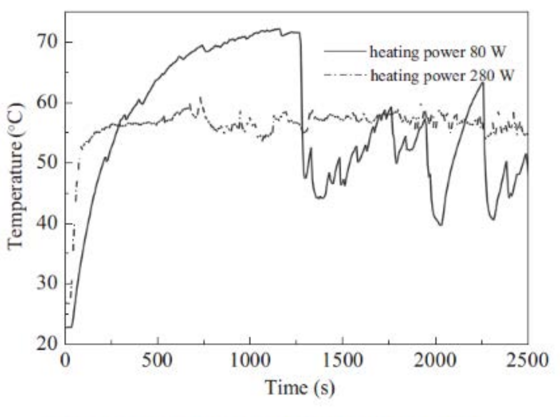

Fig. 2. Start-up process under different heating power.

Figure 2-7: Types of start-ups in PHPs [46]

2.4 Form factor variations

2.4.1 Single loop

The paper [47] involves a study of single loop of PHP to have better investigation of the PHP of multiple loops. The study was conducted using a single two-phase loop of PHP with ethanol at 60% fill ratio. The study recorded various types of flow patterns – like oscillations in 2 limbs, direction reversals followed by frequent direction reversals and finally a predominant single direction circulation as the heat loads were increased. The study suggests that the flow pattern is dependent on the filling ratio (FR) and the heat power input. The authors conclude that an ideal thermodynamic cycle is almost impossible for the single loop device due to metastable states occurring at the exits of evaporator and condenser. The authors have stated that the pressure distribution across the slugs and plugs in the vertical and horizontal orientations are different thus explaining the relatively easier operation in the vertical bottom heat mode than the horizontal mode with lesser number of turns. The authors explain the lower share of the latent heat transfer in the PHPs in wake of the overall mass quality being very low in the operational fill ratios of the PHP. The study concludes that the circulation with annular flow in up-header and slug/semi-annular flow in the down-comer results in the best thermal performance of the single loop PHP with respect to the R_{th}.

The authors in [39] have carried out a long duration study of a single closed-loop PHP. The authors have monitored the temperatures at the 4 bends and the pressure at the evaporator end. The tests were conducted only for 20 W and vertical bottom heating mode of operation. The authors have recorded 4 operating regimes (3 steady state and 1 transition state) of the same PHP over time (Figure 2-8) and attribute the start-up characteristics to the distribution of the void fraction within the PHP volume at the time of initiation of the heat load. The internal diameter used was 2.0 mm with ethanol as working fluid at 60% fill ratio. The study reveals that the best operation from heat transfer perspective occurs for the net circulation flow operation followed by the circulation with intermittent reversals. The oscillation frequency was theoretically estimated to be between 0.15 to 3.5 Hz and accordingly based on the length of the PHP the velocity scales were estimated to be in the order of 20 to 600 mm/s. The tests revealed the oscillation frequency to be between 0.1 to 3.0 Hz for various operating regimes PHP.

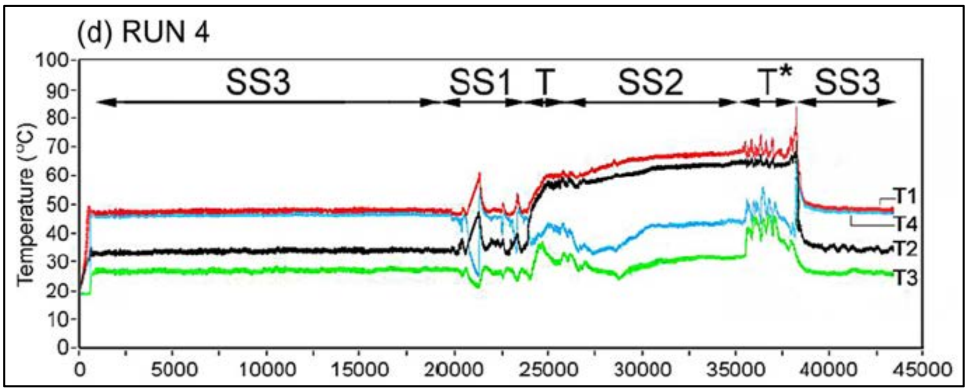

Figure 2-8: Results of multiple states of operation of a single loop PHP [39]

Saha et al. in [48] have investigated a single loop PHP made of quartz glass of internal diameter 4 mm and external diameter 6 mm. The authors performed both visualisation as well as quantitative study. The thermocouples were sampled at 1 Hz and the video recording was at 500 to 1000 frames per second. The experiments were performed with distilled water with fill ratios of 30%, 40%, 50% and 60% for inclinations angles of 0°, 10°, 30°, 50°, 70° and 90° from the horizontal for varying heat loads. The study was carried out with 4 mm internal diameter which is less than the diameter prescribed by Bond number criteria for PHP but this size of diameter is larger than what many researchers have attempted. The authors have reported that the initial slug-plug formation was highly unstable and stratification was observed with very small disturbance. However, the oscillation of slug and plug was possible at least up to the near horizontal orientation. At 90° vertical bottom heat orientation for 60% fill ratio, the flow was oscillatory with pulsations changing direction without circulation at low heat loads and oscillating circulatory flow was observed at higher heat loads with occasional change in direction. However, complete circulatory flow was not observed in any of the experiments. For 10° inclination at lower heat loads only conduction was the mode of heat transfer and no pulsations were observed. At lower fill ratios (40%) for 90° inclination the oscillatory flow was observed at moderate heat loads. The temperatures of up header and down comer was found to be fixed at higher heat loads indicating the pure circulation. The authors indicate that the circulation was always in one direction due to the fact the no PHP construction or heating can be perfectly symmetric. Thus the circulation has a preferred direction. The flow pattern changed to slug flow from annular flow at lower heat loads for lower fill ratios. The authors also plotted the probability distribution function for the adiabatic temperature which showed two peaks indicating the oscillatory flow and single peak indicating the circulatory flow. For a given heat load the flow is circulatory for higher inclinations and tend become oscillatory at lower inclinations. The authors have also carried out experiments with the evaporator thoroughly insulated to estimate the R_{th} of the configuration accurately. The study concluded that the start-up power or threshold heat flux to initiate the motion increases with the decrease in inclination angle also threshold heat flux to initiate the oscillation increases with the increase in fill ratio. The study indicates that for a lower fill ratio (30%), the resistance reduces as the loop orientation is changed from near horizontal towards vertical. This reduction continues up to an inclination angle of 70°. Thereafter, the thermal resistance remains almost constant or increases marginally. This trend continues up to a filling ratio of 50%. For a range of inclination angle from 90° to 10°, the optimum fill ratio varies from 40% to 50%. There was a unique observation that the performance of PHP does not increase monotonically with the inclination angle and may not be the highest at the vertical heating mode strongly support some of the earlier works [19] and [49]. The authors attribute this better than vertical orientation performance to the nose shape of the bubble and the associated rise velocity of the bubble. The authors have provided a flow regime map with respect to the applied heat load and the inclination angle (including the dry out limit).

Spinato et al. [50] investigated a single loop closed PHP through synchronized thermal and visual observations. The time-strip image processing technique was utilized to obtain a 2-D space-time representation of the flow inside the PHP channels, which was further processed to extract accurate qualitative and quantitative information of the thermo-hydrodynamics of PHP. The flat plate PHP consisted of 1 mm x 1 mm channel of single loop of length 830 mm charged with R245fa at a fill ratio of 60%. The temperatures were sampled at 20 Hz. The videos were recorded at 500 frames per second. The authors concluded that the FFT of the temperature and the time strip intensity profile at the corresponding location showed good agreement. The study indicated that dominant frequencies change from 0.4 Hz for the small amplitude oscillation regime to 0.7 Hz for the circulating flow regime and to 1.2 Hz for the oscillating flow regime. For the oscillating with circulation and flow reversal regime, the frequency depends on the predominant flow pattern observed during the data acquisition time period. For the oscillating flow regime, the frequency of oscillation is seen to increase with the heat load. This is attributed to the increase in system temperature and saturation pressure, which reduces the flow resistance and makes the plugs stiffer to compression and expansion. The authors conclude that the thermal oscillations are largely dependent on the flow pattern and the heat load. The predominant flow patterns were low amplitude oscillations, oscillation with circulation, flow reversals after certain time intervals, stable circulation and high amplitude oscillations. The phenomenon known as "local flow direction switch" in which circulating flow rising through the condenser briefly slows and reverses direction, is triggered by bubble nucleation at the evaporator inlet.

The authors in [51] carried out a thermal and visual investigation to systematically assess the thermal performance of a single turn CLPHP. A flat plate PHP of 1 x 1 mm^2 channel of 830 mm length was used for the investigation. The temperature data at the evaporator and condenser was measured at 20 Hz sampling rate. The thermocouple of 0.25 mm size (type K) was used for the temperature monitoring. R245fa was used as working fluid with the filling ratio varied between 10-90% in steps of 10% and the heat loads in the range of 0 to 60 W in steps of 2 W. The inclination angle with respect to horizontal was varied between 90° and 45°. The flow regimes were monitored visually by a high speed camera. The R_{th} and the flow pattern maps were generated for a particular heat load and fill ratio for a particular orientation. Based on the fluctuation of the difference in temperatures measured at evaporator and condenser the frequency of the oscillation of the slug-plug motion was estimated. A theoretical estimation of the time averaged heat transfer coefficients of the vapour, liquid and the thin film evaporation was made based on the measured temperatures of the evaporator. The salient conclusions were that the circulating motion resulted in the lowest R_{th} compared to the slug flow oscillations and circulation with flow reversals. The authors concluded that for a given fill ratio the R_{th} reduced with increasing heat loads as the flow transcends to unidirectional circulation at higher heat loads. Fill ratios lesser than 50% yielded better performance.

Ilinca et al. in [22] have carried out investigations with a single loop PHP with 2 mm internal diameter fitted with transparent adiabatic sections. The evaporator section was provided with three different heaters that was controlled individually to achieve asymmetric heating at the evaporator thereby promoting directional circulation. The PHP was also fitted with two pressure transmitters which was used to estimate the pressure drop across the adiabatic section. Ethanol and FC-72 fluids were used at 60% fill ratio. The inner diameter was chosen in such a way that for ethanol the static confinement criteria was met rendering operation to be of PHP type while for FC-72 the inner diameter would yield loop thermosyphon operation. The temperatures were sampled at 10 Hz and the pressure signal was sampled at 100 Hz. The experiments were performed with bottom heating mode with 4 different pivot angles (vertical, 30°, 60° and 90°). Minimum start up heat load required was 3 W and the start was intermittent for 3 W. However, from 6 W the PHP operation was successful. The authors have stated that the circulation had a preferred direction of clockwise even when the evaporator heating was symmetric due to the asymmetric larger thermal inertia of right adiabatic section in comparison with the left section. When the heating was done on the right section and middle section the flow tended to go upwards in the right and down wards in left thus a counter clockwise circulation. However, at larger heat loads the direction reversal did not occur even when heating asymmetry was deployed. This was attributed to the fact that the higher heating power provided results in higher void fraction in the up header and thus the higher quantity of fluid in the down-comer. It is more difficult for the vapour expansion to contrast liquid column head and momentum. Therefore, once the circulation is established in the loop in a preferential direction for such heating power input, the inertial effect reduces the effect of the non-uniform heating provided at the evaporator. At 18 W which was the highest heat load tested the flow was semi-annular and oscillating. The circulation tendency was not observed. At 18 W the dry out occurred when the tests were performed from lower heat loads but when 18 W was dissipated from the middle section after initiation of a self-sustained circulation dry out did not occur indicating that the heating history was an important parameter for dry out or otherwise. FC-72 showed better thermal performances over ethanol since is it had a prompter start up and gave a wider heat transfer capability range. The low boiling point of this liquid ensured the heat discharge to the condenser at low temperatures. An increase in pivot angle improved the flow conditions and widened the operative range of the device for both fluids. This is due to the significant gravitational assistance and the particular geometry: the evaporator section is no longer horizontal; thus circulation is promoted also by applying power at the middle heater. When the flow was from condenser to evaporator the pressure transmitters recorded a lower value and the reverse flow had the opposite trend. The pressure signals were substantially different when the flow was slug and when the flow was annular. The annular flow had higher frequency of fluctuations and the difference in pressure from evaporator to condenser was lesser while the opposite was true for slug flow conditions. The authors concluded that at high heat inputs, the flow regimes recorded for the two fluids are very similar, stressing that, when the dynamic effects (due to larger velocities) start to play a major role in the system, the device classification between loop thermosyphon and pulsating heat pipe is not that substantial though the static confinement inner diameter for the fluids was chosen differently.

2.4.2 Flat plate

Khandekar et al. [15], studied 3 different types of setup of CLPHP in terms of fill ratio, orientation, working fluid and input heat flux. The first setup was a flat plate CLPHP which can be used as an integral spreader of heat in cooling of electronics. Here the aluminium substrate was milled with grooves and a polycarbonate sheet with O-ring seal was used as a cover. In this setup the grooves were of rectangular cross-section with 2 mm width and 2.2 mm depth. The distance between the grooves being 2.5 mm. The second setup was nearly the same but the difference being the cross-section of the grooves are 1.5 mm deep and 1 mm wide in one case and 2 mm internal diameter (circular) with the circular grooves formed partially in the aluminium substrate and partially in the polycarbonate cover in another case. In the first 2 setups the number of channels was 12. The third setup was of 10 tubes (5 turns). PHP with glass tubing of inner diameter 2 mm as the adiabatic zone whereas the evaporator and the condenser were of copper tubes with the distance between tubes being 12 mm. The glass tubes acted as viewing window just like the polycarbonate cover plate. A total of six experiments were conducted. For each set of experiments for given heat load and fill ratio the orientation of the PHP was changed until the T_e exceeded 120°C. Thus the critical tilt angle was ascertained beyond which the PHP do not work. The critical tilt angle was found to be between 5-15°. The authors state that in the vertical operation, the larger internal diameter (2 mm) PHP could have higher heat transport than the smaller ones. The R_{th} of the larger tube was also less in case of vertical operation. The rectangular cross-section PHP showed lower R_{th} than circular ones of same hydraulic diameter. In the vertical operation for rectangular cross-section the optimum fill ratio for minimum R_{th} was found to be around 30%. For fill ratios less than 25% with water the oscillations were not continuous. The PHPs showed oscillations followed by dull periods of no oscillations. The rectangular section PHP with lower fill ratios showed no liquid slugs. The liquid was transported in the corners thus the PHP acted more as capillary thermosyphon than an oscillating PHP. This phenomenon was absent in circular cross-section. For fill ratios around 10% dry-out occurred for very low heat loads of 10 W. In case of horizontal operation, the dry-out occurred at 5-15° even for very low heat loads of 10 W. However, once the tilt angle was restored to the critical angle the oscillations started. The authors concluded that the larger difference in the solid-fluid contact angle (contact angle hysteresis) between the front and the rear of a bubble leads to greater resistance for flow thus hindering the PHP performance. The fluids with lower latent heat (aiding the generation and collapse of bubbles) and higher $(dP/dT)_{sat}$ enhanced the performance of PHP thus rendering that fluid as more suitable for PHP. In this regard, the authors concluded that of the fluids used in the study ethanol was better suited as working fluid than water. The authors concluded that the transverse conduction between adjacent channels leads to temperature homogenisation leading to pressure equalising which is detrimental to PHP functioning.

The authors in [23] have carried out the investigation of use of PHPs as heat spreaders to be embedded in the electronics to be cooled. In this study two variants of the spreaders (flat plate PHPs – Figure 2-9) with hydraulic diameters 2 mm with 40 parallel channels and 1 mm with 66 parallel channels both of square cross-section have been tested. A provision for visualisation was provided by using a polycarbonate sheet as cover. The study was carried out with various fill ratios from 0 to 95% with ethanol as working fluid. The orientation was varied for vertical bottom heat mode to horizontal to vertical top heat mode (3 orientations). The authors have outlined that the hydrodynamics hence the thermal performance of the rectangular channels are different than those of circular cross-section due to the angled corners in the rectangular sections. Hence at lower fill ratios the major portion of the liquid tends to accumulate at the corners in the rectangular/triangular sections whereas the circular sections do not have such provision. The fluid inventory in the non-circular section will be more than that in the same hydraulic diameter circular section. Hence the authors have stated that the tendency to form liquid slugs is more in case of circular channels than the non-circular ones. Thus the authors have concluded that the Bond number criteria prescribed for circular tubes may not be applicable for the rectangular and triangular sections with sharp angled corners. It is stated that the flow regimes of slug and annular flows may be sustained for higher gas superficial velocities. The fours modes of operation depending on the fill ratio was observed with mode of circulation yielding the maximum heat transfer with the orientation of bottom heat mode. The performance of the three orientations were comparable at 55% fill ratio for 250 to 300 W dissipation. The larger of the two channels had higher heat transfer possibility without dry out, which the authors attribute to the larger fluid inventory and lower pressure drops associated with larger channels. For the two channel sizes and the three orientations the best performance was obtained between 50% and 70% fill ratio. The authors conclude that the optimum fill ratio was wider for the bottom heat mode and gets narrower as the inclination is changed to horizontal and then to top heat mode.

Takawale et al. [16] have compared the performance of a flat plate PHP (FPPHP) and a capillary tube PHP (CTPHP) for flow regimes and thermal performance. The authors have carried out experiments with ethanol as working fluid at 40%, 60% and 80% fill ratios for heat loads varying between 20 W and 180 W. The PHPs were built to have comparable Bond number, L_e, L_c and same number of channels (17 turns) with length of each channel being nearly 180 mm. The channel size for FPPHP was 1.2 mm x 1.2 mm. The CTPHP was made of copper tubing of inner diameter 1 mm and outer diameter 2 mm. The volume of the CTPHP was more than the FPPHP. The temperatures were sampled at 1 Hz and the pressure measurement was sampled at 20 Hz. The authors reported that the pressure indicated by the pressure transmitter was higher by 30 kPa than the saturation pressure of ethanol. This was attributed to the dissolved gases in ethanol. The R_{th} of the CTPHP was higher than FPPHP due to axial conduction limited by the presence of glass tubes in the adiabatic section. The minimum heat input required for the start-up of oscillations in FPPHP increased with increase in filling ratio. At lower heat loads the cross-over of the slugs through U-turns were not observed in evaporator or condenser as the amplitude of oscillations (5 - 10 mm) was very small compared to the 180 mm channel length. An increase in heat load caused dry out at evaporator whereas in case of CTPHP even for very low heat loads the oscillation amplitude was more than 30 mm. The annular flow was not observed and this was attributed to the smaller hydraulic diameter used in the study and slug-plug flow was the dominant regime in the entire study. The authors concluded from the velocity estimate that the motion within both PHPs were oscillatory and not circulation as the velocity plot had the centre coinciding with zero. However, the velocities of oscillations in CTPHP were order of magnitude greater than the ones in FPPHP. As the adjacent channels are thermally isolated in CTPHP unlike FPPHP, high temperature gradients are possible between channels which generate the necessary pressure gradients to exhibit large amplitude oscillations even at lower heat inputs. The pressure transmitter output as well as the T_e and T_c values showed greater oscillations in CTPHP case than FPPHP which coincided with visual observation of low amplitude oscillations of FPPHP. The mean value as well as the amplitude of the pressure oscillations increased with increase in heat input. The FFT plot of the pressure signal did not indicate any characteristic frequency though a trend of frequency of oscillation tended to increase with increase in heat load. The 3D attractors were re-constructed by calculating the time delay of the pressure data. A complex pattern in the phase plots of the attractors indicates the nature of the PHP system to be chaotic without any characteristic frequency. The fill ratio of 40% was found to be better for FPPHP whereas 60% was better performing in CTPHP. As the R_{th} without fluid fill in case of CTPHP is large the value of $R_{ratio} = R_{th}/R_{dry}$ was used in comparing the performance of the two PHPs. This indicated that the CTPHP had 48% better performance than the FPPHP for the best performing data points of the two PHPs.

Figure 2-9: Flat plate heat spreader PHP [23]

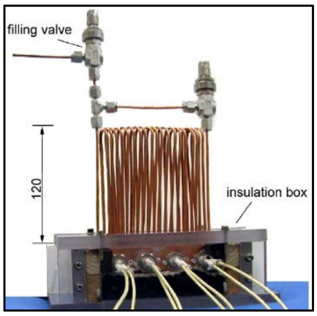

Figure 2-10: Non-planar PHP [49]

2.4.3 Multiplanar configuration

Yang et al. [24] investigated the performance and the operational limit (dry-out limit) of CLPHPs using R123 as working fluid with three fill ratios of 30, 50 and 70%. The study was carried out with two PHPs made of copper tubes of ID 2 mm and 1 mm. Both the PHPs were of 20 turns (40 copper tubes). The study was aimed to estimate the effects of inner diameter, orientation (horizontal, vertical bottom heat and top heat modes), fill ratio and input heat flux on the CLPHP performance. The evaporator consisted of a block of copper with a pocket machined to accommodate the evaporator U-turns of the copper tubes. The evaporator block was drilled with holes in the transverse direction for insertion of 4 cartridge heaters and 5 thermocouples. The evaporator length was maintained as 8 mm. The remaining part of the PHP was forced air cooled to act as condenser. The ambient air temperature was maintained as 27°C ± 1.5°C with an average air velocity of 5 m/s. Both the PHPs operated in all 3 orientations due to larger number of turns [19]. The study indicated that the smaller inner diameter PHP showed little degradation in performance with orientation with respect to gravity while the larger 2 mm inner diameter PHP performance deteriorated in the horizontal mode and more so in the vertical top heat mode. The gravity independent operation of the smaller inner diameter PHP was attributed to the dominance of the surface tension forces in comparison to the gravity forces. The dry out flux or the operational limit of the 2 mm PHP reduced with the gravity adverse mode. However, the R_{th} values of 1 mm PHP was inferior to the R_{th} of 2 mm PHP indicating that the larger tubing had greater heat transfer. The dry-out heat flux of 1 mm PHP was much higher than the 2 mm PHP. The study indicated that for both the inner diameters the best performing fill ratio was 50%. The performance of the PHP with respect to the input heat was almost linear with respect to heat flux till dry–out occurred.

The authors in [52] have investigated a CLPHP with an aim of developing a compact cooler based on PHP with orientation independent performance. The investigated PHP was of closed loop type as the authors observed in their preliminary tests that CLPHP required lesser heat loads to start-up when compared to the OLPHP. The PHP was constructed as 'Kenzan' fin type with copper tube of OD 2 mm and ID 1 mm with a length of 5.6 m. The PHP was made to make 17 turns in the evaporator region which was made out of 0.5 mm thick copper plate brazed to the PHP. The condenser region was made of radiator type fins with a surface area of 1670 cm^2 which was cooled by an axial fan capable of delivering 31.8 CFM air at 1800 RPM. The investigation was carried out for various fluids compatible with copper of distinct types – water, methanol and R141b. The PHP was tested for three orientations of bottom heat mode, horizontal or side heat mode and the top heat mode. The PHP was tested for two types of heat loads – heat applied on the entire evaporator region of 40 mm x 35 mm as well as a concentrated heat load applied over just 1 cm^2 of the evaporator plate. The tests showed that the temperature oscillations were of low frequency and large amplitude for water and vice versa for methanol and R141b. The authors attributed this behaviour of water and R141b to the fact that the saturation pressures of the two fluids were distinctly different in the temperature range of operation. However, the pulsations of temperature were almost the same at higher heat loads. The entire test setup was not allowed to exceed a maximum temperature of 100°C. Though the characteristics of pulsations and the properties of methanol and water were different both fluids yielded nearly a maximum heat load of 250 W for T_e of 100°C. However, for R141b the maximum heat load was 190 W. The authors have documented the fact that with water as the working fluid a sound was observed unlike with the other 2 fluids. This sound was perceptible from 75 W and continued to intensify with increase in heat loads. With concentrated heat load the maximum achievable load was 125 W for methanol and only 100 W for water and R141b. The PHP did not start in the top heat mode for the concentrated heat load case. The authors have concluded methanol to be the most suitable of the 3 fluids over wide heat loads in both uniform and concentrated loading conditions.

Thompson et al. in [53] investigated a novel 3D flat plate PHP with 2 layers of channels in pursuit of handling greater heat fluxes. The study was carried out with water and acetone at two different condenser cooling temperatures of 20°C and 60°C. The tests were carried out at horizontal and vertical bottom heated positions. The heat fluxes of 2 different types – one with larger area (lower flux) and another with smaller area (larger flux) was applied at various heat loads. The temperatures were sampled at 100 Hz. The channel size was 1.7 mm deep and 1.175 mm wide with 8 channels in each plane. A fill ratio of 80% was used in all experimental runs. The lowest thermal resistance was achieved with a cooling temperature of 60°C, using the larger heating area, during bottom heating with water as the working fluid. The localized heating was found to increase thermal resistance when compared to the larger heating area. This is partially attributed to the fact that when the heating area decreases, the liquid volume in the evaporator (beneath the heat load) decreases, and the higher heat flux level then directly increases thermal spreading and evaporative resistances. In the bottom heating mode, it was found that water generally provided for a lower thermal resistance than acetone regardless of heat flux. The smaller heating area results in R_{th} that is more orientation-dependent. The increase in R_{th} associated with reduction in heating area for the acetone was far more pronounced in the horizontal position than when in the vertical position. When tested with the larger heating area, acetone provided for a less orientation-sensitive R_{th}, but the opposite trend was observed during localized heating, in which water provided for less orientation sensitivity. The larger heating area resulted in similar oscillations of T_e and T_c and this was observed for both the vertical and horizontal orientations. The T_c oscillations had the same, but mirrored, spike-pattern as compared to T_e – with temperature rises in the evaporator being accompanied with simultaneous, similar-magnitude temperature troughs in the condenser. It was also observed that the temperature oscillations for water had larger peak-to-peak amplitudes than acetone. With the reduction in heating width and gravity-participation, the T_e oscillation amplitude increased. T_e oscillations as high as 30°C amplitude was observed with localized heating with water as fluid in horizontal mode. This was attributed to thermophysical and rheological properties of water such as the latent heat of vaporization, specific heat capacity, viscosity, and density. The authors have pointed out that this factor should be considered while mounting sensitive heat sources on heat sinks designed with PHP containing water. It was also found that increasing the cooling temperature decreased the average, peak to peak amplitudes T_e.

2.4.4 Flexible form factor

Qu et al. [54] have investigated the possibility of using a PHP in flexible mode with different configurations. The authors have used grooved copper tubes of approximate internal diameter 2 mm and external diameter 4 mm for the evaporator and condenser zones while the adiabatic portion was constructed out of the fluoro-rubber tubes of internal diameter 4 mm. The experiments were carried out for 4 different configurations – ‘I shaped’, ‘stair-step shaped’, ‘inverted U-shaped’ and ‘N-shaped’. The construction had 7 turns in each configuration. The L_e was 80 mm, L_c was 120 mm and L_a was maintained as 870 mm. The working fluid was deionized water with fill ratios – 50%, 60% and 70%. For every fill ratio the I-shaped configuration performed better as it resembles the regular PHP configuration. The N-shaped configuration performed the poorest even lower than the inverted U-shaped configuration as the resistance to flow due to bends was the maximum in the N-shaped configuration. The authors have also concluded that for all configurations the lower fill ratios yielded smaller start-up heat loads whereas the lower fill ratios also resulted in earlier dry outs (at lower heat loads) especially in the N and inverted U-shaped configurations.

2.5 Numerical modelling

In [11], Shafii et al. developed a numerical model to study the behaviour of both closed loop and open loop PHPs using an explicit finite difference scheme. The effects of diameter, charge ratio and T_e was studied. However, the effect of bends was not considered in the study. The heat transfer coefficient at evaporator and condenser were taken to be constants. The mass, momentum and energy equations for the slug and plug were discretized. The vapour plug pressure was calculated using the ideal gas assumption and when the vapour pressure was estimated to be lower than saturation pressure then the plug was treated as superheated and the ideal gas equation was used. If the pressure estimated was higher than the saturation pressure, then the vapour plug pressure was set equal to the saturation pressure. The flow was considered as thermally developing Hagen-Poiseuille flow. A method was suggested for determination of the position of each vapour plug by the respective end of the plug exclusively for the closed loop and the open loop configuration. The grid independence and the time step size independence was checked and a time step size of 5×10^{-6} s was chosen with non-uniform spatial grid. The method was verified by propagating a pressure impulse that was applied at one end of the PHP and the evolution of the pulse was compared with the previous work of Wong et al. [31] where an open loop PHP was modelled as a mass-spring-damper system. The number of vapour plugs was allowed evolve over time and the authors concluded that irrespective of the number plugs in the initial condition the number of plugs eventually turn out to be equal to the number of heating sections (in this case three). For an open loop PHP, the pressure, temperature and the end position of the plug indicated an oscillating pattern. The temperature and pressure of the second plug was oscillating but with

180° phase difference from that of the first plug. The two ends of the second plug was moved in the opposite direction i.e., the size of the plug elongates or shrinks. However, the third plug corresponded with the first one as the PHP considered was symmetric with three heating zones and thus three plugs. The heat transferred in and out of the vapour and the liquid slugs also show a periodic behaviour with almost 95% of heat transfer being the sensible portion and very less being latent. For an inner diameter of 3 mm it was observed that the frequency of oscillation was higher than that of the small diameter tube of 1.5 mm. It was concluded that the average temperature of the first vapour plug in both PHPs were the same as the plug entered the heating section. Due to the larger area of heat transfer, the heat exchange was much larger in case of larger diameter PHP and in this case the sensible heat transfer contributed to 97% of heat exchanged. The authors concluded that when the heating wall temperature was decreased from 120°C to 90°C the amplitude of oscillation of pressure, temperature and the displacement of the plug increased but the frequency of oscillation decreased. It was concluded that a 25% reduction in the temperature difference between heating and cooling wall sections resulted in almost 90% reduction in total heat transferred. The heat transfer reduced with increased fill ratio and was estimated to be zero at fill ratio of 89.4%. The numerical model predicted periodic behaviour in closed loop PHP as well. The numerical procedure predicted the performance of both closed and open loop PHP to be same whereas in literature it has been indicated that the closed loop performs better than open loop.

Zhang and Faghri in [55] attempted a theoretical model of an open ended PHP with improvements of considering the thin film heat transfer and accounting of surface tension. The previous models considered an assumed constant heat transfer coefficient. The model considered was sealed at one end and open at the other end. The study took into consideration the heat transfers in the film region surrounding the vapour plug as well as at the meniscus at both the evaporator as well as the condenser regions. The model was formulated by including the effect of surface tension in the momentum equation. An explicit finite difference scheme was used to solve the equations of the vapour and liquid slug. The model showed that the oscillations became steady after 0.5 seconds though the mean temperature of the slug became steady only after 5 seconds. The model also reiterated the fact that the majority of the heat transfer was sensible. However, the evaporation and condensation was responsible for the oscillatory motion leading to the heat transfer. The authors concluded that the effect of surface tension did not alter the pressure distribution but increase of surface tension enhanced the overall heat transfer rate. The change in the location of the liquid slug resulted in the oscillation frequency being the same but with a phase difference. The study also indicated that the decrease in diameter of the tube results in decrease of the heat transfer rate as the cross-sectional area as well as the heat transfer surface area gets diminished with reducing diameter. The decrease in diameter results in amplitude of the pressure oscillations being reduced and those of the temperature being increased. The authors have stated that the T_e when increased results in the increase of the amplitude of oscillations of the temperature of the vapour plug. The study also indicated that the length of the evaporator when increased results in larger amplitude of oscillation of the vapour temperature. The authors state that the heat transfer rates in the evaporator and the condenser (especially the sensible portion) showed good energy balance indicating that the PHP operated in the nearly steady state.

Zhang with his co-authors [32] investigated numerically liquid-vapour pulsating flow in a U-shaped miniature tube towards modelling of a PHP. The evaporator at the two ends of the U-tube and the condenser at the U-turn. The mass, momentum and energy equations were non-dimensionalised and the equations were solved using an implicit scheme. The non-dimensional parameters were – inherent angular frequency, temperature difference, heat transfer coefficients at condenser and evaporator, pressure of the PHP. The numerical scheme was compared with [11] and the method showed very good agreement. The model predicted that the temperature and pressure of the vapour plugs at the two ends oscillated with same frequency but a phase difference of 180 degrees. The mass of the vapour plugs also varied in the same frequency as pressure and temperature but in saw tooth manner. The value of gravity did not alter the frequency of oscillation but the amplitude was increased for the displacement, temperature and pressure. The non-dimensional pressure increased the frequency of oscillation when doubled. The increase in the non-dimensional temperature difference increased the amplitude of oscillation. The amplitude of oscillation slightly increased with increase in heat transfer coefficient. The results also showed that the initial displacement of the slug had no effect on the amplitude and frequency of oscillation. A correlation was also made for the amplitude oscillation and angular frequency in terms of non-dimensional heat transfer coefficient and temperature difference with very good accuracy.

Shafii et al. [12] carried out an improved modelling of [11] with enhancements of considering the thin film heat transfer (evaporation and condensation) and the associated meniscus apart from inclusion of surface tension as in Zhang and Faghri [55]. The heat transfer at evaporator and condenser was computed for various flow regimes (laminar, transition and turbulent) rather than the previous consideration of an assumed constant heat transfer coefficient. As in [11] the number of plugs were considered to be equal to the number of evaporator zones (precisely 3). Only the top heat mode was investigated with the pressure loss in bends considered to be negligible due to the lesser number of bends. The model showed that the pressure and temperature of the first and the last plug were same in magnitude but had a phase difference of 180 degrees. The model also established the fact that almost 95% of the heat transfer is sensible. The effect of surface tension did not alter the frequency of oscillation of the vapour plug but showed marginal increase in the amplitude of the oscillations. The model also showed that the evaporative heat transfer was higher for the higher surface tension as the liquid film thickness decreases. The velocity of the liquid slugs is also higher for higher surface tension leading to larger sensible heat transfer. The simulation predicted the oscillation frequency to decrease as the T_e was reduced. Thus the overall heat transfer decreased by 30.54% when difference in temperature between heating and cooling sections was reduced by 16.6%. The increase in diameter showed larger amplitudes of oscillation of the vapour plugs as well as their temperatures leading to higher heat transfer rates. The model showed that the heat transfer ceased to occur as the fill ratio was increased to 89.4%. The model was also used for closed loop PHPs with number of vapour plugs being 2 with the first and the last plug combined into one. The oscillations of the two plugs were having 180° phase difference. The authors have concluded in the summary that the values of heat transfer of the closed loop PHPs are lower than that of the open looped ones.

Holley and Faghri, in [14] have carried out by far the most exhaustive simulation work on the prediction of performance of PHP. The model accounted for the variation of diameter in the axial direction which resulted in bubble pumping effect. This effect enhanced the heat transfer rate. The model as well accounted for wick structure on the inner side of the evaporator and the condenser. The wick structure was introduced as it reduces the superheat temperature required for boiling and condensation. However, the model neglected the effect of turns which in actual practice affects the hydrodynamics of the PHP. The energy equation was solved for the wall, wick, liquid slugs and vapour plugs. The effect of evaporation, boiling and condensation apart from the sensible heat transfer due to slug movement was modelled. A very large set of variables like difference in diameters of the alternate tubes, fill ratios, surface roughness pertaining to the wick structure, inclination angle of the PHP with respect to gravity have been simulated. A single closed loop as well as multiturn PHP were simulated. The model also considered the actual phenomenon of liquid slugs merging and the new vapour plugs forming during the operation of PHP. This was a great addition towards realistic modelling of the PHP working. The model indicated all the possible operations like circulation (indicated by net liquid momentum), circulation with oscillation, oscillation (zero liquid momentum), flow direction reversals and complete seizure of the PHP working. The model captured the difference between the fluid temperature and the wall temperature with the difference being larger in condenser than at the evaporator. The circulatory flow indicated the larger share of liquid in the down comer relative to the up header which was consistent with the experimental works reported [47]. The model also predicted an optimum range for the axial variation of the diameters for the least T_e for a given heat load. The increase in difference between diameters after a certain threshold proved to be counter-productive. The T_e was found to be minimum for circulatory flows as indicated by the several experimental works. When the model was applied to the top heat mode of six parallel channel PHP the circulation occurred with superimposed oscillations. The model predicted that as the flow path geometry is more asymmetric with reduced diameter circulatory flow becomes more prominent. The model predicted the T_e of the top heat mode to be higher and less oscillatory compared with bottom heat mode indicating the larger oscillation amplitude and thus an enhanced heat transfer in the bottom heat mode. For variable diameter and lower fill ratios of around 40% the PHP model showed lesser sensitivity to gravity. The variable diameter showed wider range of heat loads and lower T_e for the top heat mode. The variation of Nusselt number for slug flow showed negligible effect on the heat transfer rate of the PHP as the heat transfer rate of condensation-evaporation was very much higher than the single phase flow heat transfer. The model very closely predicted the experimental results of [56], [57] and [58].

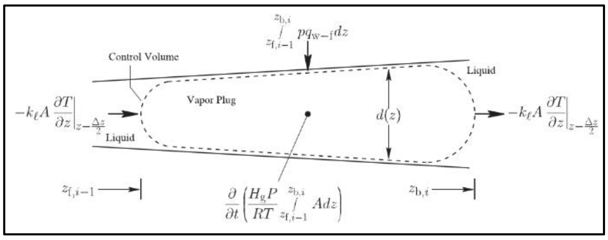

Figure 2-11: Force and energy balance for vapour plug [14]

Khandekar and Groll in [29] have elaborated on the various modelling strategies towards performance prediction of the PHPs. They have narrowed down to the semi-empirical modelling using non-dimensional groups as the most promising strategy. The authors have stated that any modelling towards PHP should address the issue of estimation of two-phase flow velocity or the mass flux as it is the direct consequence of the applied geometric and thermal boundary conditions. The authors have clearly brought out the differences in the operation of conventional heat pipes (including looped heat pipes) and the PHPs like the primary mode of heat transfer in the conventional heat pipes is latent whereas in the PHPs it is the sensible heat transfer. The capillary forces play an important role in the conventional heat pipes than in the PHPs. The authors have highlighted the importance of the two-phase flow instabilities present in the working of the PHPs. The modelling strategy for a single closed loop PHP was provided. It is stated that the single loop PHP works primarily due to the different gravity forces experienced in the two limbs and the multiturn PHP the working is more due to the bubble generation and collapsing leading to pressure difference at various locations. The authors provide the general governing equation (momentum and energy) of the single loop PHP with force balance of the gravity, two-phase friction and acceleration terms. It is also advocated that the additional constraint of void fraction of the entire PHP integrated over space to be constant as the system is closed loop. The study also highlights the change of the fill ratio from the temperature of charging to the temperature of operation. The numerical procedure was an iterative one starting from a guessed mass fraction, mass flux and operating temperature for a given geometric and thermal boundary condition. With the numerical simulation the operating design curve for various heat loads (mass flux vs operating temperature) and two fluids – water and ethanol were plotted. With the use of evaporation and condensation heat transfer coefficients based on the mass flux obtained the R_{th} of the PHP was estimated. The authors conclude that though the numerical procedure predicts the trends of the experiments so far conducted the model has the limitations like – use of simplified homogenous two-phase flow, neglect of pressure loss due to bends, neglect of driving forces like generation and collapse of bubbles.

Arabnejad et al. in [59] have simulated the working of a U-shaped (single turn) PHP with the effects of the boiling and condensation heat transfer. This study was an enhancement of detail by the inclusion of the boiling/condensation heat transfer rate along with the sensible heat transfer rate as in flow boiling the heat transfer rate is a combination of the nucleate boiling and the forced convection. The authors have considered the laminar and the turbulent flow regimes for the computation of the forced convection heat transfer rate. The model consisted of two vapour plugs and one liquid slug with top heat mode being considered. The temperature and pressure of the two vapour plugs oscillated with a phase difference of 180 degrees as the liquid slug oscillates pushing or pulling the two plugs alternately into the condenser U-turn. The authors have reported that the amplitude as well as the frequency of the oscillation of the pressure and temperature increased with increase in T_e. This resulted in enhanced heat transfer rate. As the speed of the oscillations increased the flow regime transformed to turbulent resulting in increased heat transfer. This phenomenon has been captured with concave/convex regions in the heat transfer rate curve corresponding to the decreased and increased heat transfer. In case of T_e < 100°C the sensible heat transfer dominated the latent component but after 100°C the boiling manifested as the main component of heat transfer rate. The authors have compared the model with the experimental data of [9] and demonstrated very good agreement. However, the model of [11] did not show correlation with the present study as the model of [11] was devoid of boiling (only evaporation considered) thus reinforcing the fact that the boiling and condensation heat transfer coefficients are to be accurately included in the model for realistic performance prediction.

Nikolayev [60] carried out enhancements in [11] by way of introduction of film evaporation and condensation and could accommodate PHP of varying number of turns. The model presented had the ability to account for the varying number of slugs and plugs by including the drying and deposition of the films. The model also accounted for the velocity of the slug ends relative to their centre of mass by estimating the change in volume of the slug. The code was object oriented and each slug and plug as well as the liquid film are treated as objects. Apart from these additional details of modelling the study also involved the development of the data post processing software – PHP viewer. The model predicted different regimes of the PHP working – intermittent oscillations, chaotic oscillations, periodic oscillations and bubble recondensation (two bubbles joining to form larger bubble). The author concluded that the oscillation type has a strong dependency on the liquid film thickness chosen. Lower film thickness enhances the oscillations just as the larger temperature difference leads to more oscillations. The model also indicated the chaotic variation of the heat transfer rate. The model predicted the sensible heat transfer rate in the condenser to be greater than that in the evaporator due to more liquid being present in the condenser. The model indicated that the vapour is heated well above the saturation temperature and sometimes is above the T_e as well due to the compression of the vapour. This is in contrast with the assumption that the vapour will be at saturation temperature as in [55] and [14]. The author also concluded that the model should also take into account the pressure drop in bends, viscous dissipation in the liquid films and the pressure drop across meniscus, variation of thickness of the liquid film throughout the analysis based on the slug velocity and rate of phase change.

Mameli et al. in [33] have attempted improvements in [14] with respect to both heat transfer and hydrodynamics. This work does not take into consideration the wick structure on the inner wall of the PHP tube. The authors have added the effect of local pressure loss due to turns in PHP which was assumed to be negligible in all previous numerical simulation works. However, the bends play a role as mentioned in [25] to make the PHP effective in near horizontal condition. The model accounted for the nucleation of new bubbles by stating that a new vapour plug is formed when the temperature at a location within the slug exceeds the temperature of the adjacent plugs or if the saturation pressure of the slug exceeds the pressure of the adjacent plugs. The study has monitored T_e which can be experimentally measured and the total liquid phase momentum which is very useful to characterise the flow as oscillatory, circulating, flow reversals, decay of oscillations, etc. The numerical study also included correlations for prediction of heat transfer while using various working fluids as well as various flow (like developing, laminar, transient and turbulent) types. The authors have carried out simulations for varying heat fluxes with and without bend pressure loss for 3 different fluids and found that the effect of pressure loss is not negligible. The code demonstrated the stoppage of pulsations in horizontal mode for 3 turn PHP. The authors state that with fewer turns the pressure losses are lower. This enables the liquid slugs to merge and form larger slugs leaving larger plugs at the evaporator which leads to PHP not able to function. The results indicated that for a 9 turn PHP, a heat flux of 12 W/cm² at horizontal orientation worked with and without consideration of pressure loss at bends. However, for the same conditions for heat flux of 16 W/cm² the PHP stopped working without consideration of bend losses and worked continuously with the inclusion of pressure loss. Hence the authors concluded that the presence of bend pressure losses leads on one hand to a worst heat transfer efficiency but on the other hand aids in avoiding the accumulation of a single phase in a particular zone and thereby work in a wider range of conditions. The mass flow rate (total liquid momentum) revealed that the liquid slugs have both an oscillatory component and a circulatory motion component which undergoes continuous flow reversals. These frequent flow inversions also had an effect on T_e, which shows variations due to the reversals. This effect was more visible in case of lower number of turns and lower heat fluxes. The frequencies were estimated to be in the range of 0.1-5 Hz. When the flow reversals are not predominant the frequencies are found to be in the range of 0.1-3 Hz. The authors have validated the results with the experimental values of [24] and the results show very good agreement at the lower heat loads. At higher heat loads the change of flow regime from slug to annular results in higher heat transfer in the experimental PHP but the code did not account for the annular flow regime which makes the code overestimate the T_e.

Dilawar and Pattamatta in [61] carried out numerical modelling of a single loop open ended PHP. The mass, momentum and energy equations were solved using an explicit finite difference scheme. In this model, the vapour is assumed non-isothermal by considering saturation temperature at the liquid vapour interface in calculating the phase change mass and heat transfer instead of the vapour temperature as considered in earlier isothermal models. The authors have also taken into consideration the pressure loss at bends and capillary effects at meniscus. The model was calibrated against the experimental work of [62] and compared with the numerical work of [11]. The work could show the sustenance of oscillation unlike the isothermal model of [11]. The numerical code also predicted the amplitude and frequency of the oscillation very closely for the experimental work of [62]. However, the model showed phase difference from the experimental results. This was attributed to the various assumptions made in the formulation of the model. The loss of pressure at bends was modelled using an empirical relation and the effect was seen that the bend reduces the amplitude of oscillation and also creates a phase difference with respect to the PHP working without consideration of bend loss. There was a considerable decrease in sensible heat transfer by including pressure loss at bends. The authors concluded that the effect of surface tension had negligible effect on the heat transfer and oscillations as the capillary force was much smaller than the force due to vapour pressure difference. There was a marginal phase shift in the oscillation of the liquid slug but no noticeable difference in amplitude and frequency was observed while varying the orientation angle on the heat transfer into the liquid slug. As the length of the adiabatic section is increased the amplitude of oscillation became smaller while the frequency of oscillation increased. The desired oscillation required for effective heat transport was not attained for an adiabatic length beyond 10 mm. The heat transfer was maximum without the adiabatic section. The authors observed that the n-pentane with lower saturation temperature had larger amplitude of oscillations as compared to ethanol and water. However, the heat transfer rate of n-pentane and water was similar while that using ethanol was much lower due to its higher viscosity. It was observed that the R_{th} decreases with an increase in the diameter of tube. The performance of PHP was better in the vertical mode of operation (both bottom heat as well as top heat modes showing no difference) as compared to the horizontal mode of operation. However, the bottom heat mode and top heat mode showing no difference is certainly contrary to the experiments reported in the literature. The model assumed that the PHP contained only one slug and two vapour plugs on either side of it. The model also assumed that the heat transfer coefficient at evaporator and condenser to be constant.

2.6 Correlation modelling

The work in [63] is an investigation of OLPHP in the horizontal orientation. The performance variation with respect to varying internal diameter (0.66, 1.06 and 2.03 mm), varying section lengths (50, 100 and 150 mm), 3 different number of turns (14 to 40) and fluid properties (R123, ethanol and water) was studied for horizontal operation for a fixed fill ratio of 50%. The evaporator was heated with hot water and the condenser was cooled with ethylene glycol-water mixture. Thus a temperature boundary condition was assigned to the evaporator and condenser. The authors have made observations that the variation of maximum heat flux had varying trends with different fluids. For R123 the heat tended to increase with increasing internal diameters whereas for ethanol the flux was decreasing with increase in diameter. It was observed that the longer the evaporator section lower was the heat flux. In this regard the authors have stated that this observation needs further scrutiny as the section length of the evaporator, adiabatic and condenser are same, thus the distance between evaporator and condenser is smaller for the smaller evaporator. The increase in the number of turns had heat flux decreasing. It was pointed out that with water only 2.03 mm diameter PHPs worked. So only limited number of tests could be conducted with water as the working fluid. The study also fitted a correlation for the estimation of the heat flux based on Ku, Pr, geometry of the PHP, ratio of the densities of vapour and liquid. The non-dimensional numbers of We, Bo and Fr was not used in the correlation as these numbers exhibited random pattern with respect to the results of the experiments conducted. The correlation predicted had a standard deviation of ±30%. The correlation did not account for either the temperature difference or T_e and T_c. The authors also fitted a correlation to evaluate the operational regime of the PHP in the horizontal orientation. This correlation can be used to predict whether the PHP is operational for a given heat flux in horizontal orientation. The research indicated a relationship of the useful operating inner diameter range with respect to reduced pressure. The relationship indicated that the inner diameter of an OLPHP reduced as it is made to operate at higher reduced pressure.

The paper [30] is a continuing work of [19]. It reviews the various modelling strategies available for performance prediction of PHPs and proposes that a non-dimensional number based correlation is the most suitable method for the prediction as the rest of the methods are either highly simplified due to inherent assumptions or lack experimental data to provide the right prediction. It also discusses the thermal behaviour of the PHPs with respect to the visualisation studies to emphasise the strong dependence of the performance on the flow patterns inside the tubes. The internal diameter of the tubing was 2 mm of Pyrex glass. The section lengths and the associated number of turns of the PHPs used for the visualisation were 50 mm with 10 turns, 50 mm with 28 turns and 150 mm with 11 turns. The fluid used was R123 with inclination angles being 0°, 30°, 50°, 70° and 90° starting from horizontal to vertical bottom heat mode. It also enlists various thermo-hydrodynamic phenomena that enables the working of the PHPs. The various flow regimes were captured like – the thermally best performing annular flow, semi annular flow, slug flow to the nonperforming standstill scenario. Based on the various flow regimes observed in the visualisation studies a set of relevant parameters and properties were combined into relevant non-dimensional numbers and a correlation was formulated using the 248 data points from the results of the experiments conducted in [19]. The correlation was found to be accurate for +/- 30%. The fill ratio was maintained as 50% for the entire study. In this correlation Karman number was included to provide an indirect velocity scale dependence in the prediction.

In [64] a correlation has been proposed for the prediction of the maximum heat flux before dry out for open loop PHPs. In this work the 27 PHPs on the whole – 3 internal diameters (2.03, 1.06 and 0.66 mm), 3 different numbers of turns (5, 10 and 15 turns) and 3 section lengths (50, 100 and 150 mm) were tested. Here the 3 different fluids – R123, ethanol and water with fill ratio maintained at 50% was tested. The correlation was separately proposed for the bottom heat mode of vertical orientation and the horizontal orientation. The vertical orientation correlation was inclusive of Wallis number to account for the flooding phenomenon. The standard deviation was 18% for the horizontal mode correlation and 29% for the vertical bottom heat mode.

The authors in [65] fitted a correlation to predict the maximum heat flux condition (condition just before dry-out) with a set of 36 closed loop PHPs of varying diameter (0.66, 1.06, 1.50 and 2.03 mm), evaporator lengths (50, 100 and 150 mm) and number of turns (5, 10 and 15). The fill ratio was maintained as 50% and the orientation was vertical with evaporator below condenser. The working fluids were R123, ethanol and water. The authors state that the maximum heat flux increases as the evaporator length decreases as the boiling mechanism changes from confined channel flow boiling to pool boiling. It is stated that the maximum heat flux increases with increase in internal diameter (of course within the working Bond number range) and the number of turns of the meandering tube of PHP. The study introduced the non-dimensional parameter of critical gas value (CGV) which enables the use of volume flux (superficial velocity) of the vapour in determining the maximum heat flux. This parameter of superficial vapour velocity was calculated from the heat flux and the consequent vapour generation. The work also introduced the aspect ratio of internal diameter to length of the evaporator (D_i/L_e) to capture effect of the length of the evaporator on the PHP performance, especially at dry-out. The authors also state that all the calculations of the thermophysical properties are carried out at the average temperature ((T_e+T_c)/2). The work also introduced the non-dimensional parameter for the number turns by the ratio of total length to length of evaporator (L_t/L_e). However, the authors state that the dimensionless group of the meandering turns do not capture the effect of the number turns accurately when the length of the evaporator is substantially different from the lengths of the condenser and adiabatic sections. The predicted correlation for maximum heat flux was having a standard deviation of ±24%.

Shafii et al. in [66] fitted a correlation to predict the heat flux with a series of experiments on a 5-turn closed loop copper PHP. The fill ratios were varied as 30%, 40%, 50%, 70% and 80%. The authors state that the fill ratio being less leads to dry out and fill ratio being more leads to lesser degree of freedom for the pulsations, so there exists an optimum fill ratio for which the PHP works at its best. The authors have concluded that the optimum performance of the PHP occurred at 40% fill ratio for water and 50 % fill ratio for ethanol. In this work the orientation was vertical with bottom heating mode. The working fluids used were ethanol and water. For all fill ratios the heater power was varied between 5 W to 70 W. The authors have introduced a parameter – aspect ratio (D_i/L_e) in the correlation to capture the effect of the length of the evaporator. The authors also state that all the calculations of the thermophysical properties are carried out at evaporator temperature (T_e) as the boiling occurs only at the evaporator. The Morton number which combines the effects of inertia, viscosity, buoyancy and surface tension has been included in the power law correlation. The constants for the equation was based on the fill ratio as fill ratio was varied widely in this work. The root mean square deviation of the correlation was 19.7% from the experimental data.

In [67] experimental studies were carried out with 3 copper capillary tube CLPHPs of internal diameter 1.2, 2, and 2.4 mm. The thermal performance was assessed for the vertical bottom heat mode with heating power input in a range of 15–127 W. Two working fluids - water and ethanol, were used with fill ratios of 40%, 50%, and 60%. The evaporator lengths were varied as 30 mm, 50 mm and 70 mm, while the condenser was liquid cooled with a constant length of 70 mm. The experiments were conducted for a maximum T_e of 100°C as this was considered the limit for majority of lower heat transfer applications. The authors state that the thermal performance of the CLPHPs depends on the combined effects of working fluid, filling ratio, inner diameter, evaporator length, and input heat. It was concluded that for the internal diameters of 2 mm and 2.4 mm CLPHPs had better thermal performance when charged with water whereas for 1.2 mm internal diameter ethanol was more suitable. The thermal performance of the CLPHPs was found to be better at the relatively lower filling ratios (40% and 50%). An optimum evaporator length with respect to the lowest thermal resistance was arrived at for the fill ratios. The empirical correlation based on 510 sets of available experimental data from the present study and as well as from other sources in literature was proposed to predict the thermal performance in vertical orientation. The proposed correlation agreed with the experimental data within a deviation of approximately ±40%.

The authors in [68] proposed a correlation for rotating pulsating heat pipes with evaporator at the end (periphery) and the condenser at the centre which coincided with the axis of rotation. The centrifugal force aids in transportation of fluid from condenser to evaporator. The axis of rotation was horizontal thus the 4 limbs (turns) of the PHP were alternately having the top heat mode – horizontal mode – bottom heat mode continuously. The proposed correlation was also made with the combined results of the work carried out and the previous work carried out on rotating PHPs by [69]. The experiments were carried out for two fluids – water and ethanol. The fill ratios were – 30%, 50% and 70%. The rotation speed was varied between 200 rpm to 800 rpm in steps of 200 rpm. The correlation was predicting the heat fluxes with a maximum error of 20%. The correlation accounted for rotation of the PHP by inclusion of Froude number.

Table 2-2: Various correlations for PHPs available in literature

Ref.	Year	Correlation	Remarks
[63]	2003	$Ku_0 = 0.0052\left[\left(\frac{D_i^{4.3}L_t^{0.1}}{L_e^{4.4}}\right)N^{0.5}\left(\frac{\rho_v}{\rho_l}\right)^{-0.2}Pr_v^{-25}\right]^{0.116}$	**variations** q, Di, Le, N and fluid (R123, ethanol and water) **constants** fill ratio and orientation-horizontal
[30]	2003	$\dot{q} = 0.54(\exp(\theta))^{0.48}Ka^{0.47}Pr_l^{0.27}Ja^{1.43}N^{-0.27}$	**variations** q, Di, N, fluid (R123, ethanol and water) and orientation from horizontal to vertical BHM **constants** fill ratio (50%) Exponential dependence on orientation proposed
[64]	2005	$Ku_0 = 53680\left(\frac{D_i}{L_e}\right)^{1.127}Ja^{1.417}Bo^{-1.32}$ $Ku_{90} = 0.0002\left(\frac{D_i}{L_e}\right)^{0.92}Ja^{-0.212}Bo^{-0.59}Wa^{13.06}$	**variations** q, Di, Le, N, and 3 fluids - R123, ethanol and water **constants** fill ratio (50%), orientations horizontal and vertical BHM Wallis number for flooding Only max. heat flux considered
[70]	2007	$Ku_{90} = 0.0004\left[Bo^{2.2}Fr^{1.42}Ja^{1.2}Pr^{1.02}\left(\frac{\rho_v}{\rho_l}\right)^{0.98}R_{cv}^{1.4}We^{0.8}\left(\frac{L_e}{d_i}\right)^{0.5}\right]^{0.107}$	**variations** q, Di, Le, N, Number of check valves and 3 fluids - R123, ethanol and water **constants** N, fill ratio, orientation (BHM) Included Froude number
[65]	2009	$Ku_{max} = 6.25(CGV)^{0.34}\left(\frac{D_i}{L_e}\right)^{0.91}\left(\frac{L_t}{L_e}\right)^{-0.26}$ $CGV = \frac{j_v\mu_v}{\sigma}\left(\frac{\rho_v}{\rho_l}\right);\ j_v = \frac{\dot{q}_{max}A_o}{\rho_v A_x h_{fg}}$	**variations** q, Di, Le and N 3 fluids - R123, ethanol and water **constants** fill ratio (50%) and orientation CGV included to account for vapour volumetric flux Only max. heat flux considered
[66]	2010	$Ku = a * Ja^b Pr^{-0.7}Bo^{0.85}Mo^{0.8}\left(\frac{D_i}{L_e}\right)^{0.7}\left(\frac{D_o}{D_i}\right)^{2.6}$ $a = -1258\phi^4 + 2663.1\phi^3 - 2028.9\phi^2 + 655.28\phi - 71.22$ $b = -142.5\phi^4 + 301.5\phi^3 - 227.6\phi^2 + 72.21\phi - 6.87$	**variations** q, 2 fluids (water and ethanol), 5 fill ratios (30% to 70%) **constants** Di, Le, N and orientation Inclusion of Do/Di for conduction
[67]	2013	$Ku = 8.3Bo^{-1.598}Mo^{-0.026}Pr^{-3.458}Ja^{*-0.157}\left(\frac{D_i}{L_e}\right)^{1.21}\left(\frac{L_e}{L_c}\right)^{-0.232}$	**variations** q, Di, section lengths, 2 fluids – ethanol and water, fill ratio 40%, 50% and 60% **constants** orientation, N Mo index low, effect not to be ignored
[68]	2018	$Ku = f(\phi)Bo^{-2.259}Mo^{-0.101}Ja^{1.109}\left(\frac{L_e}{L_c}\right)^{-1.111}\left(\frac{D_i}{L_e}\right)^{1.400}\left(\frac{L_e}{L_{eff}}\right)^{0.658}(\exp(0.003Fr))$ $f(\phi) = \left(0.308 - 2.220\phi + 7.331\phi^2 - 9.883\phi^3 + 4.615\phi^4\right); 0.25 \le \phi \le 0.75$	**variations** q, 2 fluids (water and ethanol), 3 fill ratios (30%, 50% and 70%), rotation speed of PHP **constants** Di, Le and N Froude number for PHP rotation

2.7 Other modelling techniques

Khandekar et al. in [34] have carried out application of Artificial Neural Networks (ANN) for prediction of the thermal performance of the PHPs. Here copper tube of internal diameter 2 mm with 5 turns in the evaporator was used as PHP. Other than the evaporator the rest of the portion was used as condenser with forced air cooling of 5 m/s. Here the fill ratio and applied heat flux was used as 2 independent variables (input) and the R_{th} was used as the output indicating the thermal performance of the PHP. The fill ratio was varied widely from 0% (dry tubes) to 100% (fully charged). The authors state that the PHP operation actually occur between 20-85% fill ratio. In this study an identity function was used for output activation and for the other nodes a sigmoid function was used for activation to perform non-linear input and output transformation. The authors conclude that 41 points out of the 52 data sets pertaining to the 20-80% fill ratio yielded a better model than the complete dataset of 76 points ranging from 0-100% as the hydrodynamic phenomenon responsible for heat transfer was different in the 20-80% range. The prediction yielded a maximum error of 6.9% when tested with the 11 datasets out of the 52 data points. The authors also mention the limitations of the ANN concept for PHP like – subjectivity in choosing the number of hidden layers and the number nodes in each layer. The authors conclude that the number parameters used in the present study was only 2 – heat flux and fill ratio but in reality a PHP operation depends on many other factors like – diameter of the tube, number of tube turns, length of the section, orientation of the PHP and physical properties of the working fluid. Hence the authors state that for ANN to be reasonably accurate in prediction of performance of PHP, a large amount of reliable experimental data is a strong prerequisite for complex systems like PHP.

2.8 Heat transfer enhancement

2.8.1 Use of check valves

In [70] the authors have investigated a CLPHP with a check valve towards enhancement of heat transfer. The PHP was made out two different internal diameters of 1.77 and 2.03 mm copper tubes. The evaporator, adiabatic and condenser lengths were maintained the same for a given prototype. The lengths were varied as 50, 100 and 150 mm. The number of turns for each prototype was maintained as 40. The fill ratio was maintained as 50% for three fluids – water, ethanol and R123. The ratio of check valves defined as number turns divided by number of check valves was also varied – 20, 8, 5 and 4. The check valves consisted of a stainless steel ball in copper tube with a ball stopper on one side and conical valve seat at the other end preventing the flow in the reverse direction. The T_e and T_c were maintained at 80°C and 20°C respectively using hot and cold water baths. The heat fluxes (heat loads) were varied for a constant orientation of vertical bottom heat mode. The PHPs showed maximum heat fluxes when the ratio of check valves are maximum for every fluid. The authors have attributed this to the effect of gravity on the ball of the check valves are lesser when the check valves are lesser in number. The aspect ratio (L_e/d_i) variation showed that the maximum heat flux could be obtained at lower aspect ratio as at higher aspect ratio boiling inside a confined channel was attributed since the evaporator is longer at higher aspect ratio. The heat flux was also found increase slightly with increase in Bond number. That is the heat flux could be higher for a larger diameter. However, in all cases, out of the three fluids, the R123 yielded highest heat flux. Also the authors have reported that the relationship of the heat flux with dimensionless parameters – We, Fr and Ku are linear in nature. The study culminates in correlation for heat flux at vertical bottom heat mode in terms of Bo, Fr, Ja, Pr, We, Ku, ratio of vapour density to liquid density, ratio of check valves and the aspect ratio (L_e/d_i).

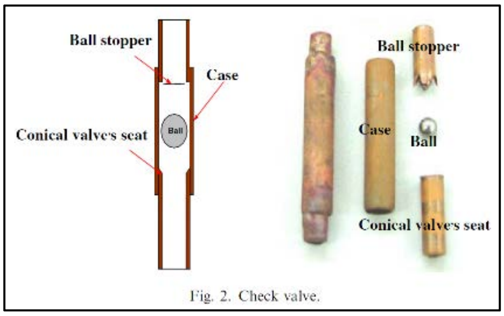

Figure 2-12: Check valves to improve unidirectional circulation [70]

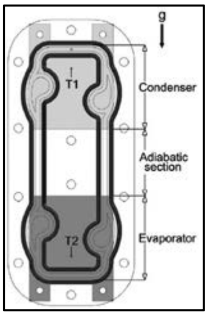

Figure 2-13: Tesla valves for unidirectional circulation [21]

Thompson et al. in [20] have investigated two flat plate PHPs - one without and another with tesla valves to enhance the directional (counter clockwise) circulation thereby enhancing the heat transfer of PHP. The PHP had 1.5 mm square channels with 6 turns. L_e and L_c were maintained as 38 mm. High purity liquid chromatography (HPCL) water at fill ratio of 70% was used to facilitate neutron radiography. The tests were carried out with only bottom heating mode. Two different cooling temperatures of 35°C and 55°C was used. The temperature measurements were sampled at 200 Hz. The fluid motion was analysed by inspecting gray-scale pixel intensities from processed neutron images using structured algorithms and routines within a MATLAB working environment. The void fraction was estimated based on the intensity of the images. Using the estimate of the void fraction the movement of the slug in the clockwise or counter clockwise direction was estimated. Inter-channel circulation of long, continuous slugs in the evaporator was clearly observed for both FP PHPs and a separate method for approximating circulatory direction was based on this observation. This method flagged images with liquid-filled evaporator turns (70% liquid) and then observed the leading/trailing edges of the evaporating liquid slug to approximate the respective flow direction. At low heat inputs static operating phases occurred for both heat pipes, where evaporator temperatures increased and internal fluid activity ceased. These static phases were disturbed when a liquid slug entered the evaporator and spurred the oscillatory/circulatory behaviour once again. These static phases may be attributed to the thermal mass of the FP PHP balancing the PHP driving force via conduction at low heat inputs. The authors have concluded from the results that the diodicity of the tesla valves increased with heat loads while the diodicity of the FP PHP without valve was always nearly 1 indicating that the PHP had no preferred direction of circulation. The authors have introduced the parameter, circulation tally ratio (CTR) which indicates which direction the circulation occurs. CTR for the PHP with valves was always greater than 1 indicating a counter clockwise circulation. The R_{th} of the PHP with tesla valves was consistently lower after the successful start-up of the PHP. The R_{th} was lower for the higher cooling temperature of 55°C. The percentage reduction of R_{th} with valves was found to range between 15% and 25% with the higher percentage reductions occurring at the higher cooling temperature. This indicates that increasing the diodicity of a PHP results in enhanced thermal performance. The authors state that the percentage increase in thermal performance is of the same order of magnitude as the percentage increase in overall diodicity for both heat pipes. The authors have also concluded that though the implementation of tesla-type check valves is a promising means for circulatory flow rectification within a PHP, but future research is needed to further optimize valve design, quantity, and alignment within a PHP.

The authors in [21] conducted the experiments for the tesla valve based PHP and established the improvement of R_{th} for a single loop PHP. The authors have designed the Tesla valve with the inlet and outlet in-line with each other with sole aim of integrating the same to PHP. The design was carried out by 2-D and 3-D simulations of single phase. The tests were conducted for the valve individually for diodicity (ability to aid flow in preferred direction and retard flow in the opposite direction) with two-phase flow with water as liquid and air as gas. The study on the valve was image processed to quantify the relative flow rates of the two fluids in the main channel and the branch channel after video recording. The liquid was mixed with dye to post process the image. The valve was integrated with PHP and tested. To benchmark the valve based PHP, a PHP without valve was also tested. The authors have quantified the improvement of R_{th} by conducting experiment with and without Tesla valve. The tests with video recording showed the diodicity enhancing the directional circulation. The authors have stated that the flow agreed well with literatures ([47] and [19]). However, the quasi-steady operation of the PHPs could not be achieved due to the T_e exceeding the maximum limit of material of construction of the PHP.

2.8.2 Deployment of channels of varying size

Chien et al. in [71] proposed a design with alternate channels of PHPs with different diameters to make the performance independent of the orientation with respect to gravity even with lower number of turns. The investigation was done by constructing two flat plate, copper substrate, CLPHPs. The overall dimensions were 122 mm x 57 mm x 5.5 mm with 8 turns. The uniform cross-section PHP had 16 parallel square channels with cross-section 2 mm x 2 mm. The non-uniform CLPHP had 8 parallel square channels with a cross-section of 2 mm x 2 mm and 8 parallel square channels having a cross-section of 1 mm x 2 mm (deep) with the alternate channels having different cross-section. The working fluid was distilled water. On the whole a total of 4 fill ratios – 40% to 70% in steps of 10% and 4 orientations 0° to 90° in steps of 30° were investigated. The investigation showed that the uniform PHP did not operate in horizontal (0°) orientation while the non-uniform one operated successfully at higher heat loads and higher fill ratio in the horizontal orientation. The possibility of the non-uniform PHP to operate in horizontal orientation is attributed to the unbalanced capillary force and flow resistance between various channels. The study also revealed that for non-uniform PHP the R_{th} values did not differ much for orientations of 30°, 60° and 90°. However, for the uniform PHP the R_{th} was nearly the same for 60° and 90° orientations while the 30° orientation showed rather high R_{th}. However, due to increased flow resistance in the non-uniform PHP the R_{th} values for the same fill ratio and heat load was found to be higher than that of the uniform PHP for the vertical (90°) orientation.

Kwon and Kim [72] in their investigations with single loop PHP with dual diameter have concluded that the difference in diameter of the adjacent limbs contributed to circulating flow in one direction (from evaporator to condenser through larger diameter tube). This has resulted in the enhancement of heat transfer and lower R_{th}. The study was carried out with 6 single closed loop PHPs. Three of the PHPS are of uniform diameter of 1.2 mm, 1.7 mm and 2.2 mm whereas the other three of them were combination of 1.2 mm - 1.7 mm, 1.2 mm - 2.2 mm and 1.7 mm – 2.2 mm. The working fluid used was ethanol and the fill ratio was maintained as 50%. The PHPs were tested from 5 W to 25 W in steps of 5 W. The orientation was varied from 90° (vertical bottom heat mode) to 10° to horizontal in steps of 10° inclinations. The L_e, L_a and L_c were maintained as 30 mm, 110 mm and 50 mm respectively with the overall length being 190 mm. The authors indicated a reduction of 45% in R_{th} from the uniform diameter to the varying diameter PHPs. The authors have attempted a numerical procedure which could predict the R_{th} and the mass flux based on the experimental results. The theoretical prediction matched the experimental results within ±15%. The authors have indicated that the latent heat contribution is less than 20% of the total heat transferred. This is in-line with the literature which consistently states that the PHPs transfer majority of heat by sensible heat transfer. The authors have recorded that the oscillation or the flow pattern changed from quasi-sine at lower heat loads to random at moderate heat loads to circulating flow at higher heat loads for the uniform PHP. While the flow pattern switched to circulation type at much lower heat loads with the narrower tube acting as down-comer and the wider tube acting as up-header in case of the dual diameter PHPs. The authors have stated that the widening of difference in diameters proves to be counterproductive if the value is too large as the gravitational force imbalance which causes the circulation in one direction gets reduced due to larger fluid mass in the larger diameter tube. The authors concluded that the ratio of the difference in diameter to the average diameter of a dual diameter PHP should be 0.25 to 0.4 for the maximum reduction in $R_{th.}$ when compared to a uniform diameter PHP.

2.8.3 Use of additional branch for asymmetry

Sedighi et al. [73] have investigated a novel design of closed single loop pulsating heat pipe by adding a branch to its evaporator and the way of heat being supplied to the evaporator. The PHP was tested against a standard single loop PHP which was 12% lesser in internal volume compared to the additional branch PHP. A pyrex glass model of the new PHP was tested for visualisation which that showed the bubble pumping, refilling behaviour of the additional branch in slug flow as well as the shooting of the mist in the annular flow regime. The actual additional branch PHP and the bench mark single loop PHP were constructed out copper tubes of internal diameter 3 mm and external diameter 5 mm. The working fluid of deionized water with fill ratios of 40% to 70% in steps of 10% was tested for varying heat loads (5 to 130 W) for 90° (vertical bottom heat mode) inclination. The most optimum fill ratio was found to be 60%. This fill ratio of 60% was tested for inclinations – 60°, 30° and 0° for various heat loads. At every heat load the additional branch PHP was found to yield lower R_{th}. The performance of the PHPs was nearly the same in vertical operation for fill ratios of

50% and 60%. While the additional branch model outperformed in 40% and 70% fill ratios, thus indicating that the additional branch PHP was less sensitive to fill ratio. For orientations other than the vertical the additional branch PHP was better than the conventional PHP. The conventional PHP did not start at all in the horizontal orientations whereas the additional branch PHP could operate in the horizontal orientation. At other inclinations the additional branch PHP was better in terms of R_{th} when compared to regular PHP indicating that the circulation is enhanced in a particular direction in case of the additional branch PHP due to asymmetric geometry and asymmetric heating.

Figure 2-14: Non-uniform diameter in flat plate PHP [71]

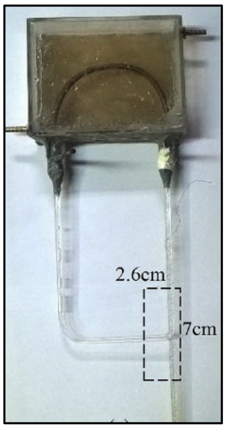

Figure 2-15: Additional branch for asymmetry [73]

2.8.4 Ultrasonic excitation towards heat transfer enhancement

In [74] Zhao et al. used the ultrasonic excitation to study the heat transfer enhancement in a six turn copper PHP (inner diameter of 1.8 mm) with variables as fluid (acetone and water), orientation, fill ratio, operating temperature (coolant incoming temperature) and heat input (15 to 200 W). The PHP had L_e = 38 mm, L_a = 53 mm and L_c = 64 mm. The study deployed lead based lanthanum doped lead zirconate titanate piezoelectric ceramics with inner diameter of 3 mm (equal to the outer diameter of the PHP tubing) at the six turns in the evaporator section. The ultrasound excitation was provided with a power of 0.1 W at 485 kHz. The enhancement of heat transfer was significant at lower heat loads and this enhancement was lower at the horizontal orientations than the vertical inclinations. The heat transfer enhancement with ultrasonic excitation increased when the operating temperature raised from 20°C to 40°C; however, the heat transfer enhancement due to ultrasonic excitation decreased when the operating temperature raised from 40°C to 60°C for acetone as working fluid. The authors have concluded that the fill ratio also affects the enhancement of heat transfer. The enhancement percentage was higher for water compared to that for acetone when the operating temperature is 20°C. A reversal of trend was observed when the operating temperature was 40°C, at which the enhancement percentage was higher for acetone compared to water.

2.8.5 Use of nanofluids

Li et al. [75] investigated PHP with working fluid of deionized (DI) water and 15 nm diameter SiO_2 nanofluid (0.268% volume/volume) with quartz glass tube of inner diameter 3.353 mm and outer diameter 5.38 mm. The evaporating section of the PHP was electrically heated by a conductive transparent thin film coated on the outer wall, with the condensing section cooled by flowing water at a temperature of 20°C. Only horizontal orientation was verified. The visualisation was captured by high speed camera (500 fps) and the temperatures were measured by infrared imaging system with uncertainty of ± 2°C. The fill ratio was between 45% and 46%. The evaporator had 3 turns of bend radius 7.48 mm. L_e was 92.1 mm and L_c was 80 mm with overall length being 320 mm. The nanofluid was more easily broken into small columns than the DI water, and its contact angle on the tube wall was smaller than that of DI water, which causes the ends of the vapour columns to be rounder in the nanofluid. The change in contact angle was attributed to a solid-like ordering of the suspended nanoparticles in the three-phase contact region and the pressure arising from this ordering, which enhances the spreading of nanofluids. Even when the oscillations were not triggered at low heat loads the nanofluid yielded lower R_{th} due the higher thermal conductivity of the fluid. The authors have concluded that the performance of nanofluid was better than DI water for all heat loads and nanofluid PHP had a much wider operating heat load (up to dry out) range. In DI water the liquid and vapour columns oscillated from their mean position. However, in the nanofluid the flow regimes of slug and annular was also found apart from mere oscillations (which is termed as column flow). One distinguishing phenomenon was documented in the nanofluid PHP where few short vapour columns shrink into small bubbles in the condensing section, which then flow into the evaporating section and were captured by the CCD camera. Since the liquid and vapour columns in the nanofluid PHP are shorter than in the DI water PHP, the overheating or sub-cooling during the absence of the liquid or vapour columns at a spot in the evaporating or condensation sections is effectively suppressed in the nanofluid PHP, which results in a lower temperature difference between the hot and cold ends of the nanofluid PHP, thus a lower R_{th}. Though the DI water PHP could not be operated beyond 42 W where the column flow stopped and dry out occurred, in the nanofluid PHP the flow regime changed to slug flow. This was triggered by the generation of large numbers of bubbles in the liquid columns in the evaporating section. These bubbles coalesced into large bubbles to form vapour plugs, so the flow turned into the slug flow. The DI water could not have this transition as the boiling nucleation is more difficult in the DI water than in the nanofluid as the particles create additional nucleation sites. The accumulation of nanoparticles at the vapour-liquid interface leads to a decrease in surface tension thus lowering the barriers for nucleation. When the heat loads were further increased annular flow with non-uniform film thickness was observed. The least R_{th} for nanofluid occurred in the slug flow regime, with a thick film surrounding vapour slugs and strong boiling in the film.

Qu and Wu in [76] conducted investigation with SiO_2/water (silica) and Al_2O_3/water (alumina) nanofluids with varying concentration of the nano particles at 50% fill ratio and compared their performance with pure water. The PHP was made out 2 mm inner diameter stainless steel pipes with 6 turns. The PHP dimensions were evaporator, adiabatic and condenser sections with 50, 105 and 70 mm in length respectively. The study showed that the silica nano fluid resulted in inferior thermal performance than the pure water whereas the alumina nano fluid yielded better performance than pure water. The addition of nano particles became counterproductive when the alumina concentration was increased beyond 0.9% by weight. The scanning electron microscope (SEM) images of the inner surface of operated PHPs revealed that the deposition in case of silica was substantially higher than that of alumina. The contact angle of sessile droplet on the three surfaces (PHP enclosure) – one exposed to pure water, second exposed to silica nanofluid and the third exposed to alumina nanofluid were measured. The silica deposited surface indicated a drastic reduction in the contact angle. An atomic force microscopic images of the surfaces were obtained. These images indicated that the silica particle deposition on the evaporator surface led to the decrease of micro-cavity density. The layer of the silica contributed to the increased thermal resistance of the tube wall. Thus the combination effects of the decreased nucleation sites, decreased contact angle and thick porous layer resulted in increased thermal resistance of the silica fluid PHP. However, the alumina deposited resulted in enhancement of nucleation sites as the particles did not agglomerate into larger ones thereby enhancing the boiling heat transfer. Although the bubbles with smaller size were created on the nano-micro roughened hierarchical surface which plays a negative role in reducing thermal resistance, the dramatic increase of the active nucleation site density and increase in the release frequency of bubbles overwhelmingly intensified the boiling. Once the alumina concentration reached the optimum level further increase resulted in agglomerated deposition on the inner surface thereby reducing the nucleation sites leading to poorer heat transfer performance.

2.9 Closure

Though the first PHP was proposed by Akachi in 1990 [8] the last decade has seen a lot of work especially experimental, being carried out on this device. The reasons are, its simplicity in construction and difficulty in the understanding of its working (or design). The experiments have been initially ([13] and [9]) devoted towards finding the right fluid (or the desired thermophysical properties of the fluid) and the optimum fill ratio. The experiments have been carried out to ascertain the right geometry of the channel – circular or rectangular [15]. The researchers have attempted to arrive at the number of turns required to make a PHP operate in horizontal or top heat mode ([19] and [25]). The investigations have been carried out to understand the working of the PHP by measurement of pressure (other than only temperatures and visual) as in case of [38]. Several studies have been carried out exclusively towards the understanding of the flow regimes [39]. Some research groups have performed investigations dedicated to estimation of PHP performance under various gravity conditions [40] and [41]. Still there exists scope for experiments to augment data on the number of turns required for gravity independent operation for various diameters of the tube.

The start-up characteristics of the PHP have been investigated as the limited investigations cited in section 2.3 states that the PHP at lower loads have a sudden start-up unlike the smooth start-up with higher heat fluxes. However, the number of research papers is limited compared to the steady state operation.

Also the simulation efforts have been carried out with simplified formulations with straight forward geometries and orientations as in [11], [55] and [61]. The more recent simulation works have been far more rigorous like [14], [60] and [33]. However, in all the simulation investigation with the exception of [33] the pressure loss at the bends of the PHP was neglected though the experimental research shows that the bends play a major role in enhancing PHP operation in top heat modes. Of all the modes of modelling the PHP, the correlation modelling with non-dimensional numbers is said to be the most promising [29] due to its simplicity and holistic nature. However, only a few correlations as summarised in Table 2-2 were fitted.

The variations of the PHP like flat plate configuration [23] and multiplanar configuration [24] and [53] where more channel densities can be packed as well as utilised directly towards cooling of electronics [42] were also investigated. However, the capillary tube configuration of the PHP was the most investigated and the researchers have reported that the flat plate configuration due to the inherent solid conduction [15] and [16] between channels perform lesser than the capillary tube configuration. The multiturn, multiplanar configuration which are relatively difficult to fabricate than the single plane capillary tube PHPs can operate successfully in all orientations as the gravity vector has a probability to assist PHP performance [19] have also been investigated [24], [52] and [53]. Despite the advantages with these flat plate and multiplanar configurations the amount of data available is very limited.

2.10 Scope of the present study

In this dissertation investigations have been carried out on

- Flat plate configuration – benchmarking of the experimental setup and investigation with respect to working fluid, fill ratio and inclination
- Single loop module – start-up characteristics, flow patterns, estimation of characteristic frequency, insulation of adiabatic section and the effect of bend radius on performance as this was found be neglected in most simulation efforts
- Multiplanar configuration – to have near gravity independent operation and compact heat transfer device
- Correlation modelling for one of the configurations investigated

The efforts were directed in these areas as the literature review shows that these are the configurations that are relatively less investigated. The closed loop PHPs are reported to be more efficient than open loop ones ([26] and [13]) due their ability to permit unidirectional circulation of the working fluid. Hence in this dissertation only closed loop pulsating heat pipes were investigated. Although the efforts towards heat transfer enhancements like addition of check valves, tesla valves, use of nanofluids are still less researched these additions/modifications make the otherwise simple device of PHP more complex. So these avenues have not been explored in this dissertation.

3 Flat plate pulsating heat pipe – Performance comparison based on working fluid, fill ratio, inclination, heat load and a proposed correlation

3.1 Introduction

PHPs are useful devices for cooling of electronic assemblies as they are less fabrication intensive compared to the conventional heat pipes due to the non-requirement of exclusive capillary wick structure. In any two-phase cooling solution, the important aspect of the cooling design is the embedding of the heat pipes or the pulsating heat pipes efficiently into the electronic assembly to be cooled. The heat pipes both conventional and pulsating ones have very high heat transfer capability. Hence if the interface of these heat pipes and the electronic assemblies have large thermal resistance due to improper contact then the benefit of high performance of the heat pipes cannot be reaped. Thus it is imperative to have PHPs in the form factor which are easy to be embedded in the assembly to be cooled. In this aspect, a flat plate PHP is more amenable for integration into a printed circuit board (PCB) due to its reduced thickness and higher density of channels within a given width of the PHP. Khandekar et al. [15] and Yang et al. [23] have investigated flat plate PHPs with the aim of using them as integral heat spreaders in electronic assemblies. Kearney and Griffin in [42] have attempted an investigation of capillary tube PHP as integral spreaders. In this study a closed loop PHP in the flat plate configuration has been considered. A flat aluminium alloy substrate, similar to that in the work of [15] was investigated. The dimensions correspond as closely as possible to the setup no. 1 of [15]. In this investigation working fluid of water was tested to benchmark the test setup with the results of [15]. This setup is chosen for the following reasons.

1. Form factor (flat) most suitable for integration in practical electronics.
2. Aluminium alloy, the most used material in terms of weight, availability and cost.
3. Experiment is amenable for visualization.
4. Other setups with narrower grooves (1 mm wide) make the manufacturing more difficult.

Although in [15] ethanol was used, in the present study methanol and FC 72 was tried, as one of the salient conclusions in the paper was that the fluid with larger $(dP/dT)_{sat}$ enhances the performance of the PHP. It is found from [27] that methanol has larger $(dP/dT)_{sat}$ than ethanol apart from being better in terms of liquid thermal conductivity, dynamic viscosity and liquid specific heat capacity which are important parameters for heat transfer in PHPs. Likewise, FC

72 with low surface tension and low latent heat of vaporization being a dielectric fluid with lower boiling point (thus a larger $(dP/dT)_{sat}$) was also tested. FC 72 also has the advantage of direct integration into an electronic system like printed circuit board due to its large dielectric strength.

Water was degassed by repeated boiling and was transferred to the PHP while still warm. However, methanol and FC 72 were not degassed as their evaporation rate was too high.

Water as a heat pipe fluid is generally not used with aluminium enclosures due to generation of hydrogen (non-condensable gas), which results in deterioration of performance over time. In this study water was chosen to investigate its efficacy for the given geometry as well as to benchmark the experimental setup. The experimental runs (for any given fluid and fill ratio) never exceeded 2 hours (either for varying heat load or for varying inclination). After which the PHP was completely purged to achieve the desired vacuum. The generation of hydrogen in the absence of alkaline catalysts is very minimal for aluminium plates exposed to water as the surface of aluminium is largely protected by the aluminium oxide layer. It is shown in Fig. 6 of [77] that it requires at least 2 hours for generation of 50 ml of hydrogen in the presence of one mole of sodium hydroxide. For the experiments carried out in the present study with water, there was no catalyst as well as the time of contact was always less than 2 hours. Hence the amount of hydrogen generated was expected to be very less.

3.2 PHP dimensions

A flat aluminium alloy plate of 3 mm thickness was used to fabricate the prototype for evaluating the PHP performance. The channel dimensions were 2.2 mm deep and 2 mm wide as shown in Figure 3-1. The distance between the channels was maintained as 2.5 mm with 6 turns at the evaporator. This yields a wall of 0.5 mm thickness separating the channels. The area for the heater ear-marked on evaporator is 30 mm x 22.5 mm. A cold plate of copper being cooled by circulating water and with an area matching with that of the condenser of [15] (30 mm x 13.5 mm) was employed for the heat removal. The channel hydraulic diameter was calculated as $D_h = 4A_{cs}/p_w = 2.1$ mm. The desired hydraulic diameter for effective slug-plug formation of the fluid is given by the Bond Number (Bo) criterion [13] of Bo < 2.

$$D_h \leq 2\sqrt{\frac{\sigma}{g(\rho_l - \rho_v)}} \tag{3.1}$$

As per the above equation (3.1), the D_h should be less than 5 mm for water and 3 mm for methanol. The PHP channel geometry thus can be used with either of the fluids mentioned

(Figure 3-2). However, the lower surface tension of FC 72 yields a diameter of around 1 mm as per Bond number criteria. In this case, the same geometry was used for testing with FC 72 as PHPs with diameters larger than the ones prescribed as per Bond number criteria were also shown to perform well in [48] and [22].

3.3 Assembly of PHP

The top side of the PHP substrate or the side on which the channels are cut was covered with 0.2 mm thick silicone sheet ([42] and [23]) before closed using a transparent polycarbonate (for visualization) sheet of 10 mm thickness. The thin silicone sheet was introduced to prevent inter-channel communication during operation of PHP while providing adequate transparency for viewing the operation. An O-ring (2 mm diameter thick) was put in the groove (1.6 mm deep x 2.1 mm wide) machined out in the polycarbonate sheet to ensure leak-free (vacuum tight to begin with) operation of the PHP. The entire assembly is illustrated in Figure 3-3.

As a precaution, before the assembly was tightened with the polycarbonate cover plate, a silicone based vacuum grease of Dow Corning make was applied over the O-ring to account for any undulations in machining which can cause leak or loss of vacuum [42]. The entire assembly of the PHP was mounted to a support plate which was clamped to a 180° swiveling vice to facilitate performance evaluation with varying inclinations. The inclinations were measured using the inclinometer mounted on the support plate (bottom inset in Figure 3-3).

3.4 Experimental setup

3.4.1 Evaporator and condenser

To apply heat load at the evaporator, two resistance heaters of flat configuration with 100 W capacity (Ohmite make - TEH100M2R00JE) were used. The two numbers of heaters each of 2 Ω resistance were used in series to have an overall resistance of 4 Ω. The two heaters were mounted on a copper plate of desired evaporator area and the assembly was fastened to the substrate by screws. The heaters were powered by Agilent make DC power supply (N5767A). To account for the drop in voltage through the connecting wires and leads the voltage was measured using a multimeter to get the actual heat power dissipated and the same was finely adjusted to achieve the desired heat load at the evaporator.

The condenser was cooled by a cold plate machined out of copper. The cold plate was fastened to the condenser zone of the PHP by screws. Water was circulated in the cold plate at an incoming temperature of 25°C to absorb the heat dissipated at the condenser of PHP.

The warmer water exiting the cold plate was cooled by passing the coolant through the re-circulating chiller (Bucchi make – F 305) as shown in Figure 3-4. The orientation was always with the evaporator below the condenser as shown in Figure 3-5.

3.4.2 Temperature and pressure measurement

The temperatures were monitored along the PHP length by 6 numbers of J-type thermocouples of Agilent make (U1185A) with accuracy ±1.0°C. These thermocouples were placed in the recesses in the PHP as shown in Figure 3-4. The responses of the 6 thermocouples were recorded with Picolog make TC-08, an 8-channel data logger which was interfaced with a computer for logging data for every one second.

A Honeywell make pressure transducer – PX2AG2XX002BAAAX with range of absolute pressure 0-2 bar was integrated into the PHP to ascertain the vacuum integrity of the PHP before charging as well as during the operation as in [42]. The entire setup was depressurized (vacuum) and left for 24 hours to estimate the leak rate. The leak rate was estimated to be of the order of 10^{-5} Torr-l/s. This was of the same order as indicated by the Adixen (Pfeiffer vacuum) model ASM182TD+ helium leak detector. The pressure data was recorded at sampling rate of 20 Hz using Keysight data acquisition system of 34980A. As seen in the literature [38] and [39] the frequency of the oscillations within the PHP is below 5 Hz. Thus the sampling rate satisfies the Nyquist criteria.

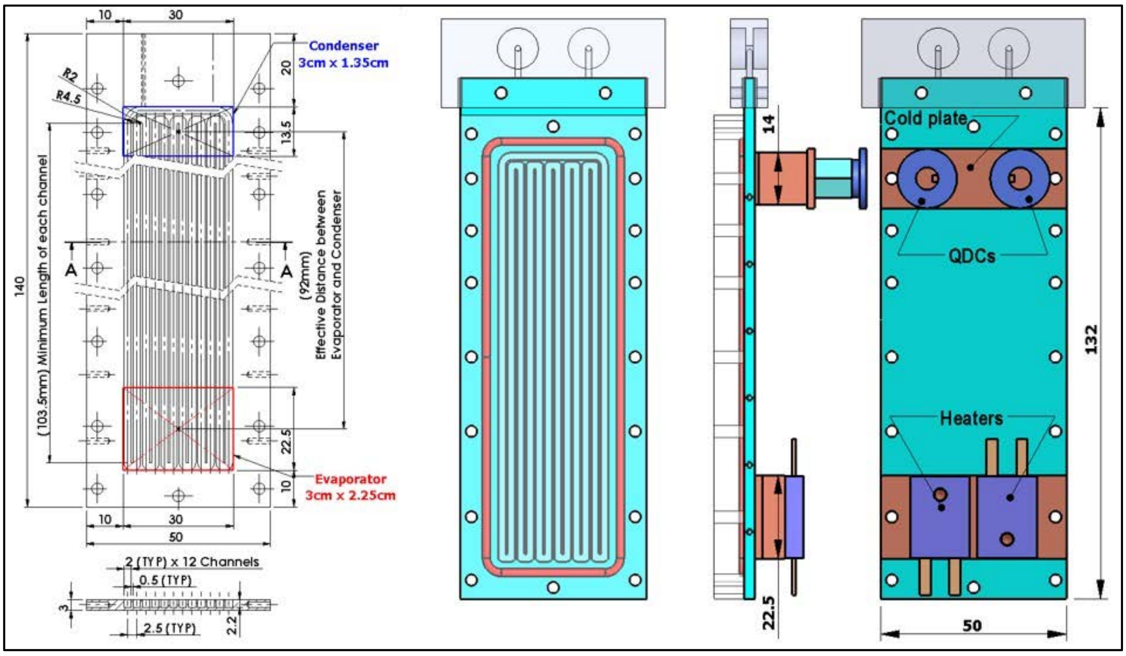

Figure 3-1: PHP substrate dimensions and details of the evaporator and condenser

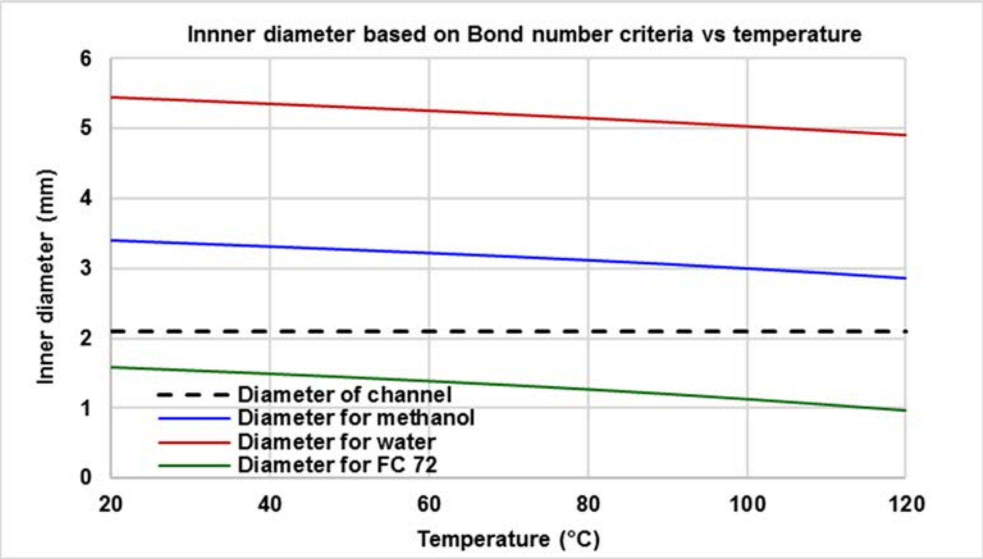

Figure 3-2: Inner diameter of the PHPbased on the Bond number criteria vs temperature

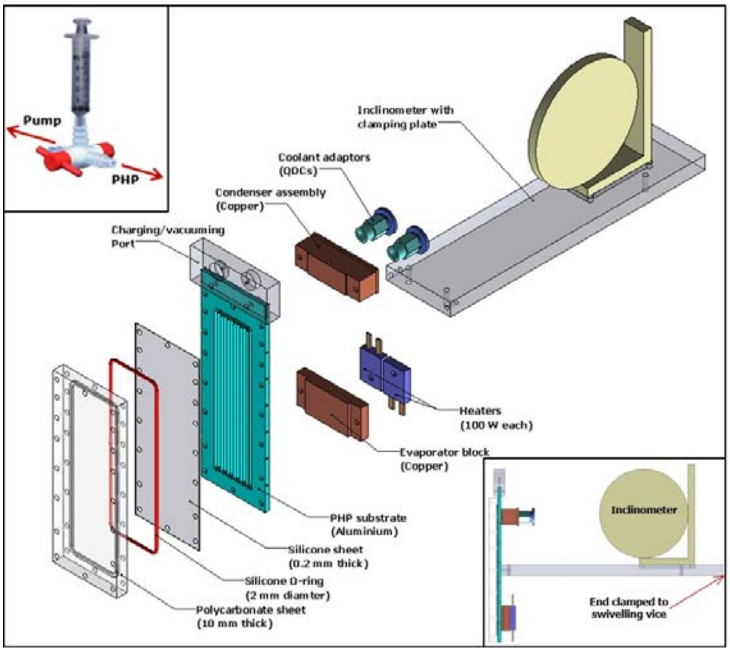

Figure 3-3: PHP assembly, charging procedure and inclination measurement

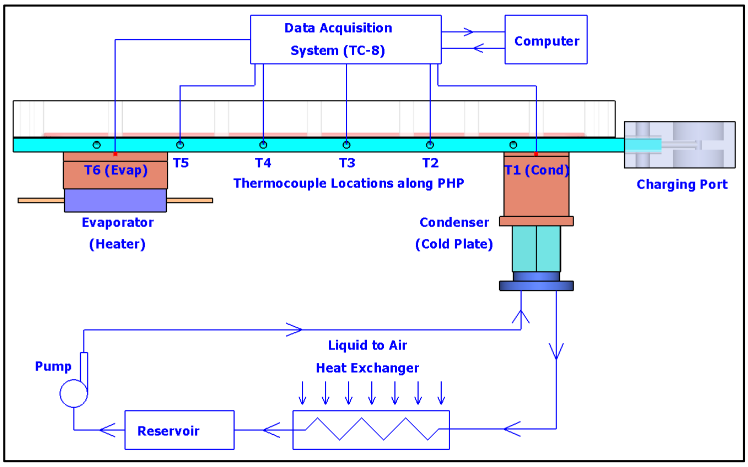

Figure 3-4: Schematic of the test setup

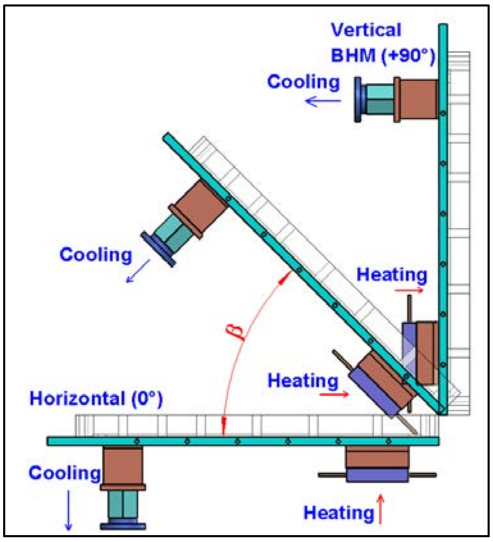

Figure 3-5: Orientation of the PHP with respect to horizontal

3.5 PHP Charging procedure

At the condenser, the PHP was provided with a charging block of polycarbonate, in which a hole was drilled to communicate with the channels. The charging block was connected to one of the ports of a Tarsons (890020) make 3-way stopcock. The second port of the stopcock was connected to a rotary-roots combination vacuum pump capable of 10^{-3} Torr (0.1 Pa). The third port of the stopcock was fitted with 5 ml syringe by which measured quantity of working fluid was admitted into the PHP. The setting up of PHP was as follows,

1. The stopcock handle was kept at 45° so that no port communicates with the other port. To begin with the stopcock handle was rotated to make the ports connecting the PHP and the vacuum pump communicate with the syringe being isolated. At this position the vacuum was created.

2. The stopcock handle was moved back to 45° position, in which all ports are sealed. The piston of the syringe was removed. The syringe was filled with the working fluid with 1 ml excess than the required charge (for example the syringe was filled with 5 ml when the charge required was 4 ml). This excess was used to prevent entry of air into PHP during charging.

3. Now the handle position was gently rotated to make the ports connecting the syringe and the PHP to communicate. Due to the atmospheric pressure being greater than the PHP channel pressure (vacuum of 0.1 Pa) the fluid entered the channel. After admitting the desired quantity of the liquid the stopcock handle was moved back to the 45° all ports sealed position. Here care was taken not to admit excess charge. The last 1 ml of the

charge was left in the syringe to act as a seal from the atmospheric condition. Now the syringe piston was put in place gently.

After the charging the working fluid self-distributed inside the channels as slug-plug combination as in shown Figure 3-6. This is due to the dominance of surface tension forces over the gravitational force (for Bo < 2) thus the liquid slugs are able to completely bridge the tube. This results in a meniscus region on either end of each liquid slug caused by surface tension at the solid/liquid/vapour interface.

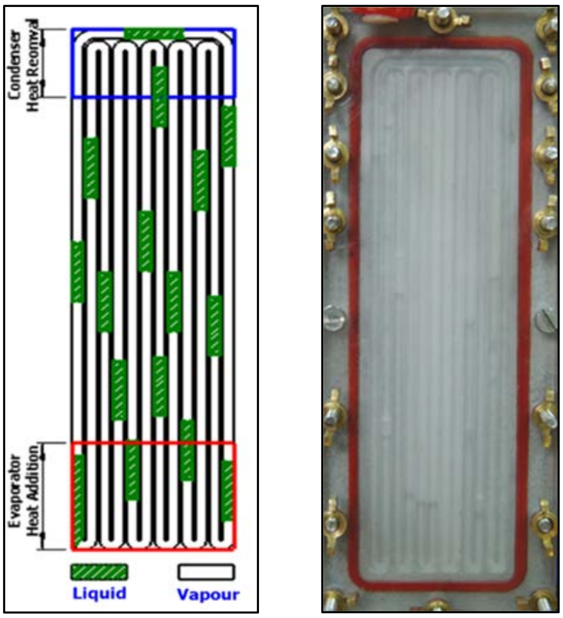

(a) Schematic b) Just after charging

Figure 3-6: Slug and plug formation of liquid and vapour after charging

3.6 Experimental protocol

The PHP was vacuumed for 60 minutes and the valve was closed towards the pump connection. Then the charging of the working fluid was done as mentioned above. The condenser cooling was switched on before heat load was applied to prevent excessive temperature rise. Once the cooling was applied to the condenser zone the computer and the interfaced data acquisition system were turned on. Then the power supply to heater was turned on and the current was adjusted to achieve the desired heat dissipation. The temperature data was recorded continuously (sampling rate 1 Hz). The test was conducted for a minimum of 15 minutes for the first data point to ensure steady state conditions. For the rest of the inclinations/loads (data points), the experiment was conducted for 10 minutes in each case as the entire assembly was already heated up and only an incremental change in temperature was expected.

3.7 Results and discussion

3.7.1 Benchmarking of the test setup

To begin with, the test setup was calibrated against the published data for 70% fill ratio of water for 50 W in the literature [15]. The results of the experiment with water as working fluid are summarized in Figure 3-7. The 90° inclination was taken as the vertical operation of the PHP with evaporator below condenser (refer Figure 3-5). In the entire study, the evaporator was always below the condenser with 7.5° being the least angle of inclination (which was close to being horizontal operation).

The PHP was then tested for the same 70% fill ratio with methanol as methanol was found to have most of the desired properties of a PHP working fluid. The PHP with water recorded a maximum temperature (as expected at evaporator) of 83°C for 90° inclination whereas the methanol yielded a temperature of 82°C. However, the T_c was almost constant for a given experiment (fluid) for all inclinations with variation of less than ±1.5 °C which can be attributed to the change in the ambient temperature during the experiment. For the PHP at 7.5° inclination the T_e reached 118°C and 99°C for water and methanol respectively.

The results show that the T_e variation up to 45° inclination was not substantial. The degradation from there on with each lower inclination was more significant. From Figure 3-8 it was evident that the temperature variation along the length of the PHP for 90° inclination for water matches fairly with the published data of [15] for the same experimental conditions. The results indicate that at 90° inclination the difference in performance between methanol and water was not substantial. In the vertical operation, as the gravity assists the transport of liquid from condenser to evaporator, water matches the performance of methanol though methanol has higher $(dP/dT)_{sat}$. However, when the inclination is far from vertical (like 45° and below) methanol having higher $(dP/dT)_{sat}$, [15], lower latent heat [27], lower density and lower viscosity was found to be a better working fluid for PHP. In the horizontal orientation, gravity does not aid the return of condensate to the evaporator for any fluid. The lower viscosity of methanol makes the pulsations better than water, thus resulting in the enhanced thermal performance in the near horizontal condition. This relatively reduced performance of water in near horizontal conditions has also been reported in [19] when fluids - ethanol and R123 were tested apart from water for various orientations.

In this study, the PHP inclination was changed from 90° in steps of 15° up to 30° for both water and methanol. Then the inclinations were changed and tested for every 2.5° up to 7.5°. The PHP continued the operation until the angle of inclination of 7.5° was reached with very low pulsations. Below this inclination the PHP failed to pulsate. Thus the critical tilt angle for this configuration of PHP was resolved to be around 10°-7.5°.

The visualization captured by video camera indicates that the oscillations are substantial until the 45° inclination and there on the oscillations become less severe with very low amplitudes between 15° to 7.5°. This phenomenon is very much evident from Figure 3-7 as the evaporator temperatures were substantially less for predominantly vertical orientations.

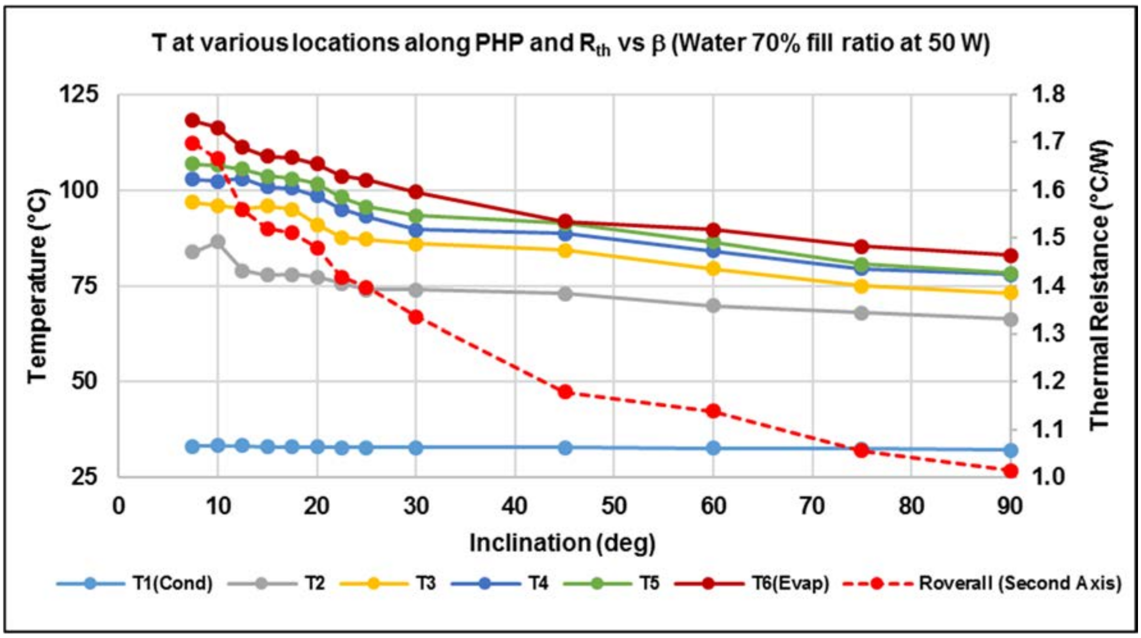

Figure 3-7: Temperatures along PHP vs inclination (water - 70% fill ratio - 50 W)

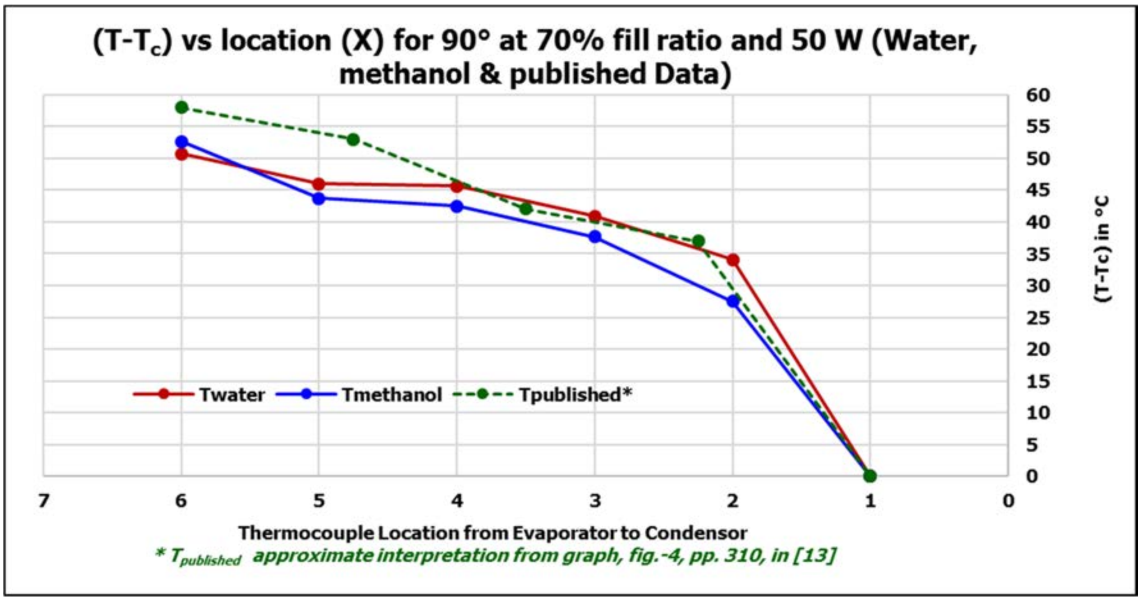

Figure 3-8: Temperature along PHP for 90° inclination and 70% fill ratio at 50 W

3.7.2 Estimation of heat loss

The heat loss to the ambient from the evaporator zone was estimated by considering the PHP as a heated vertical flat plate as this is the most favourable orientation for natural convection. Since the evaporator is restricted to 100°C, the adiabatic section is expected to be substantially lesser than 100°C. The temperature of the entire plate was considered to be 100°C (maximum allowed for safe heater operation). The calculation is as follows,

Temperature of evaporator	T_e	100	°C
Temperature of the ambient	T_{amb}	25	°C
Average temperature	$T_m = (T_e+T_{amb})/2$	62.5	°C
Acceleration due to gravity	g	9.81	m/s^2
Coefficient of volume expansion of air	$\beta_{air} = 1/T_m$	0.00298	1/K
Kinematic viscosity of air	ν_{air}	1.9×10^{-5}	m^2/s
Thermal conductivity of air	k_{air}	0.0283	W/m-°C
Characteristic length (L_e)	L	0.0225	m
Prandtl number	Pr	0.72	
Rayleigh number	$Ra = \frac{g\beta(T_s-T_a)L^3}{\nu^2}Pr$	4.98×10^4	
Nusselt number	$Nu = \left\{0.825 + \frac{0.387Ra_L^{1/6}}{[1+(0.492/Pr)^{9/16}]^{8/27}}\right\}^2$	7.81	[78]
Convective heat transfer coefficient	$htc = Nu*k_{air}/L$	9.81	W/m^2-°C
Width of the plate	w	0.05	m
Surface area for convection	$A_s = wL$	$1.125\text{x}10^{-3}$	m^2
Difference in temperature	$\Delta T = T_e-T_{amb}$	75	°C
Heat loss estimated due to convection	$\dot{Q}_{loss\_conv} = A_s * htc * (T_e - T_{amb})$	0.828	W
Emissivity of aluminium (polished)	ε	0.03	
Stefan Boltzmann constant	σ	5.67×10^{-8}	W/m^2-K^4
Heat loss estimated due to radiation	$\dot{Q}_{loss\_rad} = \epsilon * \sigma * A_s * (T_e^4 - T_{amb}^4)$	0.022	W
Total heat loss estimated	$\dot{Q}_{loss} = \dot{Q}_{loss\_conv} + \dot{Q}_{loss\_rad}$	0.85	W

Thus the heat loss is estimated to be 0.85 W for the maximum allowed temperature of the evaporator. This value is 1.7% of 50 W heat load (heat load in 106 instances out of the total 151 data points) and is considered negligible. Hence in the analysis of the data, the thermal resistance is defined for the heat load applied. The thermal resistance was used to compare the performance of the PHP for various orientations and fill ratios.

3.7.3 Effect of fill ratio with varying inclinations and fluids for a given heat load

After the calibration of the entire hardware, the experimental investigation was carried out to ascertain the effect of fill ratio on the performance of the PHP for a given heat load (50 W).

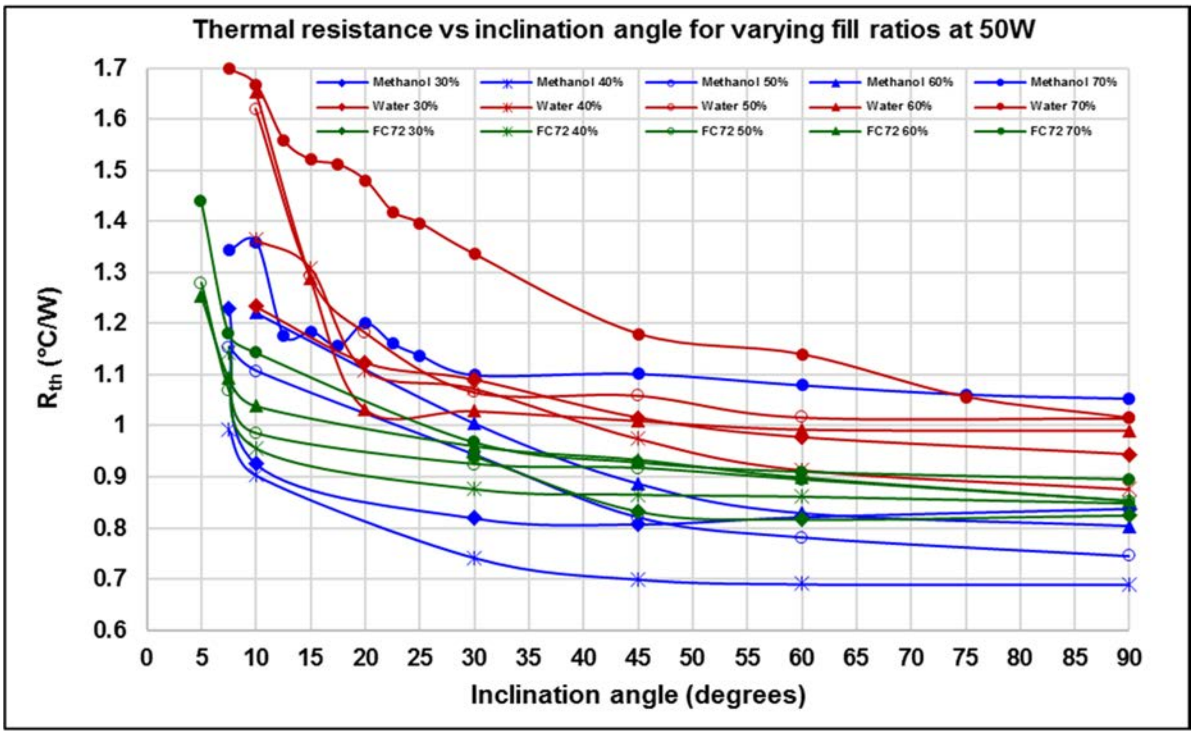

Figure 3-9: R_{th} vs inclination for various fill ratios

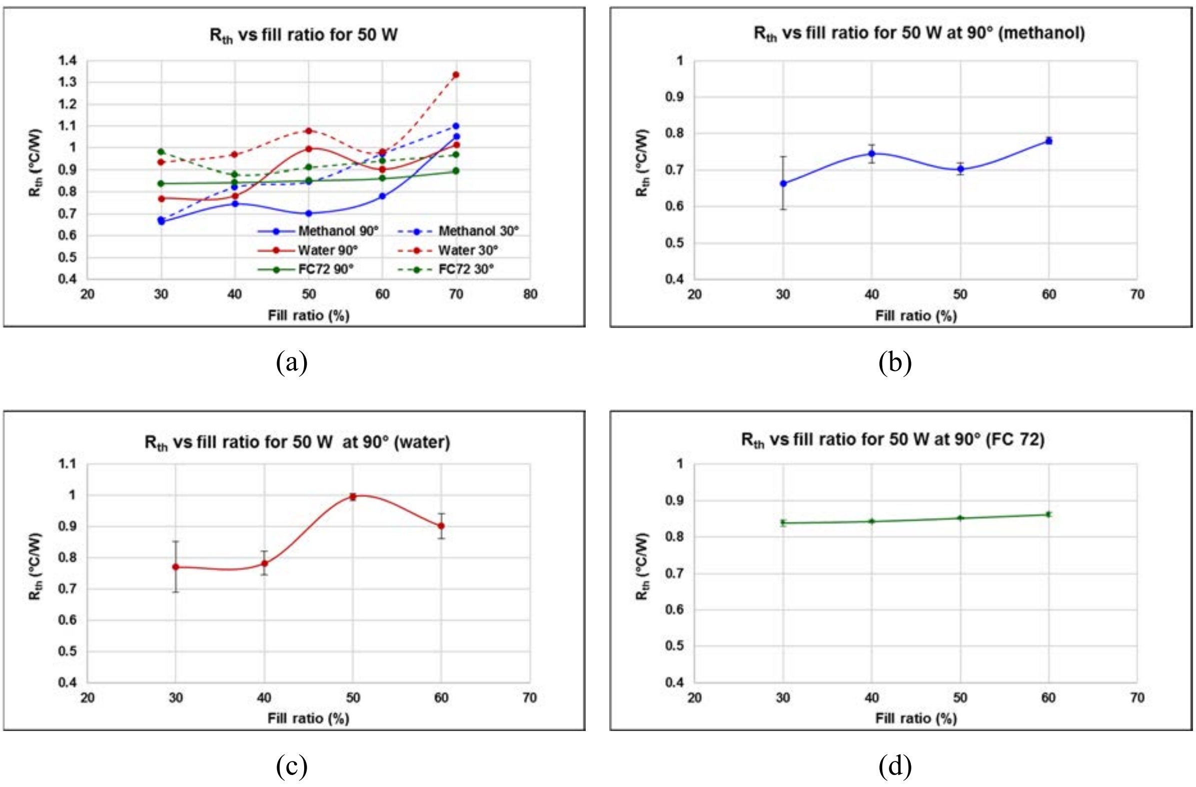

Figure 3-10: R_{th} vs fill ratio for 50 W heat load

The PHP was tested with various fill ratios – 30% to 70% in steps of 10%, with inclinations changed starting from vertical orientation in the sequence of 90°-60°-45°-30°-10°-7.5° for methanol and FC 72 whereas for water in the sequence of 90°-60°-45°-30°-20°-15°-10°. For water slightly larger angles of inclination as compared to methanol and FC 72 were chosen when investigating near horizontal orientations as the temperatures were found to fluctuate vigorously (explained in section 3.7.5) at lower angles of tilt. For each inclination minimum of 10 minutes was allowed so as to achieve the quasi steady state condition before moving over to the new inclination. The performance of the various fluids and fill ratios are compared using the parameter of thermal resistance given by

$$R_{th} = \frac{(T_e - T_c)}{\dot{Q}} \tag{3.2}$$

$$\dot{Q} = V * I \tag{3.3}$$

Figure 3-9 shows one set of trial with all three fluids. It can be inferred that the R_{th} values of 40% fill ratio was the most favourable across inclinations with least values for all the inclinations for all the fluids tested. The 40% fill ratio also yielded the least difference in R_{th} values across inclinations (most favourable vertical to least favourable near horizontal).

For all the three fluids – methanol, water and FC 72 the lower fill ratios (30% and 40%) were more effective in terms of lower R_{th}. The more volatile fluids performed well at lower inclinations owing to their larger $(dP/dT)_{sat}$ and lower viscosity. At 60% fill ratio and beyond the R_{th} values increased indicating that the fill ratios less than 50% is desirable for greater heat transfer.

The 70% fill ratio was the least effective followed by 60% fill ratio in performance as indicated by the curves in Figure 3-9. This has been reported in [23] as beyond 70% fill ratio the degree of freedom for oscillations decrease thereby resulting in diminished thermal performance. This figure also reinforces the fact that the performance of methanol and FC 72 as a working fluid is better than water and more so at near horizontal orientations for the same fill ratios. The visualization studies indicated that the corners of the channel were aiding the return of condensate from condenser to evaporator at lower inclinations (when gravity was not effective) as reported in [23]. However, due to lower latent heat and specific heat capacity of FC 72 at fill ratio of 30% the dry out occurred in the evaporator region in the PHP when tests were conducted at 10° inclination. The lower surface tension of FC 72 did not allow the return of condensate from the corners like in the case of methanol and water. Notwithstanding that the PHP with FC 72, could operate successfully at very low inclination of 5° at higher fill ratios (50%, 60% and 70%) unlike methanol and water which could not operate at angles less than 7.5°.

To ascertain the consistency of the results multiple experiments were conducted for each fill ratio for all three fluids for 50 W heat load with varying inclinations up to 30° orientation starting from vertical bottom heat position of 90° inclination. The average R_{th} values were plotted with respect to the fill ratio in Figure 3-10. The Figure 3-10 (a) also indicates that for methanol at lower fill ratios the difference in performance with respect to inclination was lesser. The optimum fill ratio for water tends to be lowest between 30% and 40%. For methanol, the good performing fill ratio was wider (30% to 50%) compared to water. FC 72 showed nearly the same performance across fill ratios in the vertical orientation but in the near horizontal orientation the lower fill ratio of 40% was favourable. From the tests conducted it can be stated that the performance of methanol was the best followed by water and FC 72 in case of near vertical orientations. In case of the near horizontal orientations, methanol was still the fluid of choice followed by FC 72.

Figure 3-10 also shows that the deviations (error bars) for the lower fill ratio of 30% is greater than that for the higher fill ratios. This can be due to the more variations in the spatial void fractions at the time of the experimental run in case of lower fill ratios leading to variations in the results.

3.7.4 Effect of heat load and inclination for a given fill ratio

The best performing fill ratio of 40% was chosen for further scrutiny with respect to varying heat loads as well as inclination. The above mentioned fill ratio was tested for only two inclinations – the best performing 90° and the near horizontal 10° (for methanol and FC 72) and 30° (for water) with varying heat loads in steps of 10 W starting with 10 W. The results are plotted as R_{th} vs heat load in Figure 3-11.

The heat loads were constrained by the criteria that the T_e should not exceed 100°C as a precaution for the safety of the experimental setup. As the inclination of 7.5° was ascertained as the critical tilt angle the tests were carried out at 10° for methanol and FC 72 and at 30° for water to ensure tests at substantial number of heat loads before reaching dry-out or prohibitively high evaporator temperatures. For water as working fluid at 40% fill ratio and 30° inclination was chosen for near horizontal orientation as water was found yielding higher evaporator temperatures at very low inclinations like 10°. The Figure 3-11 shows that the R_{th} decreases with increase in heat load as this leads to more vigorous pulsations which aids in heat transfer. This trend of lower R_{th} with higher heat loads is very similar to the ones reported in literature [71]. From Figure 3-11 it can be inferred that the R_{th} was lower for the vertical operation than for the near horizontal operation indicating the influence of orientation (gravity) on the performance of PHP.

3.7.4.1 Vertical orientation

With water as the working fluid, the heat load (maximum of 130 W) that could be attained was much more than any of the other two fluids in the 90° orientation. Methanol could be operated only up to 100 W while FC 72 could not be operated beyond 70 W. Thus water resulted as the fluid of choice in vertical orientation for higher heat loads. The tests revealed that for FC 72 lowest R_{th} occurred at 50 W and 60 W. As the heat load was increased to 70 W the R_{th} increased with heat load for FC 72. Further increase in heat load to 80 W resulted in dry out in case of FC 72. The T_e with FC 72 was always higher at every heat load tested for the 40% fill ratio in vertical orientation. However, methanol yielded comparable R_{th} to that of water up to 100 W beyond which T_e was prohibitively large hence the tests could not be continued with methanol as the working fluid.

3.7.4.2 Near horizontal orientation

When it comes to near horizontal orientation water was found yield the largest R_{th}. FC 72 could be operated only up to 30 W. FC 72 at 40% fill ratio could be tested for 50 W at 10° inclination in the changing orientation test carried out prior to changing heat loads. However, when the tests were started from 10° orientation, FC 72 could not be operated above 30 W despite repeated trials. This shows that the performance is dependent on the heating history as stated in [38] for FC 72. Methanol could be tested for 90 W but water could be tested only up to 80 W even though the inclination of test for water was only 30°. This shows that methanol can be a good fluid for PHP for most operating conditions of heat load and orientation with wider optimum fill ratio.

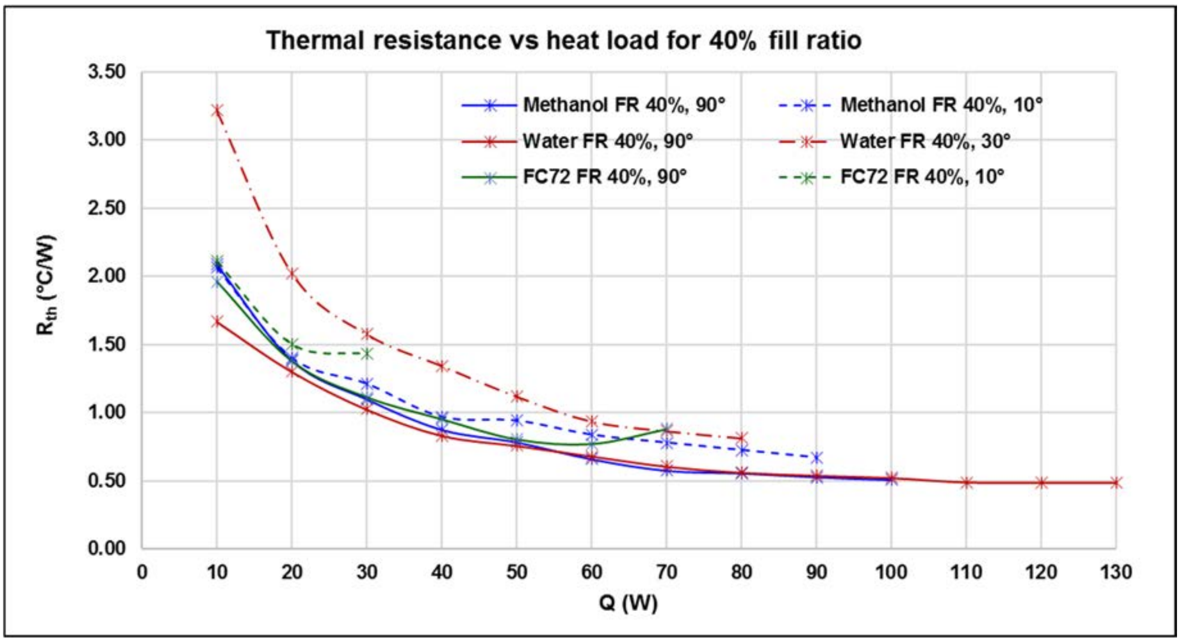

Figure 3-11: R_{th} vs heat load for 40% fill ratio at 90° and 10° (30° for water) inclinations

3.7.4.3 Flow regimes and pressure variation with heat load

For 10 W to 30 W heat loads (40% fill ratio) at 90° and 10° inclinations, the pulsations were moderate and all channels did not pulsate simultaneously. The flow regime in this case was of slug flow. The pulsations were of lower velocity up to 30 W. The slugs could not reach the top of the channel, or in other words could not travel the full length of the PHP except for FC 72 where the pulsations were comparatively larger, and could travel the entire length of the PHP at low heat loads of 10 W. The pulsations became more prominent at 30 W for FC 72 but the same could be observed only at 40 W for the other two fluids. For higher heat loads, the pulsations were vigorous and the slugs could travel the entire length and turn around at the condenser end. This manifested as reduction in R_{th} with the increase in the heat load. For the 10° inclination, at 10 W heat load the pulsations were very feeble and the slugs mostly travelled only up to half the length of the PHP channel. From 30 W heat input the slugs could complete the full length of the PHP and move to the adjacent channel at the condenser end for all the fluids.

In Figure 3-12, T_e and T_c along with the corresponding pressure (saturation) from transducer for 40% fill ratio of methanol at 90° inclination has been plotted with respect to time. Initially the PHP has the pressure equal to atmospheric pressure. The pressure transducer output was sampled at 20 Hz as the pulsations were reported to be around 3 Hz ([38] and [41]). When the vacuum pump was turned on, the lower pressure of the order of 0.1 Pa was reached. The pump is switched off and the fluid is admitted inside the PHP leading to rise in pressure equal to the saturation pressure of the fluid corresponding to the temperature of the PHP (in this case the PHP was at more than 30°C) at the time of charging. The Figure 3-12 also shows that the oscillations were very moderate until 30 W. After the initiation of 40 W, the pulsations were vigorous and the same has manifested as a dip in T_e (thus reduced R_{th}) after few minutes of 40 W heat load. Beyond this point the pulsations were of large amplitude with higher velocity. The vigorous pulsations are indicated by the large fluctuations of the pressure and temperature signals. The flow regime was of annular flow at higher heat loads (above 60 W). However, for water the flow regime was slug flow at condenser zone and was semi-annular at the evaporator zone for all the heat loads tested.

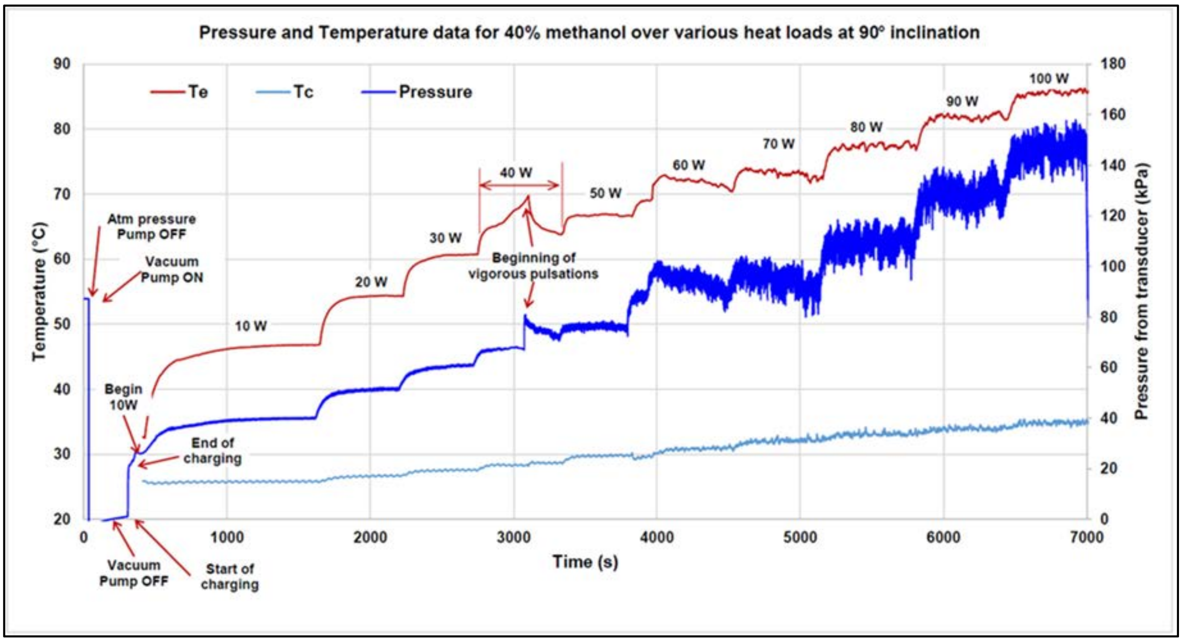

Figure 3-12: T and P vs t - 40% fill ratio; 90° inclination; methanol; varying heat load

Figure 3-13 shows the consolidated T_e and P_{sat} variation with respect to heat load (over time) for 40% fill ratio and 90° orientation for all three fluids. In this figure the initial vacuuming and the charging was not shown and the curve was plotted only from the start of the application of the 10 W heat load. The pressure was plotted as moving line average of 1200 points (corresponding to 1 minute as the sampling frequency was set for 20 Hz). Figure 3-14 shows the enlarged view of the 20 W to 40 W heat load zone of Figure 3-13. In this figure it can be clearly seen that a dip in the T_e occurs (corresponding dip in the P_{sat} as well) once the vigorous pulsations are initiated. This also followed by the decrease in T_e. This phenomenon occurs after 40 W in case of methanol and water whereas it occurs at 30 W itself for FC 72.

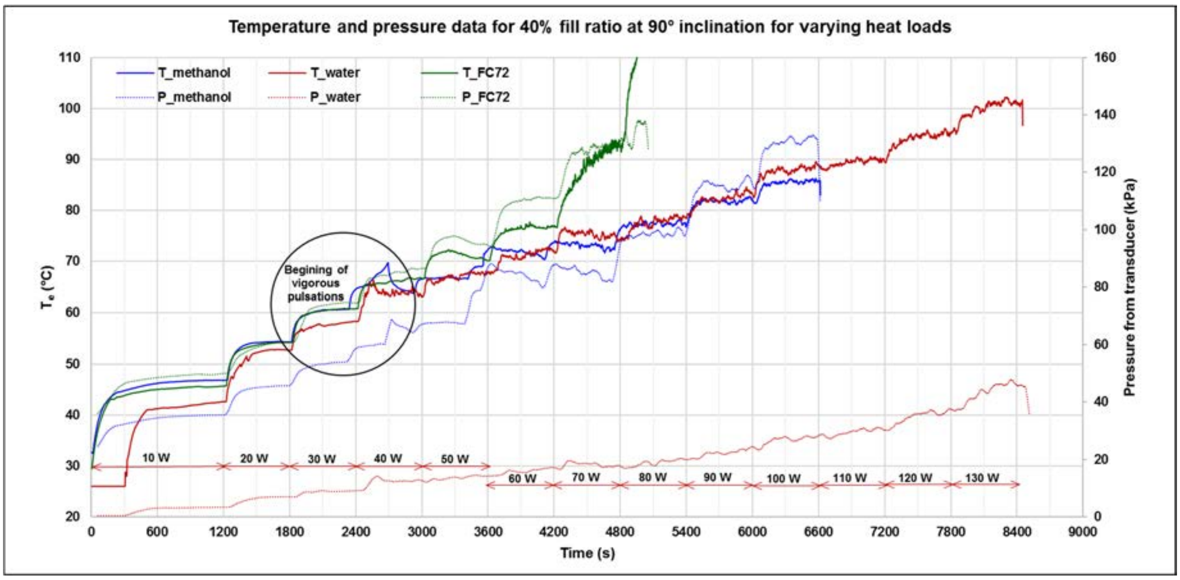

Figure 3-13: T and P vs t - 40% fill ratio; 90° inclination; varying heat load (3 fluids)

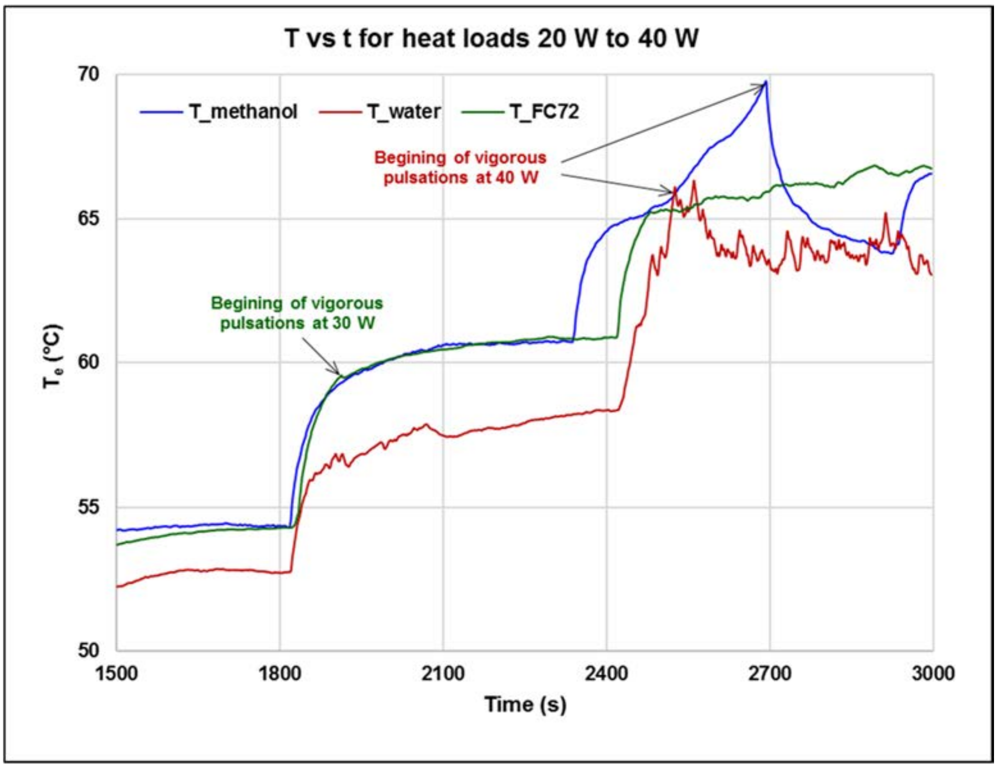

Figure 3-14: Enlarged view of T vs t at the onset of vigorous pulsations

The pressure transducer data (taken as an average of 60 s after 3500 s – not the moving line average as in Figure 3-13) is shown in comparison with the P_{sat} of the respective fluids for 50 W heat load at 90° orientation for 40% fill ratio in Table 3-1. The table indicates that the transducer pressure corresponds closely to the average of the P_{sat} at T_e and T_c though the transducer was located near the condenser. This adheres closely to the explanation of operating pressure stated in [45]. The pressure pulsations data in time domain was transformed to frequency domain using Fast Fourier Transform (FFT) and were plotted for estimation of the characteristic frequency of pulsations. FFT was performed using MS Excel (Fourier analysis under data analysis tools), where Gaussian kernel is used. The Fast Fourier transform plot shown in Figure 3-15 does not indicate any characteristic frequency as none of the peaks are seen beyond 0.5 Hz. In this PHP setup the transducer was located slightly away from the channel (a distance of 24 - 25 mm) in the PHP under study as shown in Figure 3-16. This distance between the transducer and the channel if minimised may yield more accurate measure of the pressure pulsations.

Table 3-1: T and P data comparison at 90° inclination, 40% fill ratio and 50 W heat load

Fluid	T_e	T_c	T_{avg}	P_{sat_Tavg}	P_{sat_Te}	P_{sat_Tc}	$P_{sat\_avg} = (P_{sat\_Te} + P_{sat\_Tc})/2$	P_{trans}
	°C	°C	°C	kPa	kPa	kPa	kPa	kPa
Methanol	68.95	29.68	49.32	54.1	120.4	21.6	71.0	81.8
Water	67.53	29.94	48.74	11.6	27.8	4.2	16.0	14.2
FC 72	70.63	29.78	50.21	79.3	158.4	35.4	96.9	95.1

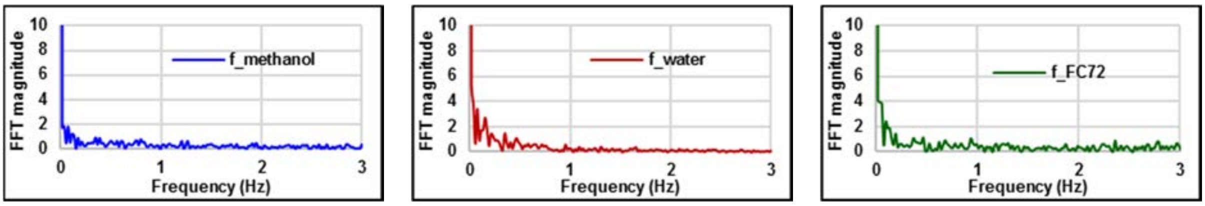

(a) (b) (c)

Figure 3-15 : FFT of pressure transducer signal - 50 W; 40% fill ratio at 90° inclination

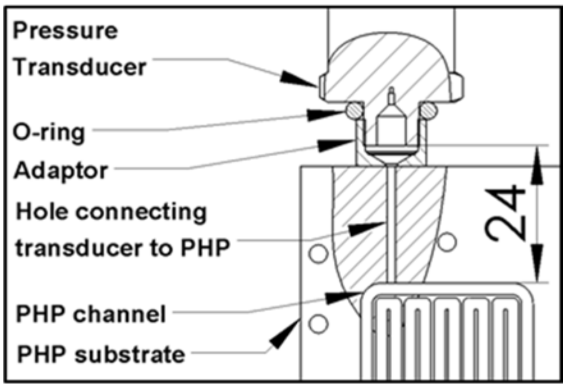

Figure 3-16: Connection and location of pressure transducer to the PHP substrate

3.7.5 Repeatability of the experiments and the critical tilt angle

The three experimental runs performed at 50 W heat load for 40% fill ratio with methanol, water and FC 72 for various inclinations starting from 90° was plotted as T_e versus time in Figure 3-17. The T_e were nearly the same for all the inclinations indicating the repeatability of the experiment. The T_e showed larger amplitude pulsations as the inclination angle was reduced to 10°-7.5°. The fluctuations were largest for water and least for FC 72. Once the inclination was changed to 5° the values of T_e started raising rapidly leading to aborting of the experiment (turn off the heat load) within few minutes after moving to 5° inclination.

In case of water as the inclination was reduced below 30° the fluctuations in the quasi steady state T_e was large that the estimation of correct steady state T_e was difficult. The T_e was ascending after 10° inclination indicating that the PHP cannot be operated beyond this inclination for water as working fluid. Figure 3-17 reinforces the fact that the critical tilt angle for the configuration of PHP investigated is between 10° to 7.5° for the tested fluids.

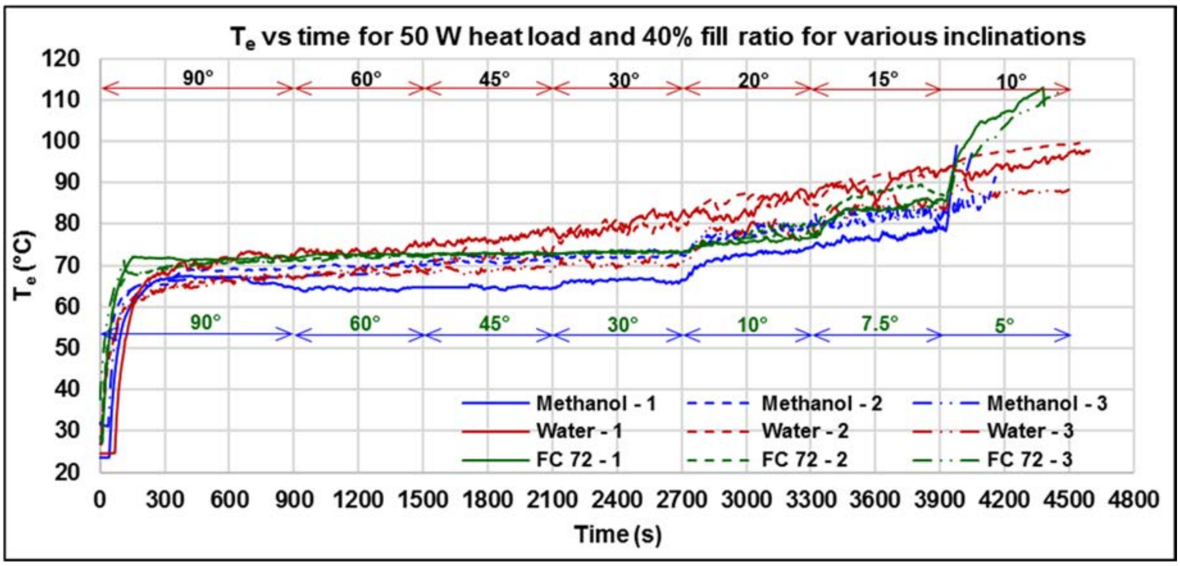

Figure 3-17: T_e vs t - 40% fill ratio; 50 W; varying inclinations 90° to 5° (3 trials)

3.7.6 Thermal resistance of PHP and the effect of PHP versus dry PHP

The overall thermal resistance of the PHP was defined by equation (3.2) as $R_{th} = (T_e - T_c)/\dot{Q}$. At 90° inclination, the overall thermal resistance with water as working fluid was 1.0 °C/W. This value has a very good match with the same configuration of experiment no. 1 of the literature [15].

$$R_{PHP} = \frac{1}{(1/R_{th})-(1/R_{Al})-(1/R_{PC})} \tag{3.4}$$

$$R_{Al/PC} = L/(kA_{cs}); \tag{3.5}$$

$$R_{th\_dry} = \frac{1}{(1/R_{Al})+(1/R_{PC})} \tag{3.6}$$

In the PHP under study, the overall thermal resistance was a combination of 3 parallel paths of heat transfer [79] – PHP effect, conduction through aluminium alloy substrate and conduction through polycarbonate cover plate as shown in Figure 3-18. The thermal resistance of the empty (unfilled) PHP of the same geometry will be given by equation (3.6). With R_{Al} being 5.2 °C/W (k_{Al} = 180 W/m-°C) and R_{PC} being 708 °C/W (k_{PC} = 0.26 W/m-°C), the $R_{th\_dry} \approx 5.2$ °C/W. The estimation of the thermal resistance of the empty PHP was also carried out experimentally with 10 W heat load (so as to keep the temperature to minimum at steady state). The temperature trace of T_e and T_c as well as the R_{th_dry} is shown in Figure 3-19. The experimental estimation of the R_{th_dry} showed the thermal resistance to be more than 3.8 °C/W. Thus the R_{PHP} can be estimated as 1.36 °C/W from the experimental value. When compared to the thermal resistance value of 1°C/W for 90° inclination and 70% fill ratio at 50 W for water from the experiment the thermal resistance can be reduced by almost 1/4th of that of an empty substrate. However, the least R_{th} of 0.5°C/W was obtained with methanol at 40% fill ratio, and 100 W heat load at 90° inclination. Thus, nearly 7.5 times enhancement of heat transfer could be achieved. This enhancement of thermal performance will be even more substantial if the substrate material is less conducting (non-metals) than that of aluminium used in this study.

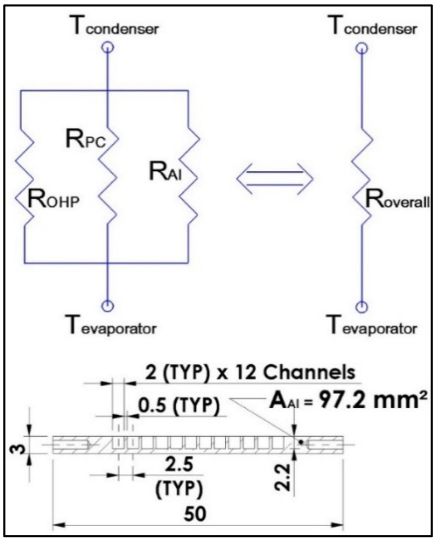

Figure 3-18: Thermal resistance network of PHP

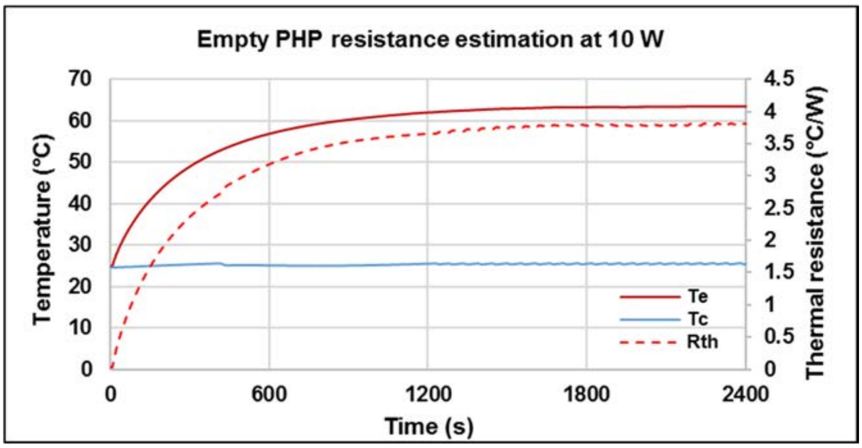

Figure 3-19: Estimation of thermal resistance of dry/empty PHP by experiment

3.7.7 Other possible factors affecting PHP performance

3.7.7.1 Contact angle hysteresis

From Figure 3-20 the contact angle hysteresis is given by $\Delta\theta = \theta_{front} - \theta_{rear}$ for liquid slug. As specified in [15], the lesser the contact angle hysteresis for a given solid-fluid combination, lesser is the resistance for the movement of the fluid. As $\theta_{front} > \theta_{rear}$, the capillary forces at the front and the rear of a slug will be $F_{cap\text{-}front} < F_{cap\text{-}rear}$ thus offering resistance to the flow. Thus more heat transfer occurs for minimum $\Delta\theta$ (contact angle hysteresis) as the pulsations will be less hindered. In this aspect methanol appears to be a fluid of choice for the PHP applications.

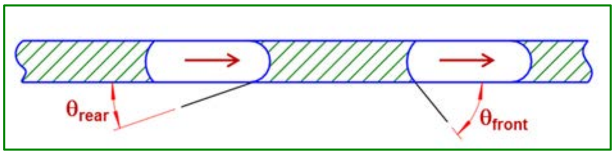

Figure 3-20: Forces across a slug with respect to moving direction

3.7.7.2 Pressure drop due to bend radius

Figure 3-21 indicates that the bend radius used in the present design of PHP is much smaller compared to the recommended minimum bend radius in piping. This smaller radius will result in more pressure drop (greater resistance) than the minimum bend radius shown adjacent. From practical stand point to pack more channels (thus more fluid inventory) sharp radii configuration is more favourable. However, a smoother bend will certainly lower the flow resistance as pressure loss in single phase flow in a smooth conduit bend is approximately the sum of pipe friction and a term accounting for the ratio of R/D where R is the radius of the bend and D is the diameter of the pipe [80]. Hence larger bend radius is beneficial from the pressure loss point of view, as this lower pressure loss will enhance the heat transfer by way of more vigorous pulsations. This aspect of flow resistance leading to reduced heat transfer performance of PHP have been reported in [23] and [71] where the authors have stated that in PHPs of comparable overall size, the ones with larger channels performed thermally better than the ones with narrower channels. The authors in [23] and [71] have attributed the diminished performance of narrower channels to the flow resistance of the narrower channel thus reinforcing the fact that lesser flow resistance leads to better thermal performance of PHP.

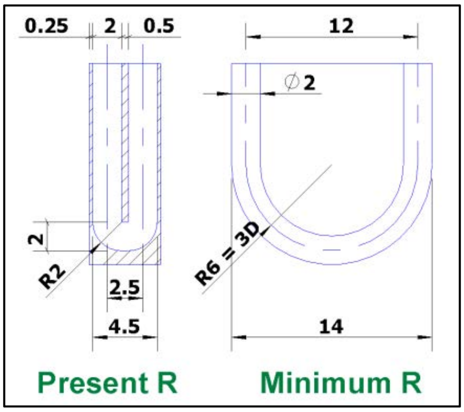

Figure 3-21: Bend radius vs flow resistance

3.7.8 Correlation modelling

3.7.8.1 Parameters for correlation

The operation of pulsating heat pipe is documented to have dependence on geometry of construction like size and shape of the channel, lengths of the evaporator, condenser and adiabatic sections and number of turns. The PHP performance is also dependent on working fluid properties like surface tension, latent heat of vaporization, specific heat capacity of liquid, viscosity of liquid, thermal conductivity of liquid, density of liquid and vapour apart from orientation with respect to gravity, difference between temperatures at evaporator and condenser and fill ratio of the working fluid. These parameters can be combined with judiciously chosen non-dimensional numbers to represent the working of the PHP.

The heat flux applied to the fluid of the PHP can be defined as

$$\dot{q} = \frac{\dot{Q}}{n(w+2t)L_e} \tag{3.7}$$

The critical heat flux (maximum heat flux) of the PHP in the pool boiling situation can be defined as

$$\dot{q_{max}} = h_{fg}\rho_v^{0.5}\left[\sigma g_{eff}(\rho_l - \rho_v)\right]^{0.25} \tag{3.8}$$

$$g_{eff} = gsin(\beta) \tag{3.9}$$

Kutateladze number from the experimental values is defined as,

$$\text{Ku}_{exp} = \frac{\dot{q}}{\dot{q_{max}}} \tag{3.10}$$

Kutateladze number can be arranged into a function of various non-dimensionless numbers as

$$\text{Ku}_{corr} = f(\text{Bo}, \text{Pr}, \text{Ja}, \text{Mo}, \phi) \tag{3.11}$$

The Bond number (Bo) represents the relative effect of buoyancy with respect to surface tension and is given by

$$\mathrm{Bo} = d\left[g_{eff}(\rho_l - \rho_v)/\sigma\right]^{0.5} \tag{3.12}$$

The Morton number (Mo) represents the interaction between the viscous, buoyancy, inertia and surface tension forces acting on a bubble formed by nucleate boiling in the evaporator section. In fluid dynamics, the Morton number is used together with the Bond number to characterize the shape of bubbles or drops moving in a surrounding fluid. Morton number also represents the effect of Froude, Weber and Reynolds numbers thus giving the combined effects of all the forces acting on the fluid within the PHP. The Fr, Re and We are not used in correlation directly as these numbers need the estimate of the velocity within the PHP which is not known upfront for any design activity. Morton number in this study is defined as given by [68].

$$\mathrm{Mo} = \frac{\mu_l^4 g_{eff}(\rho_l - \rho_v)}{\rho_v^2 \sigma^3} = \frac{We^3}{Fr * Re^4} \tag{3.13}$$

The Prandtl number (Pr) represents the ratio of momentum diffusivity to thermal diffusivity and is given by

$$\mathrm{Pr} = \frac{Cp_l \mu_l}{k_l} \tag{3.14}$$

The Jakob number (Ja) represents the ratio of the sensible heat to latent heat exchanged and is given by

$$\mathrm{Ja} = \frac{Cp_l(T_e - T_c)}{h_{fg}} \tag{3.15}$$

Another variable in this study was the fill ratio defined as the ratio of the volume of working fluid admitted inside the PHP to the total internal volume of the PHP and is given by

$$\phi = \frac{Vol_{fill}}{Vol_t} \tag{3.16}$$

3.7.8.2 Correlation for Ku

The 151 data points of the entire experiment was fitted into a correlation for Ku by multiple linear regression of all the above mentioned non-dimensional numbers which include the effects of all the parameters mentioned in the section 3.7.8.1. The general correlation of Ku is obtained as

$$\mathrm{Ku}_{corr} = 0.022\ \mathrm{Bo}^{0.153}\mathrm{Pr}^{-0.223}\mathrm{Ja}^{0.726}\mathrm{Mo}^{-0.073}\phi^{-0.47} \tag{3.17}$$

Figure 3-22 shows the comparison between the predicted values of the correlation (equation 3.17) and the experimental values for all data points. The above correlation was found to have a root mean square error of 0.259. Hence the data points of maximum deviations (summarised in Table 3-2) were removed and the correlation was refined as follows,

$$\mathrm{Ku}_{corr} = 0.022\ \mathrm{Bo}^{0.083}\mathrm{Pr}^{-0.037}\mathrm{Ja}^{0.708}\mathrm{Mo}^{-0.044}\phi^{-0.44} \quad (3.18)$$

Figure 3-23 gives the comparison of the predicted values of the refined correlation given by equation 3.18 and the experimental data points (146 points). The correlation proved more accurate with root mean square error of 0.193.

To predict the PHP performance at the most favourable orientation of 90° another correlation was made using the 42 data points obtained at 90° inclination and is given by

$$\mathrm{Ku}_{corr\_90} = 0.004\ \mathrm{Bo}^{-2.934}\mathrm{Pr}^{1.598}\mathrm{Ja}^{1.484}\mathrm{Mo}^{-0.206}\phi^{-0.43} \quad (3.19)$$

Figure 3-24 shows the comparison of the predicted values of equation 3.19 with the experimental values of the 42 data points. This correlation was found to have a root mean square error of 0.203. The details of all three correlations are summarised in Table 3-3.

Let us recall the correlation of Dehshali et al. [68] listed in Table 2-2:

$$Ku = f(\phi)Bo^{-2.259}Mo^{-0.101}Ja^{1.109}\left(\frac{L_e}{L_c}\right)^{-1.111}\left(\frac{D_i}{L_e}\right)^{1.400}\left(\frac{L_e}{L_{eff}}\right)^{0.658}(\exp(0.003Fr)) \quad (3.20)$$

Of the correlations listed in Table 2-2, the above correlation comes closest to present correlation (3.19) in terms of functional form. Comparing equation 3.19 with the above correlation, it can be clearly seen that there is a similarity in terms of the exponents of the respective non-dimensional numbers. The only difference is that in the work of Dehshali et al. [68], concerned with a rotating PHP, the role of gravity in bringing back the condensate to the evaporator is taken up by the centrifugal force.

Now let us recall the correlations for horizontal and vertical orientations proposed by Katpradit et al. in [64] also listed in Table 2-2:

$$Ku_0 = 53680\left(\frac{D_i}{L_e}\right)^{1.127}Ja^{1.417}Bo^{-1.32} \quad (3.21)$$

$$Ku_{90} = 0.0002\left(\frac{D_i}{L_e}\right)^{0.92}Ja^{-0.212}Bo^{-0.59}Wa^{13.06} \quad (3.22)$$

It is evident from equations 3.21 and 3.22 that the exponents of the non-dimensional numbers like Bo and Ja have a wide variation for different inclinations. A similar trend is observed in the present study as well for the correlations represented by equations 3.18 and 3.19. A plausible explanation for this variation is given in Section 3.7.8.3.

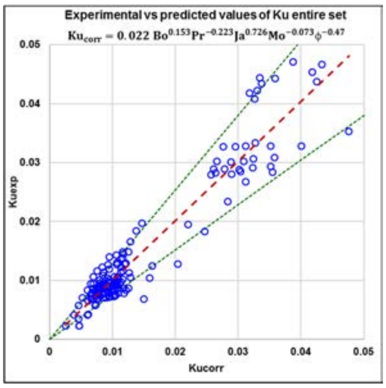

Figure 3-22: Experimental vs predicted values of Ku (entire data)

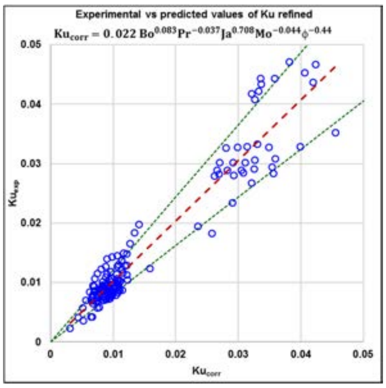

Figure 3-23: Experimental vs predicted values of Ku (refined data)

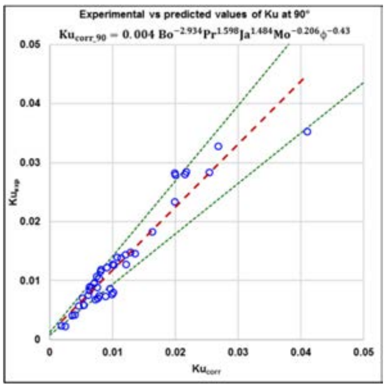

Figure 3-24: Experimental vs predicted values of Ku (for 90°)

In this study as the geometrical parameters were not varied the same have not been included in the correlation. The fluid properties (shown in Appendix – A) for the correlation were calculated using the data from [81] for methanol and from [82] for water and FC 72.

Here the RMSE is the root mean square error which is estimated as follows

$$RMSE = \left[\frac{\sum\left\{\frac{\mathrm{Ku\_}exp_i - \mathrm{Ku\_}corr_i}{Ku\_exp_i}\right\}^2}{Number\ of\ data\ points}\right]^{0.5} \tag{3.23}$$

Multiple R is the correlation coefficient which indicates the strength of the linear relationship, with 1 indicating perfect positive relationship. R^2 is the coefficient of determination which indicates the percentage of data points which adheres to the relationship predicted.

Table 3-2: Data points dropped for refinement of the correlation

Fluid	Heat load (W)	Inclination (degrees)	Fill ratio
Methanol	10	90	0.4
Water	10	30	0.4
FC 72	10	90	0.4
FC 72	10	10	0.4
FC 72	20	90	0.4

Table 3-3: Details of the correlations

Sl.No.	Correlation	Valid for angles	RMSE	Multiple R	R²
1	$\mathrm{Ku} = 0.022\ \mathrm{Bo}^{0.153}\mathrm{Pr}^{-0.223}\mathrm{Ja}^{0.726}\mathrm{Mo}^{-0.073}\phi^{-0.47}$ (151 data points)	10°≤β≤ 90°	0.259	0.94	0.86
2	$\mathrm{Ku} = 0.022\ \mathrm{Bo}^{0.083}\mathrm{Pr}^{-0.037}\mathrm{Ja}^{0.708}\mathrm{Mo}^{-0.044}\phi^{-0.44}$ (5 values dropped – 146 data points)	10°≤β≤ 90°	0.193	0.95	0.91
3	$\mathrm{Ku} = 0.003\ \mathrm{Bo}^{-2.934}\mathrm{Pr}^{1.598}\mathrm{Ja}^{1.484}\mathrm{Mo}^{-0.206}\phi^{-0.43}$ (42 data points)	β = 90°	0.203	0.96	0.92

3.7.8.3 Correlations in dimensional form

From equations 3.10 and 3.11 using the correlation 3.18, the dimensional form for the heat flux can be written as

$$\dot{q} = Ku_{corr}\,\dot{q}_{max} \propto \left[C_p^{0.671}\,h_{fg}^{0.292}\,\sigma^{0.341}\,\Delta\rho^{0.248}\,\mu^{-0.213}\,k^{-0.037}\,g^{0.248}\right] \tag{3.24}$$

Likewise, for the 90° inclination, using the correlation 3.19,

$$\dot{q}_{90} \propto \left[C_p^{3.082}\,h_{fg}^{-0.484}\,\sigma^{2.335}\,\Delta\rho^{-1.423}\,\mu^{0.774}\,k^{1.598}\,g^{-1.423}\right] \tag{3.25}$$

From equations (3.21) and (3.22), the following conclusions can be drawn.

- The exponents of the properties C_p and h_{fg} in equations 3.24 and 3.25 indicate that the relative contribution of sensible heat transfer is larger in case of the 90° orientation than for other inclinations. Thus the latent heat role is more pronounced as the PHP operates in other than vertical inclination.
- The exponents of μ and C_p indicate that in the vertical orientation the behaviour of PHP is more like forced liquid convective heat transfer.
- The surface tension plays a more dominant role for other inclinations than it does for vertical orientation.
- The exponents of $\Delta\rho$ and g in case of 90° inclination show a negative value indicating that the larger liquid density (as $\Delta\rho \approx \rho_l$) and gravity are counterproductive for the PHP operation in vertical orientation. However, the performance of the PHP at this (90°) inclination was the best. The plausible explanation for this behaviour can be that the Bo number criterion (namely, preference for smaller gravity force for a given surface tension to have slug-plug distribution) is outweighed by the larger gravity force ($\Delta\rho g$) which is responsible for better replenishment of the condensate in the evaporator. The correlation for the combined inclinations indicates less dependence on the gravity force.
- Comparison of equations 3.18 (all inclinations) and 3.19 (90° inclination), shows that the exponents of Bo and Mo are different. This can be attributed to fact that the non-dimensional numbers include acceleration due to gravity which is the main distinguishing feature of the 90° inclination.
- The exponents of Pr and Ja in both the equations (3.18 and 3.19) differ as C_p and μ are included in them. The larger contribution of specific heat capacity than latent heat of vaporisation in 90° inclination gives rise to rather wide variation of the exponents.

Table 3-4: Summary of the study vs the published data

	Parameter	Unit	**Literature** [15]	Present Work	Remarks
Experimental Details	L x W x D	mm	130 x 45 x 3	136 x 50 x 3	Additional 6 mm to accommodate charging port/valve
	Material		Aluminium	Aluminium	Same as [15]
	Fluid		Water	Water, Methanol and FC 72	Methanol and FC 72 - larger $(dP/dT)_{sat}$
	Number of channels	Nos.	12	12	Same as [15]
	Length of channel	mm	104	103.5 - 107.5	Same as [15]
	Distance between channels	mm	2.5	2.5	Same as [15]
	Channel dimension	mm x mm	2.2 x 2.0	2.2 x 2.0	Same as [15]
	Evaporator Area	mm x mm	30 x 22.5	30 x 22.5	Same as [15]
	Condenser Area	mm x mm	30 x 13.5	30 x 13.5	Same as [15]
	Effective distance between evaporator and condenser	mm	95	92	considered as distance between centres of evaporator and condenser
	Minimum fill ratio	%	10	30 (1.8 ml/5.77ml)	Water, methanol and FC-72; 30, 40, 50, 60 and 70% fill ratios
	Maximum fill ratio	%	70	70 (4 ml/5.77 ml)	
Results	Q (Q_{max})	W	50 (70)	10 to 130 W	In steps of 10 W
	$R_{th} = (T_e - T_c)/Q$	K/W	1-1.1	1	Reasonably good match with [15] for water at 50 W for 90° inclination
	Critical tilt angle for dry-out	degrees	5°-15°	7.5°-10°	At 7.5° very feeble oscillations; T_e relatively large compared with rest of the inclinations

3.8 Closure

A flat plate closed loop PHP was experimentally investigated for its performance with respect various orientations, different heat loads and fill ratios with 3 different working fluids – methanol, water and FC 72. The first experiment (with water) was used to bench mark the testing procedure and the test setup with the published data of [15]. The PHP test data was found to have very good agreement with the published data (comparison shown in Table 3-4). A pressure transducer was attached to the PHP to continuously monitor the integrity of the PHP for leakages. For a given heat load of 50 W various fill ratios of each fluid was tested. The best performing fill ratio was tested for varying heat loads for the favourable vertical (90°) and the near horizontal orientation (10°).

The salient observations are as follows,

1. For the inclinations in the range $45° \leq \beta \leq 90°$ ($0.707 \leq \sin \beta \leq 1$) (Figure 3-5), the difference in performance between the fluids across fill ratios was not substantial. However, methanol showed a better performance (though marginally) even in vertical orientation of 90°.

2. The degradation in the PHP performance occurred after 45° inclination for all the fluids up to which the performance was nearly the same.
3. The thermal resistance of methanol for predominantly horizontal operation was less than that of the other two fluids due to the combined effect of lesser density, lesser viscosity and higher $(dP/dT)_{sat}$ of methanol when compared to other fluids.
4. The lower fill ratios are better from heat transfer perspective than the higher fill ratios for water and methanol - like 30% to 40% for water, 30% to 50% for methanol, whereas for FC 72 the performance was more or less same from 30% to 60%. Thus the optimum fill ratio was wider for FC 72 and narrow for water.
5. Even in near horizontal inclinations the lower fill ratios were better performing but the optimum range was narrower compared to the vertical orientation for all fluids (refer Figure 3-10 (a)).
6. The lower fill ratio of 30% showed greater deviation (10%) while the higher fill ratios showed lower deviation (less than 5%) in R_{th} values thus higher fill ratios provide consistency of performance.
7. Even at the best fill ratios (for example 40%) the gravity had influence on the performance as indicated by higher R_{th} for lower inclinations for all heat loads when compared with 90° inclination.
8. For all fill ratios and tilt angles methanol R_{th} was lower than that of water and FC 72.
9. An attempt was made to resolve the critical angle below 15° (up to which was attempted in [15]) beyond which the PHP stops working. The critical tilt angle was ascertained as 10°-7.5° and the PHP restored its normal operation once the angle of tilt is reinstated to greater than the critical tilt angle.
10. The thermal performance of the substrate geometry (compared to empty or dry PHP) could be enhanced by nearly 8 times (R_{th} = 0.5 °C/W in case of 40% fill ratio of methanol at 90° inclination at 100 W with respect to dry PHP) due to the PHP operation.
11. At lower heat loads the pulsations were less prominent and with increase in heat loads the pulsations were more vigorous leading to reduction of R_{th} with increase of heat loads.
12. The flow regime was slug flow for heat loads less than 30 W. The flow regime was annular for methanol and FC 72 at heat loads above 50 W and 30 W respectively. However, for water the flow regime was semi-annular at evaporator and slug flow at condenser even for heat loads above 80 W.

13. A correlation was evolved with deviation of less than ±20% for Kutateladze number (prediction of heat flux) with 146 data points across fluids, fill ratios, inclinations and heat loads.

A part of the work pertaining to this chapter has been published as *Experimental investigation of flat plate closed loop pulsating heat pipe*, **P. Srikrishna, N. Siddharth, S. U. M. Reddy and G. S. V. L. Narasimham,** Heat and Mass Transfer, Springer, (2019)55:2637–2649– DOI: 10.1007/s00231-019-02607-z

4 Single loop pulsating heat pipe – Start up characteristics

4.1 Introduction

A single loop PHP is considered to be the building block of a PHP heat transfer device [47] of multiple turns which are either in single plane or sometimes arranged in multiple planes as in [36] and [52]. Though a PHP can operate successfully for all orientations, including both horizontal and vertical when number of turns in evaporator is more [10] and [19], a single loop configuration was chosen to understand the fluid dynamics (flow regimes) better. The results of the single loop were perceived to provide details towards realization of a robust numerical model for a multiturn PHP [47]. The single loop was pursued to have minimum joints thus have better reliability of the realization of the PHP with respect to sealing from the external atmosphere. In this study, focus was given to start up characteristics of the PHP as this aspect of the PHP is relatively less investigated. According to [44] two types of start-ups are possible for a PHP – one which is a sudden start with an overshoot of temperature at lower heat input and another with a more smoother rise of temperature without overshoot occurring at higher heat loads. Hence a range of heat loads starting from 10 W to 70 W in steps 10 W was tested at single fill ratio of 50% for single inclination of vertical bottom heated orientation.

4.2 Selection of fluid

A variety of fluids have been investigated and their properties with respect to the usage with PHP have been compared in [27]. The fluid to be used in PHP should have larger specific heat as most of the heat exchange occurs by sensible heat transfer [10]. It is also desirable to have fluid with lower viscosity to reduce pressure drops during operation. A fluid with lower latent heat is preferred due to shorter time for bubble formation thus quicker start-up. Apart from these desirable properties for a PHP fluid, another important factor is the rate of change in pressure with respect to temperature at saturated conditions, $(dP/dT)_{sat}$. This property affects the rate at which bubbles grow and collapse with respect to changes in temperature. At a high values of $(dP/dT)_{sat}$, the difference between vapour pressures in the evaporator and condenser will be increased and the performance of a PHP will be improved by enhanced oscillatory motion of liquid slugs [15].

Based on the above considerations and the compatibility with most metals that can be used for PHP construction, methanol was selected as the fluid for the present study, though water is the most commonly available fluid. The choice of acetone with even higher $(dP/dT)_{sat}$ was not pursued due to the perceived incompatibility with the epoxy adhesives used for glass to copper joints.

4.3 Selection of inner diameter

The internal tube diameter is one of the important parameters which essentially defines a PHP. The physical behaviour adheres to the 'pulsating' mode only under a certain range of diameters [13]. The critical Bond (Bo) number defines the diameter above which the PHP does not operate satisfactorily. Thus the critical diameter above which the PHP does not function effectively is given by equation 3.1 (chapter -3). For diameters lesser than the one given by equation (3.1), the fluid forms a slug-plug formation of liquid and vapour as shown in Figure 4-1. This critical diameter varies with temperature of operation as the properties of the fluid vary with the temperature. Figure 4-2 shows the variation of the critical diameter requirement with temperature. In the present study an inner diameter of 2.5 mm is chosen to have a favourable Bond number throughout the range of operation of temperatures.

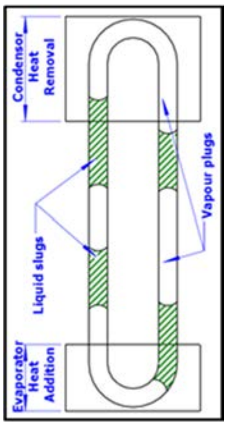

Figure 4-1: Single closed loop PHP - slug-plug formation

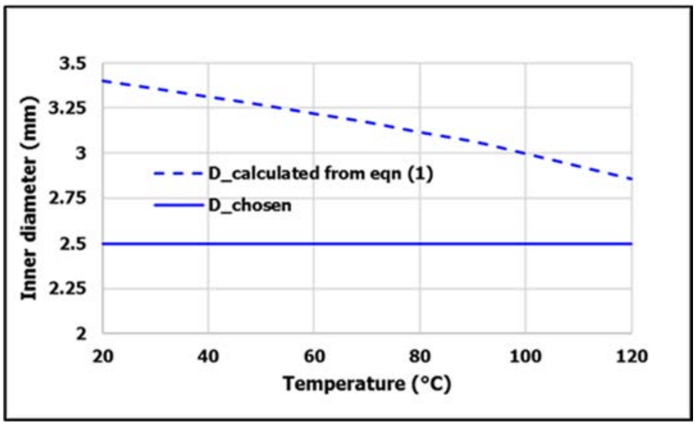

Figure 4-2: Inner diameter based on Bond number for varying temperature

4.4 PHP construction and geometry

The single closed loop PHP was constructed with copper blocks as evaporator and condenser. The evaporator and the condenser blocks were machined with channels of diameter matching the outer diameter (4 mm) of the copper tubes used for the PHP. The evaporator and condenser blocks were brazed with copper tubes for better heat transfer. The intermediate adiabatic section was formed using glass tubes (OD 4.8 mm and ID 2.5 mm) which were connected to copper tubes with copper adaptors to form the loop of PHP. The glass tubes were used to have a viewing window to study the flow regimes of operation of PHP for various heat loads. The copper tube to copper adaptor joints were carried out by brazing, whereas the copper adaptor to glass joints was completed using epoxy adhesive. The overall length of the PHP was 190 mm and the distance between the two limbs was 12 mm (with the bend radius being 6 mm). The constructional (with various parts) details and the geometry of the PHP fabricated are shown in Figure 4-3.

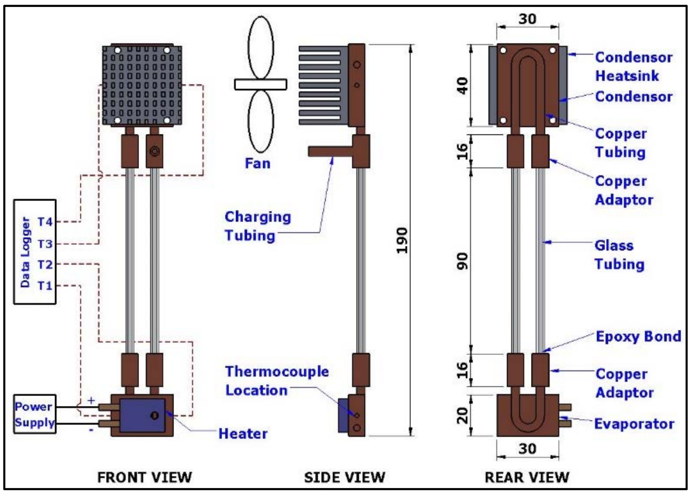

Figure 4-3: Geometry and constructional details of SLPHP

4.5 Charging procedure

The PHP was brazed with a copper tube for charging at the adaptor connecting the glass and the copper tube near the condenser. One of the ports of the Tarsons make (890020) 3-way stop cock was connected to the charging copper tube. Another port of the stop cock was connected to the turbo molecular vacuum pump capable of achieving vacuum of the order of 0.01 Pa. The third port of the stop cock was connected with a 2.5 ml syringe. The total volume of the PHP was estimated as 1.6 ml. The additional volume of the charging tubing and stopcock was estimated to be 0.4 ml. Hence to have a 50% charging ratio (volume of fluid admitted/ volume of the PHP) 1.2 ml of fluid had to be admitted to account for 0.4 ml that would remain in the additional tubing and stop cock. Thus only 0.8 ml will be admitted inside the PHP resulting in 50% charging ratio. The charging ratio of 50% was chosen as best performance with respect to heat transfer was reported to occur above 40% charge ratio [19] and [83]. The setting up of the PHP is as follows,

1. The 3-port stopcock handle is kept at 45° so that no port of the stopcock communicates with the other port to begin with. As one of the port is connected to the vacuum pump, the stopcock handle is rotated to make the ports connecting the PHP and the vacuum pump to communicate and at the same time keeping the syringe attached to the third port isolated. Now the vacuum is created to an order of 0.01 Pa.

2. The stopcock handle is moved back to all ports sealed 45° position. The piston of the syringe was removed. The syringe was filled with the working fluid with 1 ml excess than required charge (for example the syringe was filled with 2.2 ml as the charge required is

1.2 ml). This excess is done to avoid entry of ambient air into the PHP during the charging. The excess 1 ml will be left out in the syringe.

3. Now the handle position was gently rotated to make the ports connecting the syringe and the PHP to communicate. Due to the atmospheric pressure being greater than the PHP internal pressure (vacuum) the fluid was admitted inside the PHP. Here care was taken not to admit excess charge. The last 1 ml of the charge was left in the syringe. Now the charging copper tubing was pinched-off (cold welded) using a hydraulic pinch-off tool.

After the charging the working fluid (methanol) self-distributed inside the channels in the form of slug-plug combination as shown in Figure 4-1.

4.6 Experimental set up

4.6.1 Evaporator and condenser

Heat was supplied at the evaporator through a thin film resistance heater of CADDOCK make – MP 9100 of 8 Ω resistance and maximum capacity of 100 W. The heater was powered by APLAB make DC power supply (32 V and 10 A maximum) to get desired heat loads ranging from 10 W to 70 W in steps of 10 W. To account for the voltage-drop in the connecting wires from the power supply to the heater leads, the voltage was measured at the heater leads using a multimeter of ±0.1 V resolution.

The condenser was cooled using an aluminium heat sink with an axial fan of 80 mm × 80 mm × 25 mm. Hence at both evaporator and the condenser a constant heat flux boundary condition prevailed in the testing.

4.6.2 Data collection

A total of four J-type thermocouples (accuracy ± 1°C) – 2 thermocouples on either side of the evaporator and the condenser were used for monitoring the temperatures at the evaporator and the condenser. The thermocouples were planted in the holes drilled on either side of the evaporator and the condenser. The temperatures were logged using a 4 channel data logger (RS1384) with a sampling rate of 1 Hz for each channel. The schematic of the power supply and the data collection is shown in the front view of Figure 4-3. The entire data logging was interfaced with a computer for further post processing of the temperature data obtained over time for each heat load. The entire test setup is shown in Figure 4-4.

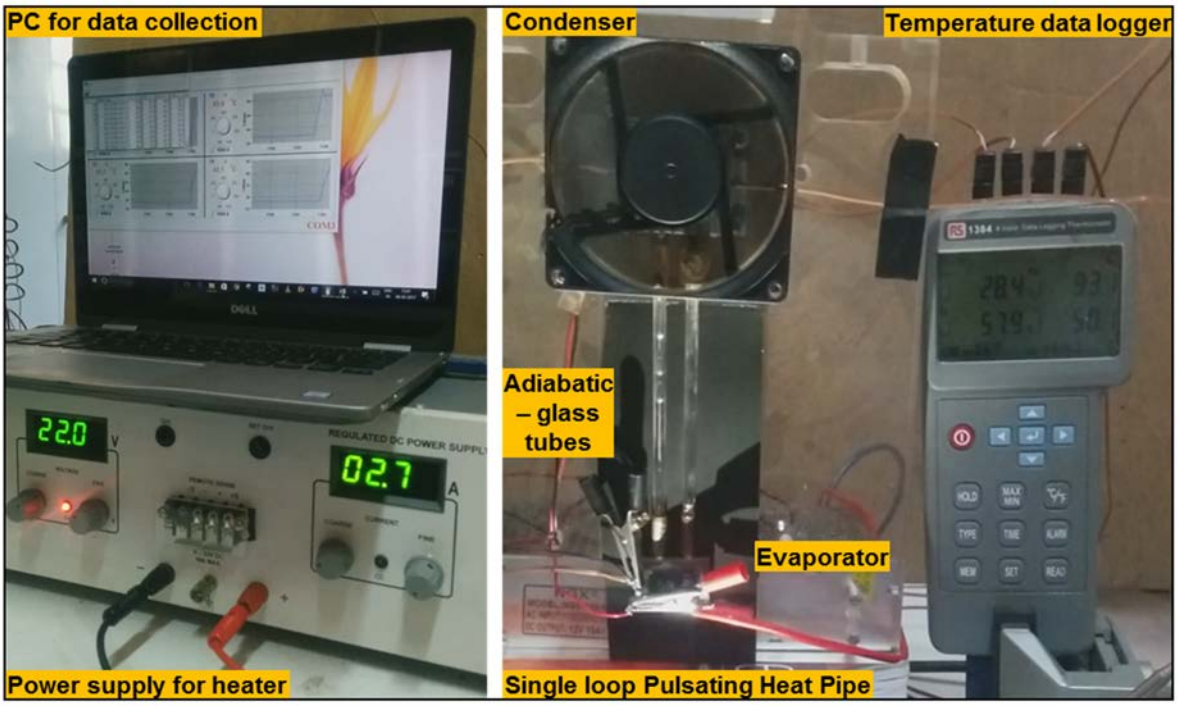

Figure 4-4: Experimental setup and the PHP

4.7 Experimental Protocol

The PHP after charging was clamped in the vertical position with the evaporator below the condenser. Hence throughout this study the orientation of the PHP was not varied. Since the PHP was pinched off, the fill ratio was also not varied in this study. The 4 thermocouples were planted in the respective recesses made in the hardware. The condenser fan was switched on before the evaporator heat load was applied to prevent any excessive temperature raise. Then the interfaced data logger was turned on. The power supply was switched on and the current was adjusted to achieve the desired heat dissipation. The temperature data was recorded for every 1 second for each channel. The start-up and the steady state data was recorded. The test was conducted for each heat load for a minimum of 10 minutes to ensure steady state operation. After each heat load the heater was turned off for at least 30 minutes. The PHP was allowed to reach the ambient temperature before the next heat load was tested. For higher heat loads the tests were conducted for 15 minutes to ensure steady state (less than 1°C change in 5 minutes for all thermocouples).

4.8 Results and discussion

The tests were conducted for heat loads of 10 W to 70 W in steps of 10 W. The tests were repeated for all heat loads for three trials on 3 different days to check the repeatability. During the course of the experiment the ambient temperatures were also noted at the end of each heat load. The ambient temperatures across 3 trials for all heat loads ranged between 26°C to 28°C.

4.8.1 Estimation of heat loss

The heat loss from the evaporator was calculated as follows:

The surface area (for the dimensions refer Figure 4-5(a)) of the evaporator block is given by

$A_e = 2*2*(W+B+D) = 232 \times 10^{-6} m^2$ (4.1)

Rayleigh number, $Ra = \frac{g(T_e - T_{amb})L^3}{\nu_{air}^2 T_m} = 4.9 \times 10^4$ (4.2)

where

Surface temperature, T_e = 111°C (maximum T_e occurring at 70 W is considered)

Ambient temperature of air, T_{amb} = 26°C

Acceleration due to gravity, g = 9.81 m/s²

Characteristic length, $L = B$ = 20 mm (as per geometry)

Mean temperature, $T_m = (T_e + T_{amb})/2 + 273.15$ (4.3)

Kinematic viscosity of air, $\nu_{air} = 1.996 \times 10^{-5}$ m²/s

Thermal conductivity of air, k_{air} = 0.02881 W/m-°C

Using the Nusselt number correlation from [78]

$$Nu = \left\{0.825 + \frac{0.387 Ra^{1/6}}{\{1+(0.492/Pr)^{9/16}\}^{8/27}}\right\} = 7.78 \quad (4.4)$$

Heat transfer coefficient, $htc = Nu * k_{air}/L$ = 11.21 W/m²-°C (4.5)

Heat loss, $\dot{Q}_{loss} = A_e * htc * (T_e - T_{amb})$ = 0.22 W (4.6)

The heat loss estimated is very small. This quantity will be not substantial even if radiation effects are included. This loss of heat is only a fraction of the input power even for the lowest heat load of 10 W. Hence the loss of heat from evaporator surface was neglected for further calculation and post processing of the results.

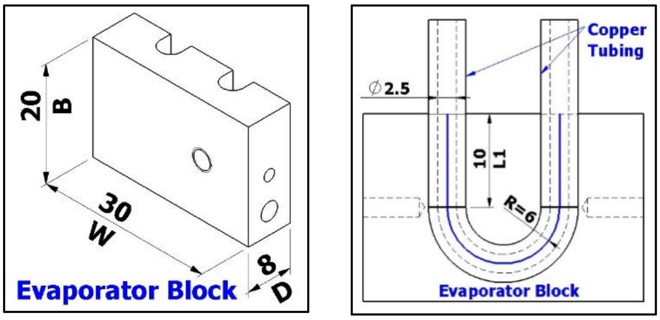

(a) (b)

Figure 4-5: Geometry of evaporator

4.8.2 Estimation of evaporator heat flux

The internal heat flux which is instrumental for the pulsations of fluid was calculated as follows,

$A_s = \pi * d * (2 * L_1 + \pi R) = 3.05\ cm^2$ (4.7)

$\dot{q} = \dot{Q}/A_s$ (4.8)

The dimensions for the calculations are shown in Figure 4-5(b).

4.8.3 Start-up characteristics

1. Figure 4-6 to Figure 4-8 shows that the operation of the PHP was in the diode mode throughout the heat load of 10 W. The pulsations started after considerable time (more than 2 minutes) but after the start the pulsations were not continuous but intermittent. This can be observed from the fact that the T_e oscillates substantially with a very low frequency unlike the other heat loads where a steady state value was observed. The PHP operated like a diode. The pulsations occur bringing down T_e, after a lower threshold of T_e was reached the pulsations stopped resulting in increase of T_e till an upper threshold was reached beyond which the pulsations reoccurred. This kind of operation was reported for the lower heat loads in [22]. This also manifests into relatively large R_{th}. This indicates that the PHP was not fully operational for the 10 W heat load.

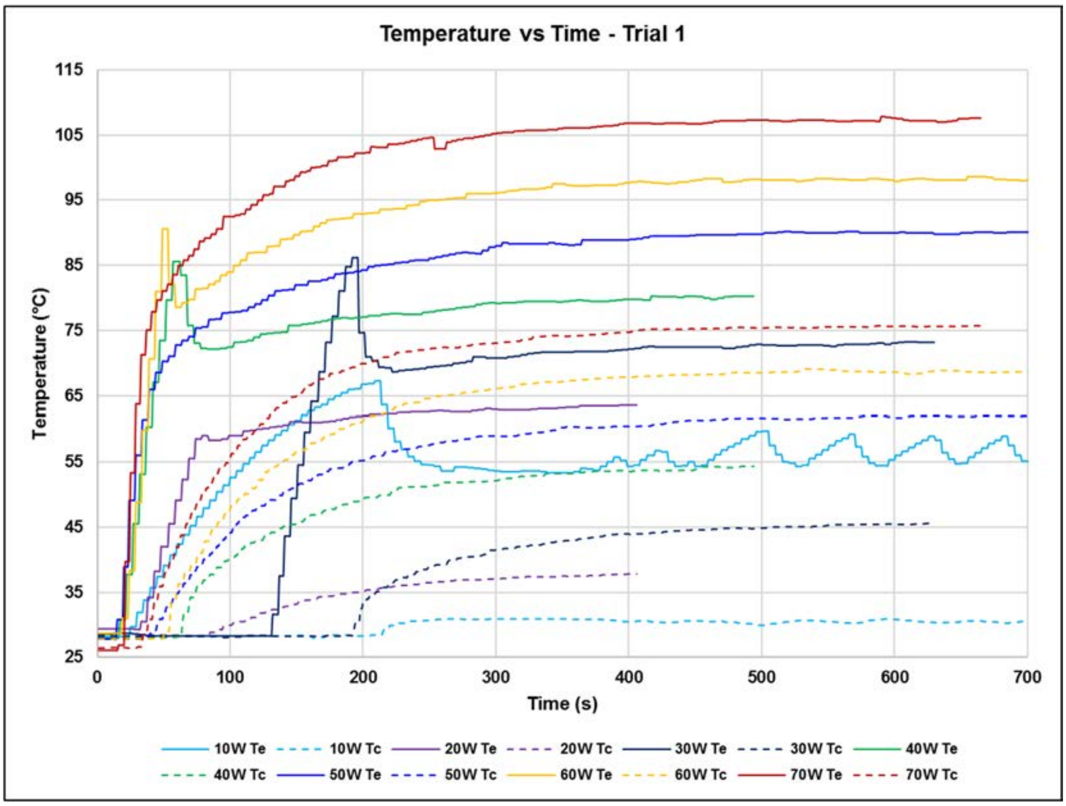

Figure 4-6: Temperature vs time - SLPHP - Trial 1

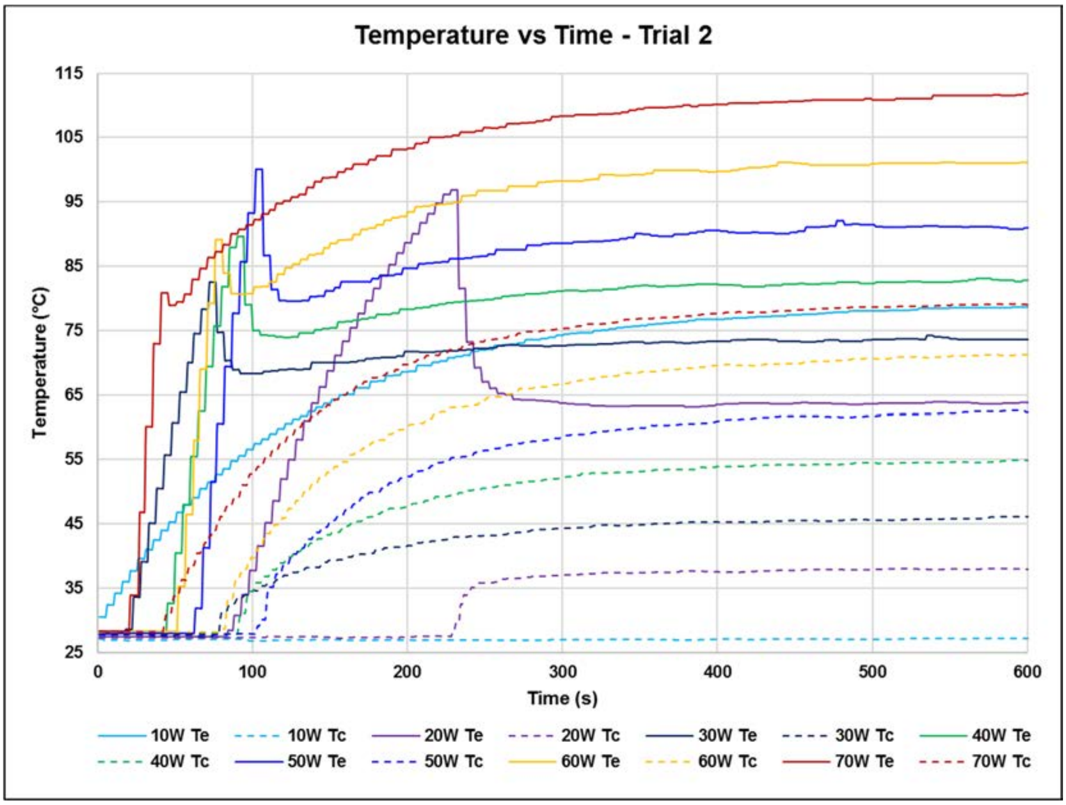

Figure 4-7: Temperature vs time - SLPHP - Trial 2

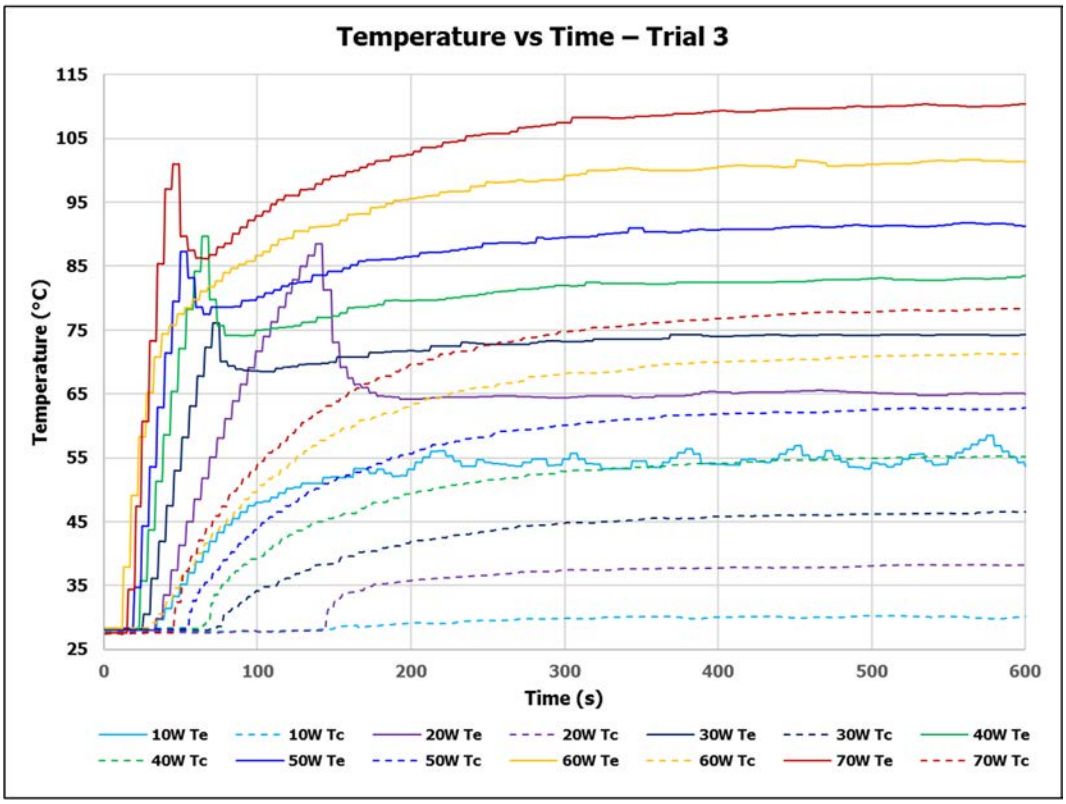

Figure 4-8: Temperature vs time - SLPHP - Trial 3

2. The two types of start-up were observed for various heat loads. One was the sudden start up mostly at lower heat loads where the T_e initially rises monotonously till the pulsations occur. Once the pulsations start the T_e comes down with simultaneous rise of T_c (refer curves for 30 and 40 W in Figure 4-6) indicating the heat transfer from evaporator to condenser. This is due to requirement of more time to accumulate energy needed to initiate the PHP to start up. This was described as a ‘‘sudden start-up mode” in [46]. For higher heat loads T_e change was smooth during the start-up and reached a steady value which was higher than the initial start-up value (refer curve for 70 W in Figure 4-6). This was described as a ‘‘smooth start-up mode” in [46].
3. The sudden or smooth start-up was not restricted to low and high heat loads across trials as reported in [44] and [46] as one can see sudden start-up even for the highest heat load of 70 W in trial 3 (refer Figure 4-8). Hence the kind of start-up not only depends on the heat load but also on the void fraction distribution at the beginning of application of the heat load. The other reason for various kinds of start-up for the same heat load may be due to the fact that only up to 70 W could be tested ($T_e < 100$°C). For the configuration of PHP tested, heat loads higher than 70 W might have consistently yielded the smooth start-up.

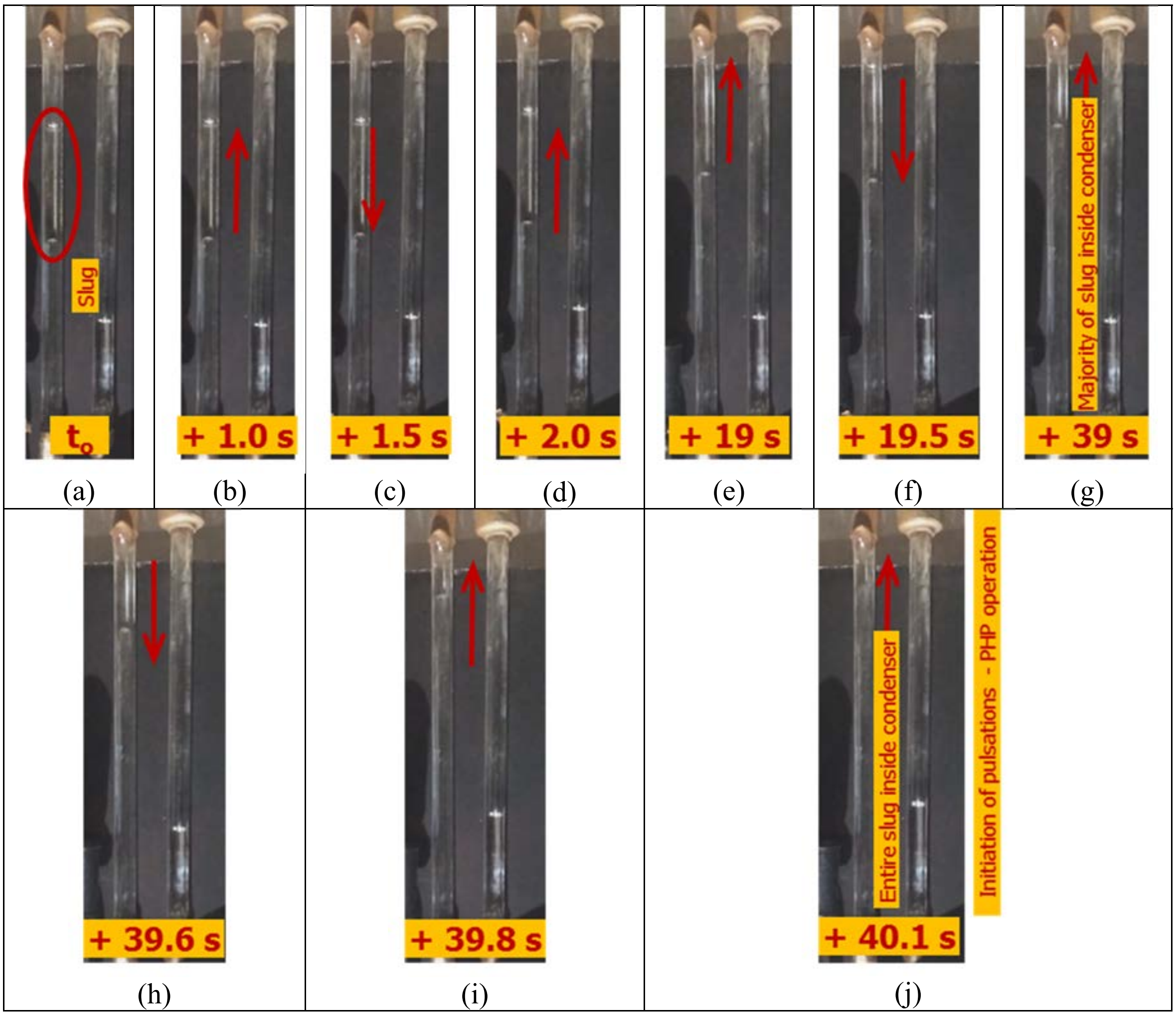

Figure 4-9: Start-up details of 10 W heat load

4. Though sudden start was observed at higher heat load the T_e at the time of start was less than the steady state T_e. Whereas in case of lower heat loads T_e at start was higher than the steady state value of T_e. Hence to have a PHP operating satisfactorily in a practical application it is desirable to have a threshold heat flux for start-up or else the maximum allowable temperature should be higher than the start-up T_e. Otherwise the start-up temperature at evaporator might exceed the steady state values thus resulting in failures. This is evident from Figure 4-8 where the start-up T_e of 20 W and 40 W was higher that the steady state value of 50 W.
5. Not only the time to start reduced with heat load but also the time between the peak start-up T_e and the time to establish steady state value (i.e., T_e just after the dip) reduced with increase in heat loads.
6. Apart from recording the temperature data for every 1 second, to observe the flow regimes the PHP operation at various heat loads were video graphed and observed with slower play back speeds as low as 0.125 X of the actual speeds. Figure 4-9 shows the

evolution of the start-up for 10 W heat input. The pictures shown are taken after certain time of application of heat load and t_0 is not the time of beginning of the heat load. The instance of t_0 indicates the beginning time after which the pictures presented in the above figure are captured. The bubble in the evaporator zone expands making the slugs above it (in both limbs) to move up wards. However, the net upward motion actually occurs with oscillatory motion as shown in the subsequent pictures in Figure 4-9. The figure indicates that in the initial stages the oscillation frequency is lower while at the instance just before the pulsations begin (Figure 4-9 (g) to (j)) – that is around the 39 s to 40 s mark, the frequency of oscillation increases. The PHP pulsations begin to occur once the entire slug is confined within the condenser. Till the PHP operation takes place the T_e raises to a higher value. The moment the pulsations begin to occur the T_e reduces accompanied by the rise in T_c indicating the heat pipe effect. This kind of start-up results in T_e overshoot at the start compared to the quasi-steady state value.

4.8.4 Thermal resistance at steady state

From Figure 4-10 to Figure 4-13 it can be observed that R_{th} comes down as the heat loads increase. The fact that the R_{th} at 10 W is substantial in comparison to the rest of the heat loads indicates that the PHPs are supposed to be operated beyond certain threshold heat fluxes for their satisfactory operation. The values plotted in Figure 4-13 are average of the 3 independent tests carried out on 3 different days for the same set of heat loads. The error estimates at the higher heat loads being negligible indicates that the steady state operation at higher heat loads are highly consistent.

The equivalent thermal conductivity of the PHP was estimated as follows

$$\frac{L_{eff}}{k_{equiv}A_{cs}} = R_{th} \tag{4.9}$$

where

$$L_{eff} = 0.5(L_e + L_c) + L_a \tag{4.10}$$

$$A_{cs} = (n\pi D_o^2)/4 \tag{4.11}$$

Thus the k_{equiv} of PHP at 20 W and 70 W was estimated to be 3840 W/m-°C and 10935 W/m-°C respectively.

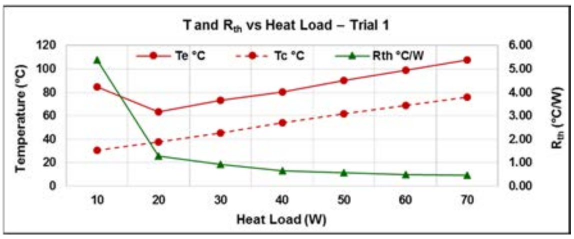

Figure 4-10: T_e, T_c and R_{th} vs heat load - Trial 1

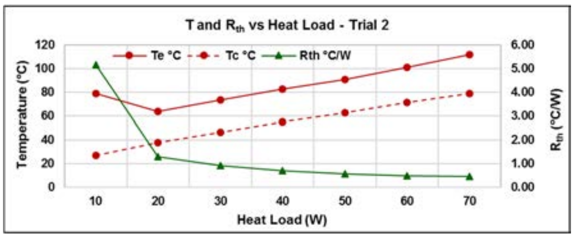

Figure 4-11: T_e, T_c and R_{th} vs heat load - Trial 2

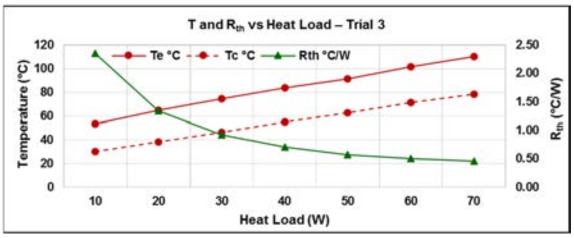

Figure 4-12: T_e, T_c and R_{th} vs heat load - Trial 3

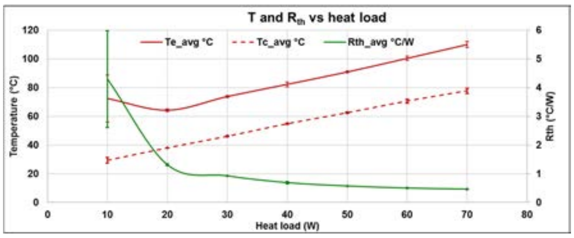

Figure 4-13: Average values of T_e, T_c and R_{th} vs heat load

4.8.5 Flow regimes

1. From the videos and as illustrated in Figure 4-14 (a), it was inferred that at lower heat loads like 20 W the oscillations were of less amplitude. The bubbles did not travel the full length of the PHP for most of the time. Thus the bubbles were confined only in the same limb of their origination. At 20 W the oscillations showed that the flow regimes in each limb alternated between slug flow (Taylor bubbles) and semi-annular flow. The movements were more or less in the same direction with small phase difference in the both limbs. At 20 W the down comer usually had the slug flow and the upward movement was of either semi-annular or longer bubbles.
2. As the heat load was increased, at around 50 W as indicated in Figure 4-14 (b), the flow was of slug-flow type but with longer bubbles. The oscillation amplitude was also higher and the travel of the bubble was nearly to the entire length of the PHP with substantially higher velocity. The bubble movement direction in each limb was distinctly different (i.e., in one limb when the movement is upward in the other it was downward).
3. At 70 W as shown in Figure 4-14 (c), the oscillation was of slug flow with further elongated bubbles. The amplitude was further increased thus the bubbles were travelling beyond the length of the PHP. Thus the bubble movement in each limb was almost totally opposite. This resulted in a near net circulation or complete unidirectional movement of the bubbles. This situation/occurrence did not last long. The flow direction reversed within few circulation cycles. Hence unidirectional circulation could not be observed. As the amplitude of oscillations increased with higher heat loads the heat transfer performance was improved as indicated by the reduced R_{th}.

4. For the heat loads tested the flow regime was mostly slug flow and semi-annular flow. As the flow was observed to be slug in one limb the other was usually near semi-annular [83]. For all heat loads the down-comer tended to have slug flow relative to the up-header where more vapour manifested with annular flow.

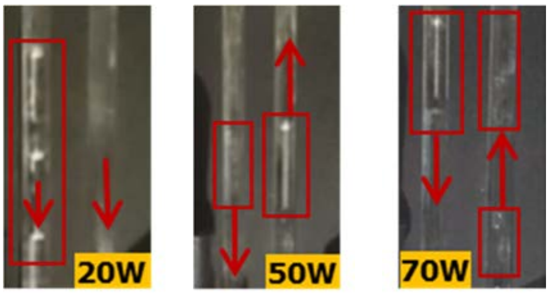

(a) (b) (c)
Figure 4-14: Flow patterns for various heat loads

4.8.6 Estimation of liquid film thickness

The liquid film thickness around the vapour was estimated from the visuals for some of the heat loads and the same is shown in Figure 4-15. The width in the photograph was compared with a known reference distance (outer diameter of the tube) to obtain the scaling. The distance from the outer side of wall to the bubble was measured in the photograph and the scaling was used to estimate the actual distance. Then the film thickness was obtained by subtracting the tube wall thickness (1.15 mm) from it. With increasing heat loads the liquid film thickness surrounding the Taylor bubbles tended to be smaller as stated in [84].

The film thickness was also estimated from equation 4.12 obtained from equations (12) and (13) of [84].

$$\dot{q} = \frac{\frac{kR'T_v^2}{h_{fg}} ln\left[1+\frac{2\sigma}{P_v}\left(\frac{1}{r_n}-\frac{1}{2(r_{in}-\delta_l)}\right)\right]}{r_{in} ln\left(\frac{r_{in}}{r_{in}-\delta_l}\right)\left[1-\frac{R'T_v}{h_{fg}} ln\left[1+\frac{2\sigma}{P_v}\left(\frac{1}{r_n}-\frac{1}{2(r_{in}-\delta_l)}\right)\right]\right]} \tag{4.12}$$

In this calculation of the film thickness, δ_l, the temperature of vapour, T_v was assumed to be 90°C as for most of the heat loads the evaporator temperature was nearly 85°C to 95°C (from Figure 4-6 to Figure 4-8) just before the start-up (peak). Here R' denotes the particular gas constant. The r_n which is the *Ra* (surface roughness) value of the copper tubing inner diameter, was measured as 0.8 μm. This was done by cutting open the tubing (Figure 4-16(a)) and inspecting using surface profilometer. The film thickness estimated was plotted in Figure 4-16(b). The values show a very good qualitative match with Fig. 8 of [84] and a reasonable quantitative match as well. For example, the values corresponding to heat flux of 10 W/cm² was found to be nearly 10 µm. For the lower heat loads the film thickness estimated from videos were reasonably close to the predicted values from equation 4.12. However, for higher heat loads of 60 W and 70 W the film thickness could not be resolved with the available video quality as the film thickness for the higher loads tended to be very small.

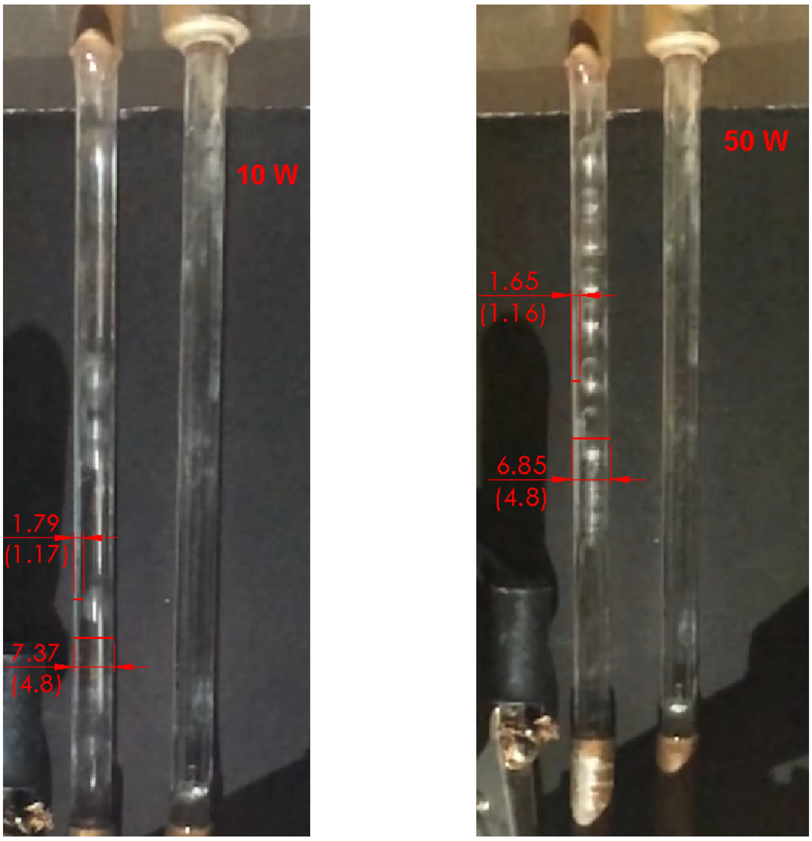

10W – 3.3 W/cm² – 15.8 µm 50W – 16.4W/cm² – 6.2 µm

Figure 4-15: Estimation of liquid film thickness for various heat loads

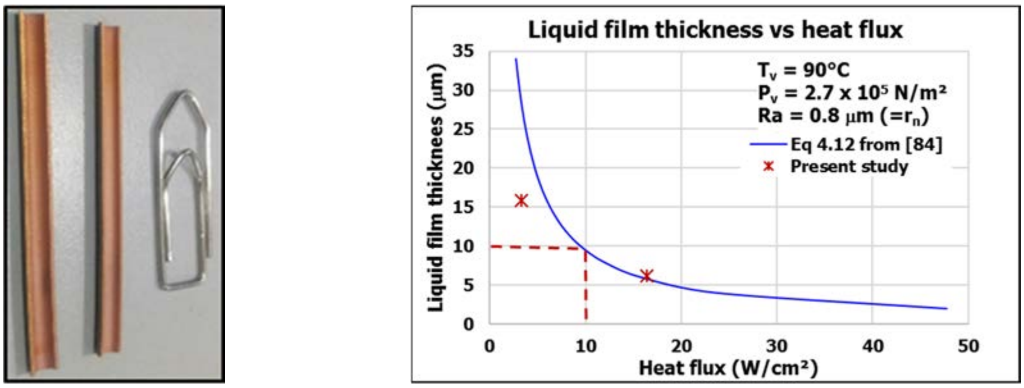

(a) (b)

Figure 4-16: Estimation of liquid film thickness

4.9 Closure

A single closed loop PHP was constructed and tested with evaporator down mode. Methanol was chosen as the working fluid as it fulfilled most of the requirement of a PHP fluid as well as was compatible with most metal substrates. The tests were carried out for heat loads ranging from 10 W to 70 W in steps of 10 W and start-up characteristics (transient) were recorded. The salient conclusions from the tests are as follows,

1. For 10 W the heat flux was insufficient for a satisfactory start-up and continuous PHP operation.
2. The flow regime was slug flow or semi annular in most cases. The up header was more annular and the down comer had predominantly slug flow.
3. The R_{th} reduced with increasing heat load. The tests were not conducted beyond 70 W as the T_e was exceeding the temperature limit for the heater.
4. At lower heat loads direction of motion of the bubbles (fluid) was in the same direction with a small phase difference in both the limbs for large periods of time with occasional travel of the bubbles for the entire length of the PHP.
5. At higher heat loads direction of motion of the fluid was opposite to each other in each of the limbs. At 70 W (highest) heat load the bubble travelled beyond length of PHP. Hence there was a tendency to have net circulation. However, net circulation never occurred for sustained periods of time.
6. Most heat loads (on lower side) indicated a sudden start up. Hence for practical cooling application care should be taken that the minimum heat flux is available for start-up as T_e at start-up was higher than T_e at steady state for at least up to 50 W.
7. Higher heat load if experimented with enhanced condenser cooling (by liquid cooling) with T_e being below the safe limit, probably would have resulted in unidirectional circulation. The net circulation at higher heat loads may further improve the heat transfer (lesser R_{th}). This additional higher heat loads would have probably given consistent smooth start-up across trials as it was reported in literature that larger heat inputs have smoother start-up.
8. Estimation of δ_l with practical values was carried out for an average T_v and this estimate showed very good agreement qualitatively (decrease of δ_l with increase of heat flux) and a reasonable agreement quantitatively with Fig. 8 of [84].

The work has been published in the Proceedings of the 24th National and 2nd International ISHMT-ASTFE Heat and Mass Transfer Conference (IHMTC-2017), *Experimental investigation of a single closed loop pulsating heat pipe,* **P. Srikrishna, S. U. M. Reddy, A. R. Hari Kumar and G. S. V. L. Narasimham,** December 2017, Hyderabad, India.

5 Single loop pulsating heat pipe – Performance comparison based on bend radius and insulation of adiabatic section

5.1 Introduction

A single loop PHP (SLPHP) can be used to investigate the performance variations arising due to the bends. This aspect of PHP has been studied in a less extensive manner and mostly the bend loss has been neglected in the simulation studies carried out for PHP geometries with lesser number of bends. In reality the bend is the location where heat transfer occurs (evaporator or condenser usually located at the bends) in most configurations of the PHP and also the location where the maximum change in fluid momentum happens. The fact that minimum number of bends are needed depending on the inner diameter of PHP [19] to make the PHP orientation independent indicates that the phenomenon at the bends cannot be left without investigation. As stated in chapter 3, section 3.7.7.2, a smoother bend radius will result in lower resistance to flow thus can permit larger pulsations leading higher heat transfer rate. Hence in this chapter the focus has been given towards comparison of two single loop PHPs with varying bend radius and estimating their performance with respect to heat fluxes, inclinations, and varying working fluids (methanol and water) for a fill ratio of 60%. One of the SLPHP was tested with the adiabatic section insulated to compare the performance change with respect to the bare copper tubing in the adiabatic section. The SLPHP was also investigated for estimation of characteristic frequency of oscillations occurring inside the PHP which can give an estimate of the velocity scales which will be useful for any design activity of PHP. As is well established in literature that a PHP with one turn is strongly affected by gravity, the PHPs in the present study were tested from horizontal (0°) to the vertical position (90°).

5.2 PHP – geometry and construction

To ascertain the impact of bend radius on the performance of the SLPHP two PHPs with substantially varying bend radius – 6 mm (R6) and 10 mm (R10) was made out capillary copper tube of inner diameter 2 mm and outer diameter 3 mm. The T-joint was made at the condenser portion of the SLPHPs where the charging and discharging valve (Aignep 6310) was located. Similarly, a SLPHP of radius 7.5 mm (R7.5) was also constructed with two T-joints at the adiabatic sections of the PHP. The T-joint in the left hand side was used to have a pressure transducer (Honeywell - PX2AG2XX002BAAAX). The right hand side was provided with another T-joint to locate the charging valve. The two T-joints were located on either side of the PHP so as to preserve the SLPHP symmetry to a large extent such that the construction does not bias the flow directions in the PHP during its operation. The pressure transducer was avoided in the 6 mm and 10 mm bend radius PHPs to have minimum fittings (like T-joints) so as to accurately estimate the effect of the bend radius on the performance of the PHPs in isolation. The evaporator, adiabatic section and condenser dimensions of all three SLPHPs were maintained identical. The copper plates were machined with channels of required size (as that of outer diameter of the copper tube) to act as the evaporator and the condenser plates. The copper tubing bent to the desired radius was brazed into the channels of the evaporator and condenser plates. The schematic of the three SLPHPs with their salient dimensions and the sensor (thermocouple and pressure transducer) locations are shown in Figure 5-1. The parts and sub-assemblies are shown in Figure 5-2. The actual PHPs are shown in the test fixture in Figure 5-3. The PHPs were constructed to have almost the same internal volume across all three PHPs (with the R 7.5 mm being more due to additional volume of the pressure transducer). The details of the volume of the PHPs and the filled charge (60% fill ratio) are summarised in Table 5-1. The table also provides the heat transfer areas in the evaporator and the condenser which were designed to have very small variations (less than 10%) across PHPs to have the heat fluxes nearly same during the experiments. The PHPs were checked for leak rate using helium leak detector (Pfeiffer ASM 182 TD$^+$) and the leak rate was found to be of the order of 10^{-8} Torr-l/s.

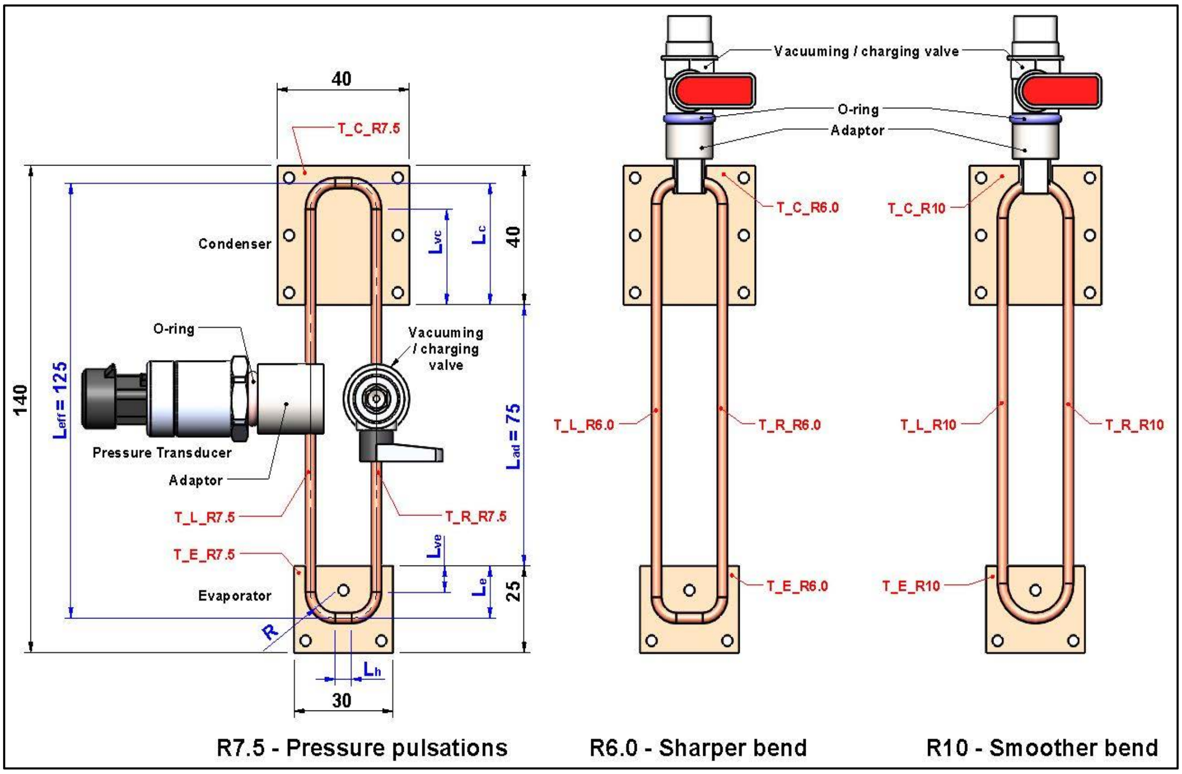

Figure 5-1: Schematic of the SLPHPs - dimensions and sensor locations

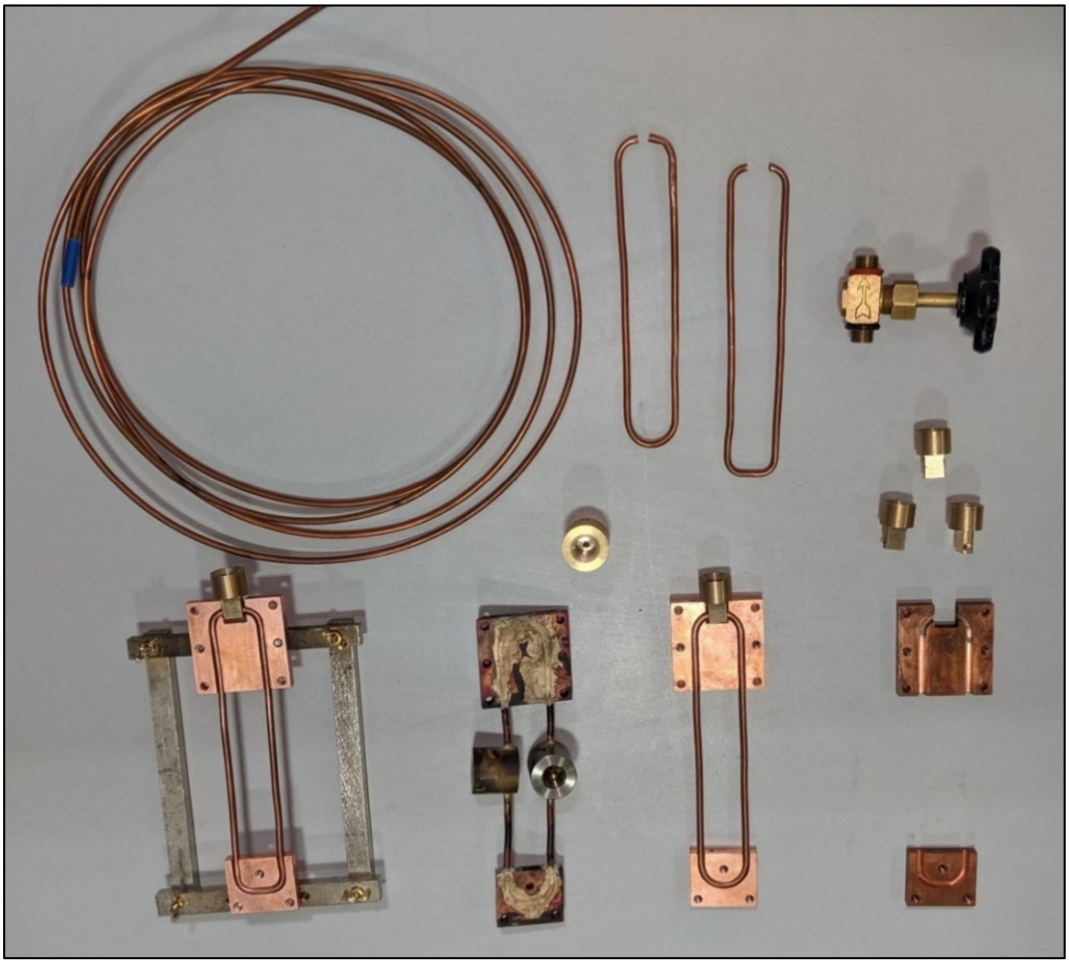

Figure 5-2: Various parts and sub-assemblies of the three SLPHPs

5.3 Experimental setup

The evaporator of each PHP was fitted with one number of 2 Ω, 100 W thin film heater (Ohmite TEH100M2R00JE). The heaters were powered by TDK-Lambda make – Z^+ 800 (60 V-14 A) power supply with ± 0.5% and ± 1% accuracies for voltage and current respectively. The condenser of each PHP was cooled by forced water cooling through a custom made copper cold plate. The chilled water was circulated through the cold plate at a flow rate of 1.5 LPM controlled by rotameters (Sunflow make – SF/ABR/206-100) from a recirculating chiller (Bucchi make – F 305) with the coolant incoming temperature to cold plate maintained at 25°C. The PHPs were mounted on fixture and attached to a rotary table (with resolution of 1° for tilt angle) to vary the inclination during the tests. The T-type thermocouples (RS PRO-621-2164) of accuracy ±0.5°C, were planted at the evaporator, condenser, left and right adiabatic limbs of each SLPHP to estimate the thermal resistance as well as information regarding the flow regime occurring inside the PHP. The thermocouple data was sampled at 1 Hz and logged using an 8-channel data logger, Picolog make-TC-08. The data from the pressure transducer was sampled at 40 Hz using Keysight data acquisition system of 34980A. The literature, [38] and [39] show that the frequency of the oscillations within the PHP is below 5 Hz. Thus the sampling rate satisfies the Nyquist criteria very well. The PHPs charging valve was connected to the dual stage rotary vane vacuum pump (Pfeiffer DUO 10 M) and vacuumed for removal of non-condensable gases (to a pressure level of less than 0.3 Pa).

Table 5-1: Summary of the geometric details of SLPHPs

Parameters	Nomenclature	Unit	R7.5 mm	R6.0 mm	R10 mm
Bend radius	R	mm	7.5	6	10
Straight length in the bent portion	L_h	mm	5	8	0
Straight length in evaporator	L_{ve}	mm	7.5	9	5
Straight length in condenser	L_{vc}	mm	27.5	29	25
Length of evaporator	L_e	mm	15	15	15
Length of condenser	L_c	mm	35	35	35
Heat transfer length in evaporator	$L_{hte}=\pi R+2*L_{ve}+L_h$	mm	43.56	44.85	41.42
Heat transfer length in condenser	$L_{htc}=\pi R+2*L_{vc}+L_h$	mm	83.56	84.85	81.42
Internal diameter	d	mm	2	2	2
Heat transfer area in evaporator	$A_{se}=\pi dL_{hte}$	mm²	273.71	281.80	260.22
Heat transfer area in condenser	$A_{sc}=\pi dL_{htc}$	mm²	525.04	533.13	511.55
Adiabatic section length	L_a	mm	75	75	75
Total length of the PHP	$L = 2*L_a+L_{hte}+L_{htc}$	mm	277.12	279.70	272.83
Area of cross-section	$A_{cs} = \pi d^2/4$	mm²	3.14	3.14	3.14
Internal volume of the PHP	$V_t = L*A_{cs}$	mm³	870.61	878.70	857.13
		ml	**0.87**	**0.88**	**0.86**
Cooling at condenser			water	water	Water
Fluids used			Methanol and deionised water		
Angle of inclination tested		deg	0° to 90° in steps of 10°		
Volume trapped in charging valve	V_{val}	ml	0.2	0.2	0.2
Volume trapped in pressure sensor	V_{trans}	ml	0.2	0	0
60% of volume of PHP	V_{fill}	ml	0.5	0.5	0.5
Amount of charge admitted	$V = V_{val}+V_{trans}+V_{fill}$	ml	**0.9**	**0.7**	**0.7**

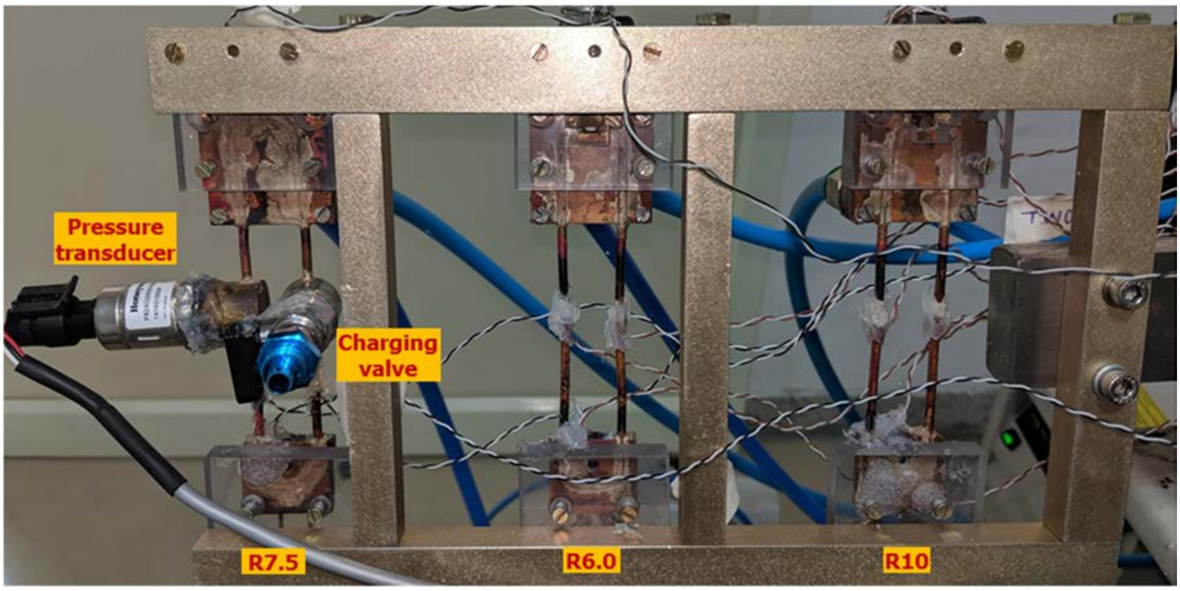

Figure 5-3: PHPs in test fixture

5.4 Experiment Protocol

After 60 minutes of purging, the valve was closed and the pump was disconnected from the valve. Now a 1 ml syringe was attached with the valve with an O-ring joint (to avoid deterioration of vacuum) and the desired quantity of the working fluid was admitted into the PHP by opening the valve. The valve was closed and the condenser cooling was started, followed by application of heat load at the heater. This protocol of vacuuming and charging was followed for each experimental trial of testing to keep vacuum deterioration over time, to be the minimum. In all the experimental runs the first load case of lowest heat load (for any inclination) was operated for a longer duration (15 minutes) and the subsequent loads were operated for reduced duration (10 minutes). This practice was followed as the initial temperatures for the first heat load will be around ambient temperature whereas for the rest of the heat loads only an incremental change in temperatures at various locations will occur. Hence to ensure steady state the first load case was operated for more duration. The temperatures were not allowed to exceed 100°C and the heat loads were not allowed above 100 W for the safe operation of the heaters.

5.5 Data reduction

The temperatures monitored at evaporator and condenser are averaged over 60 seconds for each trial and further averaged over a minimum of three trials for the estimation of thermal resistance. Thus the temperatures reported are as calculated by equation 5.1. The thermal resistance of the PHPs is calculated using equation 5.3.

$$T_k = \frac{\sum_{j=1}^{m}\left[\frac{\sum_{i=1}^{n} T_i}{n}\right]}{m} \tag{5.1}$$

Where T_k can be T_e, T_c; n = 60 (samples over a minute); m = 3 (number of trials)

$$\dot{Q} = VI; \text{where V is the voltage and I is the current applied} \tag{5.2}$$

$$R_{th} = \frac{(T_e - T_c)}{\dot{Q}} \tag{5.3}$$

5.6 Results and discussion

The PHPs with bend radius 6 mm and 10 mm were tested without any fluid for heat load of 5 W, with the condenser cooling for more than one hour. This test was carried out to estimate the dry or the fluid less R_{th} of the PHPs. This test established the adherence of the thermocouples as well, at the respective locations as the temperatures at the corresponding locations of the eight thermocouples (four from each PHP) was within 2°C variation. The temperature trace over time for the estimation of R_{th_dry} is shown in Figure 5-4. The R_{th_dry} was estimated (using equation 5.3) to be 10°C/W as the T_e was found to be 75°C for a T_c of 25°C when the applied heat load was 5 W. Further to this, the PHPs were tested for various heat loads (10 W to 100 W in steps of 10 W) and inclinations (0° to 90° in steps of 10°) for 60% fill ratio of both methanol as well as water.

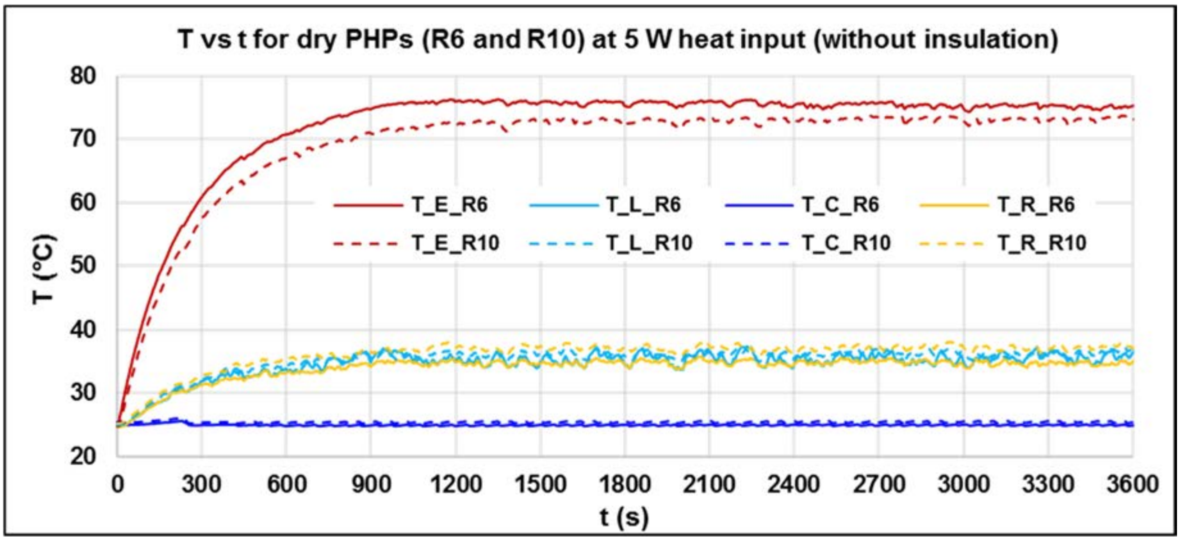

Figure 5-4: Temperature vs time for dry PHPs

5.6.1 Flow pattern for various heat loads for different bend radii

5.6.1.1 Methanol

The flow patterns differ with heat loads starting from low amplitude oscillations (LAO), followed by high amplitude oscillations (HAO), circulation with frequent reversal (CFR) in direction of circulation and ultimately unidirectional circulation (UDC) as reported in [47].

These flow regimes can be correlated by the temperatures T_L and T_R. The unidirectional circulation is the most efficient flow regime for heat transfer as will be seen in the later portions of this chapter due to the lowest R_{th}. The flow regime of frequent reversal can be further sub-divided as very frequent reversal (VFR) and less frequent reversal (LFR). The complete flow regimes are summarised in Table 5-2.

Table 5-2: Flow regime identification based on temperatures at adiabatic section

Flow regime	**Temperature pattern at adiabatic section**[47]
LAO Low Amplitude Oscillation	$(T_L-T_R) \approx 0$
HAO High Amplitude Oscillation	(T_L-T_R) vary randomly within a range of temperature
VFR Very Frequent Reversal	(T_L-T_R) is substantial but varies with time without change in sign – T_L rise accompanied by T_R fall and vice versa
LFR Less Frequent Reversal	(T_L-T_R) substantial but changes sign due to switching of flow direction but each direction occurs for longer intervals of time
UDC Unidirectional Circulation	(T_L-T_R) substantial and no change in magnitude for a given heat load and inclination

Figure 5-5 and Figure 5-8 shows the temperature trace with respect to time for R6 and R10 PHPs with methanol as working fluid for heat loads 10 W to 70 W. It can be observed that for lower heat load (10 W) in case of R6 the flow regime was LAO while for R10 it was LAO to begin with but later the oscillations subsided till the heat load was increased to 20 W. The larger oscillations within the PHP are indicated by larger temperature swing in the limbs (T_L and T_R). This is also accompanied by larger amplitude oscillation of T_e.

When the heat loads were between 20 W and 30 W, the R6 exhibited more frequent reversal in circulation compared to R10. The circulation is indicated by substantial difference between T_L and T_R. That is when the magnitude of (T_L-T_R) is large it indicates circulation as the hotter higher void fraction (more vapour) travels from the evaporator through one of the limbs (up-header) which will be warmer. This makes the condensed liquid to return from the opposite limb (down-comer) which will be certainly colder than the up header. During this regime the T_e oscillation amplitude is very much lower. The quantity (T_L-T_R) frequently changes sign indicating the LFR regime. The flow regime in up-header is always semi-annular or annular type while the slug flow manifests in down-comer as mass fraction of vapour will be much lower after the two-phase mixture traverses the condenser.

The most preferred UDC was characterised by (T_L-T_R) having substantially large value and the sign not changing for extended periods of time. This flow can be observed for heat loads 40 W and above. The flow regimes of LFR and UDC are enlarged and shown for R6 in

Figure 5-6 and Figure 5-7 respectively. The same flow regimes for R10 are shown in Figure 5-9 and Figure 5-10. During this regime, the T_e will be smooth without any oscillations.

Another flow regime of VFR can be seen in the inset in Figure 5-11 which shows the temperatures of R6 with methanol as fluid at 50° inclination. Here the magnitude of (T_L-T_R) changes frequently without change in sign. This indicates that the circulation direction changes making the temperatures in the limbs to change but immediately the direction reverses. One can observe that during this regime T_L rise is accompanied by T_R fall and vice-versa.

At heat load of 10 W for 50° inclination only LAO was seen in R10 but R6 indicated HAO (in Figure 5-11). The temperature graph of R10 with methanol at 50° inclination (Figure 5-12) shows a spike after the heat load was set to 20 W. This is the actual beginning of the PHP operation.

The same spike can be seen for 20 W heat load at 30° inclination as well (Figure 5-13 and Figure 5-14). Prior to the initiation of the oscillation in both cases either very low amplitude oscillations occurred or only expansion of vapour bubble was occurring. This inference can be made as the T_L and T_R were almost same, indicating only conduction was the mode of heat transfer. The flow regimes changed to VFR mode at 20 W for both geometries. This was followed by UDC after 40 W heat load as in the previous inclinations. For 30° inclination heat load up to 60 W only could be tested as the T_e exceeded 100°C.

For 10° inclination, the heat load up to 40 W only could be tested without T_e exceeding 100°C. In this case as well only heat load of 20 W showed the PHP operation as seen from Figure 5-15 and Figure 5-16.

In the horizontal operation R6 could not operate even at 10 W. Once the heat load was set to 20 W the PHP dry out occurred with steep rise in T_e as can be seen in Figure 5-17. At 10 W and 0° inclination (Figure 5-18) R10 operated but at 20 W dry out occurred.

At 10 W in all inclinations up to 10° the R6 operated in diode mode. The PHP operation did not start until T_e exceeded a certain value. Then the pulsations started thereby pulling down T_e. After the T_e reduced below a certain value, the pulsations ceased leading to rise in T_e. This cycle was repeated till the heat load was increased to 20 W. This phenomenon of start-stop behaviour is due to the low value of ΔP available to create fluid motion at lower T_e (which means lower ΔT). This is akin to the viscous limit of the conventional heat pipes.

The circulation direction did not have any preference and it was purely random as can be seen from Figure 5-15 and Figure 5-16 (at 10° inclination) the UDC was clockwise in R6 ($T_L > T_R$) whereas the circulation was counter clockwise in R10 ($T_R > T_L$) at 30 W and 40 W heat loads. Likewise the circulation is counter clockwise in R6 at 50° inclination (refer Figure 5-11) while it was clockwise for 30° for the same PHP at 30 W and higher heat loads. This random phenomenon was observed across trials for both geometries of PHP.

Also it can be observed that the magnitude of (T_L-T_R) for R6 was always higher than that of R10 for all inclinations and heat loads.

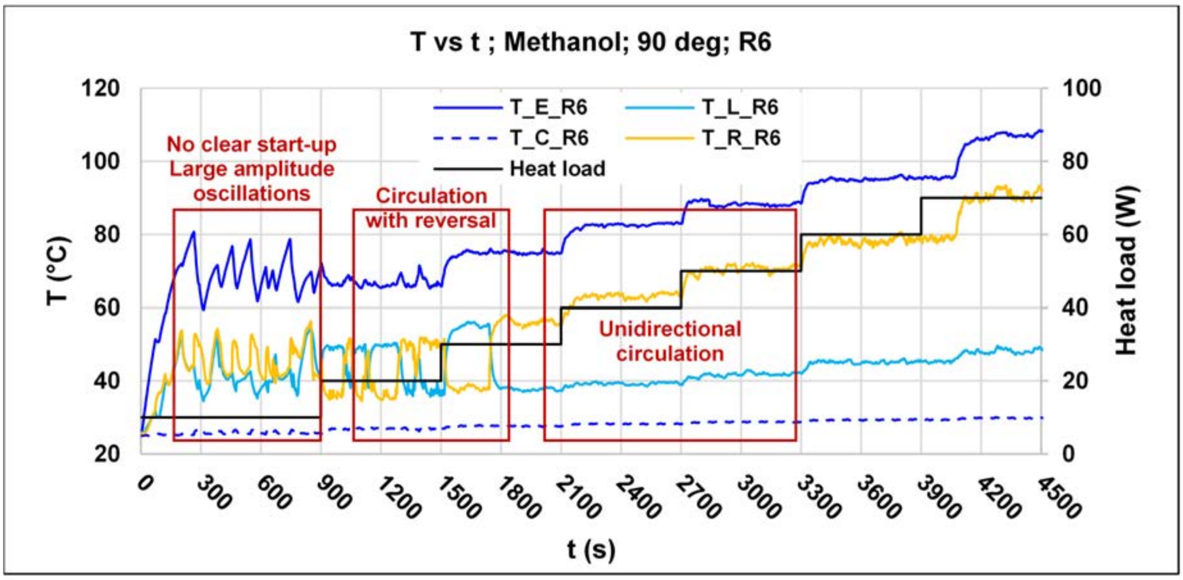

Figure 5-5: Methanol-90deg-R6 -Temperature vs time

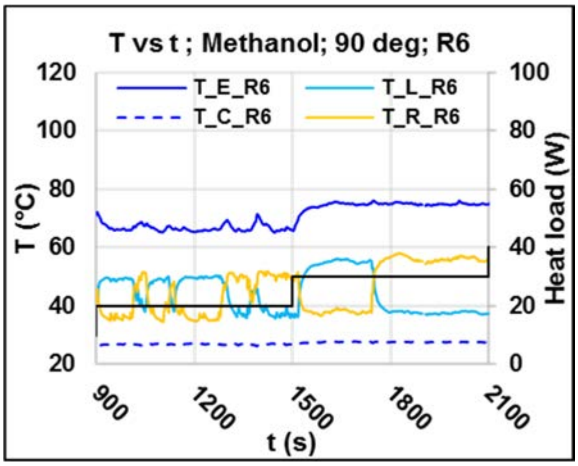

Figure 5-6: Methanol-90deg-R6-Circulation with flow reversal

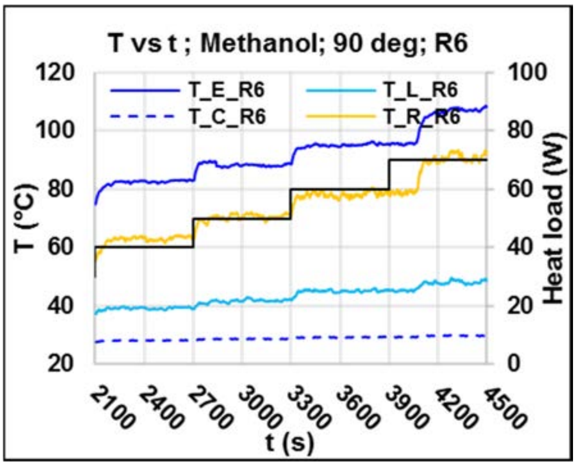

Figure 5-7: Methanol-90deg-R6 - Unidirectional circulation

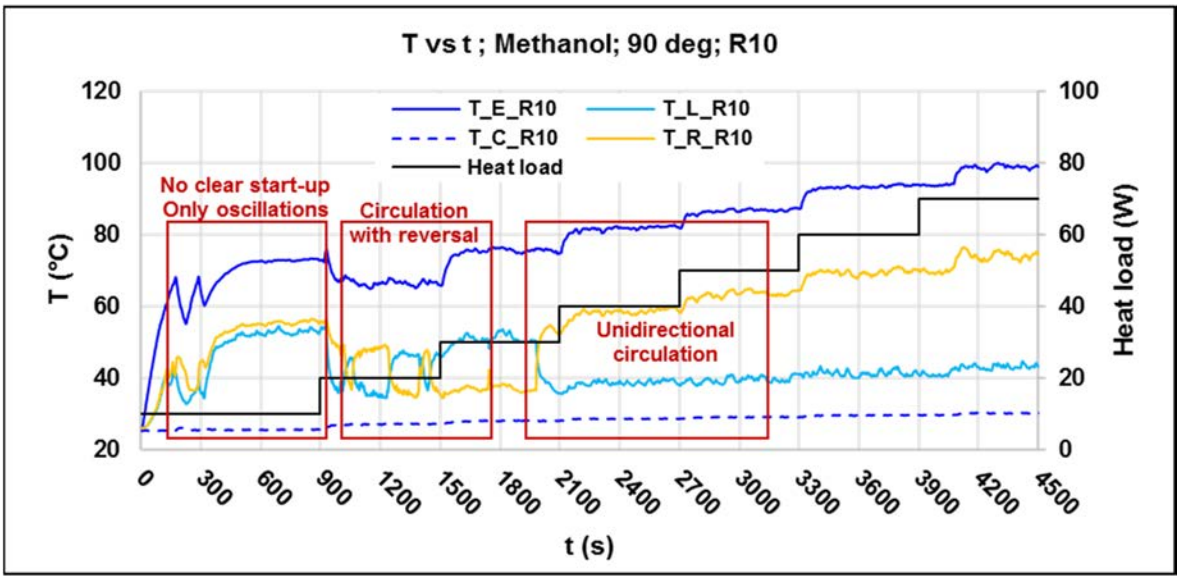

Figure 5-8: Methanol-90deg-R10 – Temperature vs time

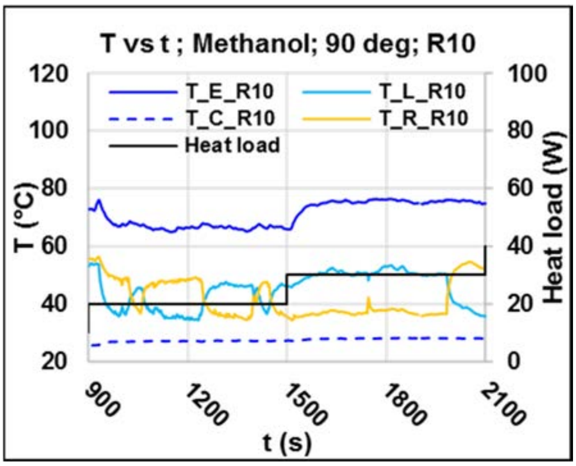

Figure 5-9: Methanol-90deg-R10-Circulation with flow reversal

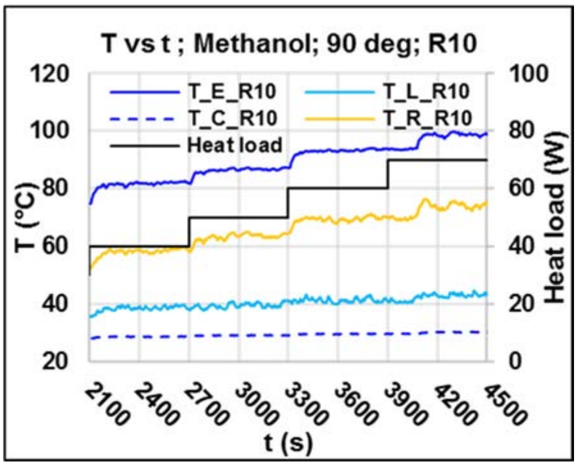

Figure 5-10: Methanol-90deg-R10 - Unidirectional circulation

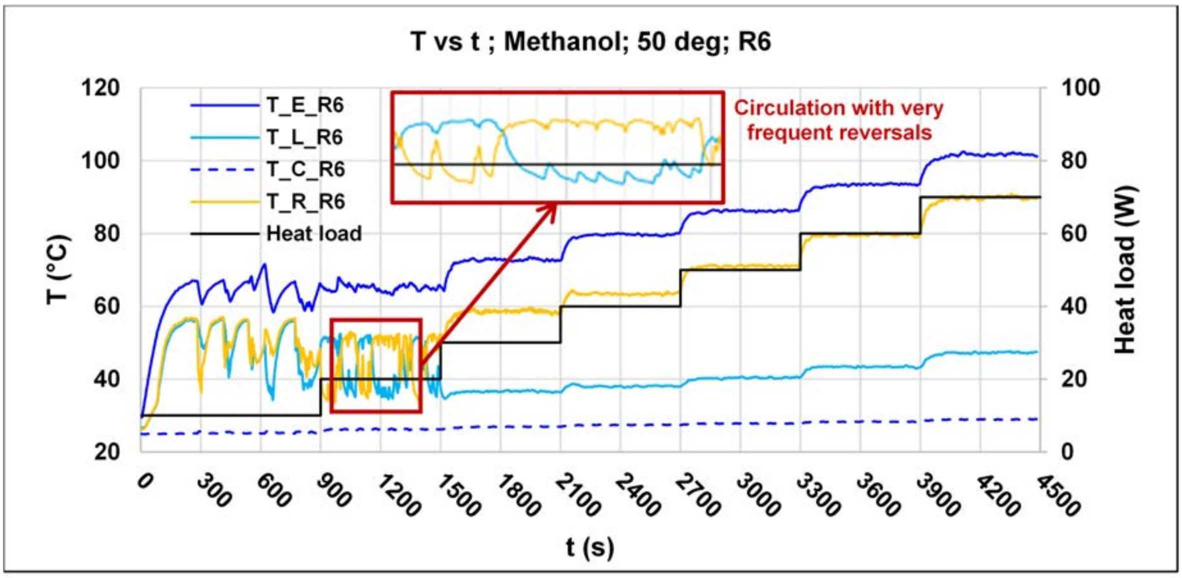

Figure 5-11: Methanol-50deg-R6 – Temperature vs time

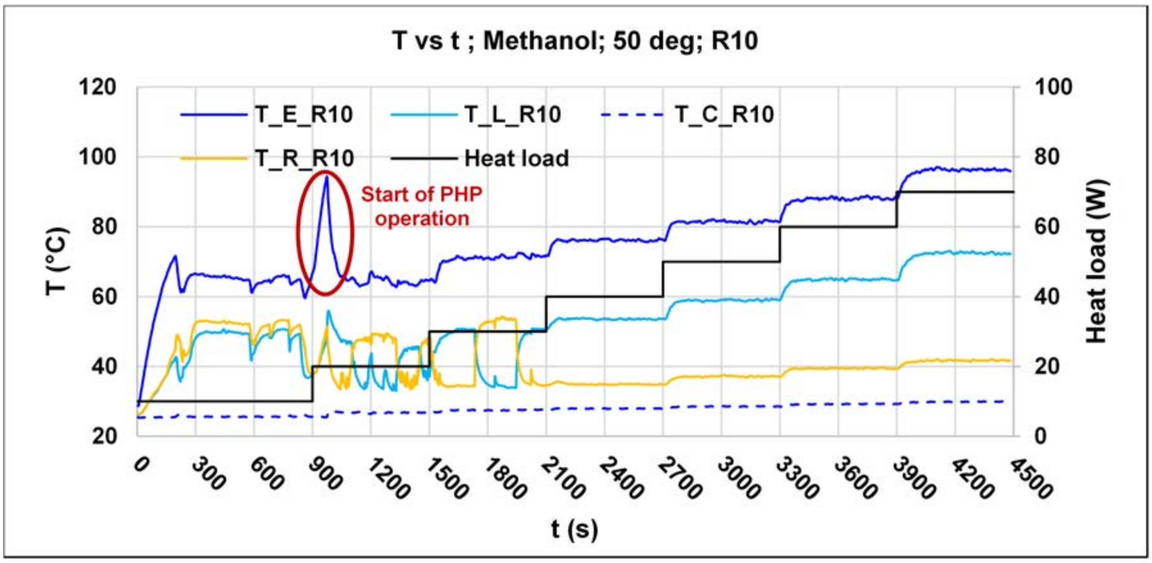

Figure 5-12: Methanol-50deg-R10 – Temperature vs time

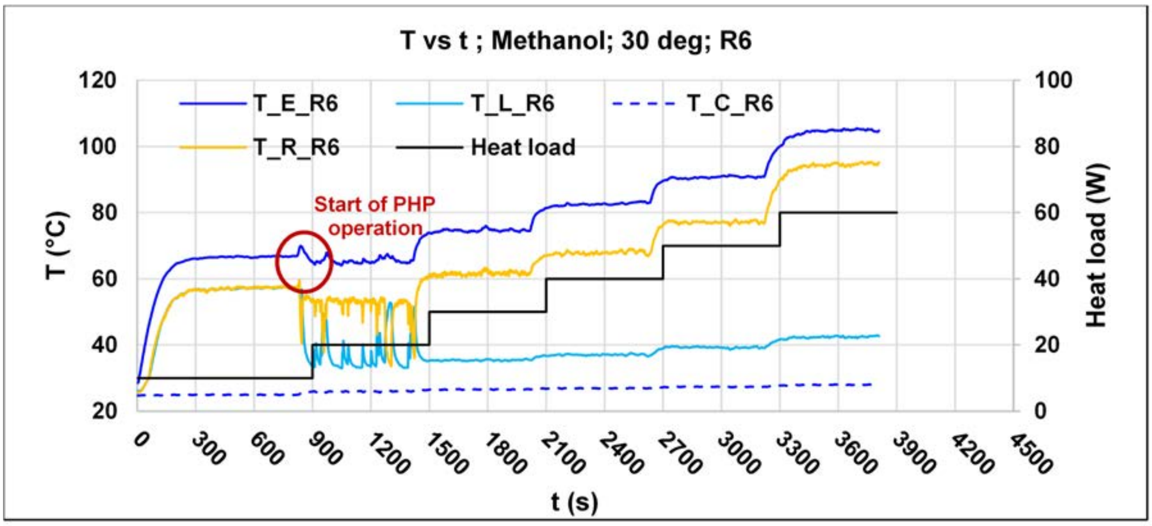

Figure 5-13: Methanol-30deg-R6 – Temperature vs time

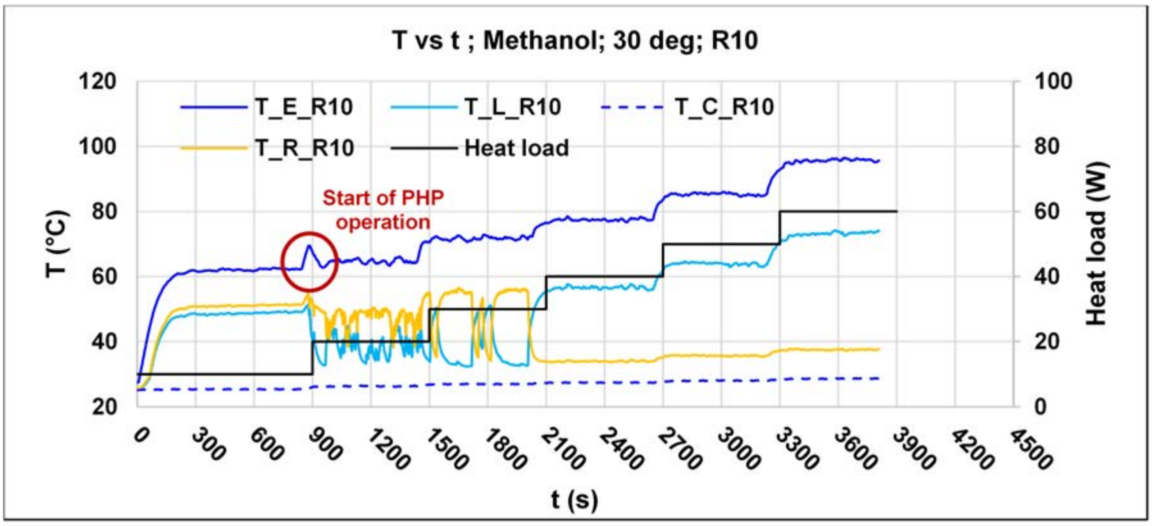

Figure 5-14: Methanol-30deg-R10 – Temperature vs time

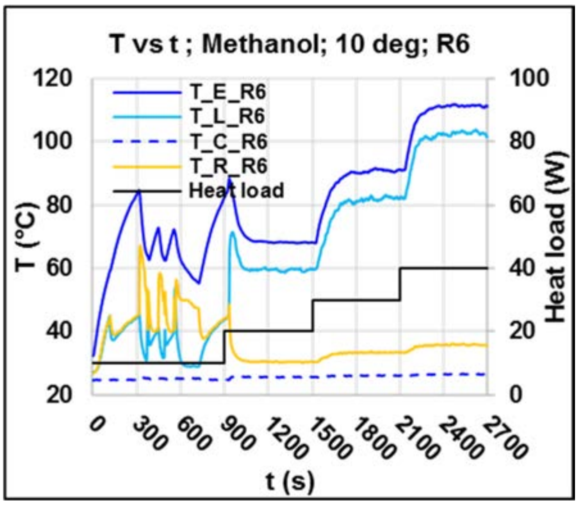

Figure 5-15: Methanol-10deg-R6 – Temperature vs time

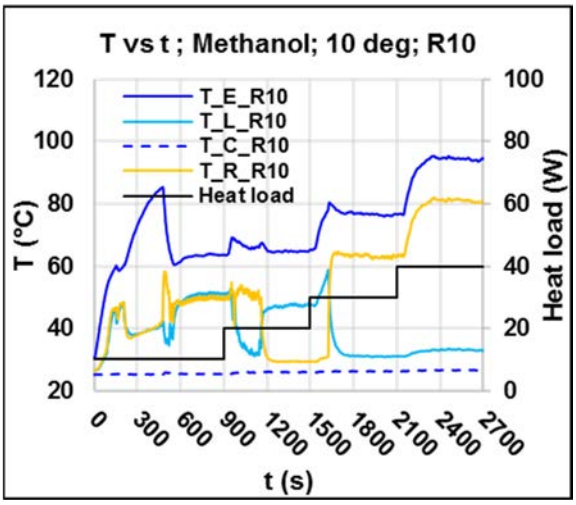

Figure 5-16: Methanol-10deg-R10 – Temperature vs time

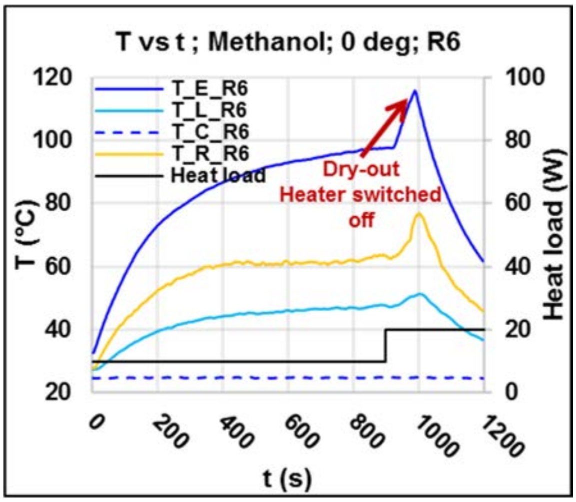

Figure 5-17: Methanol-0deg-R6 – Temperature vs time

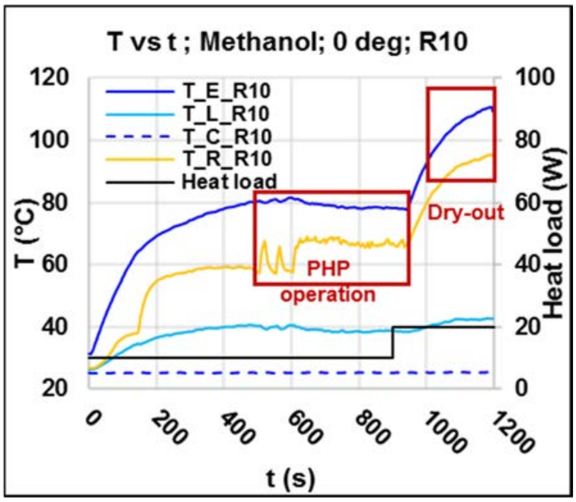

Figure 5-18: Methanol-0deg-R10 – Temperature vs time

5.6.1.2 Water

For water the same flow regimes of methanol were observed but they occurred at higher heat loads compared to methanol. The operation did not start for water until the heat loads were increased to 30 W in most favourable cases of vertical inclination. For the rest of the inclinations the operation started from 40 W only. The PHPs could be loaded up to 100 W (maximum capacity of heater) with T_e still well below 100°C, which is higher than the heat loads with methanol. This can be attributed to the thermophysical properties of water (refer Appendix –A) like larger dynamic viscosity preventing the flow, larger latent heat of vaporization requiring higher energy for bubble expansion. However, the larger specific heat and thermal conductivity of water permitted for higher heat loads without exceeding the maximum allowed temperature. The comparison of 90° inclination temperature plot for R6 and R10 (Figure 5-19 and Figure 5-21) shows that the flow regimes for the same heat loads are very different for the different bend radius. For R6, the VFR regime continued for almost up to 70 W which was followed by LFR up to 80 W (expanded and shown in Figure 5-20).

However, for R10 the VFR did not manifest. Only the LFR occurred up to 40 W (Figure 5-22) beyond which UDC was the mode of operation.

The temperature plots for 50° inclination (Figure 5-23 and Figure 5-24) as well as the ones for the 30° inclination (Figure 5-25 and Figure 5-26) also show drastic flow regime difference between configurations, R6 and R10. At 50° inclination for R6 at lower heat loads the VFR regime was found to be occurring up to 60 W whereas for the R10 case the UDC started from 40 W onwards. Figure 5-25 shows a trial where operation at 40 W did not start, but once the heat load was increased to 50 W, PHP started to operate. Thus at lower inclinations the R6 PHP had difficulty in operation especially at lower loads.

A closer look at the R6 plots across inclinations reveal that UDC began to occur at higher loads. This can be attributed to the fact that gravity does not play a part in replenishing the evaporator with the liquid; the only mode of liquid reaching the evaporator is by pushing of the liquid at the condenser by the expanding bubble at the evaporator. Thus the inertia forces dominate during these lower inclinations. Hence, once the flow starts in one direction it becomes difficult to reverse the direction. The same explanation can be extended to R10 plots also as the UDC was found to occur much more readily as the resistance to flow was much lesser in this geometry. This different response to varying bends was more pronounced for water than methanol due to the higher dynamic viscosity of water.

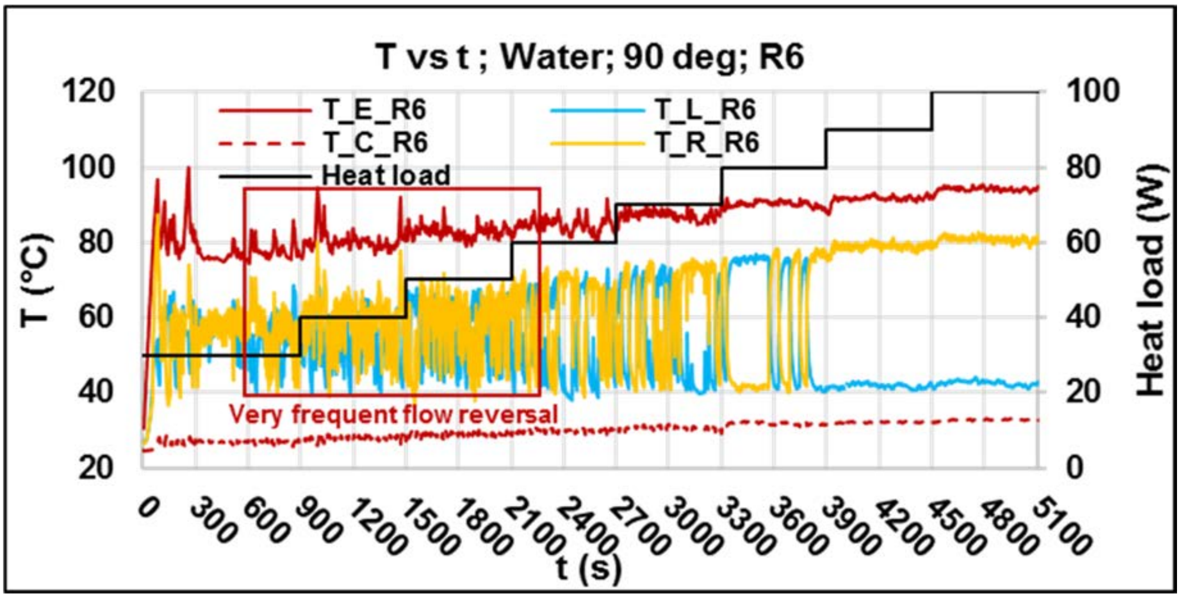

Figure 5-19: Water-90deg-R6 - Temperature vs time

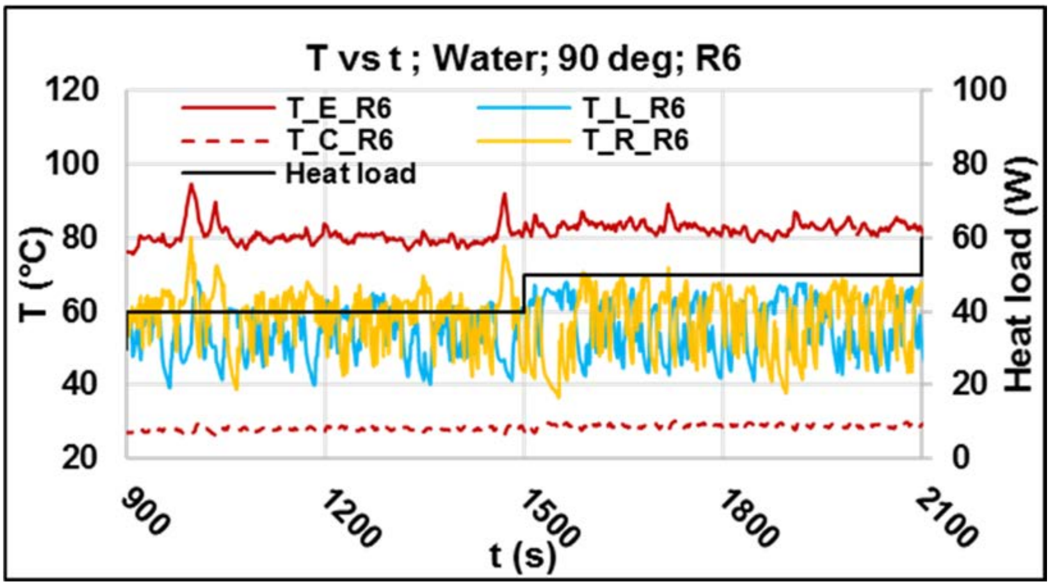

Figure 5-20: Water-90deg-R6 - Circulation with very frequent flow reversal

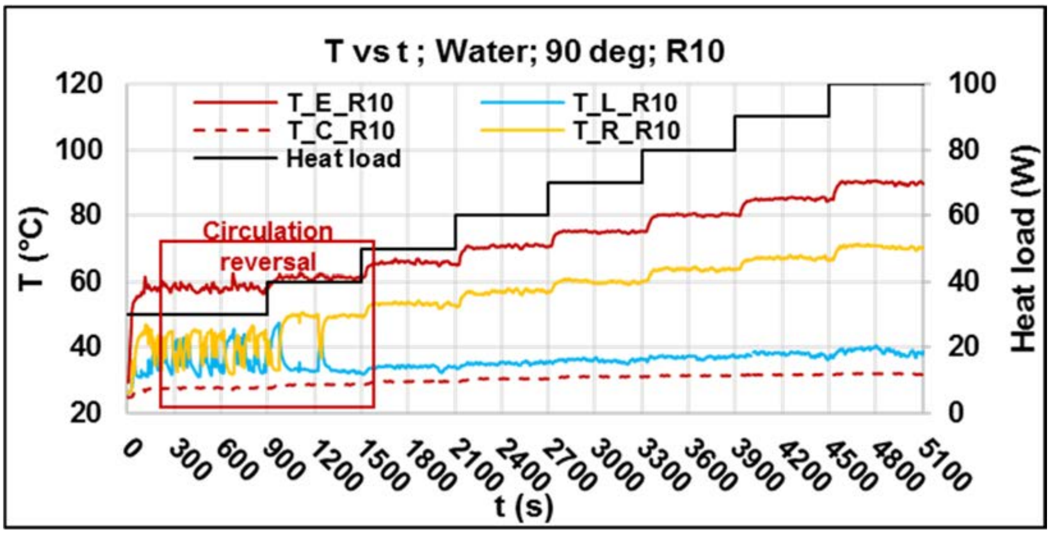

Figure 5-21: Water-90deg-R10 - Temperature vs time

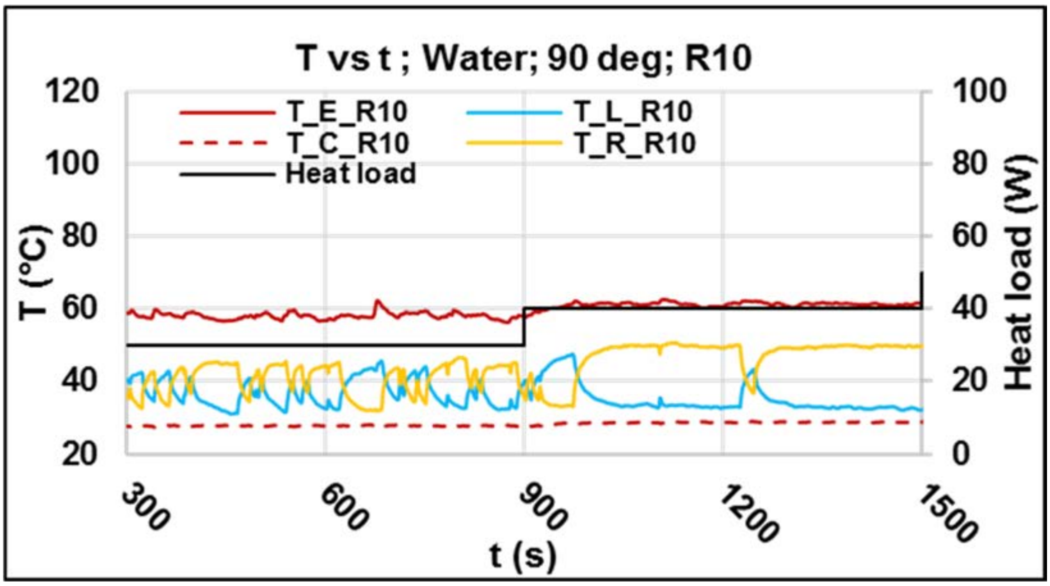

Figure 5-22: Water-90deg-R10 – Circulation with less frequent flow reversals

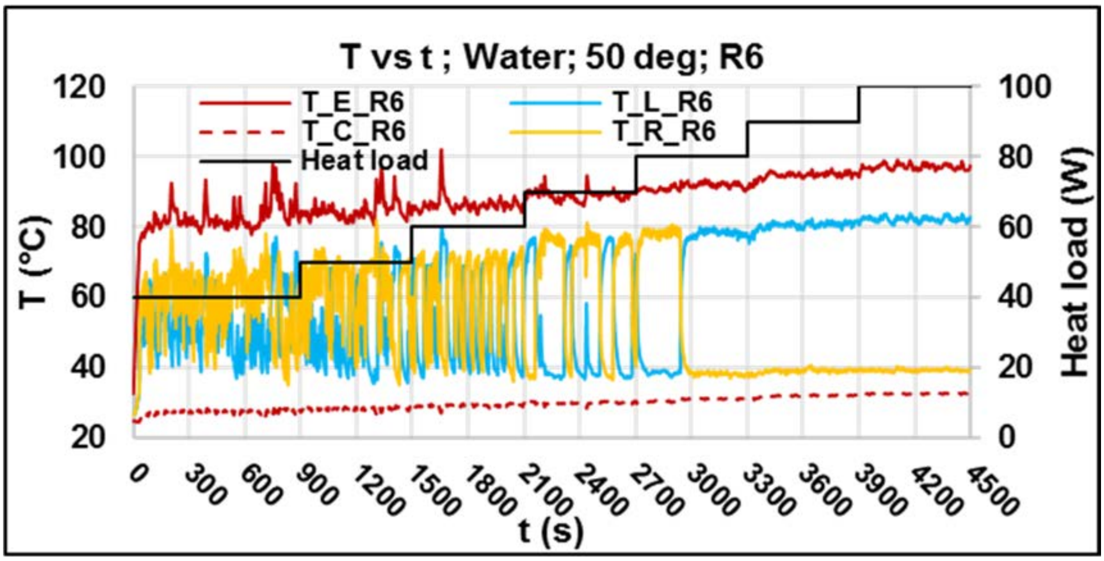

Figure 5-23: Water-50deg_R6 - Temperature vs time

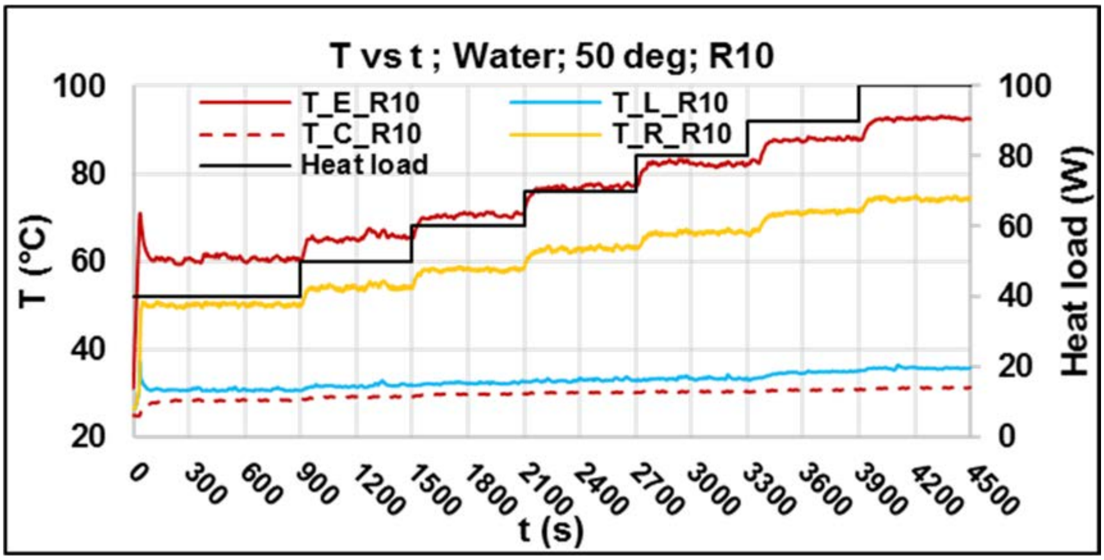

Figure 5-24: Water-50deg-R10 - Temperature vs time

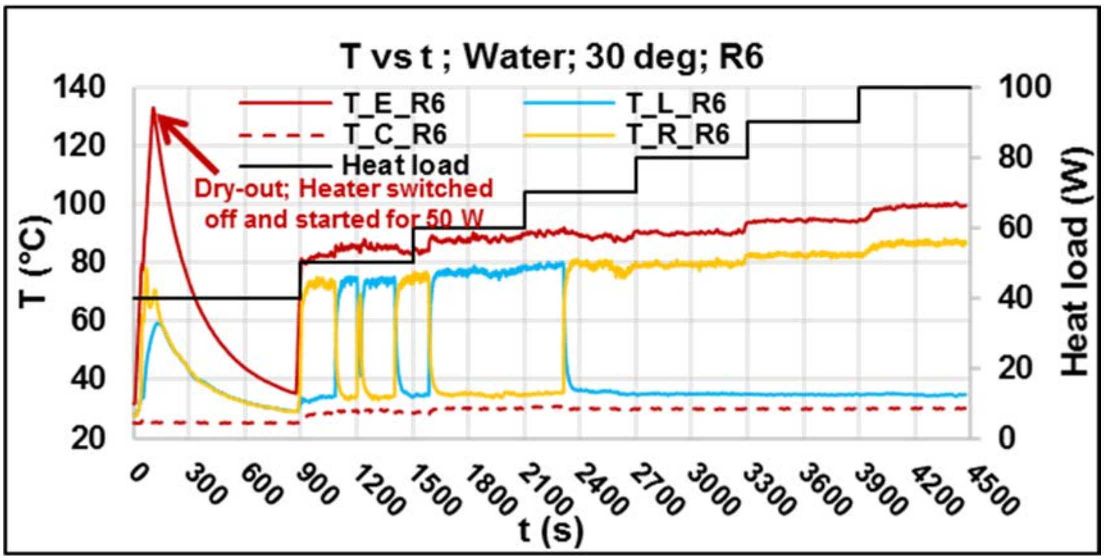

Figure 5-25: Water-30deg-R6 - Temperature vs time

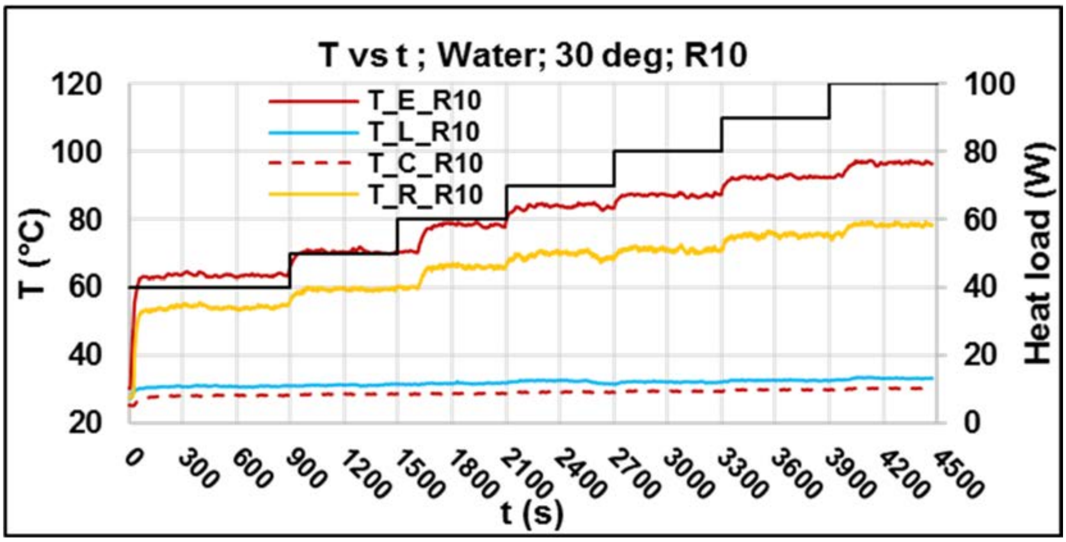

Figure 5-26: Water-30deg-R10 - Temperature vs time

5.6.1.3 Methanol versus water at a given inclination

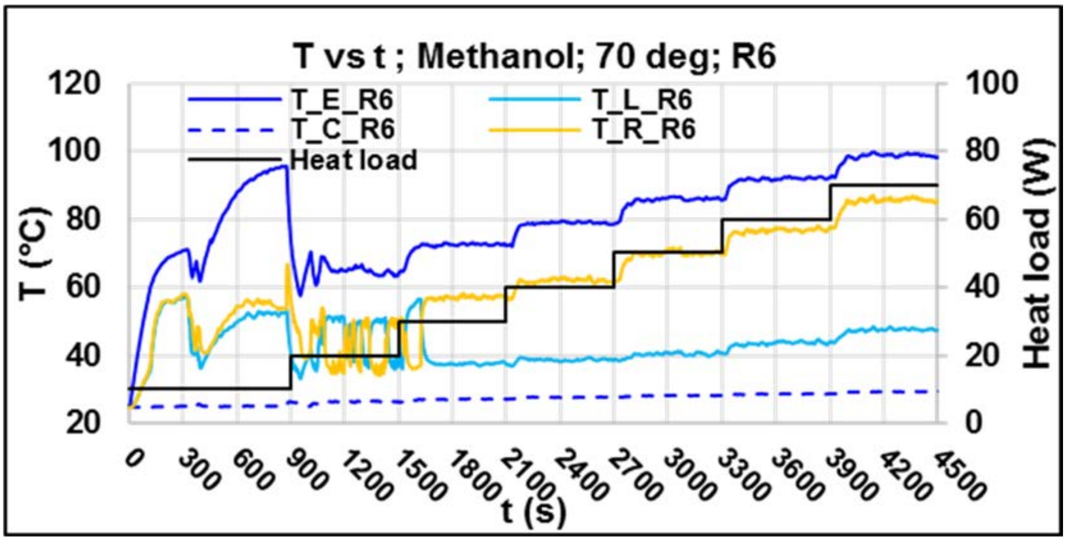

Figure 5-27: Methanol-70deg-R6 - Temperature vs time

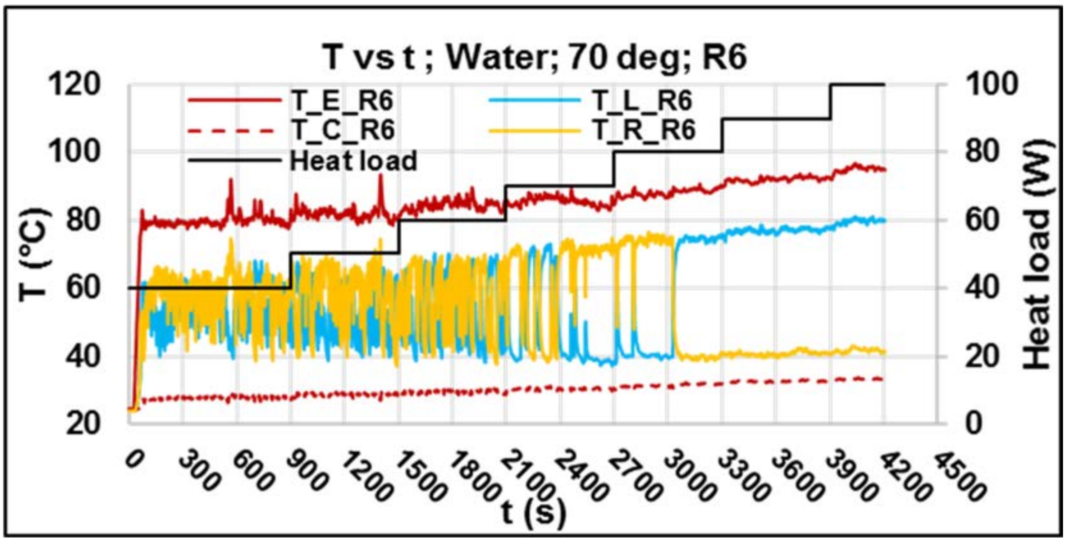

Figure 5-28: Water-70deg-R6 - Temperature vs time

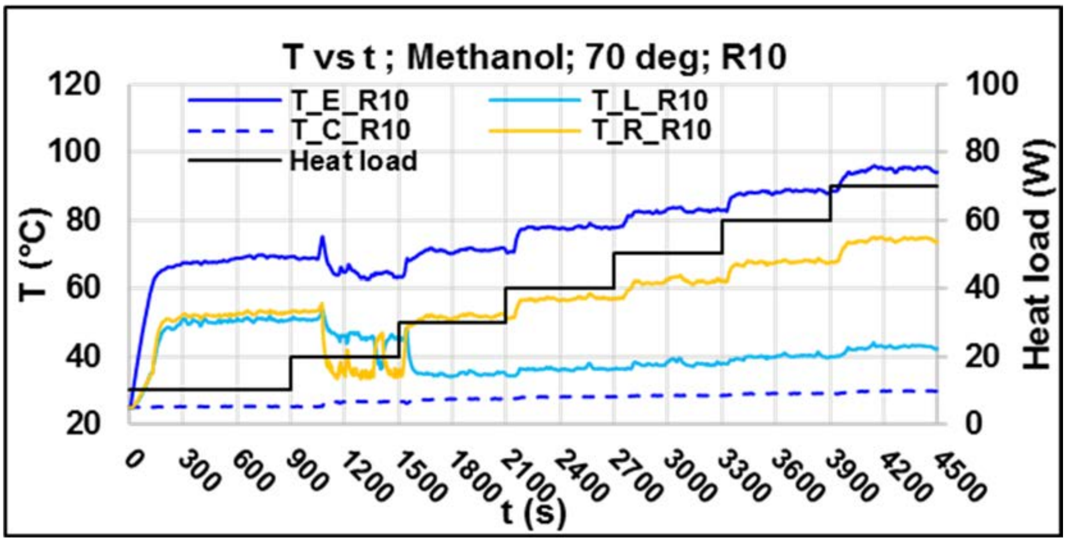

Figure 5-29: Methanol-70deg-R10 - Temperature vs time

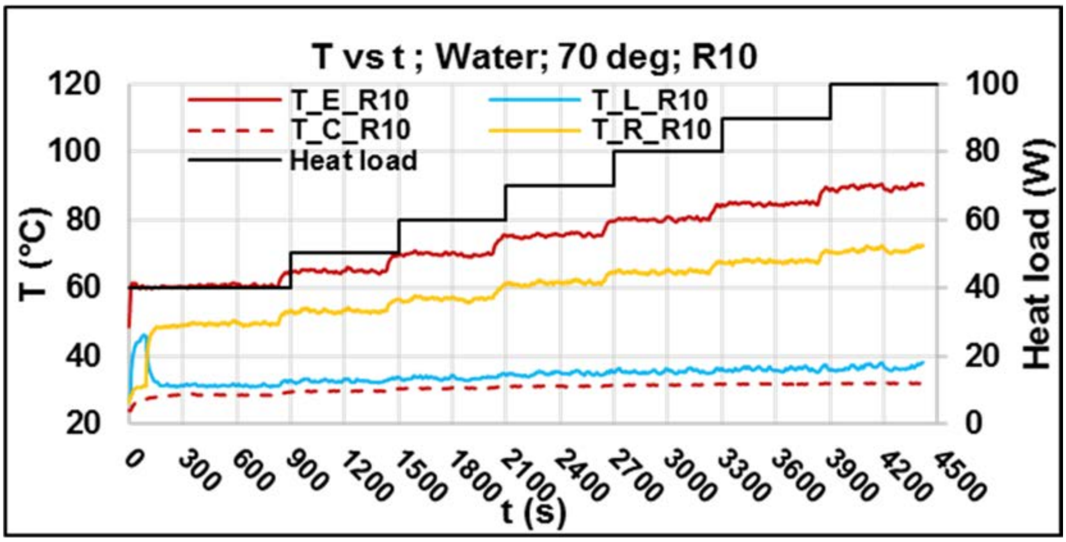

Figure 5-30: Water-70deg-R10 - Temperature vs time

Consider the 70° inclination for R6 with methanol and water as shown in Figure 5-27 and Figure 5-28. The PHP operation started at 20 W like at other inclinations in case of methanol prior to which the diode mode operation occurred. The flow regime of LFR was observed at 20 W and 30 W while UDC prevailed for the rest of the heat loads up to 70 W. However, for water for the same bend radius up to 80 W, circulation with reversal was seen with very frequent reversal up to 60 W. When the bend radius is changed to 10 mm, methanol operated with LAO at 10 W, and the actual PHP operation started (spike seen at 20 W in Figure 5-29), with LFR followed by UDC. In case of water, the entire flow regime was UDC barring one reversal at the lowest heat load of 40 W (refer Figure 5-30). Thus the flow regimes are very different for different fluids for the same geometry.

5.6.2 Effect of inclination

To ascertain the R_{th} at every data point (fluid, heat load and inclination combination) a minimum of three trials were conducted for each data point. The Figure 5-31 shows the three trials of T_e of the methanol fluid tested at 80° inclination for heat loads ranging from 10 W to 70 W in R6 PHP. The figure shows that in all the three trials the operation at 10 W was diode mode as explained in section 5.6.1.1. Hence in this section the R_{th} values of 10 W was not considered for comparison and further discussion.

To understand the effect of the inclination angle on the performance of the two PHPs the R_{th} was plotted for various inclinations for given heat load (one moderate heat load and one high heat load) in Figure 5-32. The heat loads were chosen as 30 W and 60 W for methanol. Likewise, 60 W and 100 W were chosen in case of water so as to have one moderate heat flux and one high heat flux for each fluid. However, the trend in both the heat fluxes were same.

The plots indicate that the optimum inclination in case of single loop PHP is not 90° but over a range of 60° to 70°. This was the trend reported in [47], [48] and [49] as the authors conclude that the best performing angle is slightly away from the vertical orientation. This may be due to the least resistance offered at inclination angles between 60° and 70° for both upward as well as the downward movement of the fluid as against the vertical orientation which provides a greater resistance to the upward movement of the fluid.

The figure also indicates the variation across trials for each data point. The plot shows that the error bars are wider for 90° inclination than the rest of the angles. It can be observed that the R_{th} at 80° inclination is greater than that of either 70° or 90°. At this point of time there is no possible explanation for these two occurrences.

Figure 5-32 also shows the comparison of all the four cases of – two fluids and two geometries, across inclinations at a given heat load of 60 W. The figure indicates that water performs better as working fluid for heat loads when both fluids are operational. R10 as expected was better performing than the sharper bend radius of R6 for both fluids for all heat loads.

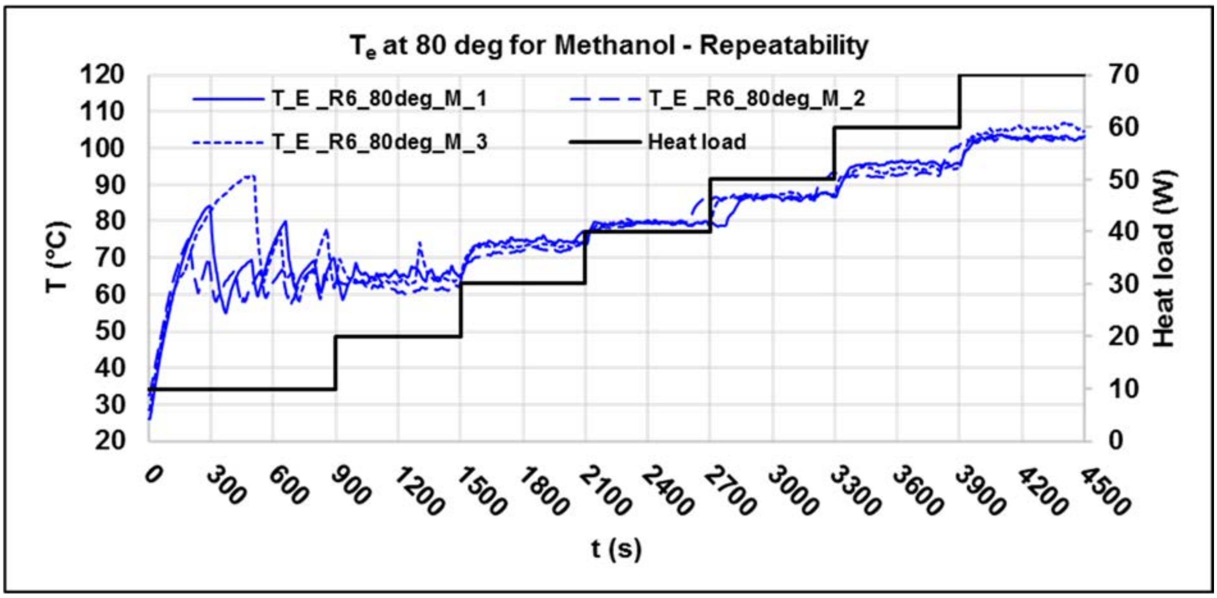

Figure 5-31: Methanol-80deg-R6 - Temperature vs time for repeatability across trials

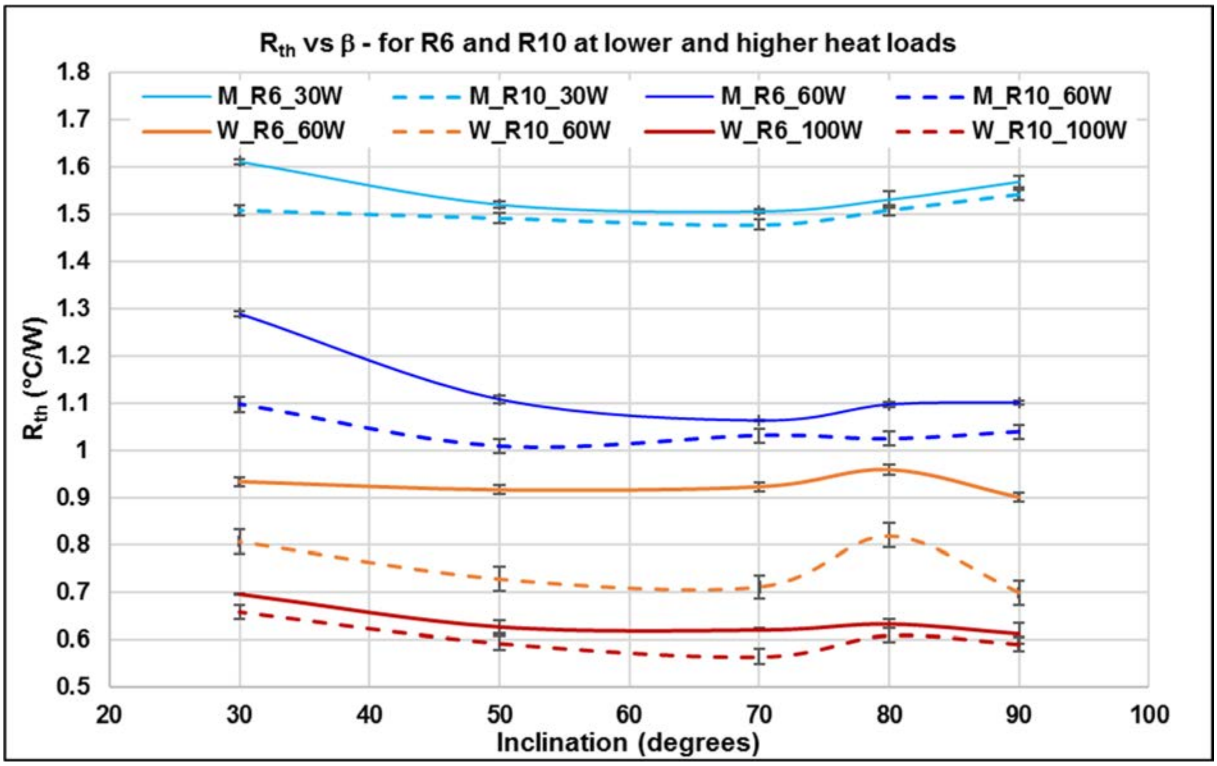

Figure 5-32: R_{th} vs inclination for both radii for low and high heat loads for two fluids

5.6.3 Effect of heat load

The effect of heat load on the thermal performance of the two PHPs under consideration with the two working fluids was plotted as bar chart for various inclinations in Figure 5-33 and Figure 5-34. The important conclusions that can be drawn are as follows

a. As the heat load increases the R_{th} comes down indicating better thermal performance. This is due to the fact that at higher loads unidirectional circulation occurs, thus there is greater heat transfer. This is true for all inclinations.
b. Also for all inclinations the difference in the performance of the two PHPs (R6 and R10) diminishes as the heat loads increase. This is more evident in water as higher heat loads could be tested with water. This can be attributed to the decrease in dynamic viscosity of the liquids (rate of decrease more in case of water) with the increase in temperature (refer Appendix – A).
c. At very low heat load of 20 W with methanol as the working fluid there is no difference in performance between R6 an R10.
d. However, for the rest of the loads R_{th} of R6 is larger than that of R10 indicating that the smoother bend results in greater heat transfer due to lesser pressure drop. The difference in R_{th} of R6 and R10 is less evident in case of methanol than water as viscosity of methanol is lesser than water hence lower resistance to flow.
e. At lower inclinations (like 50° and 30°) for 40 W heat loads the performance of water and methanol are nearly same for R6 geometry.
f. Though water did not operate at lower heat loads (lesser than 40 W) with the exception of one trial where 30 W could be tested at 90° inclination, water yielded a wider heat load range than methanol for the same maximum T_e of 100°C.

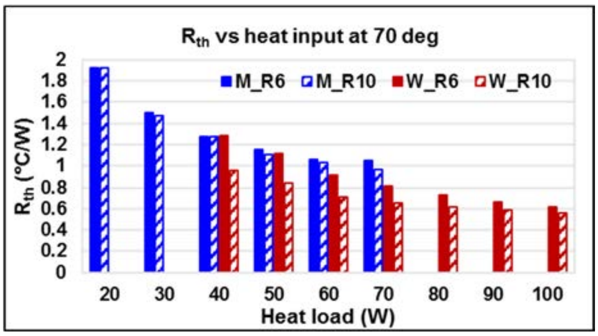

Figure 5-33: R_{th} for various heat loads for 70 degree inclination

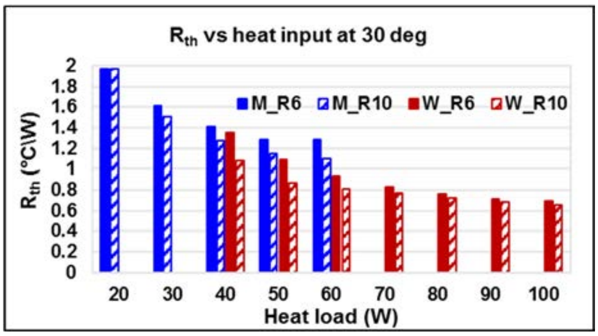

Figure 5-34: R_{th} for various heat loads for 30 degree inclination

5.6.4 Summary of the tests

For the two bend radii and the two fluids, the number of data points tested is summarised in Table 5-3 with respect to inclinations and heat load. On the whole, 48 data points of methanol and 56 data points of water could be tested. The rest of the inclinations and heat load combinations either did not operate or exceeded the heater maximum power rating or the rated temperature. Likewise, the flow pattern observed during the entire range of test is summarised in Table 5-4. The R_{th_dry} was found to be nearly 10°C/W. The best (or the lowest)

R_{th} was found to be that of R10 PHP with water as working fluid at an inclination of 70° for a heat load of 100 W with a value of 0.56°C/W. Hence with the concept of PHP, nearly 18 times enhancement of heat transfer was achieved. In case of R6, the best R_{th} was 0.62°C/W occurring with water at 70° inclination for heat load of 100 W leading to an enhancement of 16 times. The bend radius has strong impact on the performance of the PHP as evident in case of 30° and 60 W where R_{th} of R6 was 1.29°C/W and R_{th} of R10 was 1.10°C/W. This shows nearly 15% change in performance.

Table 5-3: Heat load and inclination combination for the two fluids

Fluid	Inclination (degrees)	Heat load (W)	Number of data points
Methanol	90 - 40	20 to 70 W	6 inclinations x 6 heat loads = 36
	30	20 to 60 W	5
	20	20 to 50 W	4
	10	20 to 40 W	3
Methanol – Total			48 numbers
Water	90 - 20	40 to 100 W	8 inclinations x 7 heat loads = 56
	10	No operation	
Water - Total			56 numbers

Table 5-4: Summary of flow pattern

Fluid	Inclination (degrees)	Flow pattern					
		R6			R10		
		10 W	**20 - 30 W**	**40 - 70 W**	**10 W**	**20 - 30 W**	**40 - 70 W**
Methanol	90 - 30	Diode	VFR	UDC	LAO	LFR	UDC
	30 - 10	LAO	LFR	UDC	LAO	LFR	UDC
		10 – 30 W	**40 - 80 W**	**80 - 100 W**	**10 – 30 W**	**40 – 50 W**	**40 - 100 W**
Water	90 - 50	NO	VFR	UDC	LFR	LFR/UDC	UDC
	40 - 20	NO	LFR	UDC	UDC	UDC	UDC
Diode – Start-stop operation; LAO – Low amplitude oscillations; LFR – less frequent flow reversal; NO – No operation; UDC – unidirectional circulation; VFR – very frequent flow reversal							

5.6.5 Effect of insulation in adiabatic section

In this PHP construction the adiabatic section is a conductive copper tube unlike the previous version (chapter – 4) where adiabatic section was made of glass tube. Akachi in his patent [36] states that the insulation of the adiabatic section enhances the heat transfer capability of the PHP. The performance is expected to become better as the pressure gradient responsible for the flow of fluid from evaporator to condenser and back is due the temperature gradient. Once the section is insulated the temperature gradients within the PHP tend to be large thus resulting in higher pressure gradients. So the heat transfer rate can be increased.

To determine the effect of insulation at the adiabatic section, R6 PHP was applied a 2 mm thick layer of silicone sealant and then covered with poly urethane pipe (slit longitudinally). The dry (without fluid) test was conducted for the same and the temperature plot is shown in Figure 5-35. The insulated R6 PHP is shown in Figure 5-36. The plot shows that the T_e was nearly same as that without insulation for the same heat load of 5 W and cooling conditions of condenser (T_c = 25°C). The other observation one can make is that the adiabatic limb temperatures are slightly higher (at least 5°C) than those without insulation. This is expected as the insulated limb has to be at higher temperature. Apart from that T_L and T_R trace when insulated did not have fluctuations like that of uninsulated scenario as they were not exposed to the convective heat transfer. Again the temperatures at corresponding locations were the same indicating the proper adherence of the thermocouples.

The tests for various heat loads for the two fluids were conducted at 90°, 70°, 50° and 30° inclinations only to compare the performance with and without insulation. The heat loads were changed in steps of 20 W and not in steps of 10 W as performed for the earlier investigation with bare adiabatic section.

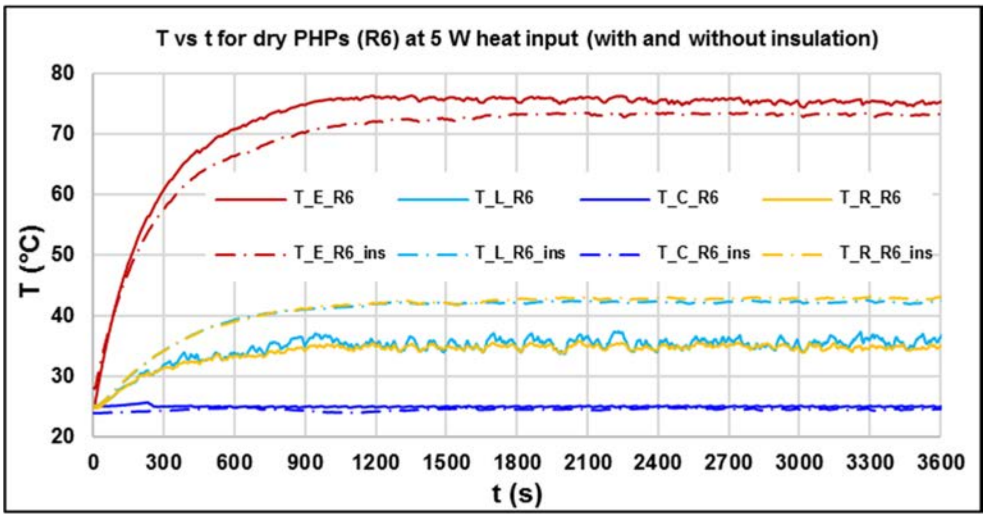

Figure 5-35: T vs t for dry PHP (with and without insulation at adiabatic section)

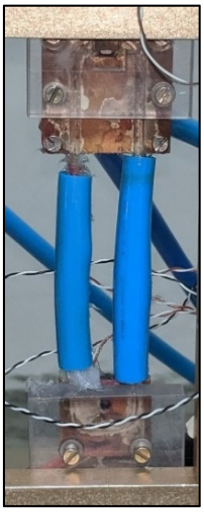

Figure 5-36: R6 adiabatic section insulated

5.6.5.1 Flow pattern variation

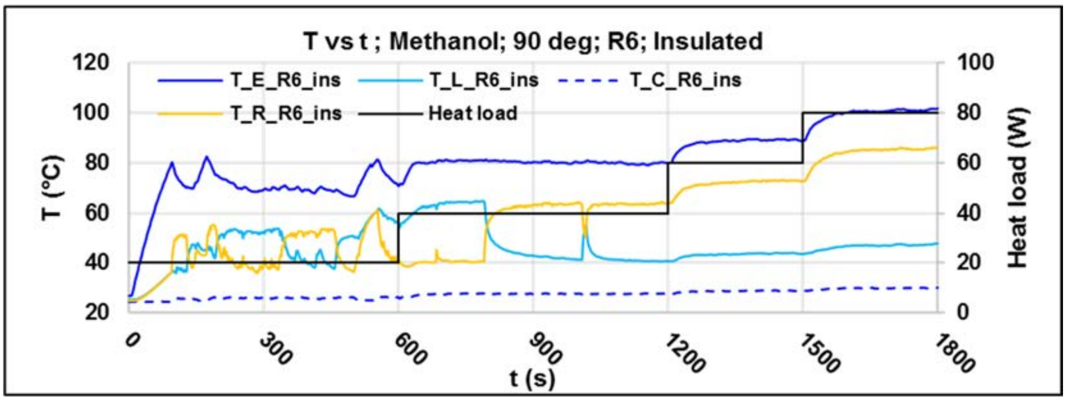

Figure 5-37: Methanol-90deg-R6 - Temperature vs time (insulated)

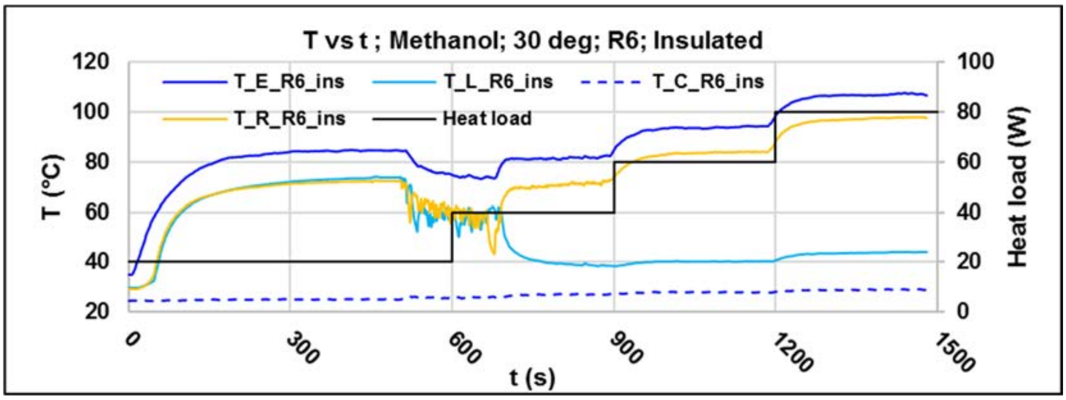

Figure 5-38: Methanol-30deg-R6 - Temperature vs time (insulated)

At 90° inclination, the pattern for methanol as shown in Figure 5-37 indicates that for 20 W heat load the reversal frequency reduced as compared to bare adiabatic section (Figure 5-5). Another important aspect was that the 80 W heat load which could not be operated as T_e exceeded 100°C could be operated at nearly 100°C. The flow became UDC at higher loads. At lower inclinations like 30° (Figure 5-38) indicated LAO at beginning of 20 W and later became HAO which was different from the flow pattern of 20 W without insulation (LFR refer Figure 5-13) but at higher heat loads the flow turned out to be UDC. The heat load of 80 W could be operated even at the lower inclination of 30° in the insulated case.

For water at 90° inclination as well as up to 30° inclination the heat load of 20 W which could not be operated with uninsulated tubes could be carried out with insulation. The flow pattern at 20 W was of HAO at 90° as seen in Figure 5-39. For 40 W at 90° the flow pattern was nearly same as that of bare PHP. At 30° the 20 W heat load initially operated in diode mode then operated with HAO (Figure 5-40). Heat load of 40 W showed more frequent reversal of circulation direction than in case of non-insulated case. Beyond 40 W UDC manifested.

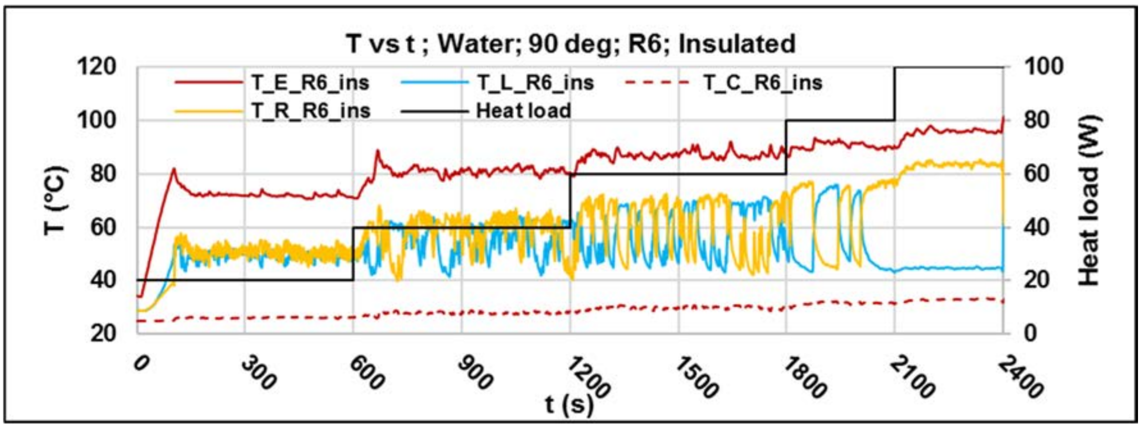

Figure 5-39: Water-90deg-R6 - Temperature vs time (insulated)

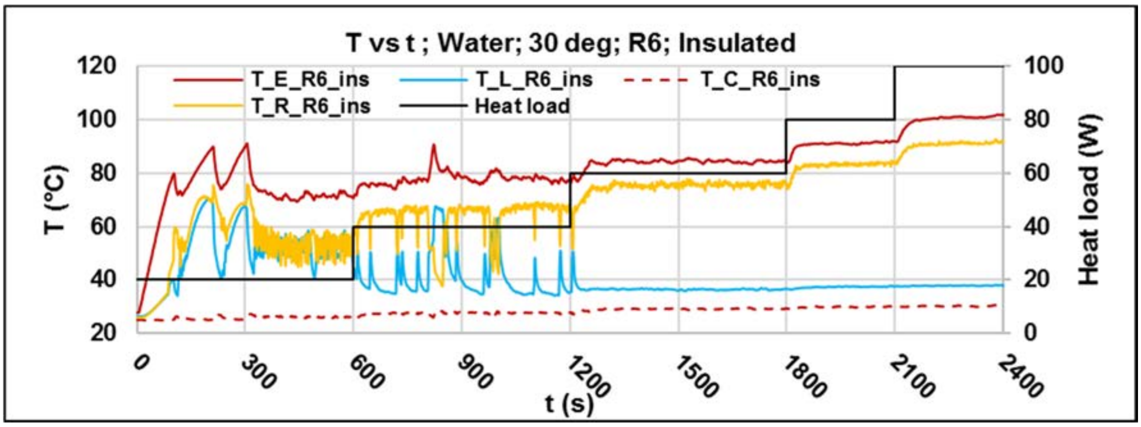

Figure 5-40: Water-30deg-R6 - Temperature vs time (insulated)

5.6.5.2 Variation with heat load

Figure 5-41 shows the variation of the R_{th} for the R6 PHP for various heat loads at 70° inclination. At lower heat load of 20 W the insulation seems to be counterproductive as the R_{th} for insulated is higher than that for bare PHP. At higher heat loads the insulation is certainly beneficial in lowering the R_{th}. This enhancement is true for both the working fluids. For instance, at 60 W heat load for both water and methanol there was a 6% reduction of R_{th}. This enhancement can be more for a PHP with more number of adiabatic tubes as greater pressure gradients may prevail at any instant of time.

5.6.5.3 Variation with inclination

Figure 5-42 and Figure 5-43 shows the comparison of R_{th} for 60 W and 100 W respectively for various inclinations. Overall it can be seen that the insulation enhanced the heat transfer capability of the PHP. However, at 90° for all loads for water as working fluid a different trend was observed – the insulated R_{th} was higher. This particular inclination with insulation needs to be further scrutinised as the curve for R_{th} shows a sudden increase only at 90° with insulation.

Figure 5-44 shows the comparison of R_{th} for various configurations tested at 60 W and 70° inclination. The insulation at the adiabatic section improved the heat transfer rate in most cases though marginally. Apart from improving the heat transfer rate the insulation of the adiabatic section aided in widening the heat load range for both the fluids. Water could be operated at 20 W (pressure gradient large enough to initiate and sustain fluid pulsations at lower loads) and methanol could be operated at 80 W (pressure gradient large to have greater velocity of flow thus lower T_e) for all inclinations (90° to 30°) both of which was not possible with the uninsulated PHP.

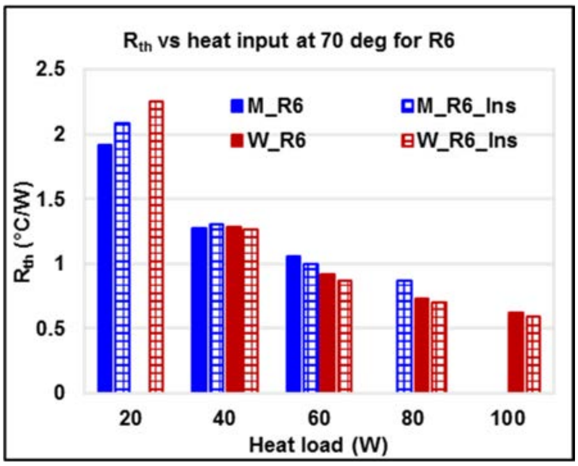

Figure 5-41: R_{th} of R6 at 70 degrees

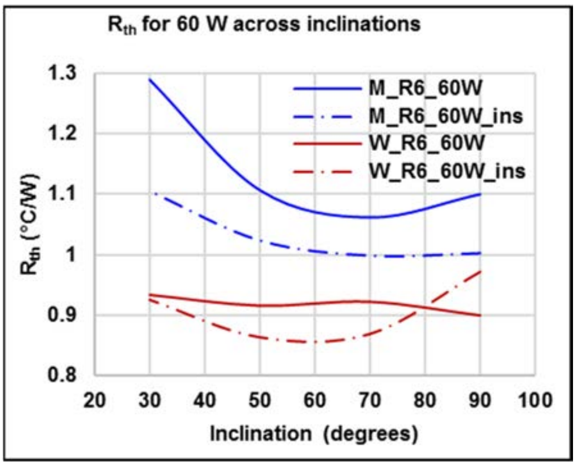

Figure 5-42: R_{th} for 60 W (R6) across inclinations

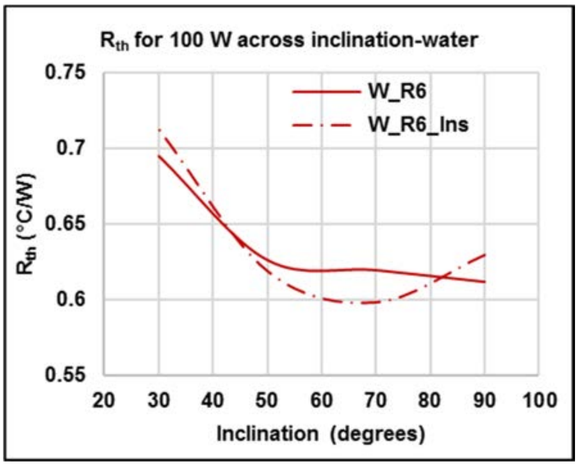

Figure 5-43: R_{th} for 100 W (R6) across inclinations

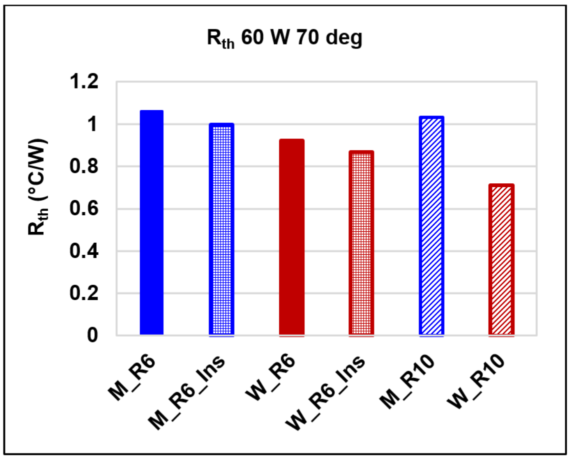

Figure 5-44: R_{th} for various configurations at 70 degree 60 W

5.6.6 Estimation of frequency of oscillation

The PHP with R7.5 was tested for various inclinations and heat loads to estimate the characteristic frequency of pulsations within the PHP. Both methanol and water was tested with this PHP which is geometrically different from the previous ones not only in terms of the bend radius but also due to T-joints at the adiabatic sections to include the pressure transducer and charging valve. To make the PHP symmetric (to avoid flow direction bias) the charging port was accommodated with a T-joint in one of the adiabatic section and the other housed the pressure transducer. In this case care was taken to fit the transducer as close to the PHP working zone as possible (refer Figure 5-45) to capture the pressure fluctuations unlike the case of flat plate PHP (refer Figure 3-16) where the sensor was located far from the PHP working zone. The presence of two T-joints made the PHP less efficient in terms of heat transfer compared to the R6 and R10. Hence the T_e as well as T_L and T_R for the configuration was always greater than the other PHPs. The flow pattern for both fluids where counter clockwise ($T_R > T_L$) though thought was given to make the PHP symmetric.

The sampling was done from the pressure transducer at 40 Hz which is much above the expected frequency of less than 5 Hz. The transducer response time is less than 2 milliseconds. The frequency estimate was done once the steady state was achieved and 2048 consecutive samples (which accounts to approximately 51 seconds) was chosen to carry out the Fast Fourier Transform (FFT) to get the power spectral density in the frequency domain from the time domain voltage signal. FFT was performed using MS Excel (Fourier analysis under data analysis tools), where Gaussian kernel is used. The FFT signal showed characteristic frequency as the sensor was located in the proximity of the flow passage. The pressure transducer data (average of 51 seconds after 500 seconds of the test) is shown in comparison with the saturation pressures corresponding to temperatures at various locations in Table 5-5. The transducer data corresponds closely to the average of the P_{sat} at T_e and T_c as in the case of flat plate PHP (chapter - 3) but in this case transducer readings are more influenced by the T_e (slightly higher than the average) as the transducer is located at around 40 mm from the evaporator. The transducer reading did not get influenced by the T_L which is the temperature measurement nearest to the transducer location.

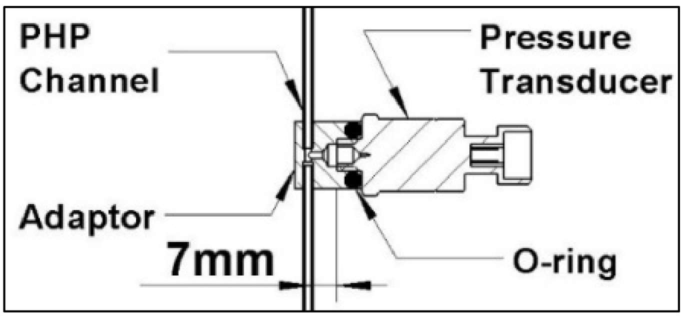

Figure 5-45: Connection and location of pressure transducer to the SLPHP

Table 5-5: Temperature and corresponding pressure data vs pressure transducer reading

Test condition	T_e	T_c	T_L	T_{avg}	P_{sat_Tavg}	P_{sat_Te}	P_{sat_Tc}	P_{sat_TL}	$P_{sat\_avg}=(P_{sat\_Te}+P_{sat\_Tc})/2$	P_{trans}
	°C	°C	°C	°C	kPa	kPa	kPa	kPa	kPa	kPa
Methanol; 90°; 30 W	81.32	27.44	44.42	54.38	67.2	189.1	19.3	43.5	104.2	128.4
Water; 90°; 40 W	79.43	29.04	37.47	54.24	15.1	45.9	4.1	6.5	25.0	38.7

5.6.6.1 Methanol

The flow pattern observed was UDC. For methanol, the saturation pressure exceeded the maximum range of pressure transducer (2 bars) for most heat loads and inclinations. Hence only a limited number of frequencies could be obtained at selected data points – like not more than 40 W at only vertical and near vertical positions of 90° and 70° (Figure 5-46 and Figure 5-47). The FFT of these data points are shown in Figure 5-48. To probe more points a heat load of 30 W was operated at 3 inclinations of 90°, 70° and 50° (Figure 5-49) so that with lower temperature of operation (thus lower pressure) more frequencies could be obtained. The corresponding FFT plots are shown in Figure 5-50. For 40 W the frequencies were in the range of 2 to 3 Hz. For 30 W the frequencies were 1 to 2 Hz for near vertical inclinations. For lower inclination of 50° the frequency was less than 1 Hz.

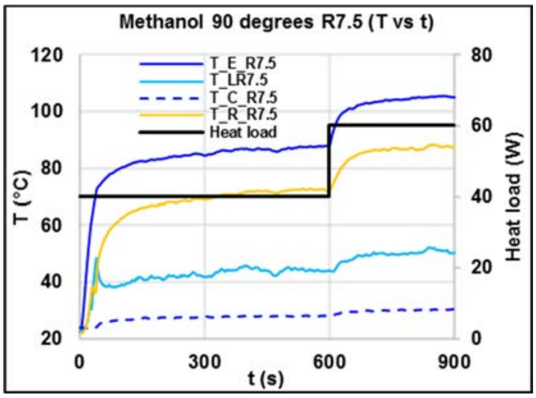

Figure 5-46: R7.5-Methanol-90deg - temperature vs time

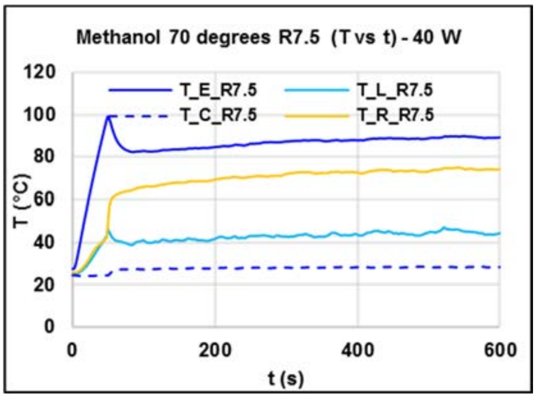

Figure 5-47: R7.5-Methanol-70deg - Temperature vs time

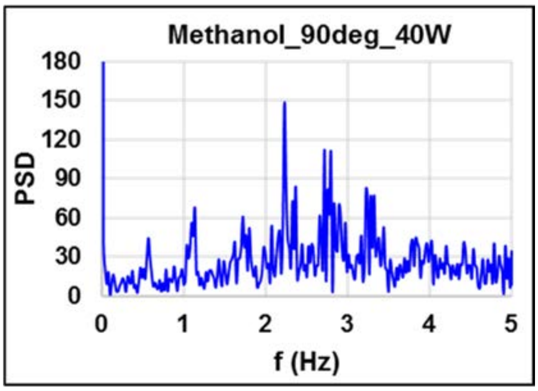

(a)

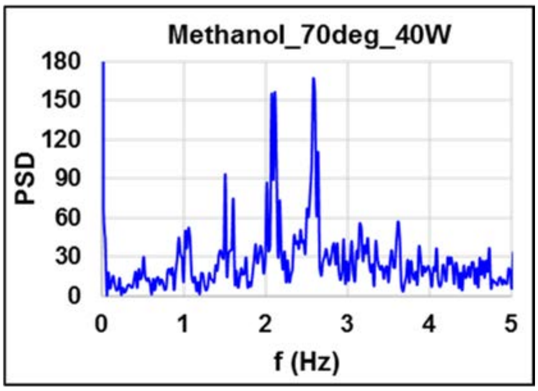

(b)

Figure 5-48: Frequency-Methanol 40W

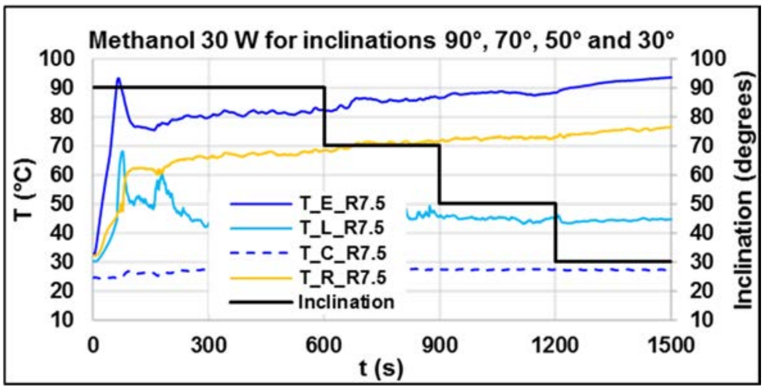

Figure 5-49: R7.5-Methanol-30W for various inclinations - Temperature vs time

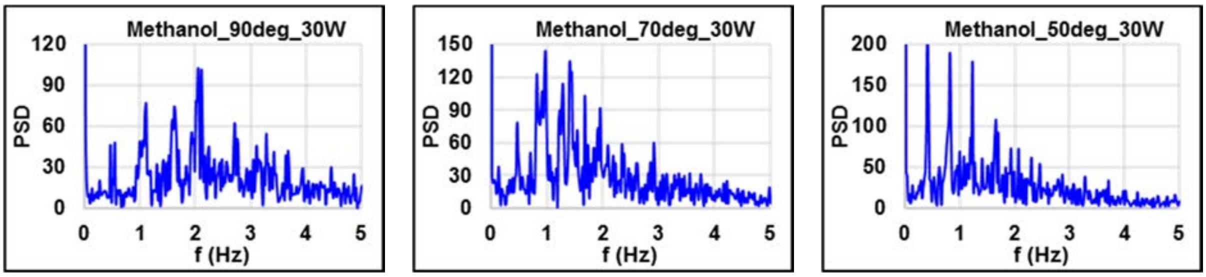

(a) (b) (c)

Figure 5-50: Frequency-methanol – 30W

5.6.6.2 Water

In case of water the saturation pressure was much lower. Hence more number of frequencies could be obtained. A total of 9 frequencies from three heat loads each at three inclinations were obtained. The inclinations tested were 90°, 70° and 50°. The corresponding temperature plots are shown in Figure 5-51, Figure 5-53 and Figure 5-55 respectively. The frequencies obtained for 40 W, 60 W and 80 W for the above inclinations are shown in Figure 5-52, Figure 5-54 and Figure 5-56.

5.6.6.3 Frequency analysis

The frequencies obtained were summarised in Table 5-6. The results show that for both methanol and water as the heat load is increased for given inclination the higher frequency components are also dominant indicating more chaotic behaviour. Figure 5-52 (c) and Figure 5-54 (c) indicates that at 80 W higher frequencies are dominant compared to 40 W and 60 W for water as working fluid. Apart from that, for the same inclination (90°) and heat load (40 W) the more volatile methanol showed the higher frequencies (Figure 5-48 (a) and Figure 5-52 (a)). With lower inclinations the frequency was lower for the same heat load as the velocities will be lesser. Thus the frequency estimate qualitatively corresponds to the velocity scales existing inside the operating PHP. However, further study with more loads and inclinations will be very useful in providing information for the design of a PHP as velocities are not known up front. The frequency ranges obtained are summarised in pictorial form in Figure 5-57.

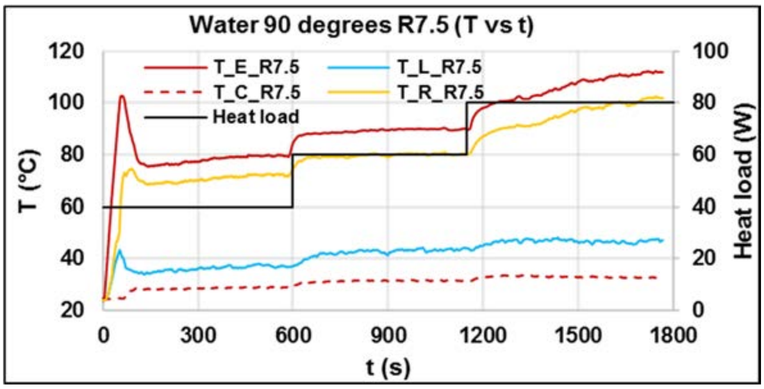

Figure 5-51: R7.5-Water-90deg - Temperature vs time

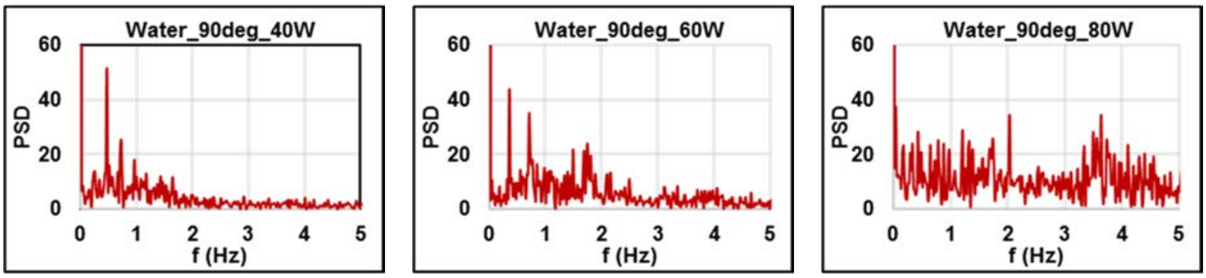

(a) (b) (c)

Figure 5-52: Frequency-water-90deg

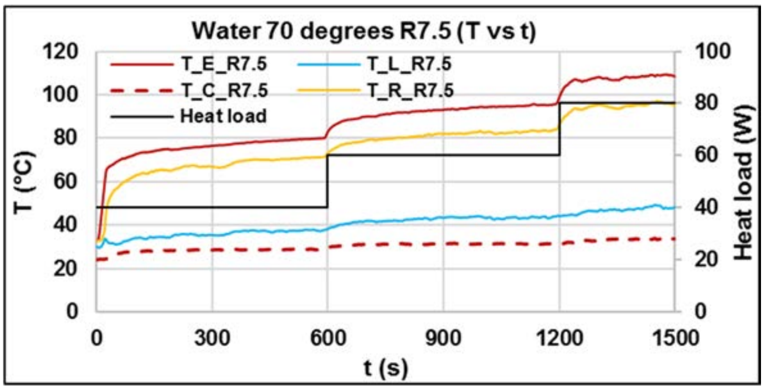

Figure 5-53: R7.5-Water-70deg - Temperature vs time

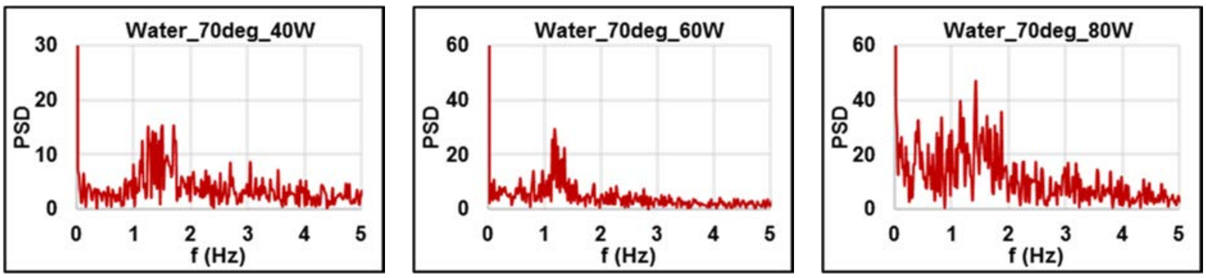

(a) (b) (c)

Figure 5-54: Frequency-water-70deg

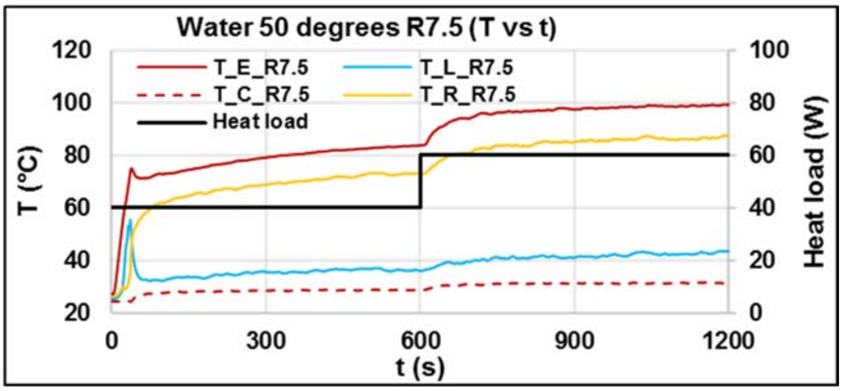

Figure 5-55: R7.5-Water-50deg - Temperature vs time

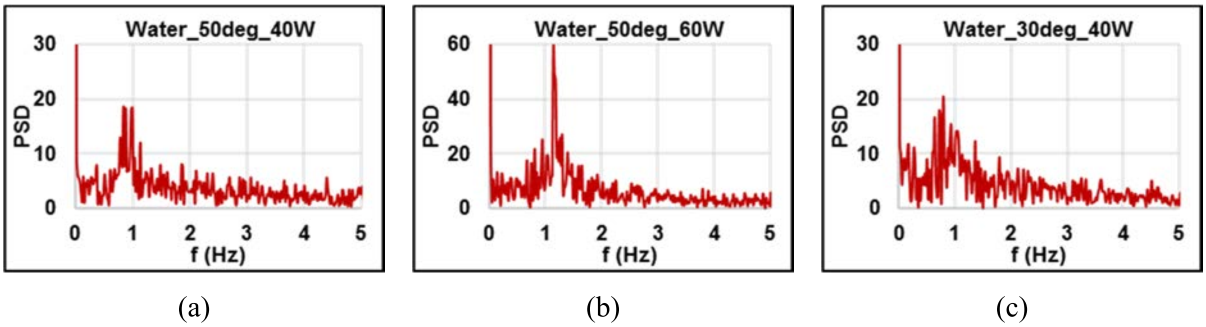

Figure 5-56: Frequency-water-50deg

Table 5-6: Summary of the frequencies for various inclinations and heat loads

Fluid	Inclination (degrees)	Heat load (W)	Time after start for estimation of frequency (s)	f (Hz)
Water	90	40	500	0.5
Water	90	60	1000	0.5-1.0
Water	90	80	1700	1.0-4.0
Water	70	40	500	1.0-2.0
Water	70	60	1000	1.0-1.5
Water	70	80	1400	1.0-2.0
Water	50	40	500	~ 1.0
Water	50	60	1000	> 1.0
Water	30	40	500	~ 1.0
Methanol	90	40	500	2.0-3.0
Methanol	70	40	500	2.0-3.0
Methanol	50 and 30 degrees	Even 40 W could not be obtained as temperatures exceeded 85°C. Hence saturation pressure of methanol was beyond transducer range of 2 bars.		
Methanol				
Methanol	90	30	500	1.0-2.0
Methanol	70	30	800	1.0-2.0
Methanol	50	30	1100	< 1.0

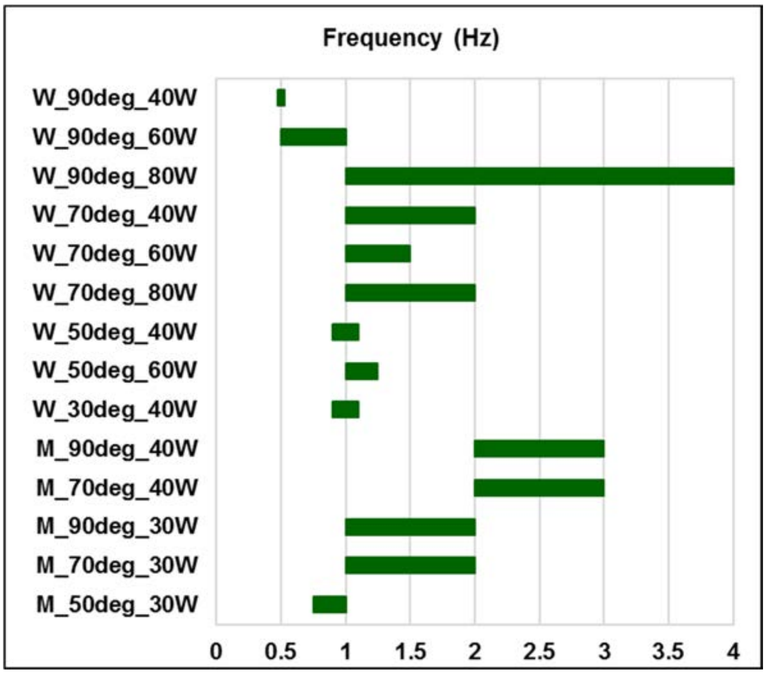

Figure 5-57: Pictorial representation of the frequency range for various data points

5.7 Closure

A study on SLPHPs was carried out with a specific focus on the performance based on the bend radius. As expected the smoother (larger radius) bend performed better than the sharper bend. The salient conclusions are as follows

- Flow regimes varied for the varying geometry and working fluids at lower heat loads. At higher heat loads unidirectional circulation manifested for all inclinations tested.
- Loss of pressure in the bends cannot be neglected even if the number of bends is small as more than 15% performance change (refer data for water with 50 W heat load at 30° from Figure 5-34) was observed at lower inclinations due to the change in bend radius.
- Contrary to the expectation the optimum angle of good heat transfer was not 90° but was found to be between 60° and 70° inclinations.
- Water turned out to be a better working fluid than methanol when both fluids could be operated.
- Effect of bend radius was less in methanol as its dynamic viscosity is much lesser than that of water.
- R_{th} was found to be decreasing with increase in heat load. This is because of the greater velocity of flow at larger heat loads.

- For all inclinations the difference in the performance of the two PHPs (R6 and R10) diminished as the heat loads increased. This is more evident in water as higher heat loads were tested with water. This can be due to the decrease in dynamic viscosity of the liquids with the increase in temperature.
- Though the PHP configuration tested was only a single loop the performance showed that the R_{th} can be reduced by 18 times (refer 100 W data for water at 70° inclination in Figure 5-33) in comparison with a dry PHP. Thus even a single loop PHP can be used for practical cooling applications if used with right fluid and heat load with predominantly vertical orientation.
- Insulating the adiabatic section resulted in marginal improvement in heat transfer of the PHP of same geometry, working fluid, heat load at almost all inclinations.
- Insulation of the adiabatic section also widened the heat load range of both the working fluids tested.
- Frequency analysis carried out by testing of R7.5 PHP showed that with increase in heat load higher frequencies manifested. The frequencies tended to be lower for near horizontal inclinations and for less volatile working fluids.

6 Multiloop multiplane pulsating heat pipe – Fins of heat sink

6.1 Introduction

The investigations on PHPs so far in this study, were confined to heat loads less than or around 100 W. In this chapter a PHP has been investigated for higher heat loads for several hundreds of watts. In this chapter the PHP tubing has not been confined to single plane but is deployed in multiple planes. Here the PHP tubes have been tested to act as fins for a heat sink base. This concept of using PHPs to act as fins was proposed by Akachi in his patents [36] and [18]. He termed these fins as "Kenzan fins". Khandekar in his doctoral thesis [49] investigated the efficacy of using the CLPHPs as fins with forced air convection and aimed at using PHPs as "super fins" of extremely high thermal conductivity. These PHPs oriented in more than one plane have been proven to work in all three orientations - bottom heat mode, horizontal mode and top heat mode in [24]. It has been reported in [19] that apart from having more turns in evaporator having loops deployed in the multiple orientation makes the PHP less dependent of orientation as the gravity forces always have some favourable components working towards bringing the condensate back to evaporator. Though these configurations of the PHP are found to have several advantages over the planar versions the investigations regarding these multiplane PHPs have been less. The PHP based forced air cooled heat sink was studied in [52] for gravity independent operation and were successful for the case of a relatively wider heat load area. Likewise, the PHP with channels in three dimensions but with a flat configuration was studied in [53] and was reported to have very good performance both in vertical and horizontal orientations. Hence in this chapter a study on PHP based fins as suitable replacement for heat sinks has been carried out with water as the working fluid for a fill ratio of 60% in three orientations with an aim to enhance the fin efficiency.

6.2 Selection of fluid and inner diameter

Though several fluids have been investigated for use in PHP [9], [26] and [27], the fluid to be used in PHP should have larger specific heat as most of the heat exchange occurs by sensible heat transfer [10]. The literature shows that of all the fluids tested water gives the scope for the largest heat load for a given configuration of PHP. Since the study was targeted at larger heat loads than what has been studied in this dissertation, water was chosen as working fluid although water does not possess the requisite high $(dP/dT)_{sat}$.

It was also stated in most literatures like [19] and [13] that 2 mm inner diameter was found to handle higher heat loads with lesser R_{th} than the smaller diameters. With water being the working fluid lower diameters will be hindering heat transfer as the viscosity is larger than fluids like methanol or ethanol. With the higher surface tension of water larger diameter tube can be used as per the Bond number criteria as well. Hence copper tubing with 2 mm inner diameter and 3 mm outer diameter was chosen for development of the PHP heat sink.

6.3 PHP construction and geometry

The heat sink was fabricated by milling the grooves of 20 mm length, 3 mm depth on a copper blank of 110 mm x 110 mm x 8 mm to make the base of the heat sink. Then, about 5 m long copper tube of 3 mm outer diameter and 2 mm inner diameter was bent into a serpentine loop that fit snugly into the grooves machined in the blank. The height of the channel of PHP which acted as the fin was 125 mm. The closed loop configuration of the PHP was chosen as the performance is better than the open loop one [19]. The number of bends in evaporator (18 in this case) was kept more than the critical number of bends as indicated by [19] to have gravity independent operation of PHP. To minimize the thermal contact resistance between the tube and the heat sink base, they were brazed together into a single component. An adaptor was given to enable charging of the PHP based heat sink. AIGNEP ball valve (06310 00 001) was used to create a vacuum in the tube and to charge deionized water into it. Figure 6-1 shows the development stages of the heat sink. An axial fan of EBM Papst make (8214 JH4 – 80 x 80 x 38 mm^3) of 24 V rating was used for forced convection cooling. A glass tube was used as a viewing window to visually characterize the operation of the heat sink.

6.4 Setting up of PHP

The PHP was checked for leak rate using helium leak detector (Pfeiffer ASM 182 TD^+) and the leak rate was found to be of the order of 10^{-6} Torr-l/s. The ball valve acted as a vacuuming port as well as a charging port for deionized water. The ball valve outlet was used for vacuuming the PHP through a dual stage rotary vane vacuum pump (Pfeiffer DUO 10 M) and vacuumed for removal of non-condensable gases (a pressure level of less than 0.3 Pa). A measured quantity of deionized water was charged into the PHP through the valve using a syringe attached to the valve. The filling ratio maintained was 60%, as the PHPs are expected to give the best performance between 40% and 60% as stated in [9]. The valve was closed and the setup was ready to be tested.

6.5 Experimental set up

The heat sink setup with the heat source (heater OHMITE make TA1K0PH8R00KE), of 1000 W, 8Ω resistance, with fan is shown in Figure 6-2. For measuring the temperature at various points on the heat sink, thermocouples were embedded as illustrated in Figure 6-3. Eight numbers of T-type thermocouples (RS 621-2164) were used for measuring the temperature. An 8-channel Picolog (TC-08) data logger was used to read the data and post-process temperature in the laptop. Two power supplies (TDK Lambda make) were used: one to power the fan (Z^{+}60-14), and the other, to power the resistance heater (GEN 60-40). The entire test setup is shown in Figure 6-4.

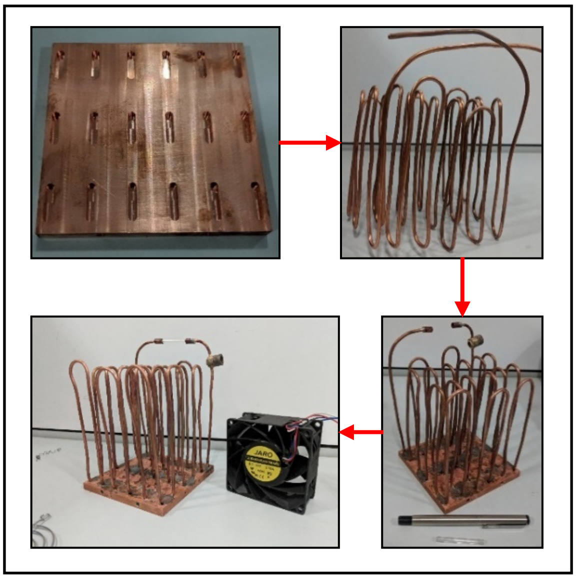

Figure 6-1: Development of PHP heat sink

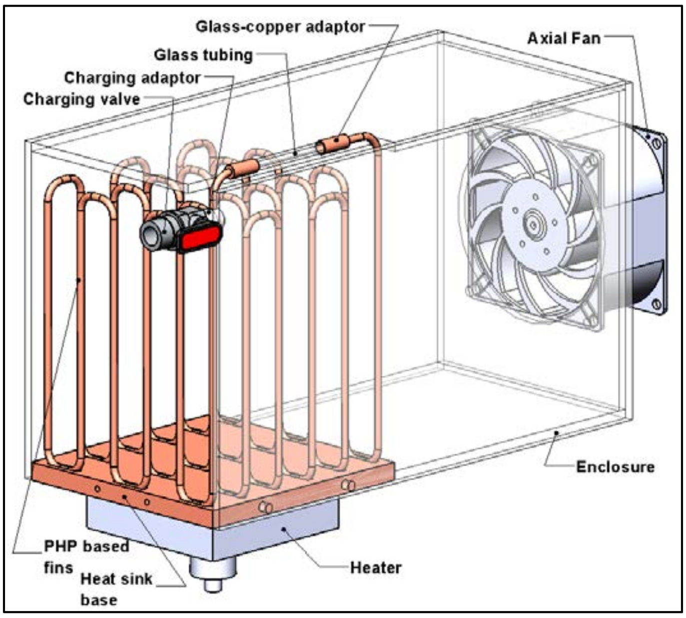

Figure 6-2: Schematic of the PHP test setup

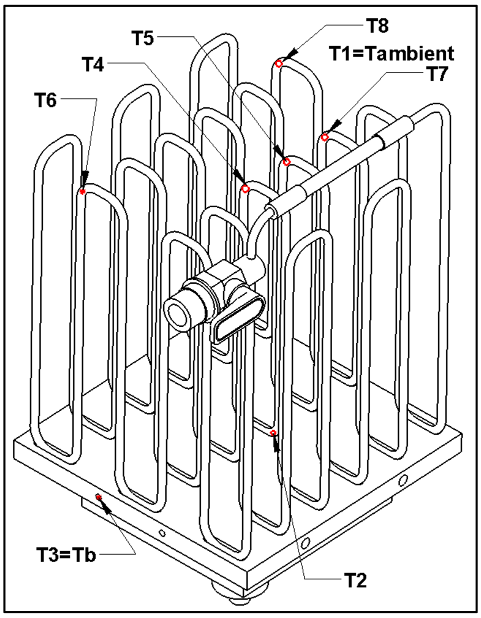

Figure 6-3: Thermocouple locations on the heat sink

6.6 Results and discussion

6.6.1 Dry PHP testing

Before carrying out the PHP testing the PHP heat sink without the working fluid charge was tested to estimate the R_{th_dry} for the configuration. The tests were conducted from 100 W to

250 W in steps of 50 W. The test was stopped at 250 W as the T_e or T_b (refer Figure 6-3) exceeded 100°C.

1. Without fluid in the PHP, the conduction path from the evaporator to the condenser was expected to be less than the phase change heat transfer, as conduction heat transfer is through the reduced cross-sectional area of the tube.
2. For heat load of 100 W, the evaporator attained steady state at 56° C. No appreciable rise in T_f was observed.
3. The steady state evaporator temperature was observed to be 70.7° C for heat load of 150 W, 87.4° C for heat load of 200 W, and 101.5° C for 250 W heat load.
4. For heat load of 250 W alone, a slight rise in the condenser temperature was observed, but this can clearly be attributed to conduction. The above characteristics are all evident from Figure 6-5.
5. Thus this trial without any fluid charged in the PHP, made it behave like a normal pin fin heat sink with forced convection.
6. The R_{th} was observed to be constant at 0.3°C/W.

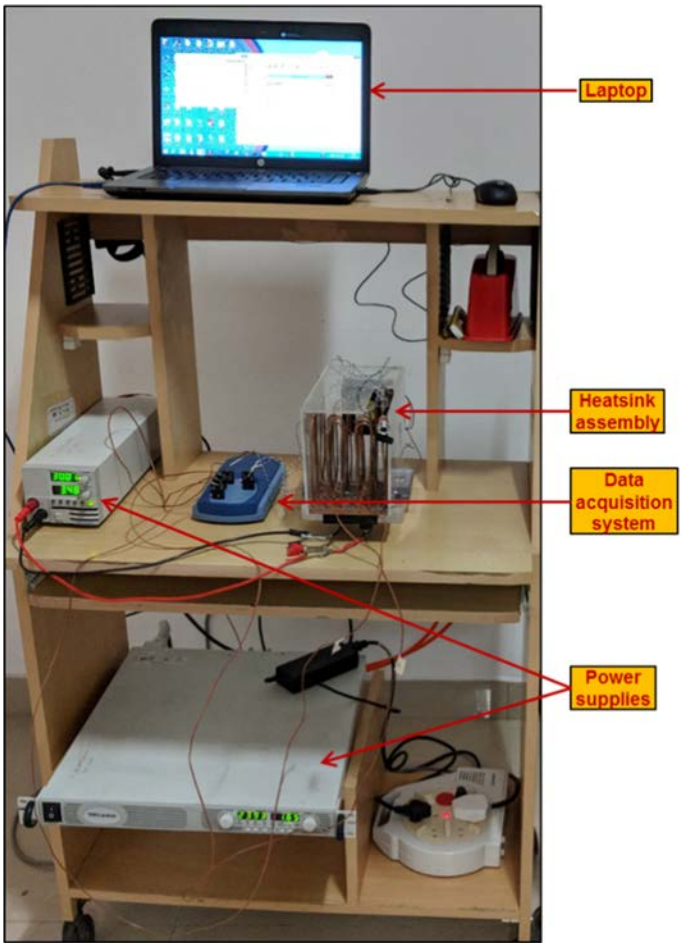

Figure 6-4: Details of the test setup

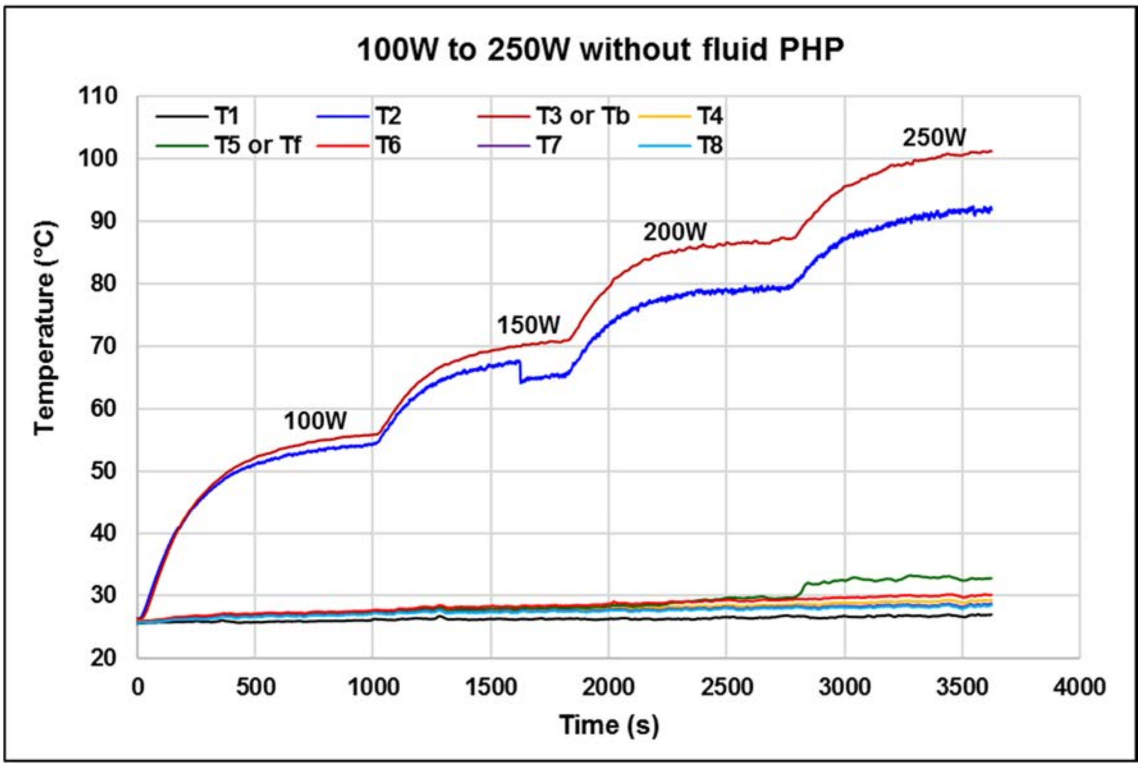

Figure 6-5: T vs t for 100 W to 250 W for dry PHP (without fluid)

6.6.2 Observations at 90° orientation

1. Discrete and weak pulses were seen through the glass window for a heat load of 100 W.
2. At 150 W, pulses were visible, but there was no preferred direction to them. Bubbles oscillated about a mean position. The flow pattern was of predominantly slug flow. At some points when the pulses were relatively rapid, the difference between the condenser and evaporator temperature, (T_b-T_f) became very less.
3. At 200 W, the pulses were faster, but the oscillations were still about the mean position only. The graph flattened after about 12 minutes into the test. The (T_b-T_f) was close to about 10° C.
4. Rapid, numerous pulses were observed for 250 W heat load. The pulses were continuous as compared to the previous values of heat loads. No circulatory characteristics were observed and only slug flow prevailed, even at 300 W.
5. As we can see from Figure 6-6, the condenser temperature, T_f violently oscillates for up to 200 W heat load after which the graphs rise smoothly. This can be attributed to the fact that the heat load did not cross the threshold value for moving the vapour bubbles continuously to the condenser. So the condenser temperature did not increase appreciably. Even if it did, it collapsed very quickly, and thus resulted in the oscillation of the T_c, as seen up to 150 W and even 200 W.

6. With operation beyond 200 W, we can see that the T_f is almost constant for a particular heat load, thus confirming that the best operating zone of the PHP has been reached. This conclusion can also be arrived at by observing the (T_b-T_f). The value comes down at higher heat loads as can be observed from Figure 6-6.

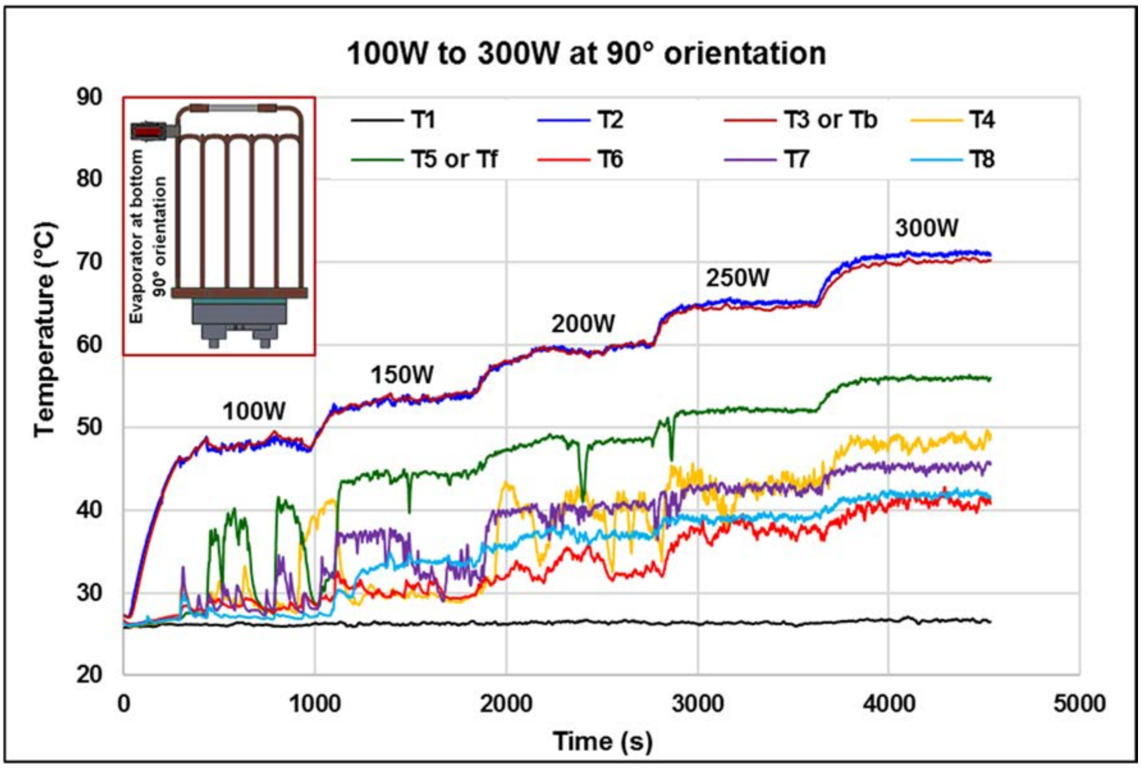

Figure 6-6: T vs t for 100 W to 300 W at 90° inclination

6.6.3 Observations at 0° orientation

1. Weak, highly intermittent pulses were observed for a heat load of 100 W. Up to about 5 minutes, the PHP remained inoperative as observed in Figure 6-7. The T_f began to rise only after that and then the oscillation continued thereon.
2. At 150 W, the operation began but with weak pulses. Participation from inner fins was also observed as seen in Figure 6-7. Vigorous pulsation of condenser temperature was observed indicating that the PHP did not attain complete quasi steady operation. It also reinforces the fact stated by several literatures that, the horizontal orientation of a PHP adversely affects the performance of PHP at lower heat loads.
3. However, at higher heat loads (from 250 W), the pulsations in condenser temperature greatly reduced and the (T_b-T_f) came down drastically; for heat loads lesser than 250 W, determination of (T_b-T_f) was difficult, owing to violent pulsing of condenser temperature.

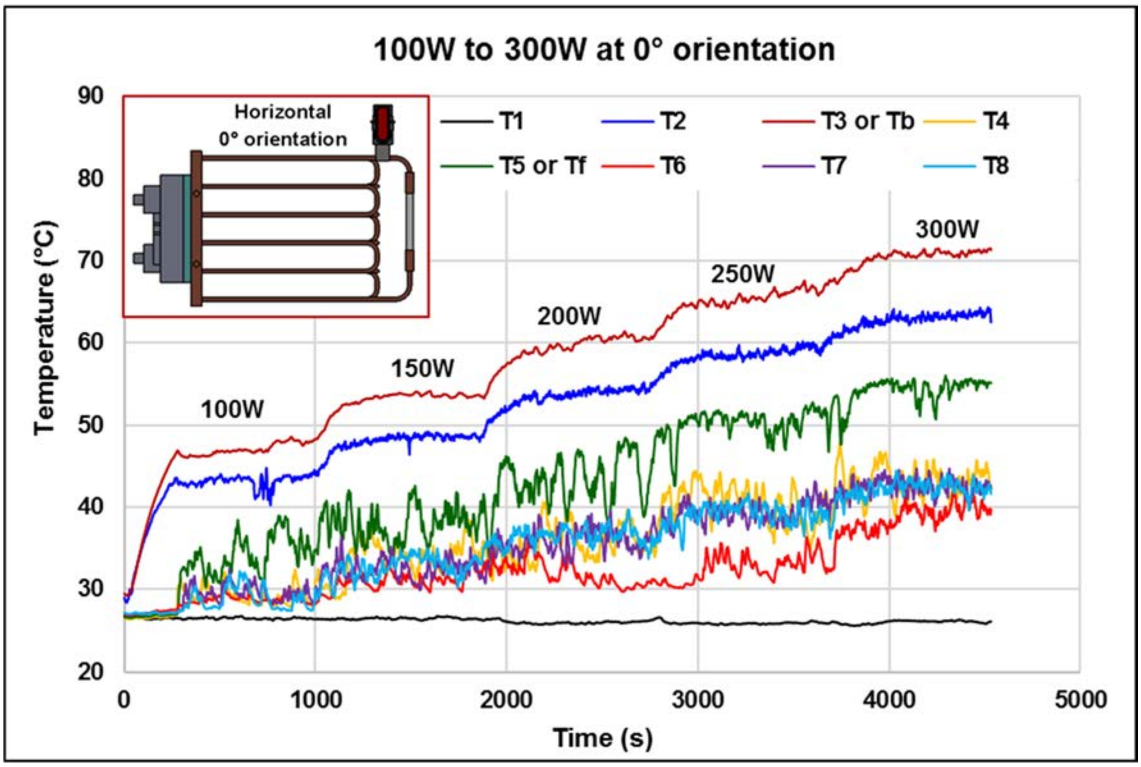

Figure 6-7: T vs t for 100 W to 300 W at 0° inclination

6.6.4 Observations at -90° orientation

1. Evaporator-up configuration is the most adverse orientation for a heat pipe to work, according to several literatures and our own experimental experiences. However, if the number of turns in the evaporator region is adequate [19], the PHP begins to work at any orientation, given that it is above the threshold heat load, so as to initiate pulsation.
2. No startup was observed even after the base temperature crossed 50°C for heat load of 100 W. Very minor pulses were seen in condenser temperature, as in Figure 6-8. No significant rise in the fin temperature was observed. The trial for this heat load was for up to 20 minutes, but no significant event occurred.
3. For 150 W heat load, there was a startup but it was very inconsistent. Two peak temperatures from each of the condenser thermocouples were observed, but the temperatures plummeted back to initial condition, indicating that the PHP did not work for this heat load as well.
4. In the next heat load of 200 W, the evaporator temperature kept rising till 82° C, immediately after which a very sudden startup occurred and the temperature dropped to 66° C, as seen in Figure 6-8.
5. From this point on, the PHP heat sink functioned. However, in the glass tube window no pulses were observed, as glass window location is the lowest point with respect to all the

other points in the heat sink for this configuration. The fluid that settled there had minimum potential energy, so it had no drive to move or pulse.

6. The experiments were carried for 20 minutes up to 200 W, and only 15 minutes for 250 to 350 W heat loads, as the evaporator temperature attained steady state.
7. The experiment was carried for 350 W to characterize the higher heat load as well. No dry out occurred even in this orientation, the most adverse of all. The heat sink worked perfectly for this heat load in this orientation.
8. Though the heat sink worked well, the temperature oscillations were very violent (of large amplitude) when compared to the other orientations, as evident from Figure 6-8. This phenomenon is the same as predicted in [52] for non-bottom heat mode with water as working fluid. The condenser temperatures measured at various locations did not show any preference of homogenization as observed in the other 2 orientations, where one condenser temperature ($T_f = T_5$) was closer to the evaporator temperature.

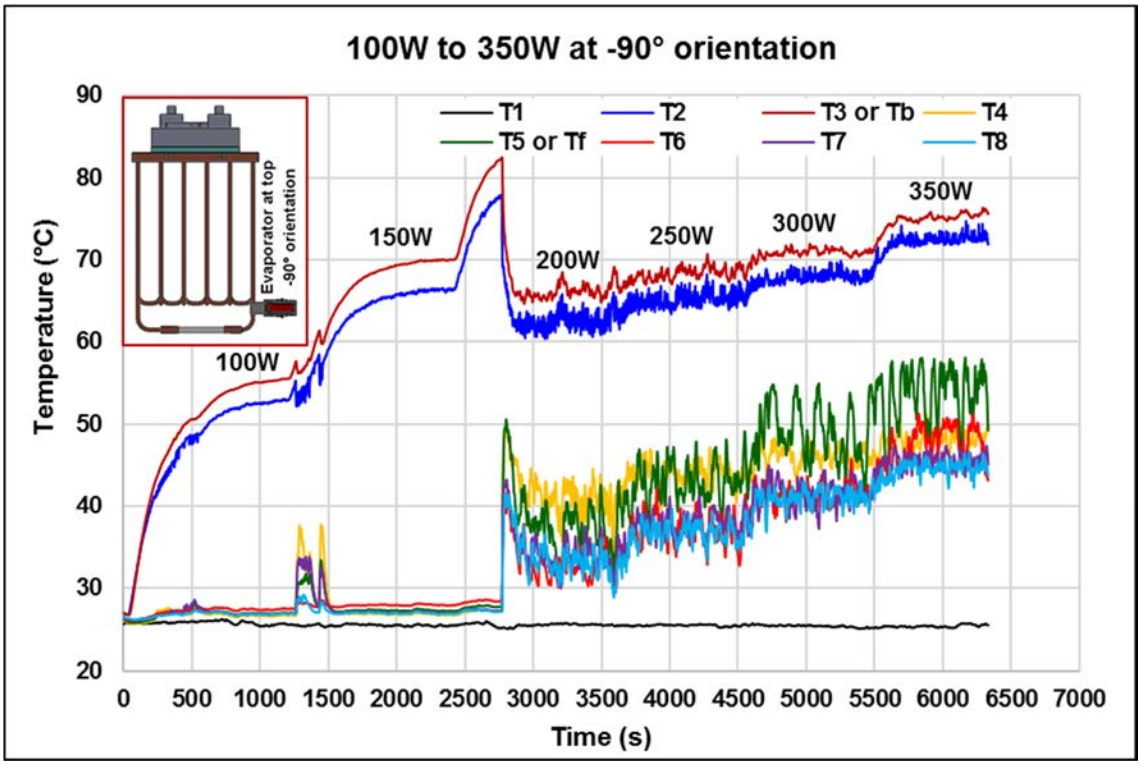

Figure 6-8: T vs t for 100 W to 300 W at -90° inclination

6.6.5 Additional tests at 350 W for 90° and 0° orientations

As the heat sink worked for the most adverse (-90°) orientation for 350 W, experiments for 350 W heat loads for the other two orientations were also performed. This is because the other orientations do not adversely affect the performance of the PHP, hence it should work even better in the other two configurations keeping the T_e within 100°C. The results were as predicted. The result for 350 W load in 90° orientation is shown in Figure 6-9 and for 0° is shown in Figure 6-10.

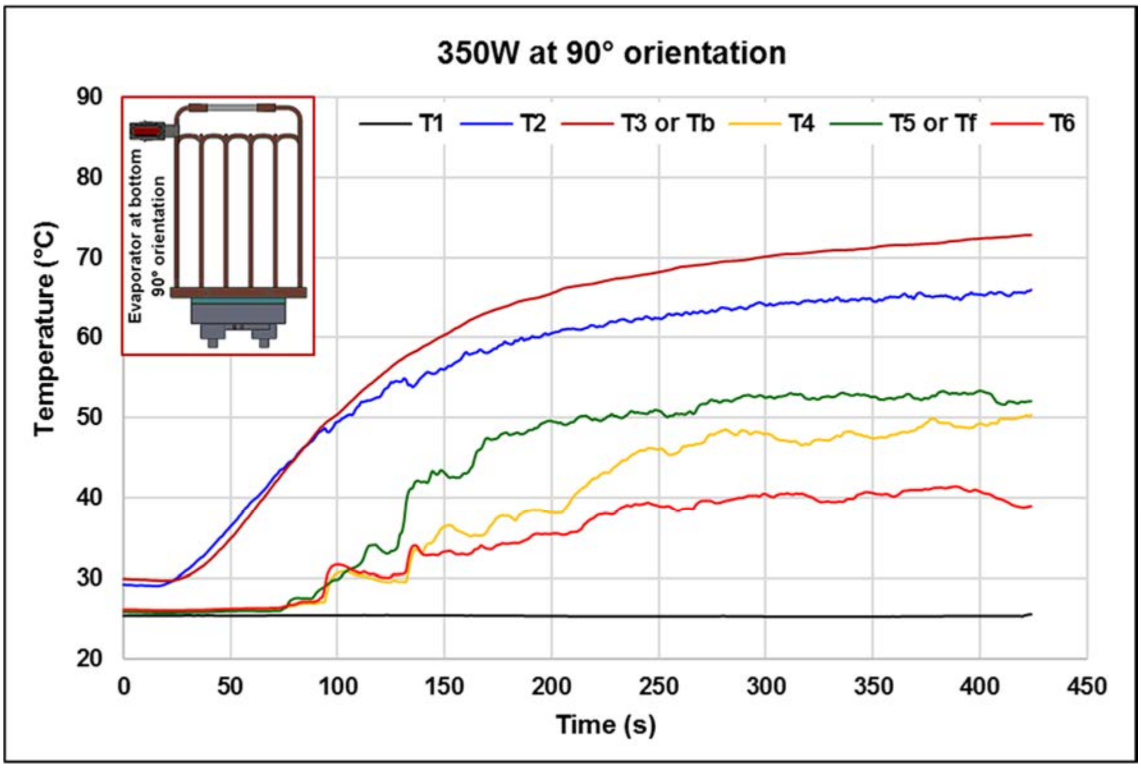

Figure 6-9: T vs t for 350 W at 90° inclination

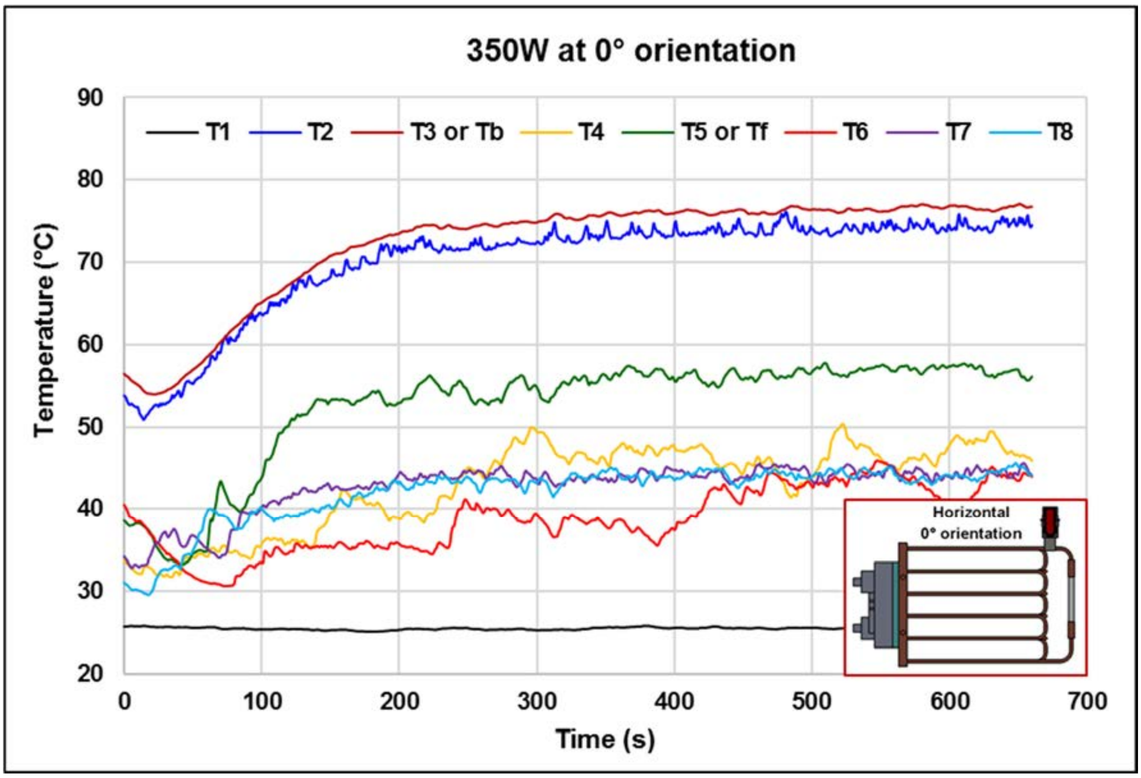

Figure 6-10: T vs t for 350 W at 0° inclination

6.6.6 Measurement of air velocity and temperature at the exit of the test duct

The velocity and the temperature of the air at the exit of the duct housing the heat sink was measured using a hot wire anemometer - Testo 405. The velocity and temperatures were measured at different locations in the exit cross-section as shown in Figure 6-11 and the values have been tabulated in Table 6-1. The average velocity of the exiting air was found to be 4.2 m/s and the air average exit temperature was 30.5°C. For the ambient temperature of 26°C the energy balance between the heat dissipated to the air and the heat supplied to the heater was within 10% for the 300 W heat input.

6.6.7 Thermal resistance of the heat sink

The R_{th} with respect to heat load is shown in Figure 6-12. Here the R_{th} was calculated as given by the following equation

$$R_{th} = \frac{T_b - T_{amb}}{\dot{Q}} \tag{6.1}$$

The figure shows that for the dry case of without working fluid the solid conduction resulted in a R_{th_dry} of 0.3°C/W which was nearly constant across heat loads. With the fluid (deionized water) the R_{th} came down for the 90° inclination and the zero inclination (horizontal) for all heat loads and the R_{th} was as expected lower for higher heat loads. In case of the top heat mode (-90°) inclination the PHP did not function for 100 W and 150 W heat load. This is reflected in the R_{th} value being same as that of the dry case. From 200 W, the R_{th} reduced indicating the operation of the PHP. At higher loads above 300 W the difference between the 3 orientations in terms of R_{th} is very marginal. This indicates that the PHP effect of the fins has a great potential to be combined as fins for higher heat loads. The tests indicate that the R_{th} was reduced to 50% from the dry case when the PHP operation was active at heat inputs above 300 W.

6.6.8 Equivalent thermal conductivity of the fin

The heat transfer coefficient for the test setup was found from the dry PHP test. When considering the heat load of 250 W, the heat transferred from the base of the heat sink is estimated as follows,

T_b = 100.6°C (at 3500 s)

T_{amb} = 26.7°C (at 3500 s)

T_f = 29.5°C (average of 5 locations measured)

v = 4.2 m/s (average of the measurements refer Table 6-1)

Width of the base (also same as the breadth) = w = 0.11 m

Re = $\rho vw/\mu$ = 2.4 x 10^4 (Hence laminar) (6.2)

For laminar flow over flat plate [79],

$Nu_{fp} = 0.664\ Re^{0.5}\ Pr^{1/3}$ (6.3)

$htc_{fp} = Nu_{fp}\ k_{air}/w$ = 24 W/m²-°C (6.4)

$\dot{Q}_b = htc(wb)(T_b - T_{amb})$ = 21.5 W (6.5)

Heat transferred through the 36 fins (2 x 18 turns),

$\dot{Q}_f = \dot{Q} - \dot{Q}_b$ = 250 – 21.5 = 228.5 W (6.6)

Heat transferred per fin,

$\dot{Q}_{fin} = \dot{Q}_f/(2N)$ = 6.35 W (6.7)

For fin with end temperatures known,

$$\dot{Q}_{fin} = M\frac{\left((T_b - T_{amb})\cosh mL_f - (T_f - T_{amb})\right)}{\sinh mL_f} \quad (6.8)$$

where,

$$M = \sqrt{htc_f\ p_f k_f A_{cs}} \quad (6.9)$$

$$m = \sqrt{\frac{htc_f p_f}{k_f A_{cs}}} \quad (6.10)$$

p_f = perimeter = πD (6.11)

A_{cs} = area of cross-section of the fin = $\pi(D^2\text{-}d^2)/4$ (6.12)

$k_f = k_{Cu}$ = thermal conductivity of the fin (for dry test) = 398 W/m-°C (6.13)

Thus the heat transfer coefficient for the fin, htc_f was found to be 500 W/m²-°C. This value is higher than that predicted by correlations for flow over cylinders or bank of tubes. This increased value can be attributed to the turbulence induced due to the fin structure.

Using this heat transfer coefficient and the temperature data for 300 W heat load of PHP testing at +90° orientation at 4000 s which are listed as follows

T_{amb} = 26.8°C

T_b = 70.8°C

T_f = 46.4°C (average of the 5 locations measured)

after accounting for the heat transferred from the base as 12.8 W (calculated as per the above mentioned procedure) the equivalent thermal conductivity of the fin was estimated to be 1900 W/m-°C using the equation (6.8). The equivalent conductivities at 250 W and 350 W for vertical operation were estimated to be around 1750 W/m-°C and 2350 W/m-°C respectively. Thus equivalent thermal conductivity of nearly 4 to 6 times of copper could be observed. Hence the device (fins) clearly qualifies as heat pipe due to the enhanced thermal conductivity.

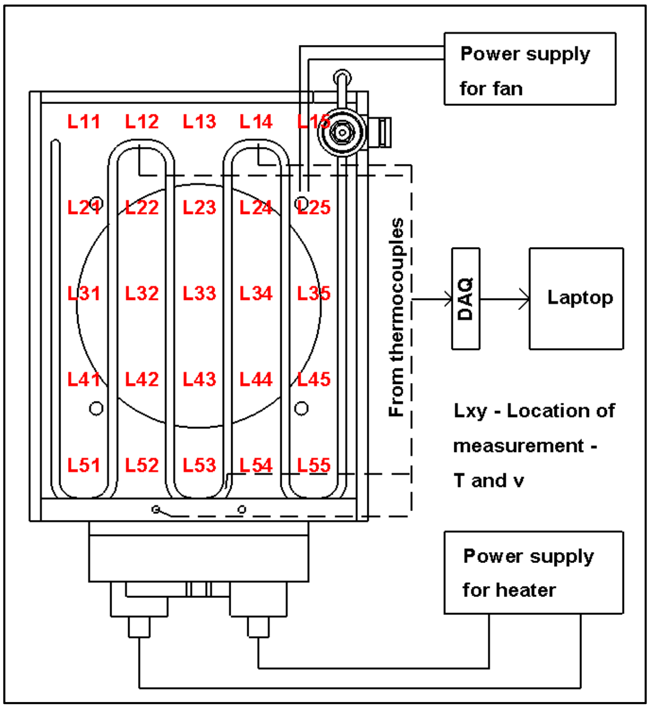

Figure 6-11: Locations of measurement of T and v of air exiting the duct

Table 6-1: Velocity and temperatures at various locations at the exit of the duct

v (T_{exit})	**1**	**2**	**3**	**4**	**5**
1	7 (27.3)	7.1 (28.5)	6 (28.7)	6.5 (29)	Valve location - NM
2	3.4 (28.6)	3.4 (29.5)	2.7 (30.3)	3.7 (30.2)	3.4 (29)
3	3.2 (30.2)	3.3 (30.5)	2.6 (30.9)	2.2 (30.3)	3.1 (29.5)
4	4.5 (31)	4.2 (31.2)	4.3 (30.9)	3.7 (30.3)	3.5 (30)
5	5.5 (34.3)	4.2 (33.6)	4.5 (33)	4.2 (31.4)	4.8 (33)
v	Velocity in m/s		Measurements carried out only for 300 W of PHP operation		
T_{exit}	Temperature in °C				
NM	Not measured				

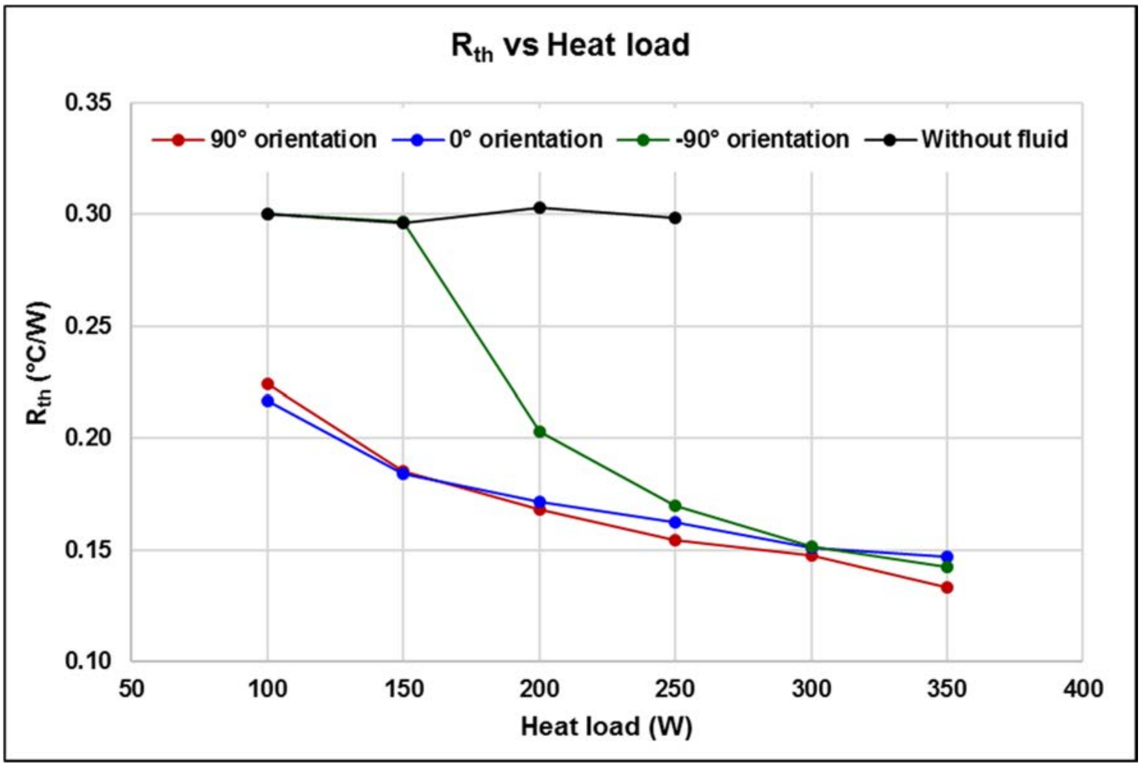

Figure 6-12: R_{th} of heat sink vs heat load for all 4 cases

6.7 Closure

A multiturn multiplane PHP was tested as a heat sink with fins being the PHP channels/tubing. The entire length of the PHP acted as condenser with the exception of few millimetres of tubing which were attached to the evaporator block. The salient conclusions are as follows,

1. The PHP based heat sink with substantial number of turns (in this case 18 numbers) can be deployed for gravity independent operation provided the heat inputs are greater than the threshold of PHP operation initiation.
2. The flow regime was always slug flow indicating that the heat sink can be tested for higher heat loads as PHP can function up to annular flow regime. The R_{th} vs heat load curve also indicates that the PHP R_{th} could still go down with increase in heat loads.
3. The fin thermal conductivity was enhanced substantially by the PHP operation that the thermal conductivity was more than 5 times of that of copper in the bottom heat mode.

7 Conclusions

Though the first engineering applications of pulsating heat pipes were proposed in the early 1990s the design philosophy for the practical deployment of pulsating heat pipes based cooling solutions are still not matured in spite of these devices being simple and cost effective. This is mainly due to the fact that the underlying phenomena responsible for the working of the PHPs are quite large and intensive from computational perspective. An entire range of activities like – bubble generation by nucleation, their agglomeration, bubble shrinkage, collapse and separation of bubbles leading to pressure variations within a constant volume system almost all of them occurring at every instant of time makes the theoretical modelling highly challenging. The number of parameters which can be varied as inputs are quite large as well – diameter of the channels, number of turns, form factor (flat or capillary tube; single or multiplane), fill ratio of working fluid apart from its thermophysical properties for a given range of heat loads and orientation of the PHP.

In this study three different form factors of PHPs of practical and academic relevance have been experimentally investigated. The set up was constructed with provision to vary the heat load, working fluid, fill ratio and the orientation so that the combined effects of the four parameters can be compared and correlated. In this study the diameter of the tubing was maintained between 2 mm and 2.5 mm as the experiments were targeted for higher heat loads (of the order of tens of watts to hundreds of watts). Hence smaller diameters were not investigated. Out of the four PHPs studied two were pursued with provision for both visualisation and quantitative analysis thus providing insight into the flow regimes of operation for different operating conditions apart from assessment of thermal performance.

Major conclusions from the study are as follows

A. The flat plate configuration which is relatively easier to be embedded into a device to be cooled as spreader showed that
   a. Methanol is a better PHP working fluid than water or FC 72 especially at near horizontal inclinations and lower heat loads due to the combined effect of higher $(dP/dT)_{sat}$ and lower viscosity.
   b. Water proved to be the fluid of choice for higher heat loads due to larger specific heat capacity and latent heat of vaporisation.
   c. Tests with FC 72 proved that PHP operation was possible even though the diameter is slightly larger than the one prescribed by static confinement criteria of Bo less than 2.

d. Thermal performance could be enhanced almost by 8 times compared to the dry PHP by addition of suitable fluids.
e. Slug flow was predominant at lower heat loads and at higher heat loads annular flow was prevalent at the evaporator zone.
f. Correlation with less than ±20% deviation was fitted with the experimental data for the flat plate configuration. Morton number seems to be a good parameter to capture the combined effects of inertia, viscosity and surface tension into a correlation. This is especially a very good parameter as the velocity of flow is not known upfront in case of the constant closed volume PHP system.
g. Also performance degradation with inclination was perceptible only below 45° inclination.

B. Single loop capillary tube configuration was investigated for better understanding of the thermo-fluid mechanism of PHP and the tests showed that
   a. Start-up characteristics were obtained for a single loop for a range of heat loads and two distinct characteristics – sudden start-up for lower heat fluxes and a smooth/gradual start up for higher heat fluxes were observed.
   b. The start-up also depended on the void fraction distribution at the beginning of application of heat input.
   c. It was observed that PHPs need minimum heat flux for start-up with the T_e at start to be less than the T_e at quasi steady state. Hence care should be taken during deployment of PHP for cooling in real time applications.
   d. Also comparative tests with different bend radius indicated that the pressure loss at the bends cannot be neglected without loss of accuracy when it comes to numerical modelling.
   e. Contrary to the expectation the best thermal performance (lowest R_{th}) of a single loop PHP occurred not at vertical 90° inclination but between 60° and 70° inclinations.
   f. The mere radial insulation of the adiabatic section of the PHP resulted in only a marginal improvement in performance. Probably the axial conduction (change of material with lower thermal conductivity at adiabatic section) should also be reduced to get more benefit in the thermal performance.
   g. Even a single loop PHP can be used for real time cooling applications if operated with minimum heat load at predominantly vertical orientations as the tests showed remarkable improvement in R_{th} with respect to fluid-less tests.

h. The frequency estimate of the oscillations showed that the higher frequencies tend to get more prominent when the heat loads are increased and also when the fluid of higher $(dP/dT)_{sat}$ is used. Thus frequency can be used as an estimate of velocity manifesting inside the PHP during operation at various operating conditions.

C. Multiloop multiplane PHP was tested for three characteristic orientations of bottom heat mode, horizontal and top heat mode to check for the gravity independent performance and the tests showed that

a. For the higher number of turns used in the study the PHP performed nearly independent of the orientation with respect to gravity after a threshold heat flux was applied.

b. When used as pin-fins for heat sink the PHP could enhance the equivalent thermal conductivity of the fin structure by a factor of about 5 with respect to copper.

7.1 Suggestions for future work

Although various research groups have studied the PHPs in detail over the last two decades still these devices remain unconquered in certain aspects. Thus the areas of research in the near future can be carried forward in the following directions,

1. Usage of PHP with narrower diameters like micro-channels with possibly lower surface tension fluids (like FC 72) as miniaturisation is the way forward.
2. Numerical modelling capturing most of the fluid mechanics phenomena occurring within the PHP as most numerical simulations till date are idealized with ample assumptions.
3. In this study the multiplane configuration was investigated with 18 turns. This is greater than the critical number of turns predicted for planar configurations for gravity independent operation. Hence multiplane configuration with reduced number of turns can be investigated to arrive the critical number of turns for the three dimensionally orientated channel configuration.
4. Study of minimum area or length of the condenser for a given area and heat flux at the evaporator can be carried out as this can determine the compactness of the cooling solution without dry outs.
5. Both experimental and numerical simulations can be carried out with single tube to get more insight into hydrodynamics as the events occurring within a single loop are fairly large and highly transient. This approach can give the investigator the freedom of using axisymmetric analysis (if not three dimensional) to capture the near wall events more accurately rather than the presently pursued one-dimensional analysis.

References

1. [Online] https://en.wikipedia.org/wiki/Transistor_count#Microprocessors.

2. E.Martin. A Medium Corporation. [Online] https://medium.com/predict/moores-law-is-alive-and-well-adc010ea7a63.

3. *High heat from a small package.* S.Oktay, R.J.Hannemann and A.Bar-Cohen. 1986, Mechanical Engineering, Vol. 108, pp. 36-42.

4. D.A. Reay, P.A. Kew and R.J. McGlen. *Heat Pipes - Theory, Design and Applications.* Sixth. Oxford : Elsevier, 2014.

5. *A network thermodynamic analysis of the heat pipe.* Z.J.Zuo and A.Faghri. 11, s.l. : Elsevier, 1998, International Journal of Heat and Mass Transfer, Vol. 41, pp. 1473-1484.

6. A.Faghri. *Heat Pipe Science and Technology.* Bristol : Taylor and Francis, 1995.

7. *Thermodynamic aspects of heat pipe operation.* R.Richter and J.M.Gottschlich. 2, 1994, Journal of Thermophysics and Heat Transfer, Vol. 8, pp. 334-340.

8. H.Akachi. *Structure of a heat pipe. 4921041* United States, May 1, 1990.

9. *Understanding operational regimes of closed loop pulsating heat pipes: an experimental study.* S.Khandekar, N.Dollinger and M.Groll. s.l. : Elsevier, 2003, Applied Thermal Engineering, Vol. 23, pp. 202-219.

10. *Advances and unsolved issues in pulsating heat pipes.* Y.Zhang and A.Faghri. s.l. : Taylor and Francis, 2008, Heat Transfer Engineering, Vol. 29, pp. 20-44.

11. *Thermal modeling of unlooped and looped pulsating heat pipes.* M.B.Shafii, A.Faghri and Y. Zhang. s.l. : ASME, 2001, Journal of Heat transfer, Vol. 123, pp. 1159-1172.

12. *Analysis of heat transfer in unlooped and looped pulsating heat pipes.* M.B. Shafii, A. Faghri and Y. Zhang. s.l. : Emerald Insight, 2002, International Journal of Numerical Methods for Heat and Fluid Flow, Vol. 12, pp. 585-609.

13. *On the definition of pulsating heat pipes: An overview.* S.Khandekar and M.Groll. Minsk : s.n., 2003. International seminar (heat pipes, heat pumps and refrigerators).

14. *Analysis of pulsating heat pipe with capillary wick and varying channel diameter.* B.Holley and A.Faghri. s.l. : Elsevier, 2005, International Journal of Heat and Mass Transfer, Vol. 48, pp. 2635-2651.

15. *Thermofluid dynamic study of flat plate closed loop pulsating heat pipes.* S.Khandekar, M.Schneider, P.Schiifer, R.Kulenovic and M.Groll. s.l. : Taylor and Francis, 2002, Microscale Thermophysical Engineering, Vol. 6, pp. 303-317.

16. *A comparative study of flow regimes and thermal performance between flat plate pulsating heat pipe and capillary tube pulsating heat pipe.* A.Takawale, S.Abraham, A.Sielaff, P.S.Mahapatra, A.Pattamatta and P.Stephan. s.l. : Elsevier, 2019, Applied Thermal Engineering, Vol. 149, pp. 613-624.

17. *Pulsating heat pipes.* H.Akachi, F.Polasek and P.Stulc. [ed.] 5th International Heat Pipe Symposium. Melbourne, Australia : s.n., 1996. pp. 208-217.

18. H.Akachi. *L-type heat sink. 5490558* United States, February 13, 1996.

19. *Closed loop pulsating heat pipes Part A: parametric experimental investigations.* P.Charoensawan, S.Khandekar, M.Groll and P.Terdtoon. s.l. : Elsevier, 2003, Applied Thermal Engineering, Vol. 23, pp. 2009-2020.

20. *Investigation of a flat-plate oscillating heat pipe with Tesla-type check valves.* S.M. Thompson, H.B. Ma and C. Wilson. s.l. : Elsevier, 2011, Experimental Thermal and Fluid Science, Vol. 35, pp. 1265-1273.

21. *Design and operation of a Tesla-type valve for pulsating heat pipes.* S.F. de Vries, D. Florea, F.G.A. Homburg, A.J.H. Frijns. s.l. : Elsevier, 2017, International Journal of Heat and Mass Transfer, Vol. 105, pp. 1-11.

22. *Fluid-flow pressure measurements and thermo-fluid characterization of a single loop two-phase passive heat transfer device.* A.Ilinca, D.Mangini, M.Mameli, D.Fioriti, S.Filippeschi, L.Araneo, N.Roth and M.Marengo. s.l. : IOP Publishing, 2017, Journal of Physics: Conference Series, Vol. 923.

23. *Performance characteristics of pulsating heat pipes as integral thermal spreaders.* H.Yang, S.Khandekar and M.Groll. s.l. : Elsevier, 2009, Vol. 48, pp. 815-824.

24. *Operational limit of closed loop pulsating heat pipes.* H.Yang, S. Khandekar and M. Groll. s.l. : Elsevier, 2008, Applied Thermal Engineering, Vol. 28, pp. 49-59.

25. *Thermal performance of horizontal closed loop oscillating heat pipes.* P.Charoensawan and P.Terdtoon. s.l. : Elsevier, 2008, Applied Thermal Engineering, Vol. 28, pp. 460-466.

26. *Pulsating heat pipes: Progress and prospects.* S.Khandekar and M.Groll. 2003. International conference on Energy and Environment. pp. 723-730.

27. *A comparative study of the behavior of working fluids and their properties on the performance of pulsating heat pipes (PHP).* H.Han, X.Cui, Y.Zhu and S.Sun. s.l. : Elsevier, 2014, International Journal of Thermal Sciences, Vol. 82, pp. 138-147.

28. *Operational characteristics of flat plate closed loop pulsating heat pipes.* H.Yang, S.Khandekar and M.Groll. Shanghai, China : s.n., 2004. 13th International Heat Pipe Conference.

29. *Roadmap to realistic modelling of closed loop pulsating heat pipes.* S.Khandekar and M.Groll. Kuala Lumpur : s.n., 2008. 9th International Heat pipe Symposium.

30. *Closed loop pulsating heat pipes Part B: visualization and semi-empirical modeling.* S.Khandekar, P.Charoensawan, M.Groll and P.Terdtoon. s.l. : Elsevier, 2003, Applied Thermal Engineering, Vol. 23, pp. 2021-2033.

31. *Theoretical modeling of pulsating heat pipe.* T.N.Wong, B.Y.Tong, S.M.Lim and K.T.Ooi. Tokyo, Japan : s.n., 1999. Proceedings of 11th International Heat Pipe Conference. pp. 159-163.

32. *Analysis of liquid-vapour pulsating flow in a U-shaped miniature tube.* Y.Zhang, A. Faghri and M.B. Shafii. s.l. : Elsevier, 2002, International Journal of Heat and Mass Transfer, Vol. 45, pp. 2501-2508.

33. *Numerical model of a multi-turn Closed Loop pulsating heat pipe: Effects of the local pressure losses due to meanderings.* M. Mameli, M. Marengo and S. Zinna. s.l. : Elsevier, 2012, International Journal of Heat and Mass Transfer, Vol. 55, pp. 1036-1047.

34. *Thermal performance modelling of pulsating heat pipes by artificial neural network.* S.Khandekar, X.Cui and M.Groll. Moscow, Russia : Proceedings of 12th International Heat Pipe Conference, 2002. pp. 215-219.

35. *Physics in a toy boat.* I.Finnie and R.L.Curl. 1963, American Journal of Physics, Vol. 31, pp. 289-293.

36. H.Akachi. *Structure of micro-heat pipe. 5219020* United States, June 15, 1993.

37. G.Smyrnov. *Method of action of the pulsating heat pipe, its construction and the devices on its base. 6672373* United States, January 6, 2004.

38. *Local heat transfer measurement and thermo-fluid characterization of a pulsating heat pipe.* M.Mameli, M.Marengo and S.Khandekar. s.l. : Elsevier, 2014, International Journal of Thermal Sciences, Vol. 75, pp. 140-152.

39. *Multiple quasi-steady states in a closed loop pulsating heat pipe.* S.Khandekar, A.P.Gautam and P.K.Sharma. s.l. : Elsevier, 2009, International Journal of Thermal Sciences, Vol. 48, pp. 535-546.

40. *Effect of gravity on the thermal instability of a closed loop pulsating heat pipe.* M.Mameli, V.Manno, S.Filippeschi and M.Marengo. Lisbon : s.n., 2013. 8th World Conference on experimental heat transfer, fluid mechanics and thermodynamics.

41. *Thermal response of a closed loop pulsating heat pipe under a varying gravity force.* M. Mameli, L. Araneo, S. Filippeschi, L. Marelli, R. Testa and M. Marengo. 2014, International Journal of Thermal Sciences, Vol. 80, pp. 11-22.

42. *An Open Loop Pulsating Heat Pipe for integrated electronic cooling applications.* D.Kearney and J.Griffin. s.l. : ASME, 2014, Journal of heat transfer, Vol. 136.

43. *Closed-loop pulsating heat pipe.* B.Y.Tong, T.N. Wong and K.T.Ooi. s.l. : Pergamon/Elsevier, 2001, Applied Thermal Engineering, Vol. 21, pp. 1845-1862.

44. *Start-up and steady thermal oscillation of a pulsating heat pipe.* J.L.Xu and X.M.Zhang. s.l. : Springer, 2005, Heat Mass Transfer, Vol. 41, pp. 685-694.

45. *Investigation of the start-up condition of a closed loop oscillating heat pipe.* N.Soponpongpipat, P.Sakulchangsatjaati, N.Kammuang-Lue and P.Terdtoon. s.l. : Taylor and Francis, 2009, Heat Transfer Engineering, Vol. 30, pp. 626-642.

46. *Experimental research on the start-up characteristics and heat transfer performance of pulsating heat pipes with rectangular channels.* C.Hua, X.Wang, X.Gao, H.Zheng, X.Han and G.Chen. s.l. : Elsevier, 2017, Applied Thermal Engineering, Vol. 126, pp. 1058-1062.

47. *An insight into thermo-hydrodynamic coupling in closed loop pulsating heat pipes.* S.Khandekar and M.Groll. s.l. : Elsevier, 2004, International Journal of Thermal Sciences, Vol. 43, pp. 13-20.

48. *Influence of process variables on the hydrodynamics and performance of a single loop pulsating heat pipe.* N.Saha, P.K.Das and P.K.Sharma. s.l. : Elsevier, 2014, International Journal of Heat and Mass Transfer, Vol. 74, pp. 238-250.

49. S.Khandekar. *Thermo-hydrodynamics of closed loop pulsating heat pipes.* University of Stuttgart. 2004. Doctoral dissertation.

50. *Time-strip visualization and thermo-hydrodynamics in a closed loop pulsating heat pipe.* G.Spinato, N.Borhani, B.P.d'Entremont and J.R.Thome. s.l. : Elsevier, 2015, Applied Thermal Engineering, Vol. 78, pp. 364-372.

51. *Operational regimes in a closed loop pulsating heat pipe.* G.Spinato, N.Borhani and J.R.Thome. s.l. : Elsevier, 2016, International Journal of Thermal Sciences, Vol. 102, pp. 78-88.

52. *Compact cooler for electronics on the basis of a pulsating heat pipe.* Y.F.Maydanik, V.I.Dmitrin and V.G.Pastukhov. s.l. : Elsevier, 2009, Applied Thermal Engineering, Vol. 29, pp. 3511-3517.

53. *An experimental investigation of a three-dimensional flat-plate oscillating heat pipe with staggered microchannels.* S.M.Thompson, P.Cheng and H.B.Ma. s.l. : Elsevier, 2011, pp. 3951-3959.

54. *Design and experimental study on a hybrid flexible oscillating heat pipe.* J.Qu, X.Li, Y.Cui and Q.Wang. s.l. : Elsevier, 2017, International Journal of Heat and Mass Transfer, Vol. 107, pp. 640-645.

55. *Heat transfer in a pulsating heat pipe with open end.* Y.Zhang and A.Faghri. s.l. : Elsevier, 2002, International Journal of Heat and Mass transfer, Vol. 45, pp. 755-764.

56. *High heat flux heat pipe mechanism for cooling of electronics.* Z.J. Zuo, M.T. North and K.L. Wert. s.l. : IEEE Transactions, 2001, Components Packaging Technology, Vol. 24, pp. 220-225.

57. *An investigation of evaporation, boiling, and heat transport performance in a pulsating heat pipe.* Q.Cai, R.Chen and C.Chen. New Orleans, LA : s.n., 2002. ASME IMECE.

58. *Oscillatory-flow heat-transport device (forced oscillatory flow type and bubble driven type).* S.Nishio. Tokyo, Japan : s.n., 1999. Eleventh International Heat Pipe Conference. pp. 39-49.

59. *Numerical investigation of the performance of a U-shaped pulsating heat pipe.* S.Arabnejad, R.Rasoulian, M.B.Shafii and Y.Saboohi. s.l. : Taylor and Francis, 2010, Heat Transfer Engineering, Vol. 31, pp. 1155-1164.

60. *A dynamic film model of the pulsating heat pipe.* V.S.Nikolayev. s.l. : ASME, 2011, Journal of Heat Transfer, Vol. 133, pp. 081504-1-9.

61. *A parametric study of oscillatory two-phase flows in a single turn pulsating heat pipe using a non-isothermal vapor model.* A.Pattamatta, M.Dilawar. s.l. : Elsevier, 2013, Applied Thermal Engineering, Vol. 51, pp. 1328-1338.

62. *Thermally induced two phase oscillating flow inside a capillary tube.* S.P.Das, V.S.Nikolayev, F.Lefevre, B.Pottier, S.Khandekar and J.Bonjour. s.l. : Elsevier, 2010, International Journal of Heat and Mass Transfer, Vol. 53, pp. 3905-3913.

63. *Correlation to predict heat transfer characteristics of a closed-end oscillating heat pipe at normal operating condition.* S.Rittidech, P.Terdtoon, M.Murakami, P.Kamonpet and W.Jompakdee. s.l. : Elsevier, 2003, Applied Thermal Engineering, Vol. 23, pp. 497-510.

64. *Correlation to predict heat transfer characteristics of a closed end oscillating heat pipe at critical state.* T.Katpradit, T.Wongratanaphisan, P.Terdtoon, P.Kamonpet, A.Polchai, A.Akbarzadeh. s.l. : Elsevier, 2005, Appled Thermal Engineering, Vol. 25, pp. 2138-2151.

65. *Correlation to predict the maximum heat flux of a vertical closed-loop pulsating heat pipe.* N.Kammuang-Lue, P.Sakulchangsatjatai , P.Terdtoon and D.J.Mook. s.l. : Taylor and Francis, 2010, Heat transfer engineering, Vol. 30 (12), pp. 961-972.

66. *Experimental Investigation of pulsating heat pipes and a proposed correlation.* M.B.Shafii, S.Arabnejad, Y.Saboohi and H.Jamshidi. s.l. : Taylor and Francis, 2010, Heat transfer engineering, Vol. 31(10), pp. 854-861.

67. *Experimental study on the thermal performance of vertical closed-loop oscillating heat pipes and correlation modeling.* J.Qu and Q.Wang. s.l. : Elsevier, 2013, Applied Energy, Vol. 112, pp. 1154-1160.

68. *Thermal performance of rotating closed-loop pulsating heat pipes: Experimental investigation and semi-empirical correlation.* M.E.Dehshali, M.A.Nazari and M.B.Shafii. s.l. : Elsevier, 2018, International Journal of Thermal Sciences, Vol. 123, pp. 14-26.

69. *Experimental investigation on performance of a rotating closed loop pulsating heat pipe.* M.Aboutalebi, A.N.Moghaddam, N.Mohammadi and M.Shafii. s.l. : Elsevier, 2013, International Communication of Heat and Mass Transfer, Vol. 45, pp. 137-145.

70. *Heat transfer characteristics of a closed-loop oscillating heat-pipe with check valves.* S.Rittidech, N.Pipatpaiboon and P.Terdtoon. s.l. : Elsevier, 2007, Applied Energy, Vol. 84, pp. 565-577.

71. *A novel design of pulsating heat pipe with fewer turns applicable to all orientations.* K.Chien, Y. Lin, Y.Chen, K.Yang and C.Wang. s.l. : Elsevier, 2012, International Journal of Heat and Mass Transfer, Vol. 55.

72. *Operational characteristics of pulsating heat pipes with a dual-diameter tube.* G.H.Kwon and S.J.Kim. s.l. : Elsevier, 2014, International Journal of Heat and Mass Transfer, Vol. 75, pp. 184-195.

73. *Experimental investigation of the thermal characteristics of single-turn pulsating heat pipes with an extra branch.* E.Sedighi, A.Amarloo and M.B.Shafii. s.l. : Elsevier, 2018, International Journal of Thermal Sciences, Vol. 134, pp. 258-268.

74. *Ultrasonic effect on heat transfer performance of oscillating heat pipes.* N.Zhao, B.Fu, H.Ma and F.Su. 2015, Journal of Heat Transfer, Vol. 137, p. 091014.

75. *Visualization of two-phase flows in nano fluid oscillating heat pipes.* Q.Li, J.Zou, Z.Yang, Y.Duan and B.Wang. s.l. : ASME, 2011, Journal of Heat Transfer, Vol. 133.

76. *Thermal performance comparison of oscillating heat pipes with SiO2/water and Al2O3/water nanofluids.* J.Qu and H.Wu. s.l. : Elsevier, 2011, International Journal of Thermal Sciences, Vol. 50, pp. 1954-1962.

77. *Production of hydorgen in the reaction between aluminium and water in the presence of NaOH and KOH.* C.B.Porciuncula, et al. 02, 2012, Brazilian Journal of Chemical Engineering, Vol. 29, pp. 337-348.

78. *Correlating equations for laminar and turbulent free convection from a vertical plate.* S.W.Churchill, H.H.S.Chu. s.l. : Elsevier, 1975, International Journal of Heat Mass Transfer, Vol. 18, p. 1323.

79. Y.A.Cengel. *Heat Transfer - A Practical Approach.* Second. New Delhi : Tata Mcgraw-Hill, 2003.

80. *Pressure losses in tubing, pipe and fittings.* R.J.S.Pigott. 1950, Transactions of the ASME, Vol. 72, pp. 679-688.

81. M.Asada. *Material characterization of alcohol-water mixtures for the numerical simulation of heat transfer in micro-channels.* University of Hawaii. 2012. Master of Science dissertation.

82. *Fluid property equations as data base for thermal design calculations.* M.Furukawa. s.l. : The Japan Society for Aeronautical and Space Sciences, 2008, Transactions of Japan Society for Aeronautical and Space Sciences, Vol. 51, pp. 203-208.

83. *Closed and open loop pulsating heat pipes.* S.Khandekar, M.Groll, P.Charoensawan, S.Rittidech and P.Terdtoon. Shanghai : s.n., 2004. 13th International Heat Pipe Conference (13th IHPC).

84. *Theoretical analysis of start-up of a pulsating heat pipe.* H.B.Ma, W.Qu and. s.l. : Elsevier, 2007, International Journal of Heat and Mass Transfer, Vol. 50, pp. 2309-2316.

85. *Describing uncertainties in single sample experiments.* F.A.McClintock, S.J.Kline and. 1953, Mechanical Engineering, Vol. 75, pp. 3-8.

Appendix – A: Fluid Properties

Methanol from [81]

Property, $\alpha = m_0 * T^4 + m_1 * T^3 + m_2 * T^2 + m_3 * T + m_4$ (A-1)

where T is in °C

Table A-1: Property table of methanol for T < 65°C

Constants	m_0	m_1	m_2	m_3	m_4
Property					
ρ_v	1.70E-08	9.07E-07	9.74E-05	3.41E-03	5.80E-02
ρ_l	-2.09E-08	-5.04E-06	2.21E-04	-9.38E-01	8.10E+02
h_v	-1.01E-04	6.04E-03	-9.73E-01	1.05E+03	1.04E+06
h_l	-4.89E-06	1.13E-02	2.26E+00	2.40E+03	-1.67E+05
Cp_l	-1.47E-07	-2.64E-06	3.26E-02	4.53E+00	2.40E+03
k_l	1.05E-11	-7.97E-09	1.83E-06	-3.87E-04	2.09E-01
μ_l	4.67E-12	-1.22E-09	1.56E-07	-1.37E-05	8.06E-04
σ_l	1.08E-12	-1.00E-09	7.23E-08	-8.46E-05	2.43E-02
P_{sat}	1.72E-03	6.92E-02	7.88E+00	2.50E+02	4.06E+03

Table A-2: Property table of methanol for T > 65°C

Constants	m_0	m_1	m_2	m_3	m_4
Property					
ρ_v	9.41E-08	-2.66E-05	3.87E-03	-2.28E-01	5.36E+00
ρ_l	-1.63E-07	5.76E-05	-9.93E-03	-2.22E-01	7.91E+02
h_v	-3.67E-05	-2.23E-02	3.36E+00	7.62E+02	1.04E+06
h_l	1.25E-04	-4.30E-02	1.08E+01	1.81E+03	-1.52E+05
Cp_l	9.63E-06	-4.20E-03	7.16E-01	-4.43E+01	3.68E+03
k_l	2.51E-11	-1.47E-08	3.01E-06	-4.76E-04	2.12E-01
μ_l	2.93E-13	-2.10E-10	6.01E-08	-9.15E-06	7.17E-04
σ_l	4.49E-12	-2.36E-09	2.79E-07	-9.86E-05	2.47E-02
P_{sat}	2.13E-03	7.89E-02	-9.32E+00	2.08E+03	5.29E+04

Water and FC 72 from [82]

$T_r = T/T_c$ where Temperature is in Kelvin (A-2)

$$\frac{\rho_l}{\rho_{l0}} = a_0 + a_1 * (1 - T_r)^{1/3} + a_2 * (1 - T_r)^{2/3} + a_3 * (1 - T_r)^1 + a_4 * (1 - T_r)^{4/3} \quad \text{(A-3)}$$

where $\rho_{l0}=10^3$ kg/m^3

$$\rho_v = \frac{1}{\frac{1}{\rho_l} + \frac{h_{fg}}{T\left(dP/_{dT}\right)}} \quad \text{(A-4)}$$

$$\frac{h_l}{h_{l0}} = a_0 + a_1 * T_r + a_2 * T_r^{\,2} + a_3 * T_r^{\,3} \quad \text{(A-5)}$$

where $h_{l0}=10^6$ J/kg

$$\frac{h_{fg}}{h_{fg0}} = c * (1 - T_r)^b \quad \text{(A-6)}$$

where $h_{fg}=10^6$ J/kg

$$\frac{Cp_l}{Cp_{l0}} = a_0 + \frac{a_1}{(1-T_r)} + \frac{a_2}{(1-T_r)^2} + \frac{a_3}{(1-T_r)^3} \quad \text{(A-7)}$$

where $Cp_{l0}=10^3$J/kg-K

$$\frac{\sigma_l}{\sigma_{l0}} = c * (1 - T_r)^b \quad \text{(A-8)}$$

where $\sigma_{l0} = 10^{-2}$ N/m

$$\ln\left(\frac{\mu_l}{\mu_{l0}}\right) = a_0 + \frac{a_1}{T_r} + \frac{a_2}{T_r^{\,2}} + \frac{a_3}{T_r^{\,3}} \quad \text{(A-9)}$$

where $\mu_{l0}=10^{-3}$ Pa.s

$$\frac{k_l}{k_{l0}} = a_0 + a_1 * T_r + a_2 * T_r^{\,2} + a_3 * T_r^{\,3} \quad \text{(A-10)}$$

where $k_{l0} = 0.1$ W/m-K

$$lnP_r = a_0 + {a_1}/{T_r} + {a_2}/{T_r^2} + {a_3}/{T_r^3} \quad \text{(A-11)}$$

$P_{sat} = P_r * P_c$ (A-12)

where,

P_c = 22060 kPa (for water) and 1868 kPa (for FC 72); T_c = 647.1 K (for water) and 448.8 K (for FC 72)

Table A-3: Property table of water

Constants	a_0	a_1	a_2	a_3	a_4	T_r	c	b
ρ_l	0.19379	1.9053	-4.054	6.5555	-3.6384	0.425 to 0.988	---	---
h_l	-2.1572	7.8877	-8.683	4.8014	0	0.425 to 0.988	---	---
Cp_l	3.6615	0.23644	1.14E-04	-1.34E-06	0	0.425 to 0.988	---	---
μ_l	-7.3265	7.4421	-3.7742	0.86393	0	0.425 to 0.988	---	---
k_l	-2.5901	29.416	-22.924	0	0	0.425 to 0.988	---	---
P_r	6.3272	-5.8316	-0.53369	0	---	0.425 to 0.988	---	---
σ_l	---	---	---	---	---	0.422 to 0.988	15.718	1.1299
h_{fg}	---	---	---	---	---	0.422 to 0.988	3.1366	0.37693

Table A-4: Property table of FC 72

Constants	a_0	a_1	a_2	a_3	a_4	T_r	c	b
ρ_l	0.46444	3.1907	-5.2421	4.6871	0	0.430 to 0.998	---	---
h_l	-0.16643	0.12051	0.25539	0		0.631 to 0.987	---	---
Cp_l	0.58955	0.69739	0	0	0	0.430 to 0.942	---	---
μ_l	-6.3179	6.4977	-2.6809	0.64281	0	0.430 to 0.942	---	---
k_l	0.89609	-0.48481	0	0	0	0.430 to 0.942	---	---
P_r	6.0126	-0.47142	-1.3647	0	---	0.430 to 0.998	---	---
σ_l	---	---	---	---	---	0.586 to 0.942	4.0433	1.2377
h_{fg}	---	---	---	---	---	0.542 to 0.998	0.15946	0.38698

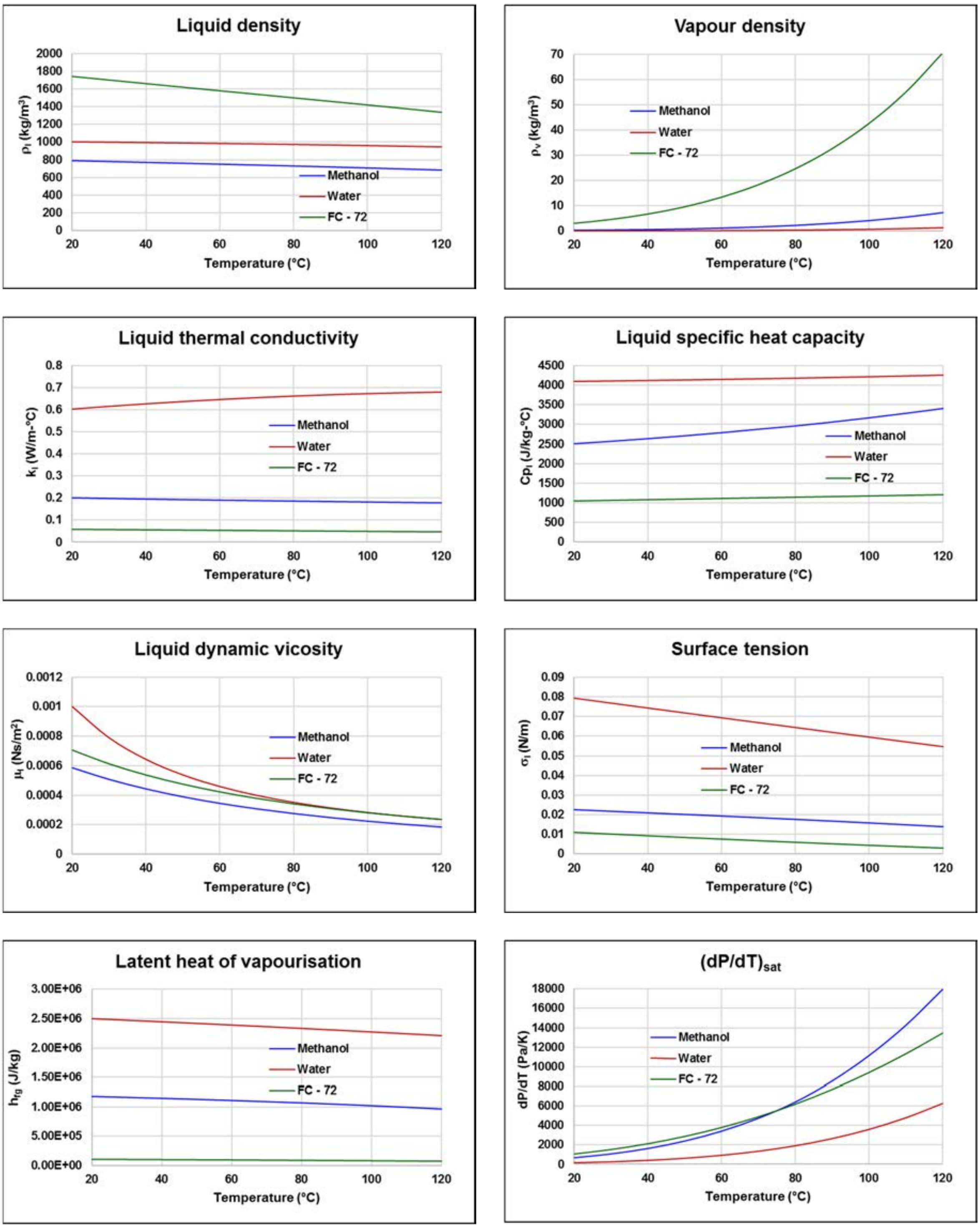

Figure A-1: Thermophysical properties with respect to temperature for methanol, water and FC 72

Appendix – B: Instruments and equipment details

Sl.No.	Equipment / Instrument	Make/Model	Size/Range	Response time/ Sampling rate	Accuracy
1	Heater – film resistor	Ohmite TEH100M2R00JE	100 W – 2 Ω 21x16x5 mm³	Not applicable	±5% of 2 Ω
2	Heater – film resistor	Caddock MP9100	100 W – 8 Ω 21x16x5 mm³	Not applicable	±1% of 8 Ω
3	Heater – film resistor	Ohmite TA1K0PH8R00KE	1000 W – 8 Ω 76x76x20 mm³	Not applicable	±10% of 8 Ω
4	Power supply – Flat plate PHP	Keysight make – N5767A	Voltage – 60 V current – 25 A	Not applicable	V ± 1%; I ± 1%
5	Power supply – Single loop PHP – Glass tube model	Aplab make – L3210	Voltage – 32 V current – 10 A	Not applicable	V ± 1%; I ± 1%
6	Power supply – Single loop PHP – Copper tube model	TDK-Lambda make – Z^+ 800 (60-14)	Voltage – 60 V current – 14 A	Not applicable	V ± 0.5%; I ± 1%
7	Power supply – Multiloop multiplane PHP	TDK-Lambda make – GEN 60-40	Voltage – 60 V current – 40 A	Not applicable	V ± 0.5%; I ± 1%
8	Data acquisition system – Flat plate PHP	Picolog TC-08	8 channels	> 1 Hz across 8 channels	± 0.5°C
9	Data acquisition system – Single loop PHP	RS1384	4 channels	> 1 Hz across 4 channels	± 1.0°C
10	Data acquisition system – Multiloop multiplane PHP	34980A with 34921A multiplexer	40 channels	> 100 Hz	determined by sensor
11	Thermocouples – Flat plate PHP	Agilent J-type (U1185A)	Wire ϕ 0.6 mm (-100 to 700°C)	less than 1.0 s	± 1.0°C
12	Thermocouples – Single loop PHP	RS PRO; T-type (621-2164)	Wire ϕ 0.2 mm (-200 to 350°C)	less than 0.5 s	± 0.5°C
13	Thermocouples – Multiloop multiplane PHP	RS PRO; T-type (621-2164)	Wire ϕ 0.2 mm (-200 to 350°C)	less than 0.5 s	± 0.5°C
14	Recirculating chiller	Bucchi make – F 305	550 W at 15°C	Not applicable	± 1.0°C
15	Rotameter	Sunflow make – SF/ABR/206-100	0.25-2.5 LPM	Not applicable	± 2% full scale
16	Pressure transducer	Honeywell make – PX2AG2XX002BAAAX	0-2 bar (Absolute)	< 2 ms	± 0.25% full scale span
17	Axial fan - Multiloop multiplane PHP	EBM Papst 8214 JH4 80x80x38 mm³	24 V DC; 38 W; 130cfm; 650Pa	Not applicable	Not applicable
18	Anemometer	Hot wire - Testo 405	0 to 10 m/s; 0 to 50°C	Not specified	± 0.3 m/s; ± 0.5°C
19	Vacuum pump	Pfeiffer (DUO 10 M) – Dual stage rotary vane pump	Less than 0.3 Pa	Not applicable	Not applicable
20	Helium leak detector	Pfeiffer ASM 182 TD^+	up to $5x10^{-13}$ Pa.m³/s	Not applicable	Not applicable

Appendix – C: Estimation of uncertainty in measurements

The temperature is the primary measured quantity in the entire study. The voltage and the current are the other primary quantity leading to the derived quantity of heat dissipated. The uncertainty in the overall thermal resistance (R_{th}) calculated was estimated in accordance with[85]. Hence,

As, $R_{th} = \frac{(T_e - T_c)}{\dot{Q}} = \frac{\Delta T}{(V * I)}$ (C-1)

$$\Delta R_{th} = \sqrt{\left[\frac{\partial R}{\partial \Delta T} . \Delta(\Delta T)\right]^2 + \left[\frac{\partial R}{\partial V} . \Delta V\right]^2 + \left[\frac{\partial R}{\partial I} . \Delta I\right]^2} \quad \text{(C-2)}$$

$$\Delta R_{th} = \sqrt{\left[\frac{1}{VI} . \Delta(\Delta T)\right]^2 + \left[\frac{\Delta T}{V^2 I} . \Delta V\right]^2 + \left[\frac{\Delta T}{V I^2} . \Delta I\right]^2} \quad \text{(C-3)}$$

A sample estimation of the uncertainty of the R_{th} was done for the flat plate PHP (chapter-3) for a heat load of 50 W. The accuracy of the readings of temperatures (thermocouples) was ±1.0 °C. The current and voltage supplied by the power supply has a maximum (full scale) error of ±0.1% (25 mA) and ±0.1% (60 mV) respectively. Thus the derived quantity of the thermal resistance, the difference in temperatures divided by the heat load would have an uncertainty of ± 0.02°C/W for the 70% fill ratio of water at the lowest inclination of 7.5° (which manifested in the largest difference in temperature between evaporator and condenser) tested for a heat input of 50 W. The same has been summarized in Table C-1.

Table C-1: Uncertainty estimation for flat plate PHP for 50 W heat load

Parameters	**Symbol**		**Value**	**Unit**
Voltage supplied	V		14.5	V
Error for voltage	dV	±	0.1	%
Uncertainty in voltage	ΔV=dV*V		0.015	V
Current supplied	I		3.5	A
Error for current	dI	±	0.1	%
Uncertainty in current	ΔI=dI*I		0.004	A
Maximum difference in temperature	ΔT		84.9	°C
Uncertainty in ΔT	Δ(ΔT)	±	1	°C
Uncertainty in overall resistance	**ΔR_{th}**	±	**0.02**	**°C/W**
Actual overall resistance	**R_{th}**		**1.7**	**°C/W**

However, the maximum uncertainty in this study was expected to arise from the fill ratio as the filling was done using the syringe by visual estimate.

Appendix – D: Other single loop pulsating heat pipes

Objective of the study

PHP was of larger bend radius (25 mm) than the one detailed in chapter – 4 which will be identified as PHP1 for further explanation. This was pursued to investigate the effect of bends on the performance of the PHPs as the larger radius bend will reduce pressure drop for the fluid during the pulsations. The reduced pressure drop was pursued with the aim of making the PHP work even at lower heat loads. The PHP was fabricated for shorter overall length (100 mm) to keep the fluid inventory nearly the same as that of the PHP1. However, there was a slight difference in the fluid volume (1.5 ml) for the second which will be identified as PHP2 for further discussion.

PHP construction

Here the copper tubes were brazed to the copper blocks such that only the end face of the tubing was in contact unlike the PHP1 where the bends were brazed surface-to-surface. Another aspect being that in PHP2, the fluid was made to flow through the evaporator and the condenser blocks directly (with drilled holes) unlike the PHP1 where the fluid had to transfer heat through the wall of the tubing. The heat transfer areas of the evaporator and the condenser in PHP2 was lesser than PHP1. The condenser was liquid cooled with liquid at 20°C inlet temperature. The constructional (with various parts) details and the geometry of the PHP fabricated are shown in Figure D-1.

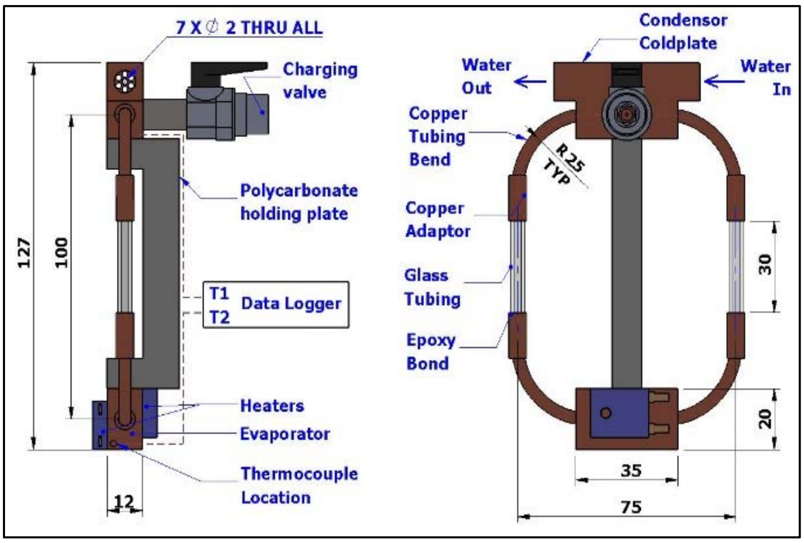

(a)

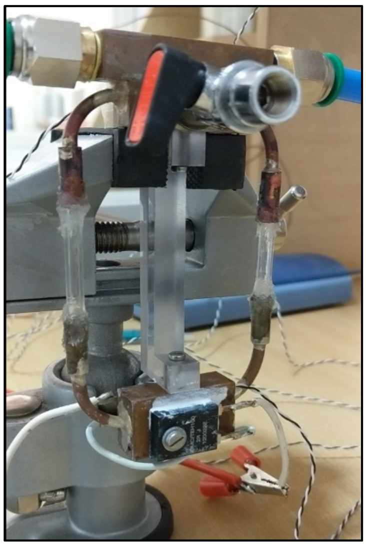

(b)

Figure D-1: Geometrical details of PHP2

Experimental setup

Heat was supplied at the evaporator through two thin film resistance heater of OHMITE make of each 2 Ω resistance and maximum capacity of 100 W connected in series on either side of the evaporator block. This was done to get more uniform heating unlike the PHP1 in which heater was placed on one side only. In PHP2, the condenser was liquid cooled to have greater temperature gradient between evaporator and condenser. The condenser was provided with an integral mini-channel based cooling arrangement as shown in Figure D-1 (a). The charging procedure was carried out as done in chapter-5. The fill ratio was 50 % as in case of PHP1. In the case of PHP2 only 2 thermocouples (one each at the evaporator and at the condenser) were used as it was observed from the PHP1 testing that the temperatures on either side did not vary appreciably.

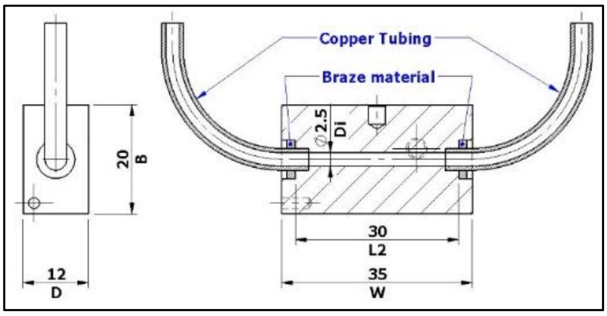

Figure D-2: Geometry of evaporator

Results

The tests were conducted for heat loads of 10 W to 50 W in steps of 10 W. The ambient temperatures across all heat loads ranged between 25°C to 26°C. The internal heat flux was calculated as follows (dimensions - Figure D-2),

$A_s = \pi d L_2 = 1.57$ cm^2; $\dot{Q} = VI$; $\dot{q} = \dot{Q}/A_s$

The salient observations from the tests conducted are summarised as follows,

1. From Figure D-3 it can be observed that a smooth start-up occurred at 10 W heat load but the pulsations were weak with low amplitudes. Thus the 10 W operation resulted into relatively large R_{th} (Figure D-4).
2. For the 20 W heat load, the evaporator steady state temperature hovered around 50° C. The pulsations were stronger as compared to the 10 W operation.
3. As the heat load increases, the time for start-up decreased as expected. For the 30 W operation, the up header had semi annular flow regime whereas the down comer had slug flow regime. The performance for this prototype PHP2 was best for this heat load. This is

evident from the fact that the evaporator temperature hovered around 48° C, 2° C lesser than the 20 W operation indicating better performance at higher heat loads, as in PHP1.

4. For the 40 W operation, the rate of rise of evaporator temperature generally had a gentle upward slope up to 60° C, and the temperature remained constant at 60° C for about 200 seconds, and then dry out occurred. Annular flow was observed in the up header of the PHP and slug flow was observed in the down comer.
5. For the 50 W operation, the evaporator dried out immediately, thus concluding the tests. In none of the tests was there complete unidirectional circulation. Only near net circulation was observed.
6. Thus the k_{equiv} of PHP2 at 20 W and 30 W was estimated to be 2150 W/m.°C and 3560 W/m.°C respectively. The 40 W and 50 W cases could not be ascertained as the evaporator dry out occurred.
7. The PHP2 showed start-up characteristics substantially different from that of PHP1, for example, there was a smooth start up even at 10 W and this was followed by sustained PHP operation unlike PHP1. Even, at 20 W and 30 W, the start-up temperatures were not higher than that of the steady state temperatures indicating smooth start-up at lower loads.
8. But dry out occurred at substantially lower heat loads than PHP1 as the evaporator and especially the condenser surface areas were very much lesser than PHP1.

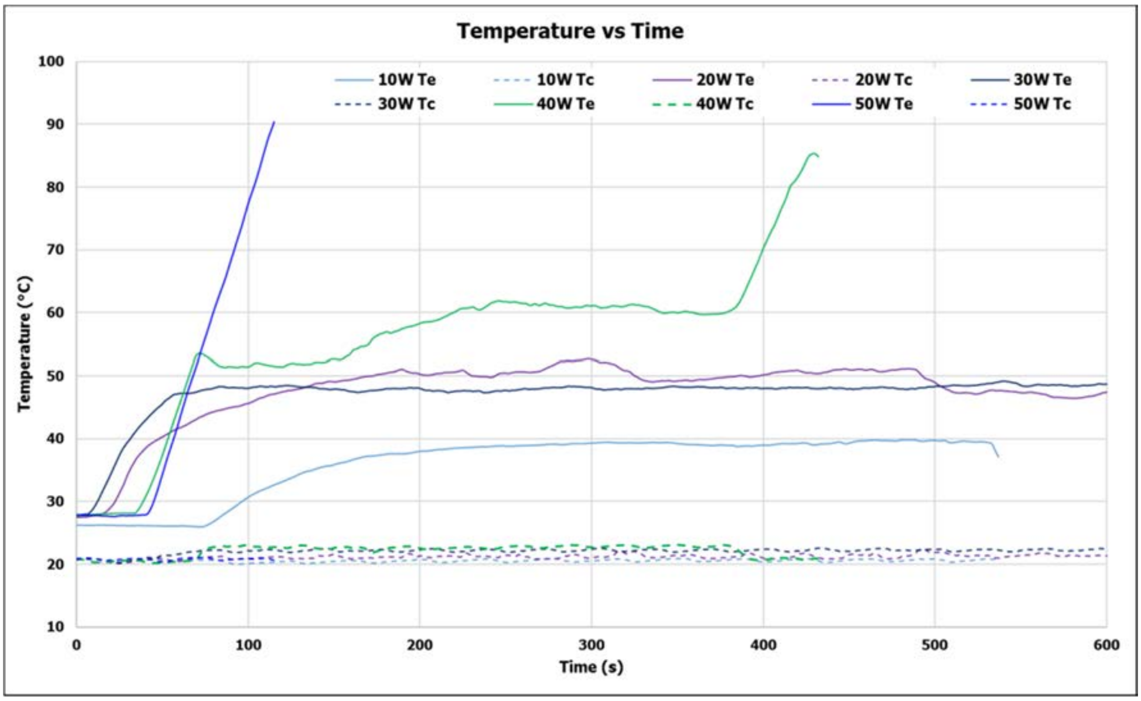

Figure D-3: Temperature vs time - PHP2

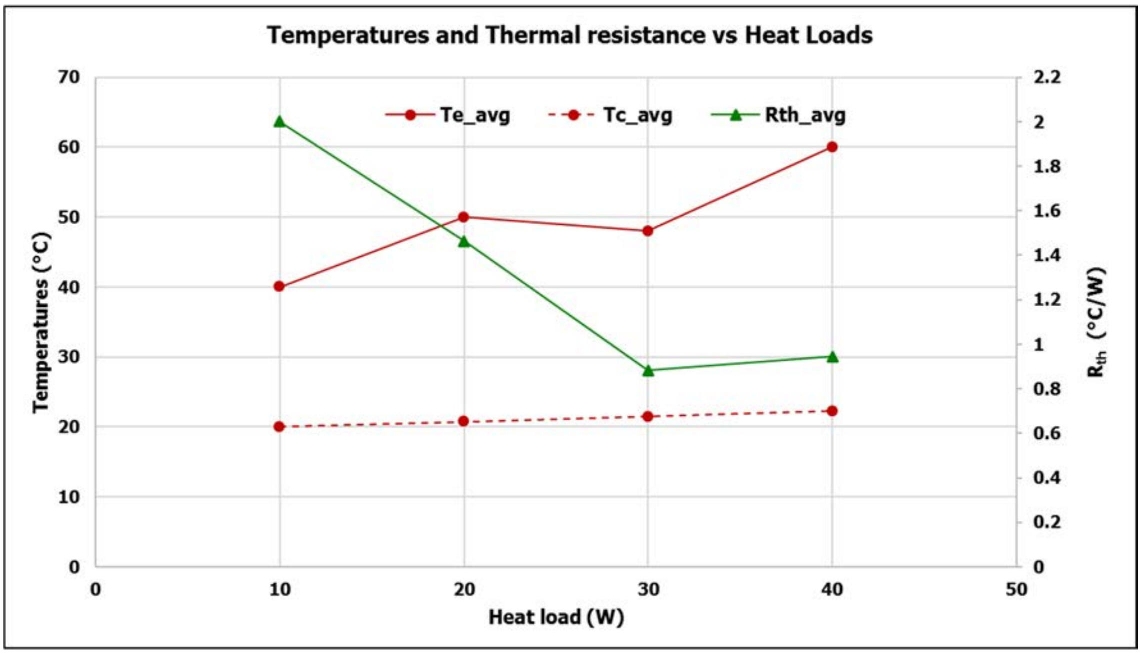

Figure D-4: T_e, T_c and R_{th} vs heat loads for PHP2